Early immune priming and activation against *Streptococcus pneumoniae* from maternal vaccination.

Jamie Pillaye

A thesis submitted to the University of Birmingham for the degree of DOCTOR OF PHILOSOPHY

Institute of Immunology and Immunotherapy
College of Biosciences
The University of Birmingham
Edgbaston
B15 2TT

December 2023

Abstract

Maternal vaccination (MV) to provide protection to the unborn infant is an attractive way to prevent infections in the early weeks and months of life. Despite this, the efficacy or mechanisms underpinning this approach are not well studied. The leading cause of child mortality by infection worldwide is *Streptococcus pneumoniae* (pneumococcus), particularly in low-to-middle-income countries (LMIC). This prevalence of infection could be due to vaccines such as Prevnar13 (PCV13) not being administered until the infant is 8 weeks old. Access to vaccination is limited in LMIC and some children might not receive vaccinations. Therefore, in children, there is a window of susceptibility to this infection that could be addressed through maternal vaccination.

In this study, we have used novel mouse models of maternal vaccination with PCV13 and challenged offspring using pneumococcus to identify the features of acquired immunity. Maternally vaccinated offspring acquired surprisingly long-lasting antibody responses as well as reduced bacterial burdens in the bronchoalveolar lavage, blood and lung suggesting protection against invasive pneumococcal disease is present. Moreover, maternally vaccinated offspring have distinct immune signatures associated with increased maternal cell populations. Maternally vaccinated offspring display distinct enhanced levels of immune control in the BAL. In addition, increased maternal B and plasma cell populations were present in the lung and bone marrow. Finally, bone marrow cells from maternally vaccinated offspring secrete PCV13-specific antibodies. Therefore, PCV13 maternal vaccination suggests long-lasting immunity to infection in offspring.

Publications

The following publications were submitted during my PhD

1. Lebeko M, Kidzeru E, Sishi N, **Pillaye J**, Mkatazo T, Arowolo A, Khumalo N. Cytotoxic Evaluation of Hair Relaxers and Straighteners Actives in Human-Derived Skin Cells. Toxicology and Industrial Health. 2023. *(Submitted, awaiting approval)*

2. Alisha Chetty, Matthew G Darby, **Jamie Pillaye,** Aishah Taliep, Matthew K O'shea, Manual Ritter, Adam Cunningham, William GC Horsnell. Induction of Siglec-$F^{hi}CD101^{hi}$ eosinophils in the lung following murine hookworm *Nippostrongylus brasiliensis* infection. Frontiers in Immunology. 2023

3. Sian E. Jossi, Melissa Arcuri, Areej Alshayea, Ruby R. Persaud, Edith Marcial-Jua´rez, Elena Palmieri, Roberta Di Benedetto, Marisol Pe´rez-Toledo, **Jamie Pillaye**, Will M. Channell, Anna E. Schager, Rachel E. Lamerton, Charlotte N. Cook, Margaret Goodall, Takeshi Haneda, Andreas J. Bäumler, Lucy H. Jackson-Jones, Kai-Michael Toellner, Calman A. MacLennan, Ian R. Henderson, Francesca Micoli and Adam F. Cunningham. Vi polysaccharide and conjugated vaccines afford similar early, IgM or IgG independent control of infection but boosting with conjugated Vi vaccines sustains the efficacy of immune responses. Frontiers in immunology. 2023.

4. Taylor M, **Pillaye J**, Horsnell WGC. Inherent maternal type 2 immunity: Consequences for maternal and offspring health. Seminars in Immunology. 2021.

5. Roberts LB, Schnoeller C, Berkachy R, Darby M, **Pillaye J**, Mackowiak C, Sedda D, Quesniaux V, Ryffel B, Vaux R, Gounaris K, Berrard S, Withers DR, Horsnell WGC, and Selkirk ME. Acetylcholine production by type 2 innate lymphoid cells promotes mucosal immunity to helminth parasites. Science Immunology. 2021(Journal front cover).

6. **Pillaye J**, Marakalala M, Khumalo N, Spearman W, Ndlovu H, Mechanistic insights into antiretroviral drug-induced liver injury, Pharmacology Research & Prospectives. 2020.

Dedication

To the experiences I never expected and the paths that were redirected.

To being brave, daring and never giving up.

To the friends and family, I found along the way.

This thesis is dedicated to my parents, Tilly and Marc Pillaye, and for all the sacrifices you have made for me. This achievement is as much yours as it is mine. *Without your endless love, support, encouragement and calls I would never have been able to complete my PhD. I love you with all my heart.*

Acknowledgements

I am incredibly fortunate to have this opportunity, for through this I have been able to meet and work with phenomenal people that have inspired me in every aspect of my life, I will be forever grateful.

I would like to send my sincere thanks to my supervisors:
Professor William Horsnell for your time, support and encouragement throughout this project and my career thus far. The lessons I have learnt from working with you are invaluable.
Professor Adam Cunningham for your guidance, encouragement and conversation. You have provided me with an environment to learn, grow and gain confidence. I will forever be grateful for your kindness.
Dr Lucy Crouch-Meyers for your kindness, empathy and support. You are the epitome of what a great supervisor should be.

To the Horsnell group, thank you for your support, kindness, motivation and friendship. I would like to specifically acknowledge and thank Alisha Chetty and Matthew Darby for your time, patience and willingness to teach and transfer your knowledge. Without you none of this work would have been possible.

I would like to thank my colleges from the Cunningham lab. Areej Alshayea, Edith Marcial Juárez and Charlie Cook. I am extremely proud to have been part of such a phenomenal team. I am awe of you and your scientific abilities. I am grateful to have worked alongside and learnt from you.

Thank you to Sian Faustini, Ruby Persaud, Elif Yilmaz and Suaad Idris for all your help, encouragement and support. I am on awe if your abilities and incredibly grateful for your friendship and kindness.

To Gabriella Morley-Scott, Fernanda Escobar Riquelme, Marisol Pérez Toledo and Rachel Lamerton. Words cannot begin to describe the how thankful I am for having you in my life. I am incredibly thankful for your constant support, love, encouragement, advice, and friendship. You are all phenomenal woman, and I am so proud to be your friend. Thank you for all of the memories, and to many more!

To Alba Llibre Sarradell, you have become my mentor during this journey teaching me valuable lessons that I will never forget. You have encouraged and motivated me every step of my journey. You are an incredible scientist but an even greater person. My soul is richer because of you.

Thank you to our collaborators Professor Tim Mitchell, Kai Toellner and Dr Yang Zhang. Your insight and knowledge was invaluable.

To the Darwin Trust of Edinburgh, thank you for funding my PhD and awarding me this opportunity.

To the BactiVac Network. You have played such a vital role in not only investing in my work but in me as a scientist as well and I will forever be grateful. I would specifically like to thank Susan Pope and Dr Johanna Dean for helping me find my passion once again.

Ronel, thank you for helping me through the most difficult period of my life. Your wisdom, empathy and kindness have made a lasting impact on my mental health. You are extraordinary at what you do and I will forever be grateful for the impact you have made in my life, this journey would not have been possible without you.

To Harriet, Holly, Alex and Carol. You have been with me throughout this journey, picked me up and encouraged me. You made me believe in myself and reminded me to enjoy life and be present. Thank you! You are amazing and I am truly grateful to have you in my life.

To my best friends and “sisters”, Chloe and Christina. Thank you believing in me, supporting me and being the best friends, anyone could ask for. I love you and you mean more to me than you will ever know.

Finally, to my family, Mom, Dad, Chantal and Phoebe. Thank you for all the sacrifices you’ve made for me. Being apart from you has been my biggest challenge but your love and support was my biggest strength. When this journey got incredibly difficult, you picked me up and kept me motivated. I have done this for you. Thank you, I love you.

Table of Contents

Abbreviations

25G	-	25 Gauge
2D	-	two-dimensional
ACK	-	Ammonium-Chloride-Potassium
ADCP	-	Antibody-dependent Cellular Phagocytosis
AID	-	activation-induced cytidine deaminase
APC	-	antigen presenting cells
B220	-	B cell isoform of 220 KDa
BAB	-	Blood agar base
BAL	-	Bronchoalveolar lavage
B cell	-	B lymphocytes
BCA	-	bicinchoninic acid
BCR	-	B cell receptor
BER	-	base excision repair
BHI	-	Brain heart infusion
BSA	-	Bovine serum albumin
CAIA	-	Cell Adhesion and invasion assay
$CD3^+$	-	Cluster Designation 3 positive
$CD4^+$	-	Cluster Designation 4 positive
CAIA	-	Cell Adhesion and invasion assay
CD19	-	Cluster of differentiation 19
CD40L	-	CD40 ligand
CD49f	-	(Integrin alpha-6),

CFU	-	Colony firming units
CFU/ml	-	Colony firming units/millilitre
CO_2	-	Carbon dioxide
DC	-	Dendritic cell
DMEM	-	Dulbecco’s modified eagle's medium
D/O	-	Days old
DN	-	Double Negative
ELISA	-	Enzyme-linked immunosorbent assay
EPO	-	erythropoietin
FACS	-	Flow cytometry, Fluorescently Activated Cell Sorter
FBS	-	Foetal bovine serum
FcRγII/III	-	Fc-gamma Receptor
FHS	-	Faculty of Health Sciences
fMC	-	fetomaternal microchimerism
G-CSF	-	Granulocyte Colony-Stimulating Factor
GBS	-	*Group B Streptococcus*
HIC	-	High income countries
HRP	-	Horseradish peroxidase
HSC’s	-	hematopoietic stem cells
Hsp	-	Heat shock proteins
IL-1β	-	Interleukin-1 beta
IL-4	-	Interleukin - 4
IL-6	-	Interleukin - 6

IL-10	-	Interleukin - 10
IL-13	-	Interleukin - 13
IL-17	-	Interleukin -17
IL-22	-	Interleukin - 22
INF-y	-	Interferon gamma
ID	-	Identity
I.N	-	Intranasal
I.P	-	intraperitoneal
IVIS	-	in vivo imaging system
LMIC	-	low-to-middle-income-countries
LPS	-	lipopolysaccharides
mMC	-	maternofetal microchimerism
mTECs	-	medullary thymic epithelial cells
MV	-	Maternal vaccination
NaN3	-	Sodium azide
NHEJ	-	non-homologous end joining
NK	-	natual killer
NO	-	nitric oxide
NTS	-	non-typhoidal Salmonella
OD	-	Optimal density
PBS	-	phosphate buffered saline
PAMPs	-	Pathogen Associated Molecular Patterns
PCV13	-	Prevnar13

PFA	-	Paraformaldehyde
P.I	-	Post infection
PLY	-	Pneumolysin
pNPP	-	p-Nitrophenol phosphate
PGCT	-	Protein Glycan Coupling Technology
PRRs	-	Pattern Recognition Receptors
PspA	-	surface proteins
ROS	-	reactive oxygen species
RPMI 1640	-	Roswell Park Memorial Institute 1640
PMA	-	phorbol 12-myristate 13-acetate
RLU	-	Relative light units
RSV	-	Respiratory Syncytial Virus
SARS-CoV-2-	-	Severe acute respiratory syndrome coronavirus 2
SAVC	-	South African Veterinary Council
Sca-1	-	(Stem cell antigen-1),
SHM	-	Somatic hypermutation
STm	-	Salmonella Typhimurium
t-SNE	-	t-Distributed Stochastic Neighbour Embedding
T4P2	-	TiGR4 serotype 2 strain
TdT	-	Terminal deoxynucleotidyl transferase
TH1	-	T helper 1
TH2	-	T helper 2
T Cell	-	T lymphocytes

TIGR4	-	*S. pneumoniae* serotype 4 strain
TMB	-	3,3',5,5'-Tetramethylbenzidine
TNF-α	-	Tumor Necrosis Factor-alpha
TPO	-	Thrombopoietin
UCT	-	University of Cape Town
VDJ	-	variable, diversity, joining gene
W/O	-	Weeks old
WT	-	Wild type

List of figures

Chapter 1: Introduction

1.1 Streptococcus pneumoniae

Streptococcus pneumoniae (S. *pneumoniae*) is a gram-positive bacterium and is currently the leading cause of pneumonia in children under the age of five years old(1). Pneumonia accounts for 14% of mortality due to infection of children under 5 years old, killing approximately 738, 974 children in 2019 **(Figure 1.1)**. *S. pneumoniae* is associated with the colonisation of the nasopharynx but can also lead to invasive disease(1, 2).

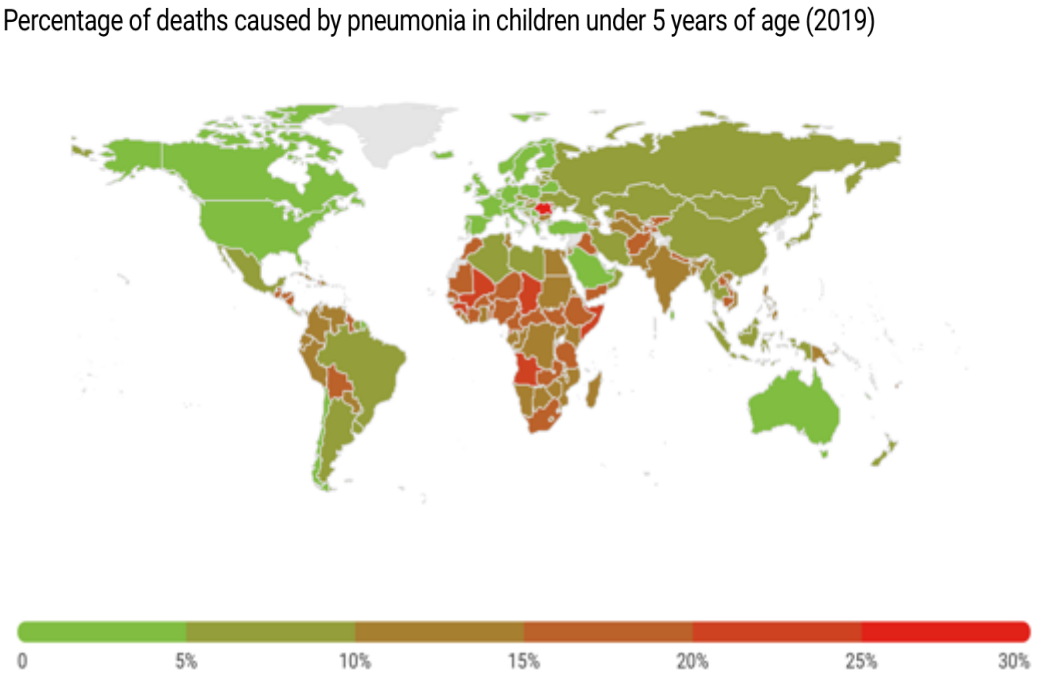

Figure 1.1: Percentage of deaths caused by pneumonia in children under 5 years of age in 2019.
Pneumonia has been the leading cause of death by infection globally since 2000 and due to pneumococcal vaccine intervention, total deaths have reduced. The pneumonia disease burden remains the leading cause of death by infection as of 2019.
Source: WHO and the Maternal Child Epidemiology Estimation group (MCEE) 2020

There are more than 90 identified *pneumococcal* serotypes however, only a small percentage of these serotypes account for most infections in infants. Each serotype has unique characteristics which range in virulence and structure(2, 3). A unique characteristic identified is the absence of the polysaccharide capsule, these strains are classified as non-typable serotypes. The absence or presence of a capsule aids in the serotype invasiveness and pathogenesis(4, 5). The capsule is the major target for protective antibodies and vaccine strategies which include purified capsular polysaccharide proteins of serotypes of *S. pneumoniae*.

1.1.1 Disease burden

Pneumonia due to *S. pneumoniae* is the leading cause of child mortality by infection worldwide, accounting for approximately 1 million child deaths annually **(Figure 1.2)**(1). Despite the use of antibiotic treatment, polysaccharide-based and conjugated vaccine strategies, pneumococcal disease and mortality is disproportionally high in low-to-middle-income countries (LMIC)(3, 6).

Deaths of children under five by infectious disease, 2000 vs 2019

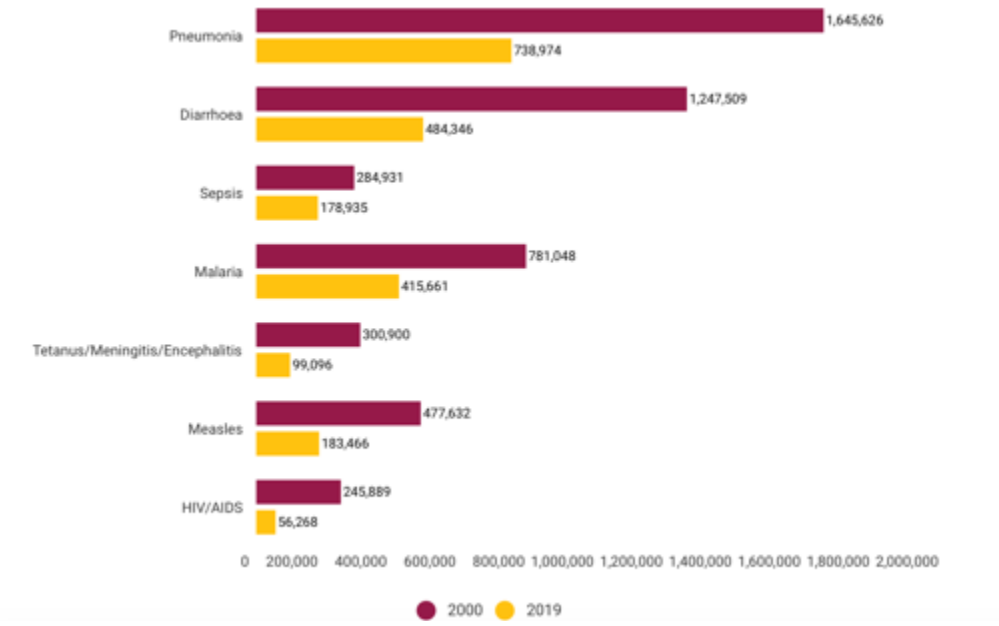

Figure 1.2: Deaths of children under the age of five by infectious diseases. Pneumonia has been the leading cause of death by infection globally since 2000 and due to pneumococcal vaccine intervention, total deaths have reduced. The pneumonia disease burden remains the leading cause of death by infection as of 2019.
Source: WHO and the Maternal Child Epidemiology Estimation group (MCEE) 2020

Pneumonia caused by bacteria can be treated with antibiotics, however only 33% of children with pneumonia receive the antibiotics needed **(Figure 1.3)**. A range of antibiotics have been widely used to manage and control the spread of *S. pneumoniae*, however, more than 30% of infections are caused by pneumococcal serotypes that have developed antibiotic sensitivity or resistance to one or more clinically relevant antibiotics. The highest rate of resistance of *S. pneumoniae* in children under the age of five was found to be penicillin, tetracycline and erythromycin. Moderate resistance was found in chloramphenicol, clindamycin and trimethoprim-sulfamethoxazole(7-9). These antibiotics should be avoided in treatment strategies however remain the most used antibiotics globally.

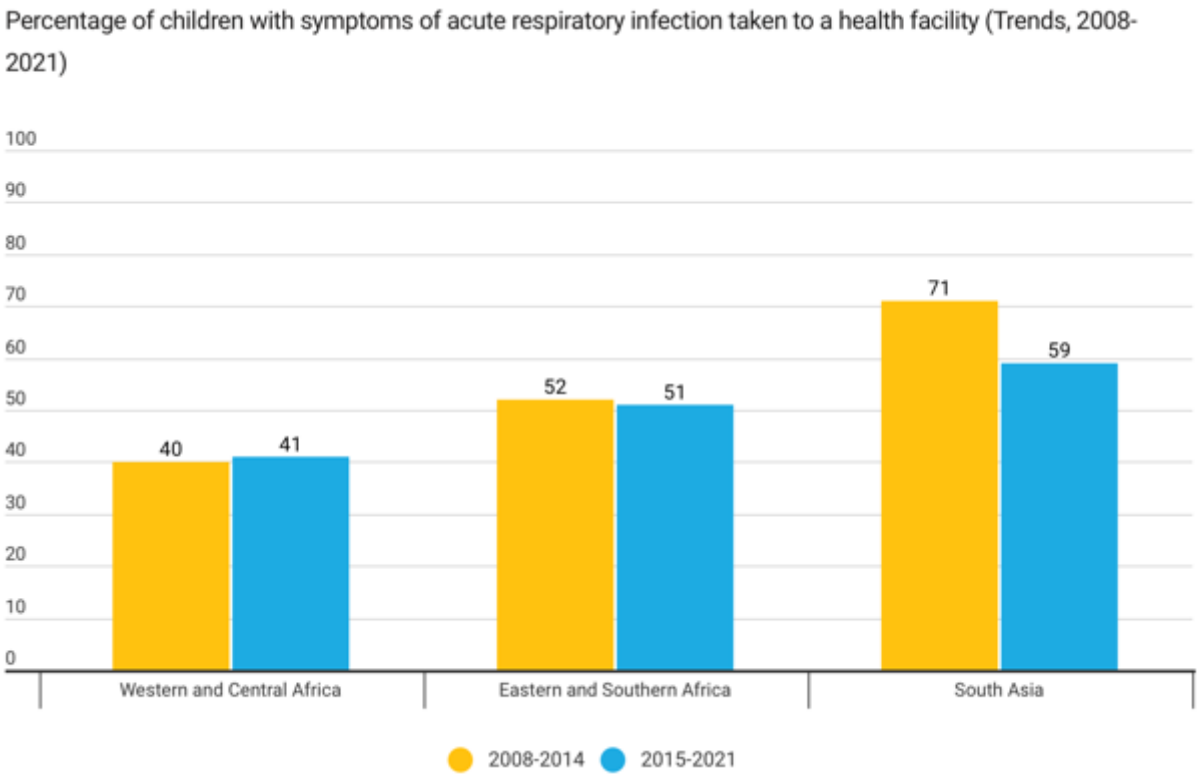

Figure 1.3: Percentage of children with symptoms of acute respiratory infections taken into health facilities.
Children in LMIC's have limited access to health care facilities.
Source: UNICEF global databases, 2022, based on MICS, DHS and other nationally representative household surveys

In LMIC's, antibiotic sensitivity and resistance is not regularly tested in patients and therefore incompatible and high concentrations of the more commonly available antibiotics are prescribed for a prolonged time(7-9). This may lead to adverse side effects such as gastrointestinal distress, allergic reactions, cardiovascular effects, secondary infections as well as liver and kidney damage. These factors increase the difficulty of treating patients and due to the associated challenges, the most effective way to prevent pneumococcal infections is through vaccination.

1.1.2 Pneumococcal colonisation and disease

Pneumococcal colonisation occurs primarily in the upper part of throat that lies behind the nose, more commonly referred to as the nasopharynx **(Figure 1.4)**. Pneumococcal colonization typically occurs when infectious droplets are released through the air and inhaled(5, 10, 11). Colonized bacteria in the nasopharynx may multiply and establish as pneumonia in the lower respiratory tract, which includes the bronchi and alveoli of the lungs(5, 10). If pneumonia is not effectively treated, the pathogen can enter the bloodstream this can lead to bacteraemia and spread to other organs such as the spleen and liver which is a hallmark of sepsis(11, 12). Bacteraemia may also spread to the blain and lead to meningitis. Sepsis can lead to further complications such as organ dysfunction and heart failure **(Figure 1.4)**.

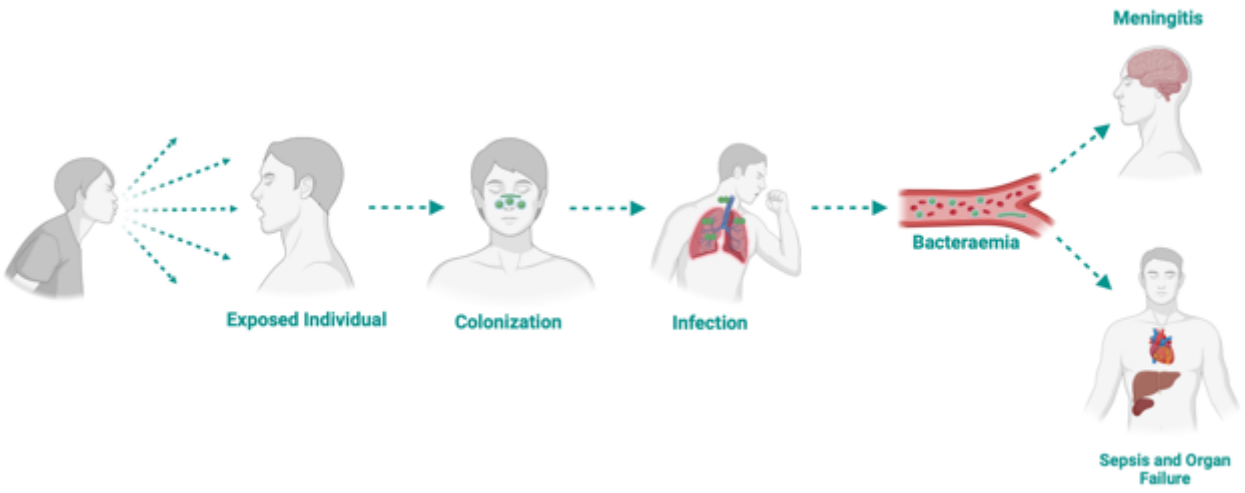

Figure 1.4: Pneumococcal colonisation and spread of disease.
After *Pneumococcal* exposure, colonisation occurs in the nasopharynx. Bacteria multiplies and establishes as pneumonia in the lower respiratory tract in the lung. Pneumonia if not treated can enter the bloodstream lead to bacteraemia which may lead to sepsis and meningitis.

1.2 Vaccines

1.2.1 Current Vaccine strategies

Current pneumococcal vaccines can be classified into two categories: pneumococcal conjugate vaccines (PCV's) and pneumococcal polysaccharide vaccines (PPSV's). The most globally administered PPSV is Pneumovax23® which provides protection against certain *S. pneumoniae* serotypes (1, 2, 3, 4, 5, 6B, 7F, 8, 9N, 9V, 10A, 11A, 12F, 14, 15B, 17F, 18C, 19F, 19A, 20, 22F, 23F, and 33F), but unfortunately does not work effectively in children under the age of two due to a lack of response to free polysaccharides(1, 2, 4, 7). The most widely used conjugate vaccine is Prevnar13® (PCV13) which includes purified capsular polysaccharide of 13 serotypes of Streptococcus pneumoniae (1, 3, 4, 5, 6A, 6B, 7F, 9V, 14, 19A, 19F, 18C, and 23F) conjugated to a nontoxic variant of diphtheria toxin known as CRM197. PCV13 is the leading vaccination strategy for children but is expensive, has limited serotype coverage and can only be administered to children after 6 weeks of age.

PCV13 is classified as one of the most expensive vaccines to develop and manufacture and is currently priced at ~£140 per dose. Global organisations such as the World Health Organisation (WHO), governments agencies including the Centre for Disease Control and Prevention (CDC) and local governments have recommended PCV13 as a routine vaccine for children, however PCV13 is not financially supported by governments(2, 7). In LMIC's, where the pneumococcal disease burden is extremely high, children require four PCV13 boosts at 2, 4, 6 and 12-15 months which increases the financial burden(3, 8). The financial costs contribute to the difficulty of vaccine rollout as many individuals in

LMIC cannot afford to vaccinate children and therefore increase the spread of *S. pneumoniae.*

There are more than 90 identified serotypes of *S. pneumoniae* identified globally. PCV13 and Pneumovax23® only protect against limited serotypes creating a serotype bias. To overcome the serotype bias present in current vaccine strategies, a vaccine that does not target specific serotypes but rather universal *S. pneumoniae* proteins could reduce incidence of early life *S. pneumoniae* infections in vulnerable populations globally. In LMIC's and regions with limited access to healthcare and vaccination rates can be extremely low and children might not receive any treatments or pneumococcal vaccines. In LMIC's, the incidence of pneumonia in children younger than 2 months of age is extremely high and the lack of protection for infants creates a window of opportunity for the bacteria to infect. Identifying a way to decrease this window of susceptibility in infants is essential to reduce the spread of infection.

1.2.2 Serotype replacement

Serotype replacement is due to the introduction of pneumococcal vaccines, this reduces the prevalence of vaccine targeted serotypes and allows for non-vaccine serotypes (NVT) to thrive and become more common(4, 13, 14). This directly increases the incidence of early life *S. pneumoniae* infections in vulnerable populations and places strain on health care infrastructure. Surveillance and monitoring of pneumococcal serotypes are constantly reported on in an attempt to notify vaccine developers to constantly add serotypes to enhance protection. The turnaround time and financial development of these

vaccines is costly and slow however, this does not solve the issues facing serotype replacement.

In studies, clinical isolates of children from a range of LMIC's were sequenced and NVT were identified. These strains include 16F, 34, 35B indicating that serotype replacement is a factor that needs to be investigated to protect individuals in countries where *S. pneumoniae is* prevalence is high(15). Therefore It is imperative to explore the potential to vaccinate against these unprotected serotypes.

1.2.3 Novel Vaccine strategies

Current vaccination strategies could be improved by utilising novel vaccine approaches. The lack of broad spectrum protection highlights the need for the current "gold standard" of vaccines to be revised. Pneumococcal proteins have been widely studied and characterised according to their role and colonization, pathogenesis and virulence. These proteins have the potential to function as antigens in a multi-valent protein vaccine that confers capsule independent protection and in turn removes any serotype bias. The protein expression should be highly conserved across the serotypes, have adequate surface expression and should be easily recognised by antibody. Studies have shown that a combination of pneumococcal proteins confers superior protection compared to single antigens in mice(16-18).

S. pneumoniae proteins such as NanA, PiuA, PspA and Sp0148 are important for ensuring colonization in the nasopharynx. These proteins are responsible in aiding the

survival and replication of *S. pneumoniae* bacteria(19-21). Studies have shown that new vaccine targets using Protein Glycan Coupling Technology (PGCT) can protect mice against *S. pneumoniae* infections. One examples would be *S. pneumoniae* serotype 4 capsular polysaccharides linked to proteins NanA, PiuA, and Sp0148 protected mice against meningitis and septicaemia with the same efficacy as vaccination with Prevnar-13(21). These data demonstrate that a vaccine made by PGCT is as effective as Prevnar-13 and demonstrates that linking capsular antigen to S. pneumoniae protein antigens has additional protective benefits that could provide a degree of serotype-independent immunity(19, 20).

Current vaccine strategies against *S. pneumoniae* are created around capsular polysaccharide technologies. Serotypes are selected and incorporated into conjugated vaccines however serotype replacement has led to nonvaccine serotype replacement disease(22, 23). An alternative serotype independent strategy using multiple-antigen vaccines (MAV) prepared from *S. pneumoniae* TiGR4 serotype lystaes enriched with heat shock proteins (Hsps), surface proteins (PspA) and pneumolysin (Ply)(23-25). Mice vaccinated with MAV induced antibody responses to multiple serotypes, including nonpneumococcal conjugate vaccine serotypes(22, 25). This data suggests that MAV potentially could provide serotype-independent protection against S. pneumoniae.

1.2.4 Maternal Vaccination strategies

Maternal vaccination (MV) refers to the practice of immunizing pregnant woman to protect both the mother and the unborn child from infectious disease(26-28). Pregnancy can

weaken the immune system causing pregnant woman to become more susceptible to infection(29). The aim of MV is to increase the transfer of antibodies from the mother to the fetus through the placenta. This can provide the newborns with passive immunity during the early weeks to months of life which are particularly vulnerable to infections and not yet eligible for their own vaccinations(26). The timing of MV is crucial for increasing the transfer of protection to the infant. Once the baby is born, passive transfer can be transferred through breastmilk as well however not every vaccine has the same mechanism of action and each MV study needs to investigated independently. Therefore MV can benefit and protect the both the mother and the fetus.

Maternal vaccinations against Respiratory Syncytial Virus (RSV), Influenza, Group B Streptococcus (GBS), SARS-CoV-2, and pertussis have been shown to provide immune protection in infants (30-33). The Centre for Disease Control (CDC) highly recommends that pregnant woman receive pertussis, Influenza and SARS-CoV-2 vaccines during pregnancy.

MV is showing clinical promise for GBS and RSV. The timing of GBS disease suggests that a maternal vaccine given in the late second or early third trimester of pregnancy would prevent most maternal cases(34, 35). MV can lead to a reduction in maternal and child GBS colonisation lasting up to 89 days after exposure (29, 32). A study evaluating the safety and immunogenicity of an investigational trivalent GBS vaccine in US pregnant woman indicated antibody concentrations were substantially higher in women with

detectable pre-vaccination antibody concentrations(36). Infant IgG and breast milk IgA were higher in the vaccine vs the placebo group at all timepoints(36).

Pertussis infection in infants can cause severe illness and death. Pertussis MV during the third trimester (at approximately 28-31 weeks) gestation was effective in preventing pertussis infection in infants aged 8 weeks and younger(37, 38). In addition, Pertussis MV is associated with a lower risk of infection among infants through 8 months of age(39, 40). Due to the clinical trial data the Tdap (tetanus, diphtheria, acellular pertussis) vaccine has proven to be highly effective in infants and therefore has become a routine vaccination in infants(38, 40).

It is likely that maternal vaccination against *S. pneumoniae* is a tractable approach to provide offspring with early life protection. Understanding when the optimal time is to vaccinate a mother to provide not just passive immunity but also a long lasting active immune response would represent an important biomedical benefit.

1.3 The immune system

The immune system is a complex and vital defence mechanism that consists of cells tissues and organs that has a purpose of protecting the body from harmful infections and diseases such as bacteria, fungi, parasites, and viruses. The immune system's primary function is to distinguish between self and non-self. The body's own cells are regarded as self while a foreign substance or pathogen would be regarded as non-self. This is crucial for maintaining the body's homeostasis and tolerate the hosts own cells and tissues but also prevent autoimmune reactions whereby the body mistakenly attacks its own tissues. If a foreign pathogen is detected by host cells, a coordinated response is trigged to eliminate the targeted pathogen in a rapid way. Control of an immune response is essential as an incorrect immune response may result to immune-pathology and cause a detrimental inflammatory immune response.

Blood cells are consistently produced in the bone marrow through expansion and differentiation of progenitor cells that originate from hematopoietic stem cells (HSC's)(41, 42). Hematopoiesis starts with HSCs which are proliferative and multipotent cells that are localised in specialized regions of the bone marrow called niches(43). These niches have stromal cells, extracellular matrix components, and signalling molecules that support the survival, proliferation, and differentiation progenitor cells(44).

HSCs can self-renew to not only maintain their population but also differentiate into a range of blood cell lineages. HSCs can differentiate into two different progenitor cells lines: Myeloid progenitor and Lymphoid progenitor cells(41).

Myeloid progenitor cells can further differentiate into several distinct types of cells, each with specialized functions. The first subgroup of cells is known as Megakaryocytes which are large cells that fragment to form platelets with the stimulation of Thrombopoietin (TPO)(45). The function of platelets is essential for blood clotting and wound healing. Myeloid progenitor cells differentiate into myoblasts which further matures into Granulocytes under the influence of Granulocyte Colony-Stimulating Factor (G-CSF)(43). Granulocytes can be categorised into Neutrophils, Eosinophils and Basophils(42, 45). Neutrophils are responsible for phagocytosis mainly involved with bacteria and fungi while Eosinophils and Basophils are predominantly involved with parasitic infections, allergic reactions, and inflammation(43). Erythrocytes are the largest proportion of Myeloid progenitor cells chich are derived from erythroblasts stimulated by erythropoietin (EPO)(42, 46). These cells are responsible for transporting oxygen from the lungs to the tissues while carrying carbon dioxide ($C0_2$) from the tissue to be exhaled from the lungs(42). Monocytes are the final subgroups of Myeloid progenitor cells(45). Monocytes mature into monocytes which circulate in the blood and migrate into tissues where they become macrophages or dendritic cells(46). Macrophages and dendritic cells are involved in phagocytosis and antigen presentation which is essential for the immune response **(Figure 1.5)**.

Lymphoid progenitor cells can further differentiate into various lymphocytes that are essential for the adaptive immune response. Lymphoid progenitor cells migrate to the thymus where they mature into various T lymphocyte cells (T cells)(42, 45). T cells are primarily involved in cell-mediated immunity, directly killing infected cells, and regulating immune responses(43, 46). Lymphoid progenitor cells can further differentiate into Natural Killer (NK) cells which are essential for the innate immune system(42, 43). NK cells can recognise and kill virus-infected cells without prior exposure to antigen. The final subgroup of Lymphoid progenitor cells is B Lymphocyte cells (B cells)(42, 45, 46). Mature B cells migrate to secondary lymphoid organs such as spleen and lymph nodes. B cells can also differentiate into plasma cells that can secrete antibodies **(Figure 1.5)**.

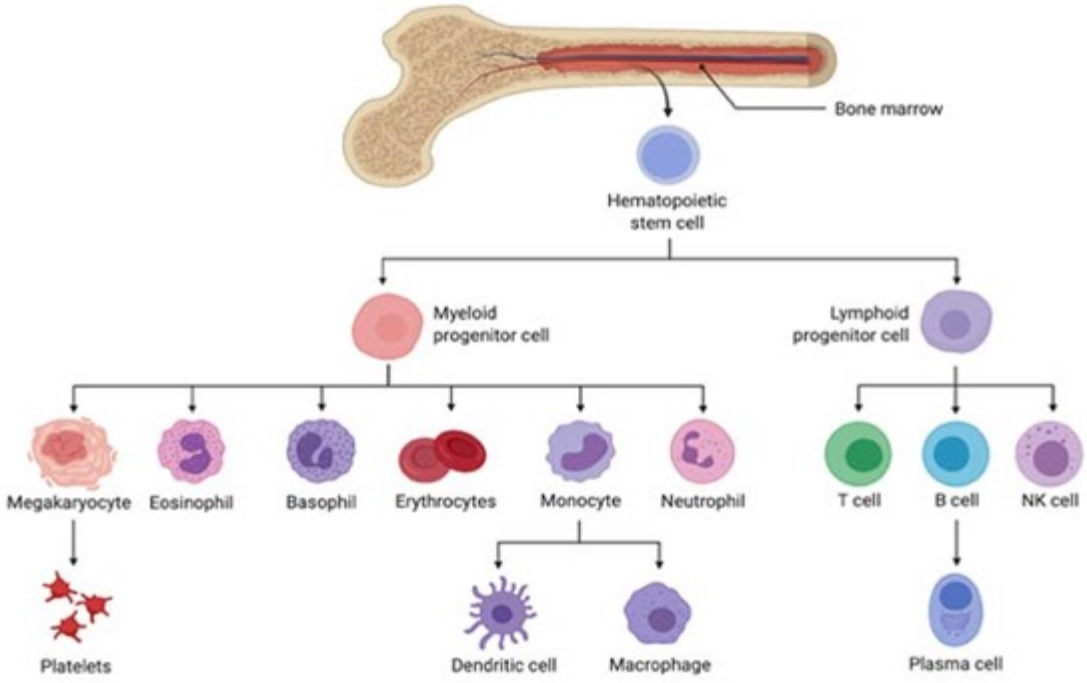

Figure 1.5: Hematopoiesis in the bone marrow
Blood cells are consistently produced in the bone marrow through expansion and differentiation of progenitor cells that originate from hematopoietic stem cells (HSCs). HSCs can differentiate into two different progenitor cells lines: Myeloid and Lymphoid progenitor cells. Myeloid progenitor cells can further differentiate into platelets, eosinophils, basophils, erythrocytes, dendritic cells, macrophages and neutrophils. Lymphoid progenitor cells can further develop into T, B, plasma and Natural killer cells.

The immune system can be broadly characterised into two branches: the innate and adaptive immune system. The innate and adaptive immune response function together to provide the body with a comprehensive defence to fight off pathogens. The innate system recognises a spectrum of pathogens and provides the body with a non-specific first line of defence(47). The adaptive immune response is a secondary defence which is slower and specific. The adaptive response can develop memory cells to a specific infection and therefore upon re-exposure to the same pathogen a quicker and more targeted response can be generated.

The innate immune system has distinct cells which act as the initial first line of defence. Some of the key cells involved are granulocytes, natural killer (NK) cells, dendritic cells, neutrophils and phagocytes(47, 48). In addition, the complement system is an essential part of the innate immune response. The adaptive immune system is characterised by its specificity and memory. The key cells involved are antigen-presenting cells (APC's), B lymphocytes (B cells), T lymphocytes (T cells) and memory cells(48, 49).

1.3.1 Innate immunity

The innate immune system functions through a series of mechanisms. Innate cells express Pattern Recognition Receptors (PRRs) which recognise highly conserved Pathogen Associated Molecular Patterns (PAMPs). These PAMPs include lipopolysaccharides (LPS), DNA, double stranded RNA and flagellin. In the presence of a pathogen, innate cells will recognise the foreign antigen and differentiate into short-lived effector cells.

Phagocytic cells such as macrophages and neutrophils are effector cells that detect and bind foreign pathogens(50). These phagocytic cells surround and engulf the pathogen which results in the formation of the phagosome. The phagosome undergoes maturation which includes the fusion of the lysosome. The lysosome is an acidic environment whereby enzymes can degrade pathogens and break them into smaller fragments which are expelled through exocytosis(50).

Macrophages are present in most tissues and act as scavengers and supervisors which play a key role in initiating the innate response. Macrophages have the ability to recruit other phagocytes to the site of infection by secreting chemokines. Chemokines. As macrophages encounter different types of pathogens, tissues or inflammatory signals they can produce a range of chemokines into the surroundings to create a concentration gradient that recruits and guides other immune cells towards the site of infection(51). Macrophages secrete CCL2 which attracts monocytes, CCL3 and CCL4 which recruits T cells and dendritic cells, CCL5 which attracts monocytes and eosinophils as well as CXCL10 which is responsible for attracting activated T cells to the sites of infection. Macrophages play a role in orchestrating the recruitment and ultimately shaping the immune response to a pathogen(52).

Macrophages can be sub divided into M1 and M2 macrophages. M1 macrophages are involved in promoting a range of pro-inflammatory responses and antigen presentation(52). M1 macrophages contribute to the development of a T helper 1 (TH1) responses characterised by the release of pro-inflammatory cytokines such as Tumor Necrosis Factor-alpha (TNF-α), Interleukin-1 beta (IL-1β) and Interleukin-6 (IL-6)(53). M1 macrophages play a crucial role in microbial defences specifically against bacterial, viral and fungal infections(52). M1 macrophages produce reactive oxygen species (ROS) and nitric oxide (NO)(53). M2 macrophages are predominantly involved in phagocytosis and promoting the development of T helper 2 (Th2) responses(50, 52, 54). M2 macrophages are involved in downregulating inflammation and release anti-inflammatory cytokines such as interleukin-4 (IL-4), interleukin-13 and interleukin-10 (IL-10). Understanding the

balance and regulation between M1 and M2 macrophages is important for maintaining proper immune responses and tissue homeostasis.

1.3.2 Adaptive immunity

The adaptive immune system is a critical part of the body's defense mechanism, providing a specific and long-lasting response to pathogens such bacteria, and other foreign invaders(55). It differs from the innate immune system in that it is highly specific to antigens and has the ability to remember previous encounters with pathogens, leading to a more efficient response upon re-exposure(55). The adaptive immune system has key features that contribute to the role of the immune system. The adaptive immune system is highly specific and can distinguish between different pathogens and target them specifically(56). If a specific pathogen is identified, the adaptive immune system remembers it and a more robust response can be identified upon exposure. The adaptive immune system can differentiate between self and non-self therefore preventing autoimmunity and allowing for self-tolerance(56, 57).

The main components of the adaptive immune system are lymphocytes which are white blood cells and can be further characterised into B and T cells. T cells originate from hematopoietic stem cells in the bone marrow(55, 56). T cell development is a finely tuned process that ensures the generation of a functional and self-tolerant T cells. This process involves several stages, including thymocyte migration, differentiation and selection. T cell progenitors, called thymocytes, originate from hematopoietic stem cells in the bone marrow and migrate to the thymus through the bloodstream(58). Thymocytes at this stage

enter the cortex and do not express CD4 or CD8 co-receptors. The Double-Negative (DN) stage is classified into four sub-phases based on the expression of surface markers: DN1, DN2, DN3 and DN4(59). In stage DN1 to DN2, thymocytes proliferate and begin to rearrange their T cell receptor (TCR) beta chain genes(60, 61). Following successful rearrangement of the TCR beta-chain genes, phase DN2 to DN3 allows for the expression of the pre-TCR complex, leading to proliferation and differentiation(58, 60, 62). In phase DN3 to DN4, thymocytes begin to rearrange their TCR alpha chain genes(60). In the Double-Positive (DP) stage, thymocytes express both CD4 and CD8 co-receptors and TCRs on their surface(63). This stage is crucial for the selection processes that ensure the functional competence and self-tolerance of T cells(64). The first stage is positive selection, which thymocytes with TCRs that moderately bind self-MHC-peptide complexes receive survival signals and are selected for further maturation(60, 65). This ensures that T cells can recognize self-MHC molecules. Negative selection includes thymocytes with TCRs that bind strongly to self-MHC-peptide complexes undergo apoptosis. This process eliminates potentially auto-reactive T cells, ensuring self-tolerance(61). The final stage is the Single-Positive (SP) stage(60, 65). Thymocytes differentiate into either $CD4^+$ or $CD8^+$ T cells based on their TCR specificity. $CD4^+$ T cells are produced if antigens presented by MHC class II molecules and typically become helper T cells while CD8+ T cells are produced if antigens presented by MHC class I molecules and typically become cytotoxic T cells(63, 65) **(Figure 1.6)**.

Final maturation occurs whereby further selection occurs in the thymic medulla to ensure self-tolerance through interactions with medullary thymic epithelial cells (mTECs) and

dendritic cells presenting self-antigens. Successfully selected and matured T cells leave the thymus and enter the peripheral circulation as naive T cells(59). These cells are now capable of recognizing and responding to foreign antigens presented by MHC molecules. This process is essential for maintaining immune homeostasis and effective immune responses against pathogens(59).

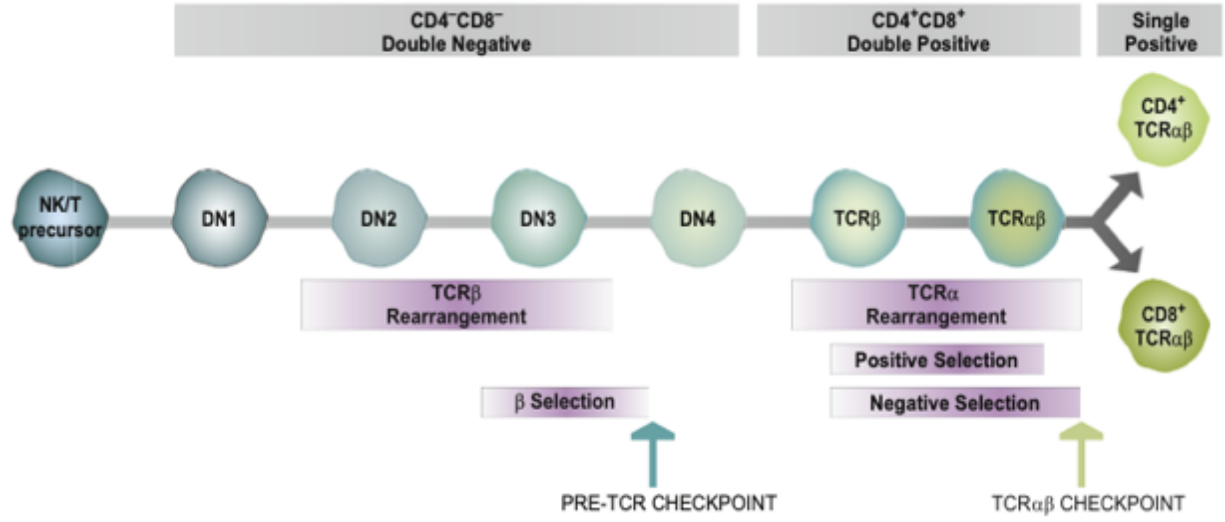

Figure 1.6 Checkpoints of T cell Development
NK/T precursors pass through the DN1-DN4 stages of the double negative (DN), double positive (DP) and single positive (SP) stages of thymocyte development. Most DN3 thymocytes become αβ T cells, but some generate γδ T cells. Most DP thymocytes that survive various thymic selection processes become $CD4^+$ or $CD8^+$

B cells are a fundamental component of the adaptive immune response and can be further described according to their function(66). Naïve B cells are a crucial component of the adaptive immune system and plays and essential role in the initial stages of the immune response. Naïve B cells express specific surface markers including CD19, CD20, CD21, CD22 and B cells receptors (BCRs(66)). Naïve B cells exit the bone marrow and circulate

in the peripheral blood and lymphoid organs and then migrate to secondary lymphoid tissues such as lymph nodes, spleen, peyer's patches where they await to encounter specific antigens. When a naïve B cell encounters antigen, it becomes activated which is a complex process(67). B cell activation involves key steps such as antigen recognition, co-stimulation, clonal expansion and differentiation. Antigen recognition is triggered when a specific antigen binds to the BCR(67, 68). After binding the B cell internalizes the antigen-BCR complex through endocytosis and the antigen is processed into smaller fragments within the B cell(68). The processed antigen fragments are relocated to the surface of the B cell and presented on the surface of the B cell in conjunction with Major Histocompatibility Complex (MHC) class II molecules(68). This antigen fragment presentation is essential for subsequent interaction with $CD4^+$ helper T cells which provides co-stimulatory signals for B cell activation(57). Activated B cells acquire enhanced potential for antigen presentation with upregulation of MHC-I and II and co-stimulatory molecules, such as CD40 ligand (CD40L) on $CD4^+$ T cells binding to CD40 on B cells(61). Another example is CD80/86, further activating both CD4+ and CD8+ T cells(57, 61). Also, CD27 is upregulated in activated B cells, and interaction between this molecule and CD70 on the membrane of memory CD8+ T cells promote their maintenance and facilitates their activation in an antigen-independent manner(61). CD8+ T cell activation leads to efficient cell proliferation and production of potent inflammatory mediators, such as granzymes, perforin, and IFN-γ. Once activated, B cells proliferate extensively, creating a clone of cells that all recognize the same antigen. This clonal expansion increases the number of B cells available to combat the specific antigen **(Figure 1.7)**.

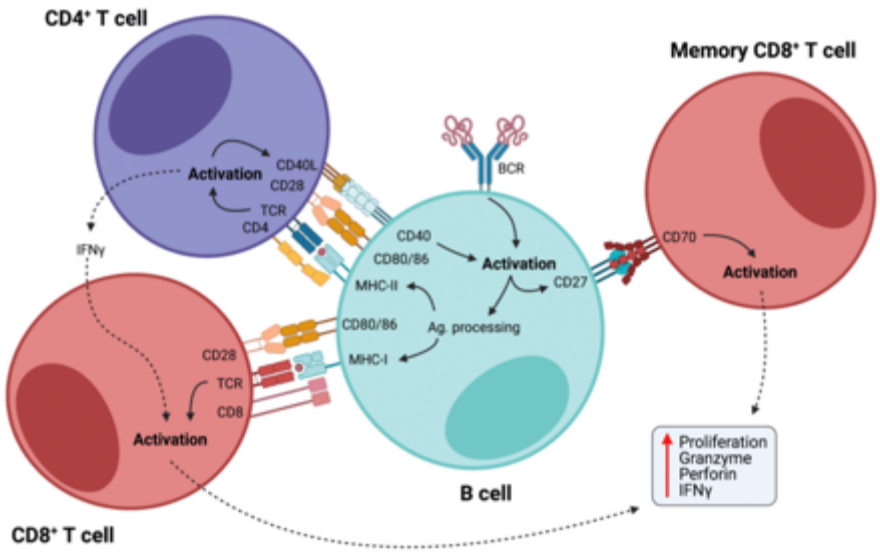

Figure 1.7 B cells as activators of cellular immunity.
B cells are initially activated by antigen recognition through the BCR. Internalized antigens are then presented through class II MHC to $CD4^+$ helper T cells, which provide co-stimulatory signals for B cell activation. Activated B cells acquire enhanced potential for antigen presentation with upregulation of MHC-I and II and co-stimulatory molecules activating both $CD4^+$ and $CD8^+$ T cells.

Activated B cells can differentiate into plasma cells. Plasma cells are effector B cells that secrete large amounts of antibodies specific to the antigen. These antibodies help neutralize the pathogen, mark it for destruction by phagocytes, or activate the complement system. Through a process called V(D)J recombination, a diverse repertoire of antibodies by randomly combining variable (V), diversity (D), and joining (J) gene segments(69). This creates the initial diversity necessary for recognizing a wide array of antigens, while an additional process called somatic hypermutation (SHM) fine-tunes and enhances antibody affinity, ensuring effective and robust immune protection(70, 71). Other activated B cells become memory B cells. These cells do not immediately participate in the current immune response but remain in the body for long periods, ready to respond rapidly and robustly if the same antigen is encountered again(68).

VDJ recombination is a process that generates diverse antibodies by randomly assembling VDJ gene segments(69, 72). This process occurs in developing B cells within the bone marrow and is crucial for creating the vast repertoire of antibodies capable of recognizing numerous antigens. In the heavy chain genes, one D segment joins a J segment first, followed by the addition of a V segment to the DJ complex(72, 73). Light chain genes, which lack D segments, undergo a simpler VJ recombination. The recombination is initiated by the RAG1 and RAG2 proteins, which introduce double strand breaks at specific recombination signal sequences(69, 72). The resulting DNA breaks are repaired by the non-homologous end joining (NHEJ) pathway, with additional diversity introduced by the enzyme Terminal deoxynucleotidyl transferase (TdT), which adds random nucleotides at the junctions. This combinatorial and junctional diversity ensures that each B cell produces a unique antibody, equipping the immune system to respond to a wide array of pathogens(73).

Somatic hypermutation (SHM) is a critical process in the adaptive immune system that enhances the affinity of antibodies for their specific antigens(70, 74, 75). This process occurs in mature B cells within the germinal centers of secondary lymphoid organs, such as lymph nodes and the spleen, after B cells have been activated by antigen exposure(70, 74, 75). SHM is initiated by the enzyme activation-induced cytidine deaminase (AID), which deaminates cytosine bases in the DNA of the variable regions of immunoglobulin genes, converting them to uracil(70, 74, 75). The resulting uracil bases are recognized as errors and are processed by error-prone DNA repair mechanisms, including base excision repair (BER) and mismatch repair (MMR), introducing point mutations. These mutations

create a diverse array of antibody variants. B cells expressing antibodies with higher affinity for the antigen are selected for survival and proliferation in a process known as affinity maturation(71, 75). SHM, therefore, works in conjunction with this selective pressure to produce high-affinity antibodies, enhancing the immune system's ability to effectively neutralize and eliminate pathogens.

Vaccination primes the immune system by activating naive B cells specific to the vaccine antigen(76). These B cells undergo clonal expansion and differentiation. As part of the adaptive immune response triggered by vaccination, SHM introduces mutations into the variable regions of the antibody genes in activated B cells(77-79). This process occurs in germinal centre’s where B cells interact with follicular dendritic cells and T helper cells. Through affinity maturation, B cells that produce antibodies with increased affinity for the antigen are selected(77-79). This results in a more effective and robust immune response. The high-affinity antibodies produced are better at neutralizing the pathogen if encountered in the future. Memory B cells generated during the vaccination process undergo SHM, leading to a pool of high-affinity memory B cells. These cells can rapidly respond to subsequent exposures to the pathogen, providing long-term immunity(78, 79). Therefore, vaccination leverages the body's natural immune mechanisms by stimulating the production and maturation of high-affinity antibodies, vaccination ensures robust protection against infectious diseases, underscoring the crucial role of SHM in adaptive immunity and vaccine efficacy(76).

1.3.3 The immune system in the context of a pneumococcal infection

During a pneumococcal infection, neutrophils and macrophages are crucial as the first responders. During a pneumococcal infection, neutrophils and macrophages are rapidly activated as part of the body's innate immune response. The presence of *Streptococcus pneumoniae* is detected by pattern recognition receptors (PRRs) on the surface of neutrophils, such as Toll-like receptors (TLRs), which recognize pathogen-associated molecular patterns (PAMPs) specific to the bacteria(80-83). Upon recognition, these receptors trigger intracellular signalling pathways that activate the immune cells. Neutrophils are recruited to the site of infection by chemotactic signals (CXCL8, CXCL1, CXCL2, CXCL5) and cytokines Interleukin-8 (IL-8)(81-83). Chemokines released by infected tissues and other immune cells bind to the appropriate receptor. Once activated, neutrophils engage in phagocytosis, engulfing and digesting the bacteria, and release antimicrobial substances like reactive oxygen species (ROS) and enzymes to kill the pathogens(81-83). Macrophages, which reside in tissues, also recognize and engulf the bacteria, and upon activation, they secrete additional cytokines to amplify the immune response, attract more immune cells, and present antigens to T cells, thereby linking the innate and adaptive immune responses. This coordinated activation of neutrophils and macrophages is critical for controlling and eliminating the pneumococcal infection.

Dendritic cells (DCs) play a pivotal role in controlling a pneumococcal infection by bridging the innate and adaptive immune responses. DCs recognize the bacteria through pattern recognition receptors (PRRs) such as Toll-like receptors (TLRs)(84, 85). This recognition triggers the maturation and activation of dendritic cells, prompting them to engulf and

process the bacterial antigens. These antigens are then presented on the surface of dendritic cells bound to major histocompatibility complex (MHC) molecules. Migrating to the lymph nodes, dendritic cells present these antigens to naïve T cells, leading to the activation and differentiation of T cells into helper T cells (CD4+ T cells) and cytotoxic T cells (CD8+ T cells)(84-86). Helper T cells, in turn, stimulate B cells to produce specific antibodies against the pneumococcal bacteria, enhancing opsonization and phagocytosis of the bacteria. Moreover, DCs secrete cytokines such as Interleukin-12 (IL-12), Interleukin-6 (IL-6), Tumor Necrosis Factor-alpha (TNF-α), Interleukin-1β (IL-1β), Interleukin-10 (IL-10) and Interferon-gamma (IFN-γ) that is crucial for shaping the immune response(84).

Together, through these mechanisms, DCs initiate and regulate the adaptive immune response, essential for the effective clearance of the pneumococcal infection.

1.4 Neonate Immune system

During early life, neonates have a reduced ability to elicit and control an immune response. Due to a lack of immune memory, new-borns are highly susceptible to infections. In 2018, 5.3 million children under the age of 5 died from infectious preventable diseases. In addition, pneumonia was the leading cause of death and nearly 50% of recorded deaths were in new-borns (87).

Neonates receive important immunity from their mother in the form of maternally derived antibody and other immunogenic components such as cytokines and antigen (88). The transfer of cytokines or antigen is less likely than antibodies, except in instances whereby the mother has an active infection during pregnancy or breastfeeding. This transfer of protection can occur across the placenta or via breastfeeding. Nursing alone provides important protection to offspring against both infectious and non-infectious diseases. This transfer of maternal antibodies is vital for infant immunity as the protection is stable for long periods of time and are specific to the pathogens they interact with (89).

IgG is the most abundant antibody class to cross the placenta in humans. The crossing of IgG is mediated by neonatal Fc receptors and evidence has shown that IgG transfer is dependent on the concentration of maternal IgG during pregnancy. Preferential transport occurs for IgG1, followed by IgG4, IgG3, and IgG2. Breastmilk adds additional immune benefits for offspring and consists of many nutrients, lactoferrin, IgA antibodies as well as maternal B and T cells (90). Breastfeeding has been shown to decrease the risk of respiratory tract infections and breastfeeding by stimulating infant immune system by anti-

idiotypic antibodies and the uptake of lymphocytes which may contribute to long term protection in infants (2).

1.5 Aim of this thesis

This project will address the following questions:

1. When is the appropriate time to vaccinate a mother (dam) to elicit the highest antibody titres and greatest vaccine induced cellular immune response?
2. Does pregnancy have an effect on vaccine efficiency?
3. Does maternal *S. pneumoniae* vaccination using PCV13 transfer passive and or active immunity against *S. pneumoniae* to the offspring?
4. Do the effects seen differ in an allogeneic setting?
5. Does IL-4 play a role in transfer of protection?

Chapter 2: Materials and methods

2.1. Bacterial growth conditions and storage

TiGR4 (*S. pneumoniae* serotype 4 strain) and T4P2 (bioluminescent derivatives of *S. pneumoniae* serotype 4 strain, TIGR4) were streaked and grown on blood agar base (BAB) agar plates supplemented with 5% horse blood and antibiotics (strain dependent). Optochin discs were placed on streaked areas to ensure stocks were free of contamination and bacteria were grown for a maximum of 16 hours at 37°C in a static incubator. *S. pneumoniae* was inoculated aseptically in 10mL of brain heart infusion (BHI) broth supplemented with antibiotic when applicable. Strains were grown statically in a 37°C water bath until an OD_{600nm} of O.6 was reached. The cultures were centrifuged at 4000 rpm for 10 minutes, the supernatant discarded, and the pellet resuspended in sterile BHI supplemented with 15% sterile glycerol. 1 mL aliquots were prepared and stored at -20°C for 24 hours. Glycerol stocks were streaked on BAB plates supplemented with 5% horse blood and optochin discs were applied to ensure glycerol stocks were free of contamination, thereafter glycerol stocks were moved to -80°C for long term storage.

2.1.1 Viability counting of *S. pneumoniae* glycerol stocks

After glycerol stocks were cleared for contamination, stocks were thawed on ice. 20 µL of glycerol stocks were mixed with 180 µL of sterile phosphate buffered saline (PBS) and used to make serial 10 fold dilutions from 10^{-1}-10^{-6} in a 96 well round bottom plate. A BAB plate was divided into 6 equal parts and 3 X 20 µL of each serial dilution was spotted in one section of a BAB plate supplemented with 5% horse blood. Plates were left to dry in

aseptic conditions and incubated overnight at 37°C. After 16 hours, dilution factors with colonies between 30 and 100 were chosen. colony forming units/ml (CFU/ml) were calculated according to Equation 1. These stocks were used for further experiments.

Number of Colonies (Spot 1 + spot 2 + spot 3) = N

$$\textbf{Average of three spots } (\mathbf{A}) = \frac{\mathbf{N}}{\mathbf{3}}$$

$$\mathbf{A\ X\ 50 = Number/ml}$$

Number/ml X dilution factor = CFU/ml

Equation 1: Equation used to calculate the CFU/ml of S. pneumoniae glycerol stocks.

2.1.2 Bacteria Antigen preparation

S. pneumoniae was inoculated aseptically in 10mL (in triplicate) of Brain heart infusion (BHI) broth supplemented antibiotic if need be. Strains were grown statically in a 37°C water bath until an OD_{600nm} of O.6 was reached. The cultures were centrifuged at 10 000 rpm for 10 minutes, the supernatant discarded, and the pellet resuspended in 1 mL of RIPA lysis buffer containing protease inhibitor (Sigma Aldrich). Triplicate tubes were combined into one tube and centrifuged at 10 000 rpm for 10 minutes. Supernatants were collected and separated into 500 µL aliquots and stored at 4°C. Protein concentrations were quantified by bicinchoninic acid (BCA) assay (Pierce™, Thermo Scientific) and antigen was used for coating antibody ELISA plates **(section 2.6.1)**

2.1.3 Haemolytic Assay

$1X10^9$ CFU, determined from viability counting **(Section 2.1.1),** was plated in a round-bottomed 96 well plate and serially diluted in 1X PBS from $1X10^9$-$1X10^1$. In addition, 1X PBS and 10X Triton-X controls were added to the plate and 15% horse blood was added to each well. The plate was incubated for 1 hour at 37°C and following incubation centrifuged for 10 000rpm for 5 minutes. The supernatants were transferred to a new plate and absorbances were measures at 540 nm. Total cell lysis was measured by the absorbance of each sample and expressed as a percentage of the Triton-X control absorbance.

2.2. Animal work

2.2.1 Mice experimental procedures, animal unit and ethics

All experiments were carried out in accordance with protocol 019/031 approved by the Faculty of Health Sciences Animal Ethics Committee from the University of Cape Town and all experiments were performed by SAVC (South African Veterinary Council) accredited animal technicians. Mice were bred and housed in specific pathogen–free conditions at the Animal Unit at the Faculty of Health Sciences (FHS) of the University of Cape Town (UCT), South Africa. All experimental mice used were between 10 days and 11 weeks of age with age-matched littermate controls, where appropriate. Mice were killed by halothane inhalation and death was confirmed either by cardiac puncture or cervical dislocation.

2.2.2 Immunization

BALB/cJ mice (Balb/C) and C57BL/6J mice (C57BL/6) were purchased from Jackson Laboratory and maintained at the University of Cape Town, Department of Pathology for experiments. 7-week-old (W/O) Balb/C female mice were vaccinated with the *pneumococcal* conjugate vaccine Prevnar13 (PCV13) **(Table 1).**

Table 1: Concentration and route of vaccinations

Vaccine	Abbreviation	Route of Vaccination	Concentration (dams)
Pneumococcal conjugate vaccine	PCV13	Intraperitoneal (I.P)	0.224µg

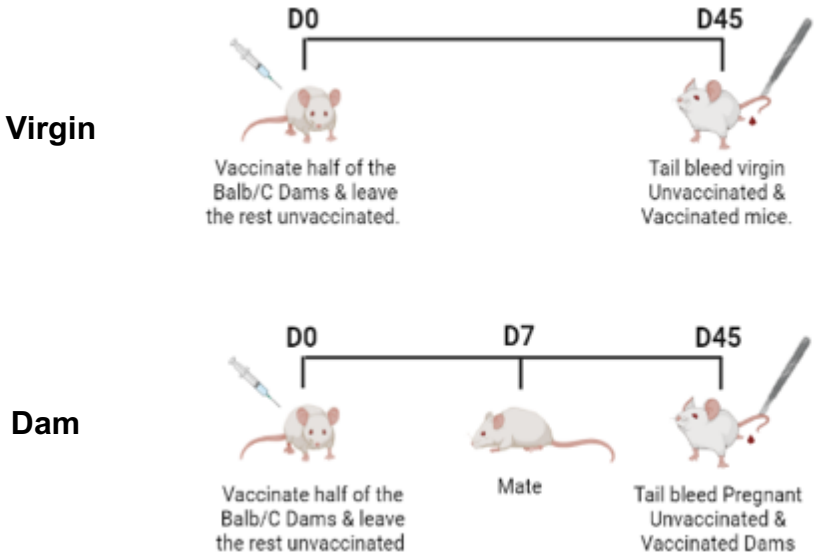

Figure 2.1: Vaccination and tail bleed model in virgin and dams.
At 7 weeks of age female Balb/C mice were either left unvaccinated or vaccinated intraperitoneally with PCV13. Mice that were not mated were classified as virgin mice while mice mated were classified as dams. Virgin and Dams were tail bled at day 45 for antibody detection using ELISA.

2.2.3 Pneumococcal challenge

Glycerol stocks of *pneumococcal* strains **(Table 2)**, of known concentration were thawed on ice and centrifuged at 8000 rpm for 10 minutes to pellet the bacteria. The supernatant was removed and the pellet was resuspended in an equal volume of cold sterile 1X PBS. Once resuspended, bacteria were kept on ice and aliquoted accordingly to concentrations needed for desired experimental procedures.

Table 2: Names, concentration and route of vaccinations

	Description	Antibiotic resistance	Inoculum concentration
TiGR4	Serotype 4 strain	N/A	$1X10^7$
T4P2	Serotype 4 TIGR4 strain with lux genes inserted in SP_1886 under the control of promoter P2.	Kanamycin	$1X10^7$

2.2.3.1 Intranasal (I.N) challenge

Mice were anaesthetized via I.P with 150 µL of appropriate anesthetic [1.2 mL of ketamine and 0.8 mL of xylavet added to 8 mL of 1X sterile PBS] and monitored until they showed signs of unconsciousness (i.e., limb movement reflex had been lost). Mice were infected with $1x10^7$ CFU in 10 µl into each of the nasal flares of 7 week old offspring. The anaesthetized mice were monitored until they regained consciousness.

2.2.4 Tail bleeds

Mice were warmed using an infra-red light to promote tail vein vasodilation. Mice were restrained using a restraining tube and a small incision in the tail vein or artery was performed and a 25G needle was used to draw a maximum of 73µl of blood **(Equation 2)**. Blood flow was stopped by applying pressure on the blood sampling site for approximately 30 seconds or until the bleeding stopped.

An average mouse has approximately 58.5 mL of blood per kg therefore 58.5mL x 0.025kg (average weight of a mouse) = 1.46mL of blood in a mouse. For all mice we will take a maximum of 5% of blood which is approximately 73

Equation 2: Equation used for tail bleed blood withdrawal.

2.2.5 Syngeneic model

7 W/O female wild type (WT) BALB/c mice were mated with WT BALB/c males. One male WT BALB/c was placed in a cage with 3-4 females and after one week the male was removed. Females were weighed routinely to measure weight gain and due to these scores, pregnancy was confirmed by day 12. Once pregnancy was confirmed, females were considered to be dams and moved to cages with a maximum of 2 dams. Dams gave birth approximately 21 days after fertilisation. Once offspring were born, they were observed on a daily basis. Offspring were weaned at 3 weeks of age and separated from their mothers according to sex. 7 W/O offspring were infected I.N with $1X10^7$ T4P2 CFU and culled 48 hours post infection (P.I) **(Figure 2.2)**.

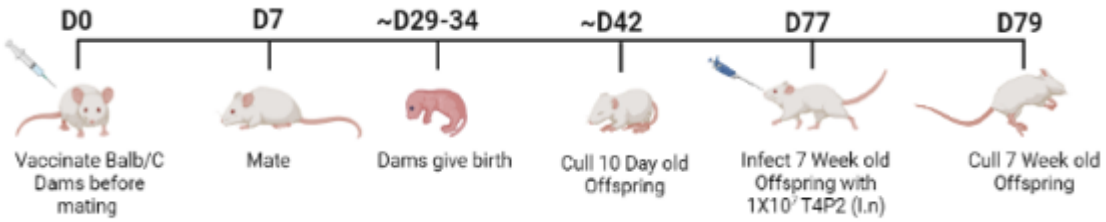

Figure 2.2: The Syngeneic maternal vaccination experimental model.
At 7 weeks of age female Balb/C mice were either left unvaccinated or vaccinated intraperitoneally with PCV13 one week before mating. These females were then mated with Balb/C males. At approximately day 30, offspring were born and 10 days later 3-5 offspring were culled to collect blood and breastmilk pellets. At 3 weeks of age, the remaining offspring were weaned and separated according to sex. Once offspring were 7 weeks of age, half were infected with $1X10^7$ T4P2 and culled 48 hours later.

2.2.6 Allogeneic model

7 W/O female WT or IL-4R$\alpha^{-/-}$ BALB/c (H-$2^{d/d}$) mice were mated with WT or IL-4R$\alpha^{-/-}$ C57BL/6J (H-$2^{b/b}$) males. One C57BL/6J male mouse was placed in a cage with 3-4 females and after one week the male was removed. Females were weighed routinely to measure weight gain and due to these scores, pregnancy could be confirmed by day 12. Once pregnancy was confirmed, females were considered to be dams and moved to cages with a maximum of 2 dams. Females gave birth approximately 21 days after fertilisation. Heterozygous offspring (H-$2^{b/d}$) were born and monitored on a daily basis. Offspring were weaned at 3 weeks of age and separated from their mothers according to sex. At 7 weeks of age, H-$2^{b/d}$ offspring were either vaccinated with PCV13 before mating or left unvaccinated. H-$2^{b/d}$ offspring were mated with WT or IL-4R$\alpha^{-/-}$ H-$2^{b/b}$ males which resulted in both H-$2^{b/d}$ and H-$2^{b/b}$ offspring. 4 W/O Offspring were tail bled and blood was processed and stained for flow cytometry to determine the genotype of each offspring. H-$2^{b/d}$ offspring were culled and H-$2^{b/b}$ offspring were reserved for when they reached 7W/O. half of the 7 W/O offspring were infected I.N with $1X10^7$ T4P2 CFU and culled 48 hours post infection (P.I)**(Figure 2.3)**.

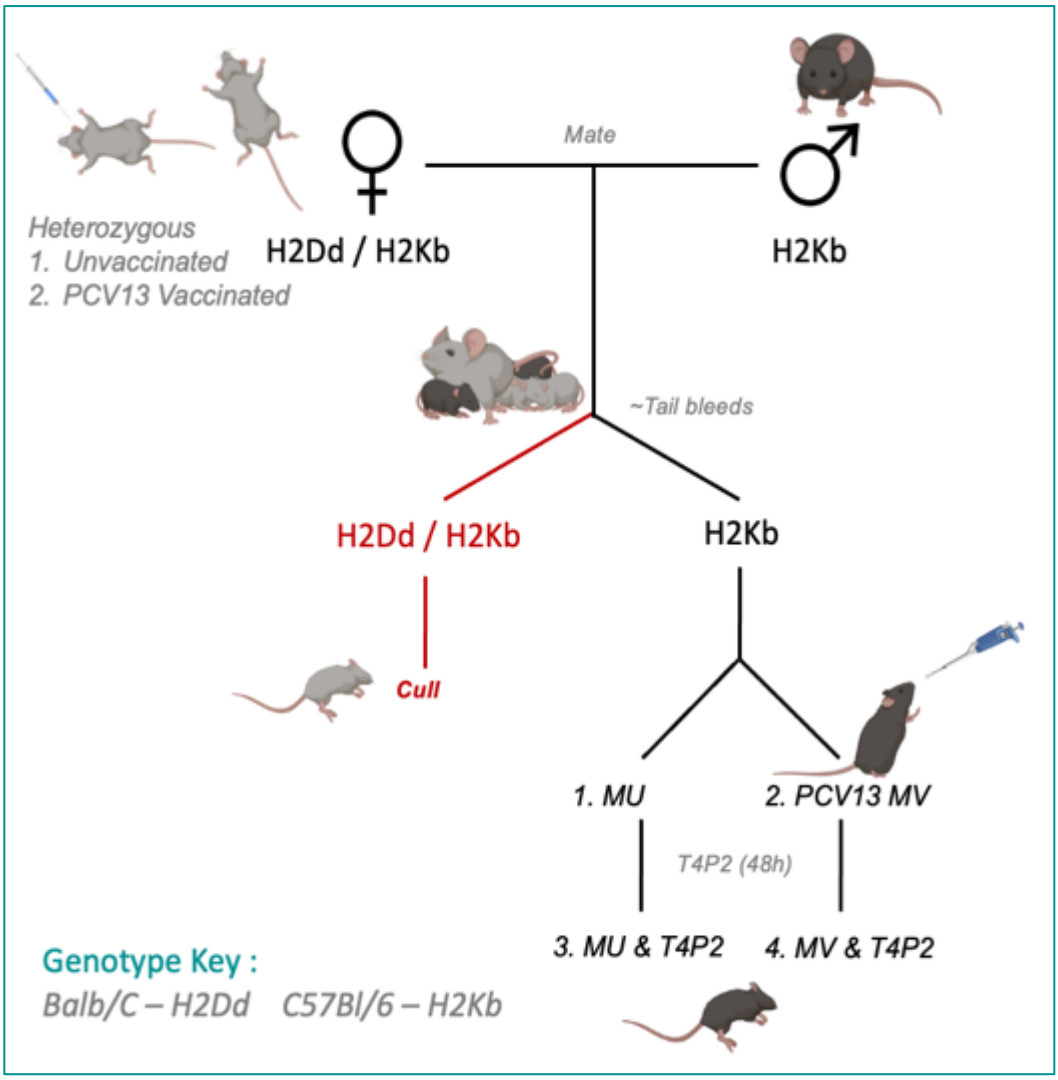

Figure 2.3: The Allogeneic maternal vaccination experimental model.
At 7 weeks of age, H-$2^{b/d}$ female mice were either vaccinated intraperitoneally with PCV13 before mating or left unvaccinated. These females were then mated with H-$2^{b/b}$ males resulting in H-$2^{b/d}$ and H-$2^{b/b}$ offspring. The H-$2^{b/d}$ offspring were culled and half of the H-$2^{b/b}$ offspring were infected with T4P2 intranasally and euthanized 48H post infection.

2.2.7 In *vivo* imaging system (IVIS)

7 week old maternally unvaccinated and vaccinated mice were infected with T4P2 via I.P and 24h later mice received D-luciferin solution (150 mg/kg) I.P. After 10 minutes, mice were immediately anesthetized in an oxygen-rich induction chamber with 2% isofluorane. Mice were placed in the nose cone delivery device to keep the mice anesthetized during image acquisition (IVIS 100; Xenogen). Mice were imaged for 5 minutes, images were displayed using the same settings in Living Image software to allow for consistency between experimental groups. Mice were monitored for at least 5 minutes after imaging to make sure mice regained consciousness and normal activity.

2.2.8 Experimental End point

Offspring were culled 48 hours after an intranasal challenge and cardiac punctures were performed to collect peripheral blood in serum separation tubes. Bronchoalveolar lavage's (BAL), lungs, spleens and bone marrows were collected under sterile conditions.

2.3. Cell and tissue Processing

2.3.1 Breastmilk pellets

Breastmilk pellets were isolated from the stomachs of 10 day old offspring and placed in 1 mL of 1X PBS. Breast milk pellets were passed through a 70 μM filter and the resuspended sample was centrifuged at 4000 rpm for 5 minutes. Supernatants were collected and stored at -20°C for antibody ELISA analysis.

2.3.2 Axillary and Illiac lymph nodes

The axillary and illiac lymph nodes were located, and excess fatty tissue was removed. The lymph nodes were placed in 1 mL Roswell Park Memorial Institute (RPMI) 1640 and carefully passed through a 40 μM filter to create a single cell suspension. Single cell suspensions were centrifuged at 4000 rpm for 5 minutes and resuspended in RPMI 1640 with 10% Foetal bovine serum (FBS) and temporarily stored on ice in preparation for cell staining for flow cytometry.

2.3.3 Bronchiolar Lavage

The bronchioles were flushed with 0.8 mL of sterile 1X PBS. The flushed fluids were collected in an eppendorf tube whereby 0.7 mL was processed for Flow cytometry and ELISA while 0.1 mL was aliquoted for bacterial viability counting.

2.3.3.1 Bacterial viability counting

The BAL was processed according to the method described in **Section 2.1.1.** BAL samples were plated in triplicate from neat to 10^{-4}, serially diluted 10-fold in sterile 1X PBS in a 96 well round bottom plate.

2.3.3.2 Flow cytometry and ELISA

0.7 mL of the BAL was centrifuged at 4000 rpm for 5 minutes. The supernatants were transferred and aliquoted into smaller volumes to avoid multiple thawing cycles. The supernatants were later processed according to **section 2.6.1** to perform antibody ELISAs. The BAL pellets were collected and further processed for flow cytometry according to **section 2.5**. Samples were stored at -20°C for short and -80°C for long term storage.

2.3.4 Blood

Blood was collected in serum separation tubes and 20 µL of each sample was transferred to 96 well round bottom plates to perform viability counting as explained in **section 2.1.1**. The remaining blood was centrifuged at 10000 rpm for 5 minutes to separate serum and red blood cells. Serum was collected and further aliquoted into smaller volumes to avoid multiple thawing cycles. Serum was stored at -20°C for short and -80°C for long term storage.

2.3.5 Lung and spleen

The lungs were removed from mice immediately after being culled and placed in 2mL RPMI 1640. The lungs were carefully passed through a 40 µM filter to create a single cell suspension. The cell suspensions were centrifuged at 4000 rpm for 5 minutes and cell pellets were incubated with 0.9 mL of Ammonium-Chloride-Potassium (ACK) lysis buffer (Gibco – A10492-01) for 5 minutes to remove red blood cells. Cells were centrifuged at 4000 rpm for 5 minutes and resuspended in RPMI 1640 with 10% Foetal bovine serum (FBS) and temporarily stored on ice in preparation for cell staining for flow cytometry. The cell concentration was established under a microscope using a haemocytometer **(section 2.5)**.

2.3.6 Bone Marrow

Cells from the bone marrow were obtained by cutting the off the ends of both the femur and tibia of the rear legs of the mouse and flushing the marrow out using 2 mL RPMI 1640 and a 25G needle. Cells were passed through a 40 µM filter to create a single cell suspension. The single cell suspensions were centrifuged at 4000 rpm for 5 minutes and pellets were resuspended in 0.9 mL ACK Lysis Buffer for 3 minutes to remove red blood cells. Cells were centrifuged at 4000 rpm for 5 minutes and resuspended in RPMI 1640 with 10% FBS and temporarily stored on ice. Cells were counted using a haemocytometer and processed further for flow cytometry **(section 2.5)**.

2.4. In vitro cell culture

2.4.1 Restimulation

Bone marrow single cell suspensions in complete RPMI 1640 media were plated at $1x10^7$ cells per well in 96 well round bottom plate. Cells were incubated in a 37°C water jacket CO_2 Incubator for 24 hours. The plate was centrifuged at 400 g for 5 minutes and supernatants were collected and aliquoted into eppendorf's. Samples were stored at -20°C for short term storage and -80°C for long term storage. Samples were used for antibody ELISA detection.

2.5. Flow cytometry

Flow cytometry was used to analyse the BAL, lung, spleen and bone marrow of offspring in order to quantify and explore different immune cell populations. Single cell suspensions were prepared and 200 µl of each sample was transferred to a 96 well plate. The plate was centrifuged at 400 g for 5 minutes and media was removed carefully by inverting the plate. The cells were resuspended in 25 µl antibody master mix containing 2% Rat serum, 1% anti-FcRγII/III and the required antibodies diluted to the correct concentration in FACS buffer for 30 minutes on ice. Cells were further processed for intracellular staining **(section 2.5.1)** or plates were centrifuged at 400 g for 5 minutes and the staining mix was removed by carefully inverting the plates. Cells were resuspended in 150 µl of FACS buffer and transferred to FACS tubes in preparation for acquisition.

2.5.1 Intracellular staining

Cells were fixed with 100 µL 4% para-formaldehyde (PFA) for 20 minutes in the fridge, covered in foil due to light sensitivity. Cells were washed twice with 1X PBS and centrifuged at 400 g for 5 minutes. Cells were stained with intracellular antibodies **(section 8.1.1)** in 50 µL of perm wash for 45 minutes at 4°C covered in foil. Samples were centrifuged at 400g for 5 minutes and washed with 1X PBS. Cells were resuspended in 150 µL FACS buffer and transferred to FACS tubes, ready for cell acquisition **(section 2.5.2)**.

2.5.2 Cell acquisition and analysis

The cell samples were acquired on a BD LSR Fortessa (BD Biosciences). The data was collected by using DIVA© BD (San Diego, CA) and analysed using FlowJo© (Treestar Ashland, OR). Appropriately stained compensation beads and unstained controls were used to run cell compensation to account for spectral overlap between fluorochrome emissions. For all cell gating strategies, refer to Appendix A **(Section 8.2.1)**.

2.6. Enzyme-linked immunosorbent assay (ELISA)

2.6.1 Antibody ELISA

BAL, serum, breastmilk and bone marrow supernatant antibody levels were determined by ELISA. For all solution and antibody details for cytokine ELISAs, refer to Appendix A **(Section 8.1.1)**.

A 96 flat bottom plate (Nunc, Maxisorp) was coated with 10 µg/ml of Total IgG, IgA, Prevnar13 or bacteria antigen **(Table 3)** in 1X PBS and incubated overnight at 4°C. Post incubation, plates were washed 3 times with wash buffer. 200 µl of blocking buffer was added to each well and left to incubate at 37°C for 2 hours. Wells were washed twice with wash buffer. Serum processed in **section 2.3.2** was added to the first well and serially diluted in dilution buffer and plates were incubated overnight at 4°C **(Table 4)**.

Plates were washed four times with wash buffer and 100 µL secondary detection in antibody diluted in dilution buffer was added to each well and incubated for 1 hour at 37°C. The plates were washed five times with wash buffer followed by the addition of 100 µL of SigmaFAST p-Nitrophenol phosphate (pNPP) (Sigma Aldritch) to each well. The plates were developed for 1 hour at 37°C and developed plates were read at 405 nm using a SpectraMax ABS Plus plate reader (Molecular Devices). Plates were placed in the fridge overnight and read after 16 hours at 405 nm. Relative antibody titres were calculated at the dilution where ELISA curves were approximately parallel.

2.6.2 Cytokine ELISA

Cytokine levels were quantified from supernatants taken from lung or spleen homogenates. For all solution and antibody details for cytokine ELISAs, refer to Appendix A **(Section 8.1.1)**. Briefly, cytokine levels were quantified by coating a 96 well flat bottom plate (Nunc, Maxisorp) in 1 x PBS overnight at 4°C **(Table 8.1)**. Plates were washed 3 times with wash buffer and blocked with 200 µL blocking buffer. The samples were added in duplicate. Recombinant protein standards were used to generate a standard curve and diluted serially at 1/2 across 11 wells. Plates were incubated overnight at 4°C. Plates were washed 4 times and 100 µl biotinlyated secondary antibody in dilution buffer **(Table 8.1)** was added to each well. Plates were incubated for 37°C for 1 hour. Plates were washed 4 times and 100 µl streptavidin-linked horseradish peroxidase (HRP) was added at a dilution of 1/5000 in a volume of 50 µl per well and incubated for 1 hour at 37°C. After washing, plates were developed with 50 µl TMB Microwell Peroxidase Substrate System (KPL), and once the titration of the standard curve was clearly visible, the reaction was stopped with 25µl 1M H_3PO_4 and the signal was read at a wavelength of 450 nm against a reference measurement of 540nm on a VersaMax microplate reader (Molecular Devices Corporation, Sunnyvale, CA). Cytokine concentrations from samples were determined from the standard curve.

2.7. Statistical analysis

The results below are expressed as either individual mice/datapoints or group means ± standard deviation (SD). One-tailed Mann-Whitney T-tests or Kruskal-Wallis tests were performed to identify P values and significance between groups. Significance was achieved if the P value was less than 0.05. ($p<0.05$ = *, $p<0.01$ = **, $p<0.001$ = ***). Statistical anals were performed using GraphPad Prism V6 (La Jolla, CA).

Chapter 3: The impact of PCV13 vaccination on pregnant vs non-pregnant Dams.

3.1. Introduction

In a non-pregnant environment, the immune system is generally in a state of balance, with both T helper 1 (Th1) and T helper 2 (Th2) responses coexisting to effectively respond to various pathogens and challenges(91, 92). During pregnancy, the maternal immune system undergoes significant changes to tolerate the developing foetus, which is essentially a semi-allograft (foreign to the mother)(93). These changes involve a shift toward a more anti-inflammatory or regulatory state to prevent the rejection of the fetus(94). This shift is often referred to as a Th2 bias, indicating a dominance of type 2 helper T-cell responses, which is an important immunological signature during pregnancy and plays a central role in influencing early-life immune programming(95, 96).

Understanding the optimal time to vaccinate a mother, whether this is before or during pregnancy, is essential to establish when maximum immune protection in the mother can be achieved. Elevated immune control in a mother is essential as this could influence the potential to transfer protection to offspring. The protection transferred must not only feature passive immunity but also a long lasting active immune response which can be crucial for fighting off severe infections.

Studies have shown that maternal vaccination (MV) is predominantly administered in the third trimester due to changes from a Th1 to a Th2 immune environment(15, 16). This is due to a more tolerant immune environment whereby B2 Cells are more involved in producing regulatory B cells and the regulatory cytokines(49, 97). In addition, B2 cells produce high affinity antibodies and generate immunological memory which is well suited for vaccination(17). During vaccination B2 cells undergo multiple rounds of selection to produce antibody secreting cells and therefore MV in this environment, could lead to more high affinity antibodies specific to the antigen produced from vaccination(17, 49).

In order investigate if PCV13 could be used as a MV, understanding how pregnant mice and virgin mice (not pregnant) respond to PCV13 vaccination is fundamental. This will help to understand how pregnancy may influence maternal vaccination efficiency in terms of both passive antibody transfer and other mechanisms, such as maternal microchimerism (a major focus of this study).

In this chapter, we aim to investigate if the optimal time to vaccinated mothers is before or after mating (during pregnancy). In addition, we aim to see if pregnancy affects vaccine efficiency in virgin (not mated) and dams (mated and pregnant). Finally, we aim to investigate the cellular differences due to PCV13 vaccination in virgin and dams.

3.2. Results

3. 2.1 PCV13 vaccination elicits higher antibody titres in dams vaccinated before mating.

7-week-old female BALB/c mice were either left unvaccinated or vaccinated intraperitoneally with PCV13. Females were either vaccinated one week before or one week after mating once pregnancy was confirmed. Mice that were mated were classified as dams while mice that were not mated were classified as virgin mice. **(Figure 2.1)**.

Serum was collected from unvaccinated/vaccinated dams and virgin mice 45 days post vaccination whereby serum was analysed using antibody ELISA's. PCV13 vaccinated dams had significantly elevated PCV13 specific-IgG and total IgG antibodies in serum. Moreover, the recorded antibody responses were significantly higher in dams vaccinated before mating **(Figure 3.1)**. Vaccinated dams demonstrated equivalent detection levels of PCV13 specific-IgG and total IgG antibodies in comparison to PCV13 vaccinated virgin mice, indicating that vaccine efficiency was not compromised due to pregnancy **(Figure 3.1)**. Therefore, protection associated antibody responses were present in dams vaccinated before pregnancy at equivalent levels to those seen in virgin vaccinated mice.

A. Total IgG and PCV13 IgG specific antibody titres in Dams.

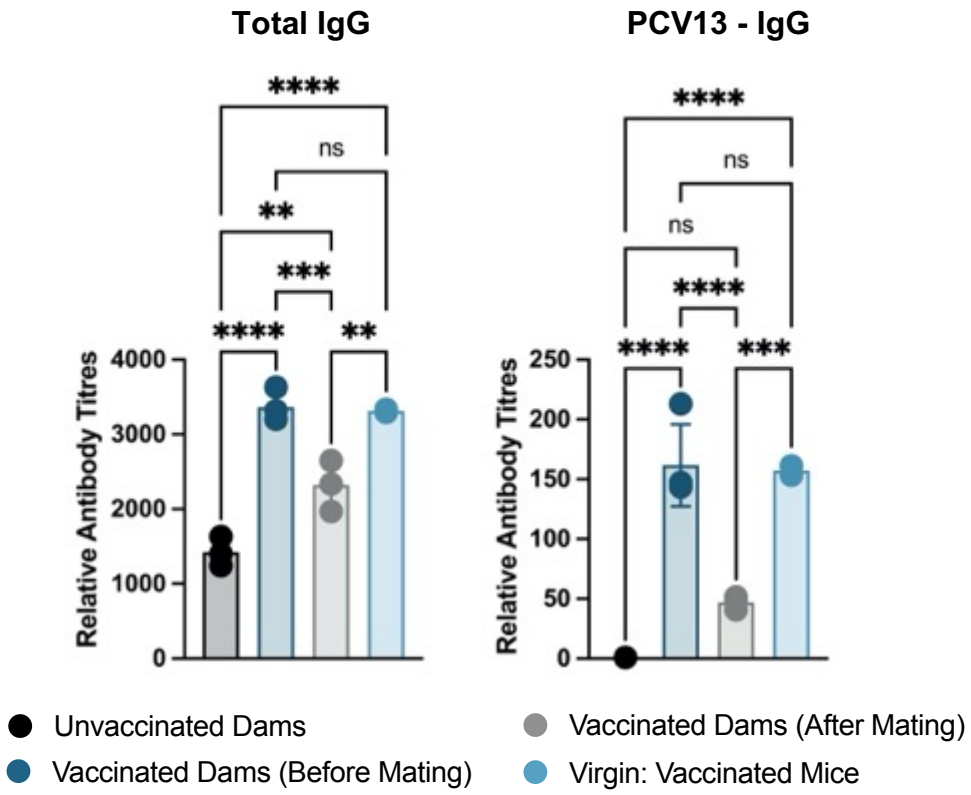

Figure 3.1: PCV13 vaccination elicits higher PCV13-specific antibody titres in dams vaccinated before mating and virgin vaccinated mice.
A. 7-week-old female BALB/c mice were un/vaccinated with PVC13 either before or after mating while female virgin mice were vaccinated. Tail bleeds were collected at 45 days post vaccination and serum analysed using antibody ELISA's specific for total IgG and PCV13-IgG. Data is representative of 2 equivalent experiments whereby n = 2-3 mice per group. Statistical analysis was performed using a Kruskal Wallis test. *$p \leq 0.05$; **$p \leq 0.01$, *** $p \leq 0.001$, **** $p \leq 0.0001$.

3. 2.2 PCV13 vaccination does not elicit differences in cell populations in the spleens of dams and virgin mice.

The immune profile of dams (pregnant) and virgin mice (Not pregnant) were investigated using flow cytometry. The effect of PCV13 vaccination was examined in the spleen, illiac and axillary lymph nodes in dams and virgin mice. $CD45^+$ immune cells were investigated in the spleens and no differences were observed in the numbers of $CD45^+$ immune cells between dams and virgin mice **(Figure 3.2)**.

A. Total $CD45^+$ immune cells in the spleen: dams vs virgin cell numbers

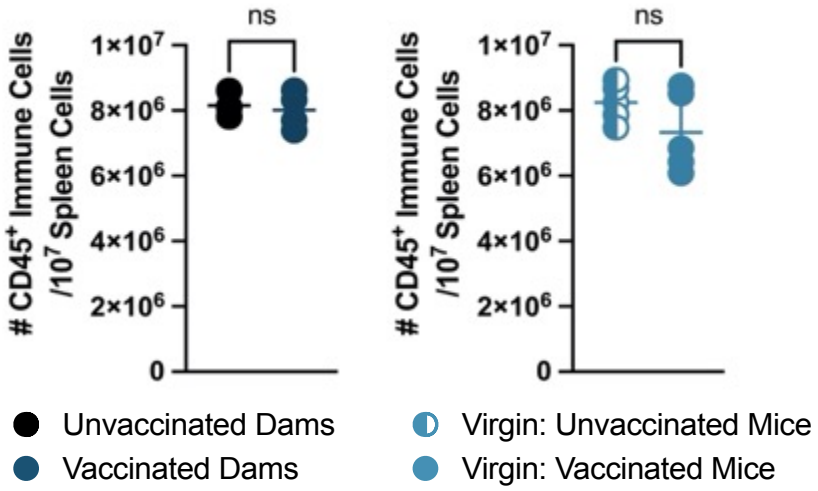

Figure 3.2: PCV13 vaccination does not alter $CD45^+$ immune cell populations in the spleens of dams and virgin mice.
A. 7-week-old female BALB/c mice were un/vaccinated with PVC13 before mating while female virgin mice were vaccinated. Spleens were processed into single cell suspensions and $CD45^+$ Immune cell populations were investigated using flow cytometry. Data is representative of 2 equivalent experiments whereby n = 2-3 mice per group. Statistical analysis was performed using a Kruskal Wallis test. *$p \leq 0.05$; **$p \leq 0.01$, *** $p \leq 0.001$, **** $p \leq 0.0001$.

Splenic B cells ($CD45^+$ $CD19^+$ $B220^+$) were investigated and no differences in B cell populations were observed between dams and virgin mice **(Figure 3.3)**. B cell subsets, namely $IgG1^+$ expressing B cells ($CD45^+$ $CD19^+$ $B220^+$ $IgG1^+$), $IgG2a^+$ expressing B cells ($CD45^+$ $CD19^+$ $B220^+$ $IgG2a^+$) and plasmoblasts ($CD45^+$ $B220^+$ $CD138^+$) were investigated between groups, however no significant splenic cell differences were observed in $IgG1^+$ expressing B cells and $IgG2a^+$ expressing B cells **(Figure 3.4).** Plasmoblast cell populations were elevated in dams however, cell numbers were reduced in virgin mice **(Figure 3.4)**. Interestingly, PCV13 vaccination had no effect on antibody and plasmoblast populations in dams or virgin mice.

A. Total CD19⁺ B220⁺ B cells in the spleen: dams vs virgin cell numbers

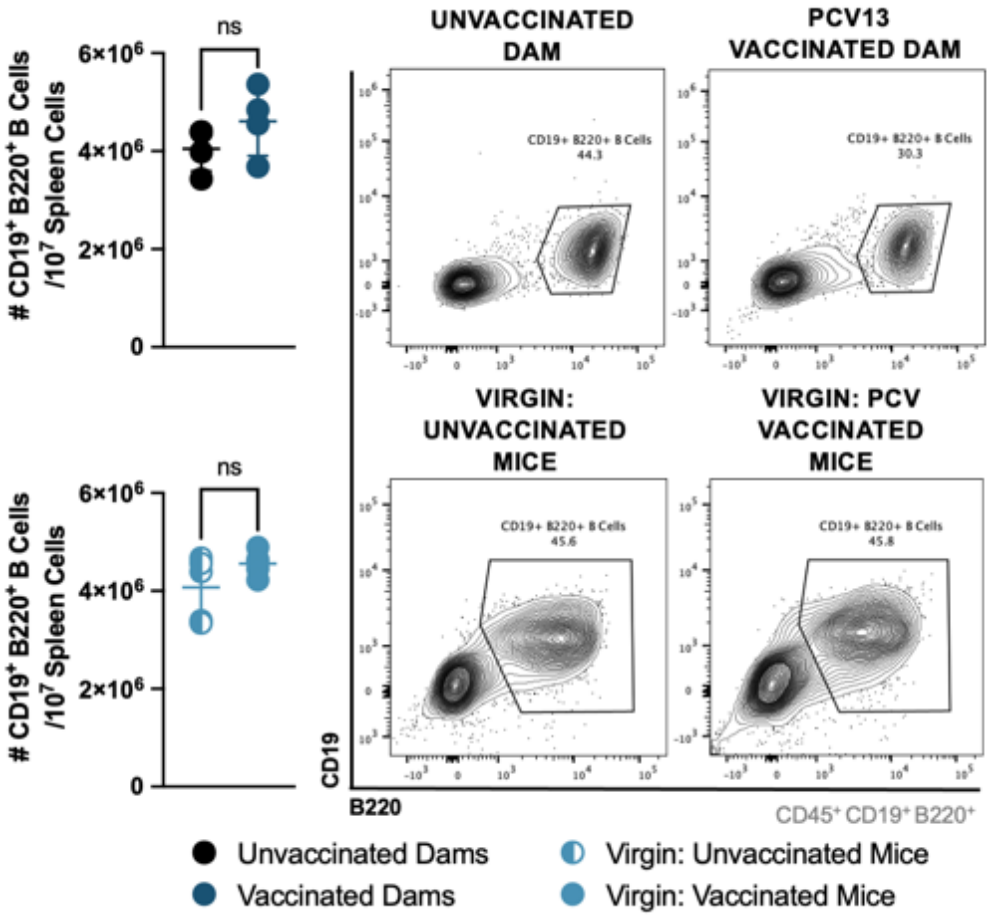

Figure 3.3: PCV13 vaccination does not alter B cell populations in the spleens of dams and virgin mice.

A. 7-week-old female BALB/c mice were un/vaccinated with PVC13 before mating while female virgin mice were vaccinated. Spleens were processed into single cell suspensions and stained to evaluate B cell ($CD45^+$ $CD19^+$ $B220^+$) populations using flow cytometry. Data is representative of 2 equivalent experiments whereby n = 2-3 mice per group. Statistical analysis was performed using a Kruskal Wallis test. *$p \leq 0.05$; **$p \leq 0.01$, *** $p \leq 0.001$, **** $p \leq 0.0001$.

A. Total IgG1⁺ and IgG2a⁺ expressing B cells and plasmoblasts in the spleen: dams vs virgin cell numbers

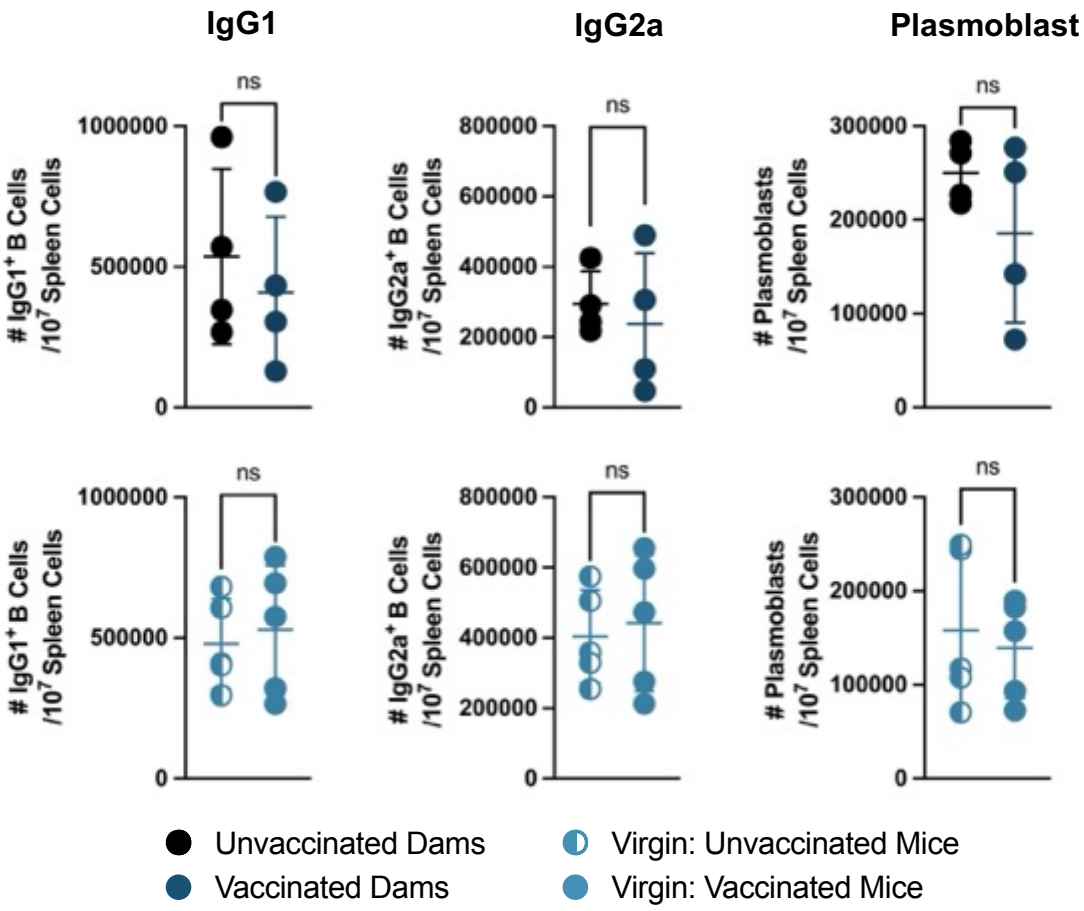

Figure 3.4: No differences in B Cell subsets were induced by vaccination between unvaccinated and vaccinated dams
A. 7-week-old female BALB/c mice were un/vaccinated with PVC13 before mating while female virgin mice were vaccinated. Spleens were processed into single cell suspensions and stained intracellularly to investigate IgG1 ($CD45^+$ $CD19^+$ $B220^+$ $IgG1^+$), and IgG2a ($CD45^+$ $CD19^+$ $B220^+$ $IgG2a^+$) expressing B cells and plasmoblast ($CD45^+$ $B220^+$ $CD138^+$) subsets using flow cytometry. Data is representative of 2 equivalent experiments whereby n = 2-3 mice per group. Statistical analysis was performed using a Kruskal Wallis test. *$p \leq 0.05$; **$p \leq 0.01$, *** $p \leq 0.001$, **** $p \leq 0.0001$.

T cell ($CD45^+$ $CD3^+$ $CD4^+$) populations were evaluated between dams and virgin mice. No differences were present between unvaccinated and PCV13 vaccinated groups **(Figure 3.5)**. The total number of T cells were reduced in virgin mice **(Figure 3.5).**

A. Total $CD3^+$ $CD4^+$ T cells in the spleen: dams vs virgin cell numbers

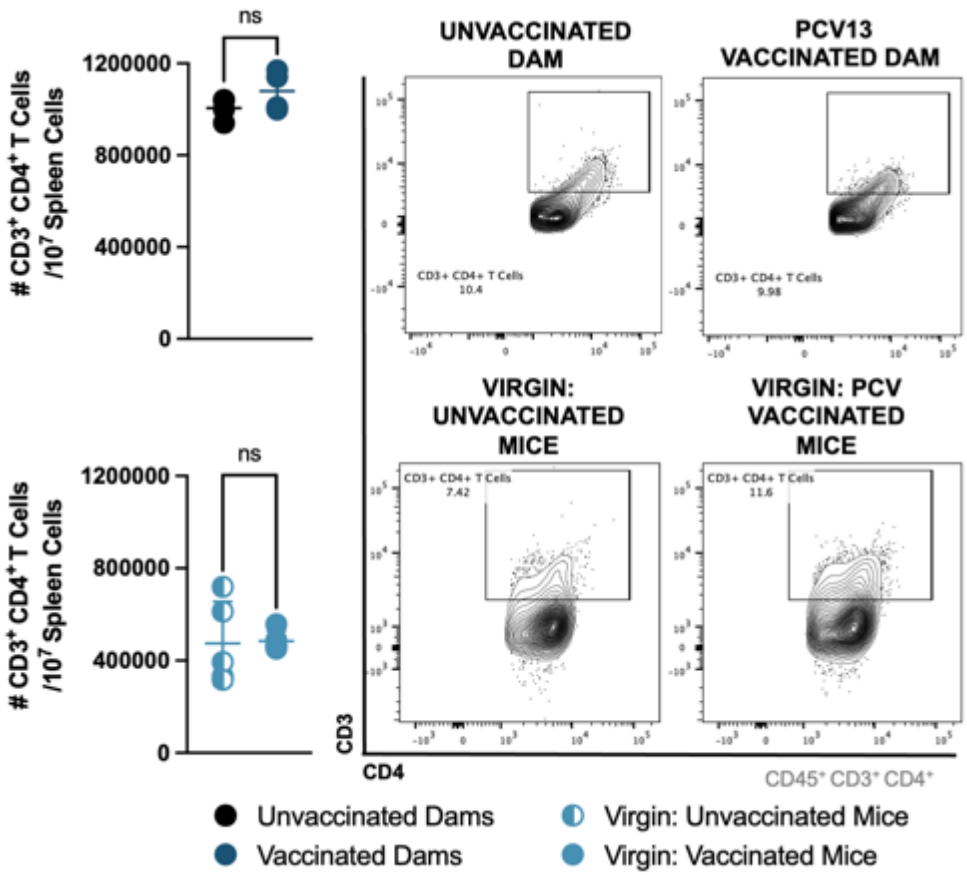

Figure 3.5: T Cell populations are reduced in the spleens of virgin mice.
A. 7-week-old female BALB/c mice were un/vaccinated with PVC13 before mating while female virgin mice were vaccinated. Spleens were processed into single cell suspensions and processed to evaluate T cell ($CD45^+$ $CD3^+$ $CD4^+$) populations using flow cytometry. Data is representative of 2 equivalent experiments whereby n = 2-3 mice per group. Statistical analysis was performed using a Kruskal Wallis test. *$p \leq 0.05$; **$p \leq 0.01$, *** $p \leq 0.001$, **** $p \leq 0.0001$.

Together this set of results indicate that PCV13 vaccination leads to no differences in overall B cells, $IgG1^+$expressing B cells and $IgG2a^+$ expressing B cells in the spleen. However, there were small differences observed in the plasmoblast populations between virgin mice and dams.

3.2.3 PCV13 vaccination elicits differences in IgG1$^+$ and IgG2a$^+$ expressing B cell populations in the illiac lymph nodes of dams and virgin mice.

The illiac lymph node was investigated to identify if PCV13 vaccination altered the immune profile. The CD45$^+$ immune cell populations were not altered in dams however there was a reduced number of immune cells in vaccinated virgin mice **(Figure 3.6)**.

A. Total CD45$^+$ immune cells in the illiac lymph nodes: dams vs virgin cell numbers

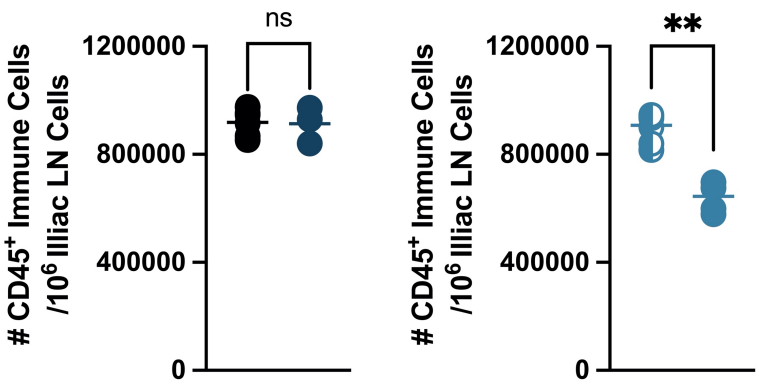

Figure 3.6: Decreased CD45$^+$ immune cell populations were identified in the illiac lymph nodes of virgin mice.
A. 7-week-old female BALB/c mice were un/vaccinated with PVC13 before mating while female virgin mice were vaccinated. The illiac lymph nodes were processed into single cell suspensions and stained to investigate CD45$^+$ Immune cell populations using flow cytometry. Data is representative of 2 equivalent experiments whereby n = 2-3 mice per group. Statistical analysis was performed using a Kruskal Wallis test. *$p \leq 0.05$; **$p \leq 0.01$, *** $p \leq 0.001$, **** $p \leq 0.0001$.

Vaccination elicited no differences in B cells ($CD45^+$ $CD19^+$ $B220^+$) in dams and virgin mice **(Figure 3.7)**. However, a reduction in B cell numbers were observed in vaccinated virgin mice **(Figure 3.7)**. Interestingly, vaccination caused a notable increase in $IgG1^+$ and $IgG2a^+$ expressing B cells in both dams and virgin mice **(Figure 3.8)**. Vaccination had no effect on plasmoblast populations however, plasmoblast numbers were slightly elevated in virgin mice **(Figure 3.8)**.

A. Total CD19⁺ B220⁺ B cells in the illiac lymph nodes: dams vs virgin cell numbers

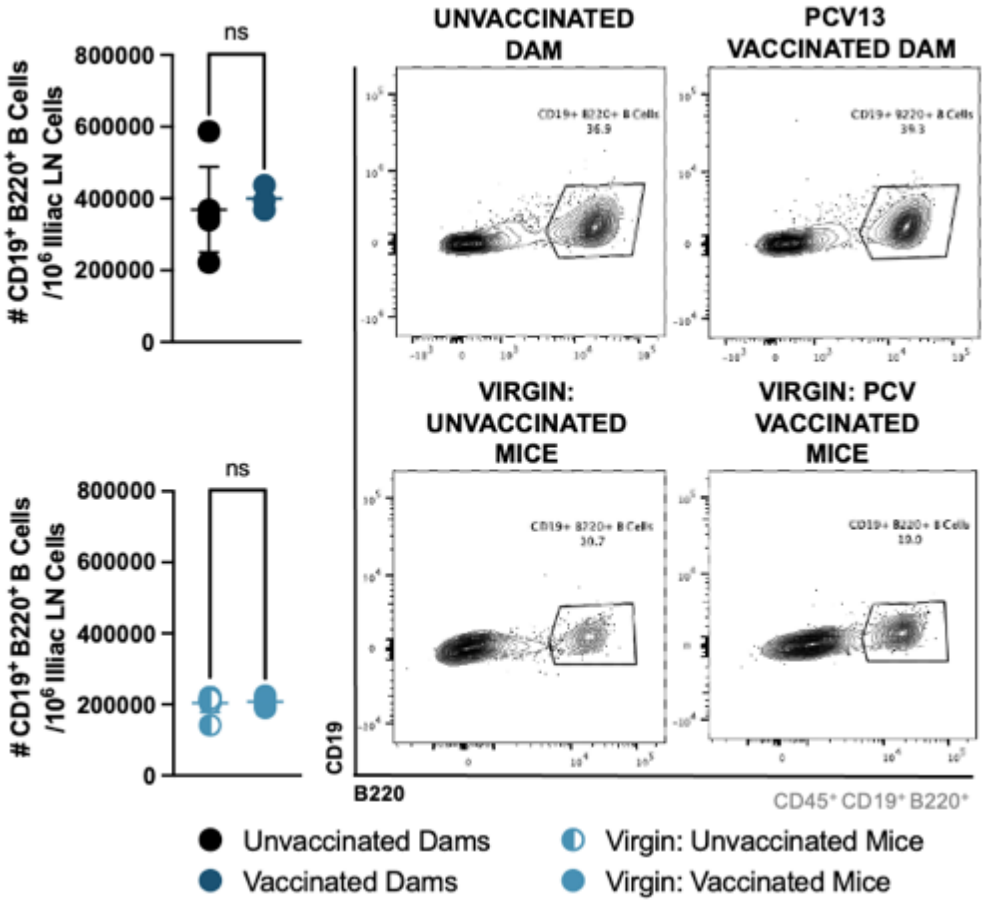

Figure 3.7: No difference in B cell populations were present in illiac lymph nodes of dams and virgin mice.
A. 7-week-old female BALB/c mice were un/vaccinated with PVC13 before mating while female virgin mice were vaccinated. The illiac lymph nodes were processed into single cell suspensions and processed to investigate B cell ($CD45^+$ $CD19^+$ $B220^+$) populations using flow cytometry. Data is representative of 2 equivalent experiments whereby n = 2-3 mice per group. Statistical analysis was performed using a Kruskal Wallis test. *$p \leq 0.05$; **$p \leq 0.01$, *** $p \leq 0.001$, **** $p \leq 0.0001$.

A. Total IgG1⁺ and IgG2a⁺ expressing B cells and plasmoblasts in the illiac lymph nodes: dams vs virgin cell numbers

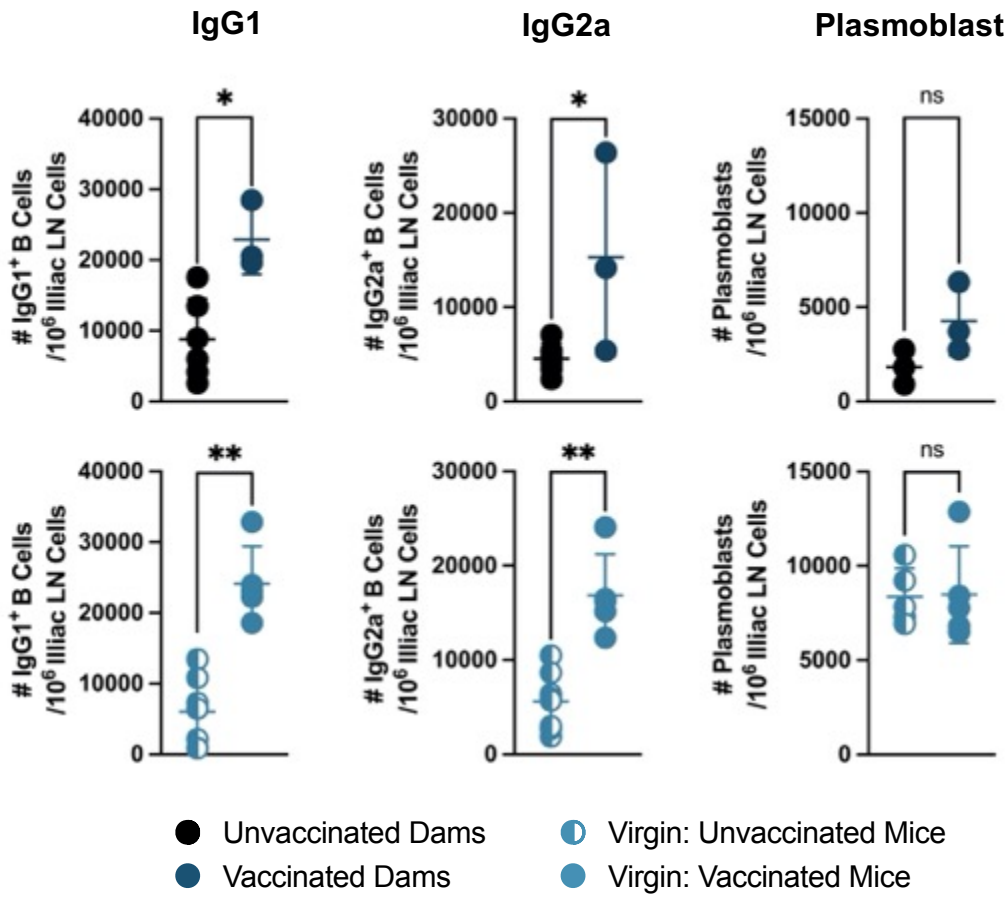

Figure 3.8: PCV13 vaccination results in increased IgG1 and IgG2a expressing B cells in the illiac lymph nodes of dams and virgin mice.
A. 7-week-old female BALB/c mice were un/vaccinated with PVC13 before mating while female virgin mice were vaccinated. Illiac lymph nodes were processed into single cell suspensions and intracellularly stained to investigate IgG1 ($CD45^+$ $CD19^+$ $B220^+$ $IgG1^+$) and IgG2a ($CD45^+$ $CD19^+$ $B220^+$ $IgG2a^+$) expressing B cells and plasmoblasts ($CD45^+$ $B220^+$ $CD138^+$) using flow cytometry. Data is representative of 2 equivalent experiments whereby n = 2-3 mice per group. Statistical analysis was performed using a Kruskal Wallis test. *$p \leq 0.05$; **$p \leq 0.01$, *** $p \leq 0.001$, **** $p \leq 0.0001$

T cell ($CD45^+$ $CD3^+$ $CD4^+$) populations were investigated, and no differences were observed between unvaccinated and vaccinated groups in the dams and virgins. A reduction was seen in the overall T cell populations between dam and virgin mice **(Figure 3.9)**.

A. Total $CD3^+$ $CD4^+$ T cells in illiac lymph nodes: dams vs virgin cell numbers

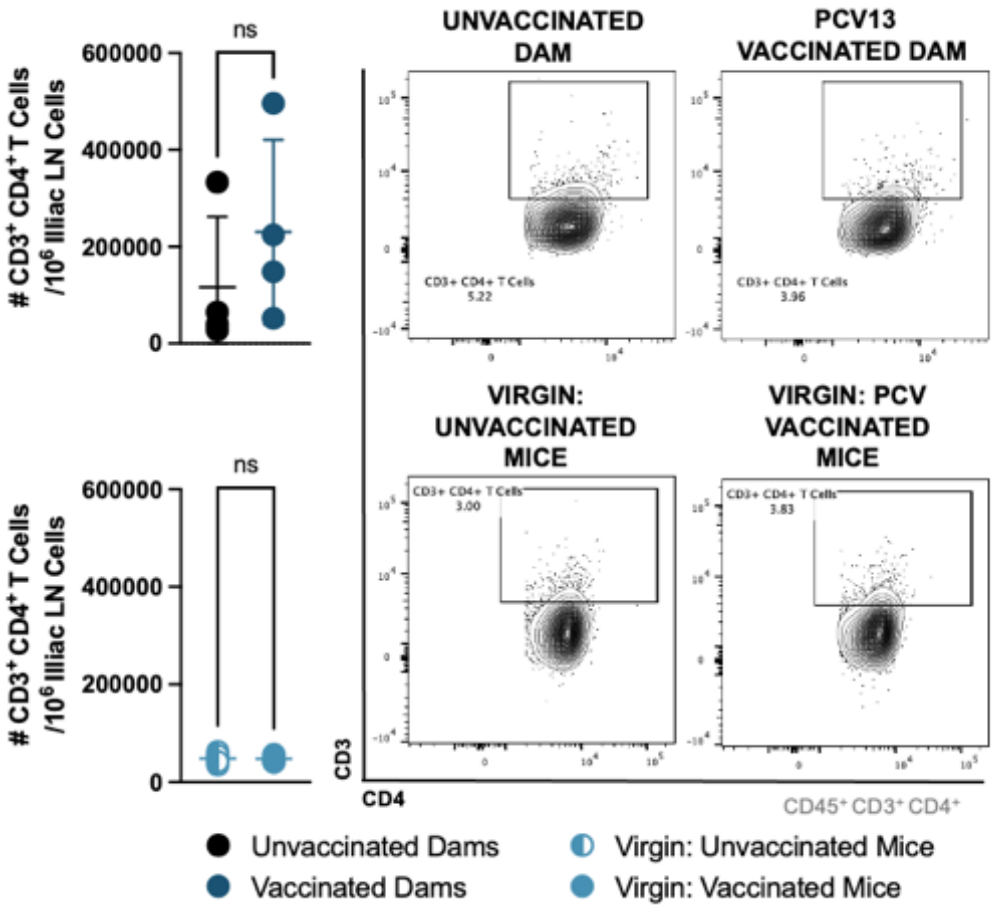

Figure 3.9: T Cell populations are reduced in the illiac lymph nodes of virgin mice.
A. 7-week-old female BALB/c mice were un/vaccinated with PVC13 before mating while female virgin mice were vaccinated. Illiac lymph nodes were processed into single cell suspensions and processed to evaluate $CD3^+$ $CD4^+$ T cell populations using flow cytometry. Data is representative of 2 equivalent experiments whereby n = 2-3 mice per group. Statistical analysis was performed using a Kruskal Wallis test. *$p \leq 0.05$; **$p \leq 0.01$, *** $p \leq 0.001$, **** $p \leq 0.0001$

3.2.4 PCV13 vaccination leads to increased IgG1$^+$ and IgG2a$^+$ B Cell populations in the axillary lymph nodes of virgin mice.

The axillary lymph node was explored to identify if PCV13 vaccination influenced the CD45$^+$ immune profile. The CD45$^+$ immune cell profile was not altered in dams however there was a reduced number of immune cells in vaccinated virgin mice **(Figure 3.10)**.

A. Total CD45$^+$ immune cells in the axillary lymph nodes: dams vs virgin cell numbers

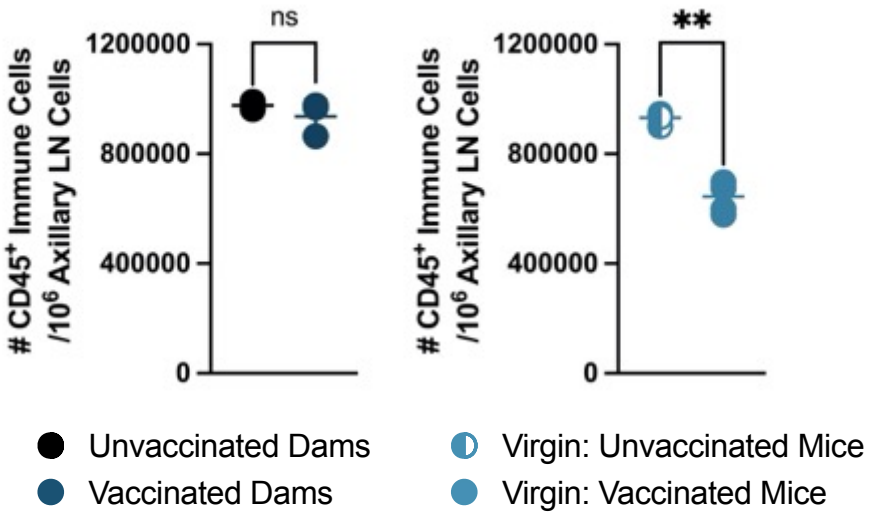

Figure 3.10: PCV13 vaccination results in decreased CD45$^+$ Immune cells in the axillary lymph nodes of virgin mice.
A. 7-week-old female BALB/c mice were un/vaccinated with PVC13 before mating while female virgin mice were vaccinated. The axillary Lymph nodes were processed into single cell suspensions and stained to investigate CD45$^+$ Immune cell populations using flow cytometry. Data is representative of 2 equivalent experiments whereby n = 2-3 mice per group. Statistical analysis was performed using a Kruskal Wallis test. *$p \leq 0.05$; **$p \leq 0.01$, *** $p \leq 0.001$, **** $p \leq 0.0001$

B Cell ($CD45^+$ $CD19^+$ $B220^+$) populations were investigated in the axillary lymph nodes and no differences were observed in unvaccinated and vaccinated dams. The same trend was observed in virgin mice, however overall B cell populations were reduced **(Figure 3.11)**.

No differences in $IgG1^+$ and $IgG2a^+$ expressing B Cells were present between unvaccinated and vaccinated dams **(Figure 3.12)**. However, $IgG1^+$ and $IgG2a^+$ expressing B cell populations were increased in vaccinated virgin mice **(Figure 3.12)**.
No differences were present in plasmoblast cell populations due to vaccination in dams and virgin mice, however an overall reduction in plasmoblast numbers were reduced in virgin mice. **(Figure 3.12)**.

A. Total CD19⁺ B220⁺ B cells in the axillary lymph nodes: dams vs virgin cell numbers

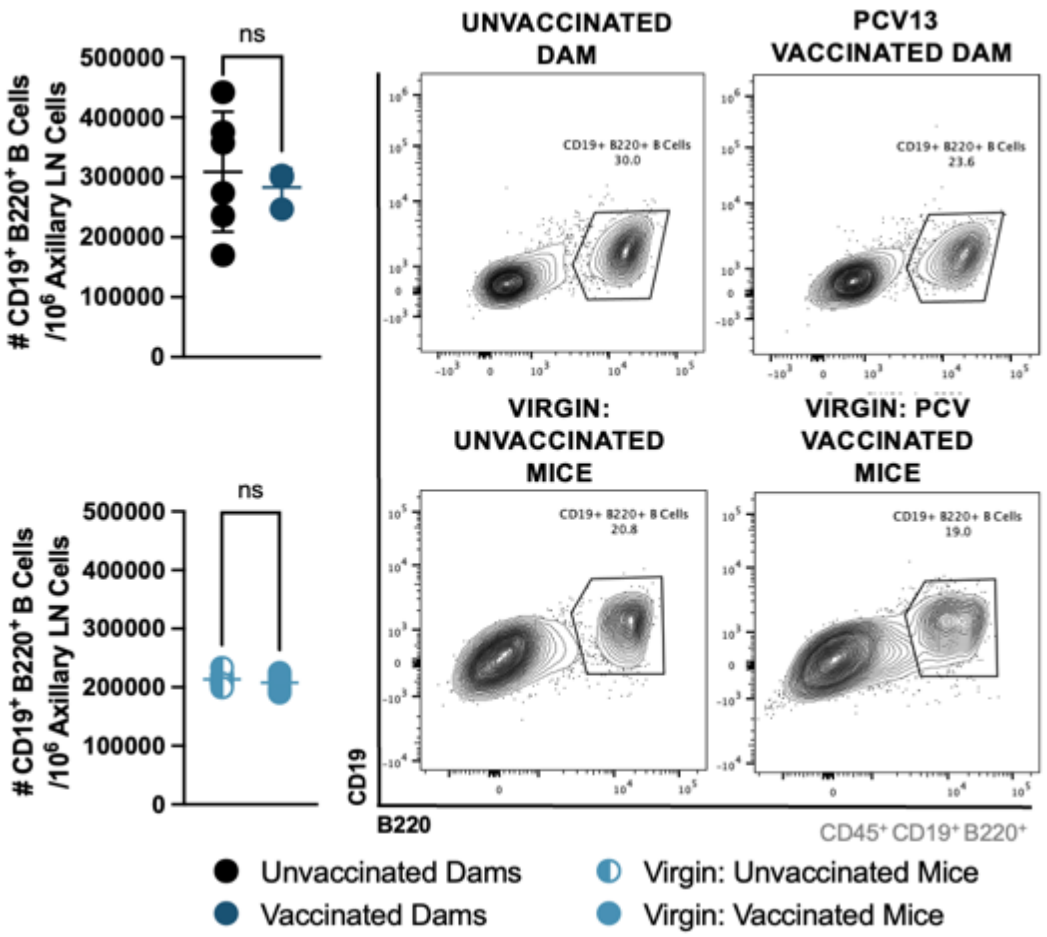

Figure 3.11: B Cell populations are reduced in the axillary lymph nodes of virgin mice.

A. 7-week-old female BALB/c mice were un/vaccinated with PVC13 before mating while female virgin mice were vaccinated. The axillary lymph nodes were processed into single cell suspensions and processed to investigate $CD45^+$ $CD19^+$ $B220^+$ B cell populations. Data is representative of 2 equivalent experiments whereby n = 2-3 mice per group. Statistical analysis was performed using a Kruskal Wallis test. *$p \leq 0.05$; **$p \leq 0.01$, *** $p \leq 0.001$, **** $p \leq 0.0001$

A. Total IgG1⁺ and IgG2a⁺ expressing B cells and plasmoblasts in the illiac lymph nodes: dams vs virgin cell numbers

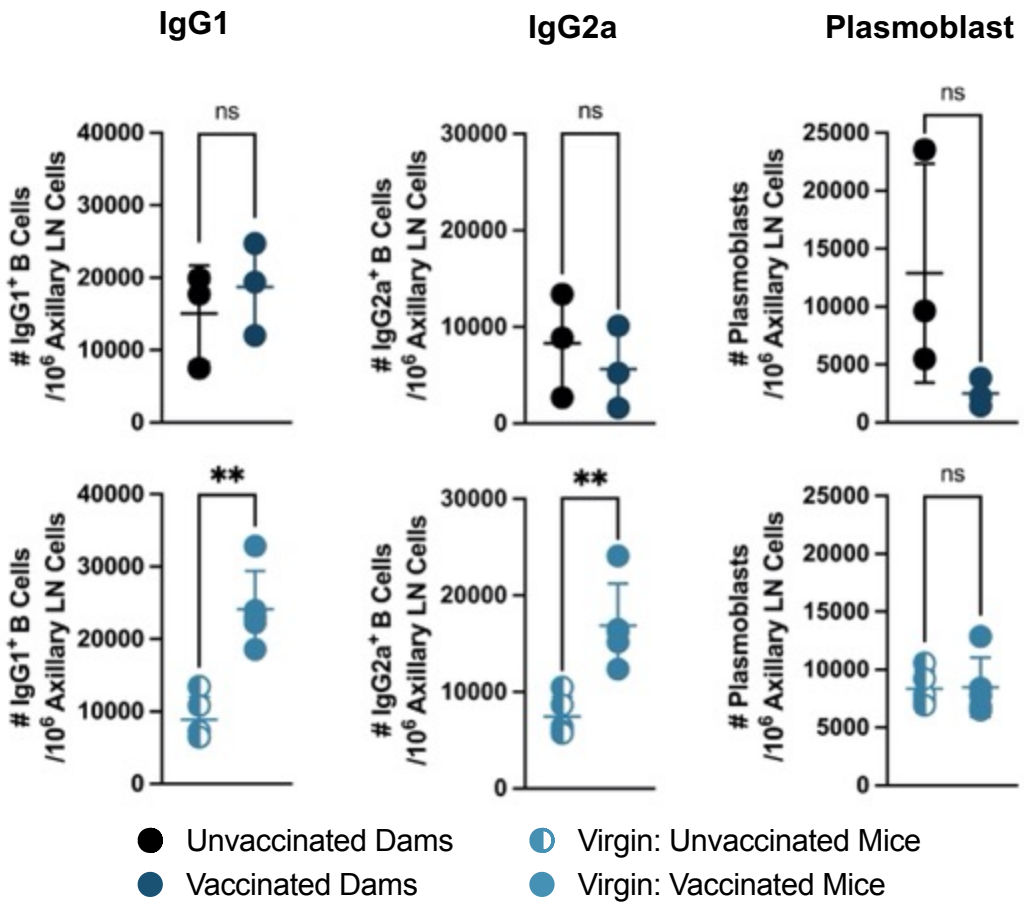

Figure 3.12: PCV13 vaccination results in increased IgG1, IgG2a antibody subsets in the axillary lymph nodes of virgin mice.
A. 7-week-old female BALB/c mice were un/vaccinated with PVC13 before mating while female virgin mice were vaccinated. Axillary lymph nodes were processed into single cell suspensions and processed to investigate IgG1 ($CD45^+$ $CD19^+$ $B220^+$ $IgG1^+$) and IgG2a ($CD45^+$ $CD19^+$ $B220^+$ $IgG2a^+$) expressing B cells and plasmoblasts ($CD45^+$ $B220^+$ $CD138^+$). Data is representative of 2 equivalent experiments whereby n = 2-3 mice per group. Statistical analysis was performed using a Kruskal Wallis test. *$p \leq 0.05$; **$p \leq 0.01$, *** $p \leq 0.001$, **** $p \leq 0.0001$

T cell ($CD45^+$ $CD3^+$ $CD4^+$) populations were slightly elevated in virgin mice however no differences were observed as a result of vaccination **(Figure 3.13)**. Overall, this set of results suggests that in the axillary lymph nodes, $IgG1^+$ and $IgG2a^+$ expressing B cells, were significantly increased in virgin vaccinated mice.

A. Total $CD3^+$ $CD4^+$ T cells in axillary lymph nodes: dams vs virgin cell numbers

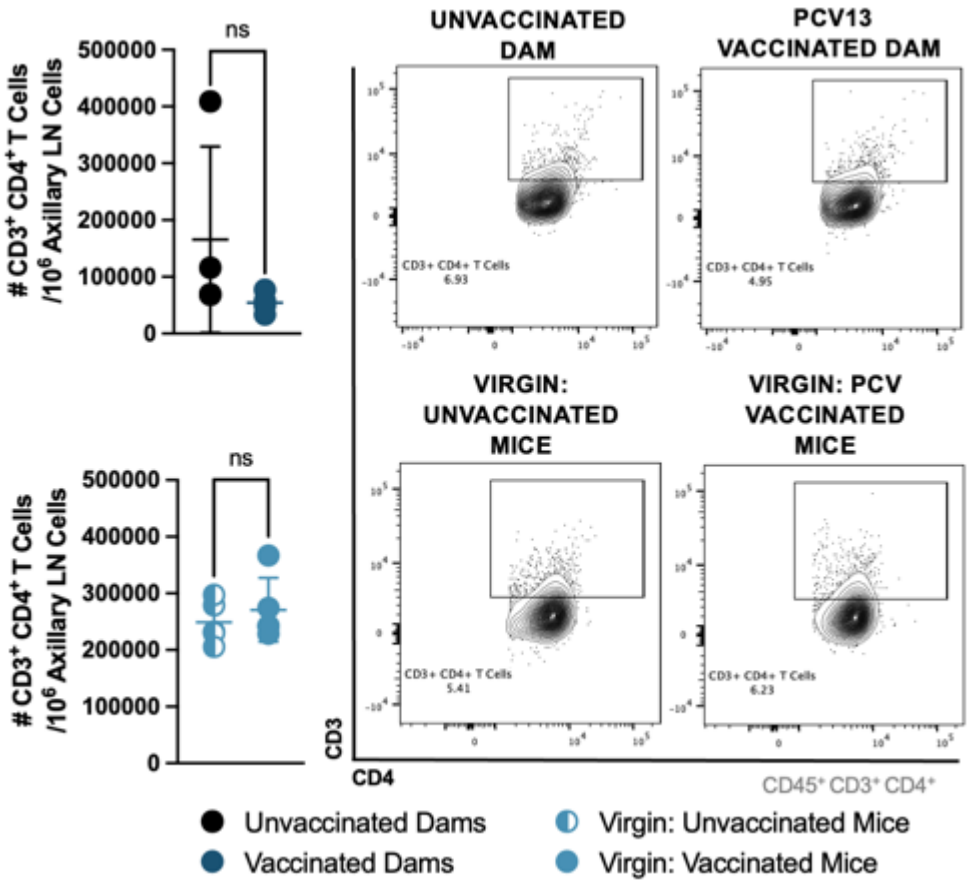

Figure 3.13: T Cell populations are increased in the axillary lymph nodes of virgin mice.
A. 7-week-old female BALB/c mice were un/vaccinated with PVC13 before mating while female virgin mice were vaccinated. Axillary lymph nodes were processed into single cell suspensions and processed to evaluate ($CD45^+$ $CD3^+$ $CD4^+$) T cell populations. Data is representative of 2 equivalent experiments whereby n = 2-3 mice per group. Statistical analysis was performed using a Kruskal Wallis test. *$p \leq 0.05$; **$p \leq 0.01$, *** $p \leq 0.001$, **** $p \leq 0.0001$

3.3. Discussion

Pregnancy induces changes to the immune profile from a TH1 to a TH2 environment which creates a tolerant environment to prevent the body from attacking the developing foetus. This altered state may affect the response to PCV13 therefore administering vaccines at certain points during pregnancy may result in a more robust immune response and better protection for both the pregnant dam and the offspring. Total and PCV13 specific antibody results indicate that dams vaccinated with PCV13 one week before mating yields greater antibody titters when compared to dams vaccinated one week after mating. In addition, to investigate if pregnancy affects vaccine efficiency, virgin (not mated) mice were vaccinated with PVC13 and compared to dams (mated). No differences were recorded between dams vaccinated one week before mating and virgin mice. These results indicate that pregnancy does not affect vaccine efficiency when dams are vaccinated one week before pregnancy.

The axillary lymph nodes serve to drain the entire upper limb and the breast while illiac lymph nodes function to drain the superior parts of the middle to anterior pelvic organs, inferior pelvic viscera and deep perineum. These lymph nodes are crucial for trapping bacteria before they migrate to other organs via the circulatory system. The illiac lymph undergoes immune system modulation whereby the lymph nodes help in establishing maternal-fetal tolerance, whereby the immune system does not attack the fetus. The illiac lymph nodes may be involved in the processing and distribution of maternal antibodies which are crucial for providing passive immunity to the fetus around the pelvic region.

This can be seen in the results as distinct differences can be seen in the illiac lymph nodes whereby $IgG1^+$ and $IgG2a^+$ expressing B cells are increased in PCV13 vaccinated dams and virgin mice. Similar results can be seen in the axillary lymph nodes, $IgG1^+$ and $IgG2a^+$ expressing B cells are also increased in the axillary lymph nodes of virgin PCV13 vaccinated mice. This result is significant as the axillary lymph nodes are responsible for filtering lymphatic fluid in the breast.

These results suggest that PCV13 vaccination was successful in the vaccination model and not only antibody titres were increased but in addition $IgG1^+$ and $IgG2a^+$ expressing B cells were increased in the illiac and slightly elevated in the axillary lymph nodes of vaccinated dams and virgin mice. Due to the successful vaccination in dams, investigating the maternal vaccination strategies could be further investigated in offspring.

Chapter 4: Investigating maternal transfer of protection in a syngeneic setting.

4.1. Introduction

Maternal transfer of immunity refers to the process whereby mothers pass immune protection to their offspring primarily in utero or via breastfeeding. The transfer of antibodies provides temporary passive immunity against pathogens to the offspring(87). Maternal antibody levels can be boosted by maternal vaccination against specific pathogens. Maternal vaccination against COVID 19, pertussis, and influenza has been widely researched and used successfully in many populations (16, 27, 32, 98, 99). In addition, maternal vaccination against respiratory syncytial virus (RSV) and group B streptococcus (GBS) have been shown to provide immune protection in infants(29, 33, 100). In pregnant woman, maternal vaccination against GBS leads to increased maternally-derived anti-GBS functional antibodies(29). These higher concentrations of maternally-derived antibody-mediated complement deposition was associated with a decreased risk of GBS colonization in infants up to day 60–89 of life(29, 101).

Due to the investment of knowledge and research towards maternal vaccination in GBS, there is a possibility that maternal vaccination against *S. pneumoniae* is a tractable approach to provide offspring with early life protection. Maternally acquired antibodies confer important passive protection against *S. pneumoniae* for at least the first 6 months

of an infant's life (2, 3, 87). This maternal influence is being appreciated as an important driver in the onset of offspring immune autonomy (87, 90, 102, 103).

Understanding if maternal vaccination using PCV13 is possible and if maternal antibodies in utero, predominantly across the placenta, and after birth through breast milk could be transferred is essential. In addition, investigating if passive immunity but also long lasting active immune responses in offspring can be achieved is crucial for understanding if PCV13 maternal transfer could be used as potential solution for reducing the disease burden in children under five years of age(1).

In this chapter, we aim to investigate if PCV13 maternal vaccination can be transferred to offspring in the absence and presence of infection in a syngeneic experimental model. If protection is successful, we aim to investigate if this is achieved in utero, via breastfeeding or a combination of both.

4.2. Results

4. 2.1 PCV13 maternal vaccination elicits higher antibody titres in the breastmilk and serum pellets of maternally vaccinated offspring.

To investigate the effect of PCV13 maternal vaccination on offspring, dams were vaccinated one week before mating. Dams gave birth and 10 days later half of the offspring were euthanized. Breastmilk pellets and serum were collected for ELISA analysis. The remaining offspring was left to age and at 7-weeks-old offspring were euthanized and serum collected for ELISA analysis **(Figure 4.1)**.

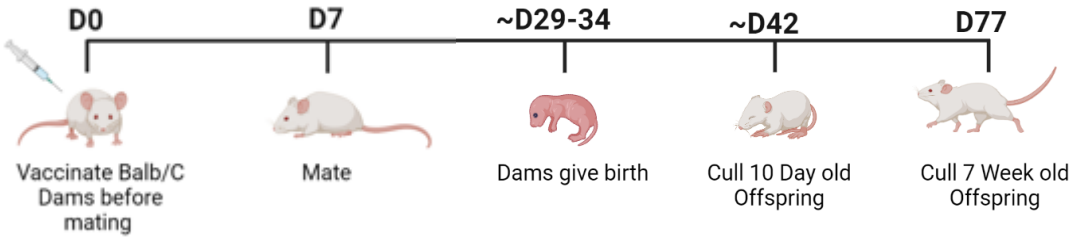

Figure 4.1 Syngeneic experimental vaccination model
7-week-old female mice (dams) were either unvaccinated or vaccinated one week before mating. Dams gave birth to offspring and were left to age. At 10 days old, half of the offspring were euthanized, and breastmilk pellets and serum were collected for ELISA analysis. The remaining half of the offspring were euthanized at 7 weeks of age and serum was collected for PCV13 specific ELISA analysis.

Breastmilk pellets were subjected to PCV13 specific IgG and total IgG ELISA analysis. PCV13 specific IgG was not detected in the breastmilk of maternally unvaccinated and vaccinated offspring. Total IgG was elevated in the breastmilk of both maternally unvaccinated and vaccinated 10-day-old offspring, but no significant differences were observed between offspring **(Figure 4.2A)**. In the serum of 10-day-old offspring, PCV13

specific IgG was significantly elevated in maternally vaccinated offspring. In addition, total IgG titres were also significantly elevated in maternally vaccinated offspring **(Figure 4.2B)**. These results indicate that due to maternal vaccination, circulatory PCV13 specific IgG antibodies were increased in 10-day-old offspring.

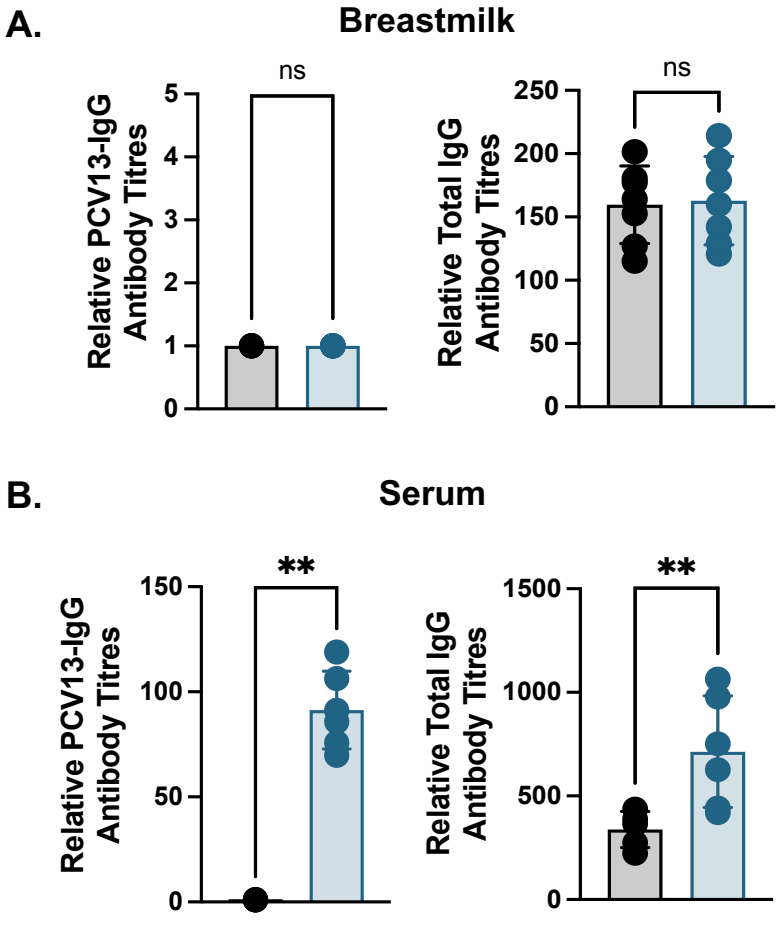

Figure 4.2 PCV13 specific and total IgG antibodies are significantly elevated in the serum of maternally vaccinated 10-day old offspring.
10-day old offspring were either born to unvaccinated or PCV13 vaccinated dams. PCV13-specific and Total IgG was investigated in **A.** breastmilk and **B.** serum using ELISA. Data is representative of 2 experiments whereby n = 4-5 mice per group. Statistical analysis was performed using a Kruskal Wallis test. P values were regarded as significant if less than 0.05 (* $p<0.05$, ** $p<0.01$, *** $p<0.001$).

PCV13 specific IgG and Total IgG titres were investigated in the serum of 7-week-old offspring. PCV13 specific IgG and Total IgG titres were significantly increased in the maternally vaccinated offspring **(Figure 4.3)**. These results indicate that maternally vaccinated offspring inherited long-lasting elevated antibody titres as a result from maternal vaccination.

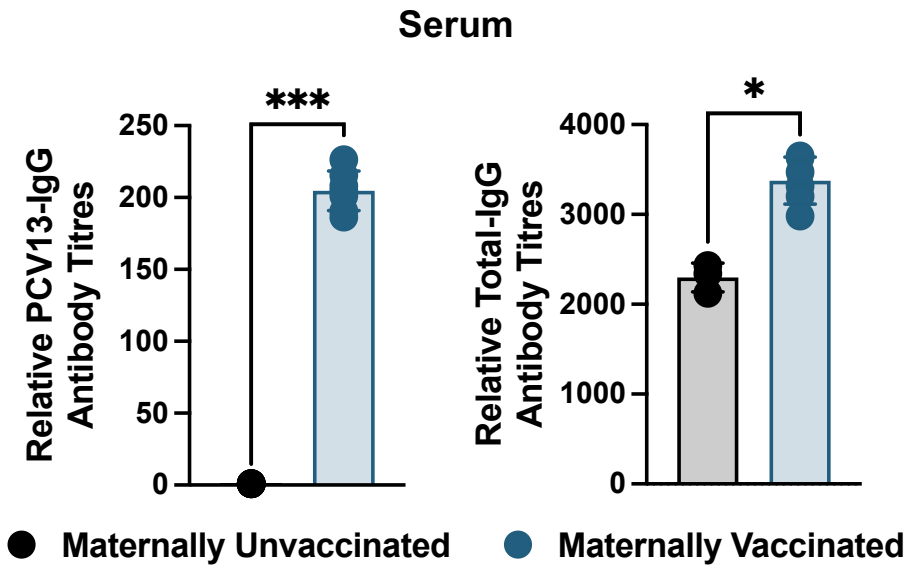

Figure 4.3 PCV13 specific and total IgG antibodies are significantly elevated in maternally vaccinated 7-week-old offspring.
7-week-old offspring were either born to unvaccinated or PCV13 vaccinated dams. PCV13-specific and Total IgG was identified in serum using ELISA. Data is representative of 2 experiments whereby n = 4-5 mice per group. Statistical analysis was performed using a kruskal-wallis test. P values were regarded as significant if less than 0.05 (* $p<0.05$, ** $p<0.01$, *** $p<0.001$).

4. 2.2 PCV13 maternal vaccination elicits reduced bacteria CFU and T4P2 bioluminescence in maternally vaccinated offspring.

The *in vivo* imaging system (IVIS) was used to enable non-invasive visualization and quantification of *pneumococcal* disease progression in 8-week-old offspring. TiGR4 is a Serotype 4 pneumococcal strain and is widely used in studies. T4P2 is a variant of TiGR4 with lux genes SP_1886 inserted under the control of promoter P2. Therefore allowing for bioluminescent imagining to be evaluated using the IVIS. T4P2 is similar to its WT, however, is slightly less virulent due to the metabolism of the bacteria being shifted towards bioluminescence production **(Figure 4.4A)**. Pneumococcal strains Xen35 and T4P3 has elicit higher levels of bioluminescence however their virulence significantly reduced. Therefore, T4P2 was selected as it most mimicked the TiGR4 strain but still produced a level of bioluminescence that was able to be detected.

To establish if PCV13 maternal vaccination could reduce the T4P2 bacterial burden in offspring, optimisation experiments needed to be performed. 8-week-old dams were vaccinated one week before mating. Dams gave birth and offspring were left to age. 8-week-old maternally unvaccinated and vaccinated offspring were challenged with $1X10^9$ CFU intraperitoneally. 24h later, bioluminescence was measured to investigate bacterial progression in maternally unvaccinated and vaccinated mice **(Figure 4.4B)**. These initial set of experiments formed the foundation of the experimental model but also allowed for the number of mice euthanized to be reduced as we could visualise the effects of bacterial progression while mice were anesthetised.

The bioluminescence of the inoculum was recorded prior to infection and was measured to be 3.694 $X10^5$ RLU **(Figure 4.4D)**. 8-week-old maternally unvaccinated and vaccinated mice were challenged intraperitoneally with $1X10^9$ CFU/ml T4P2. 24h after infection, mice were anesthetised, and bioluminescence was imaged and recorded using the IVIS. 8-week-old maternally vaccinated offspring had reduced RLU recorded in the abdomen near the site of infection in the peritoneal cavity. In addition, the bacteria were restricted to the abdomen whereas bacteria in maternally unvaccinated mice had spread to the lung **(Figure 4.4C)**. This result is indicative that bacteria spread to the circulatory system in maternally unvaccinated offspring. To ensure that RLU scores were truly reflective of bacteria growth, mice were euthanised and intraperitoneal lavages were collected and plated on BAB agar plates. RLU's and CFU's were reduced in maternally vaccinated offspring **(Figure 4.4D)**.

The preliminary IVIS results suggest that the maternal vaccination model was successful, and the infection model was effective. PCV13 maternal vaccination may result in enhanced protection against *S. pneumoniae* in offspring. However, the infection model in mice needed to mimic a natural pneumococcal colonisation infection and therefore for future experiments $1X10^7$ CFU would be inserted intranasally and 48h later mice will be euthanized.

A

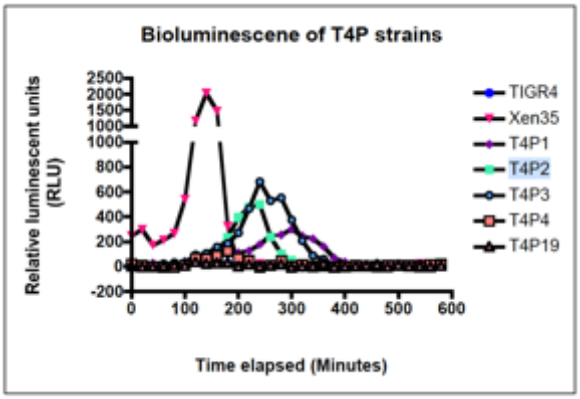

B

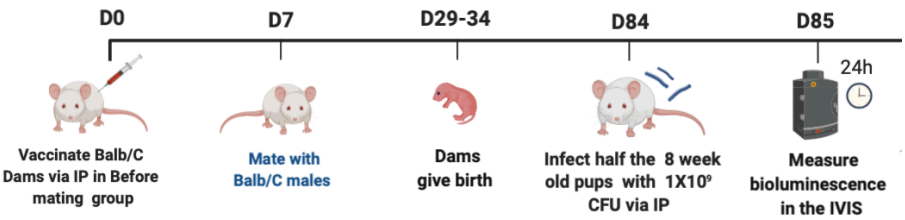

C.

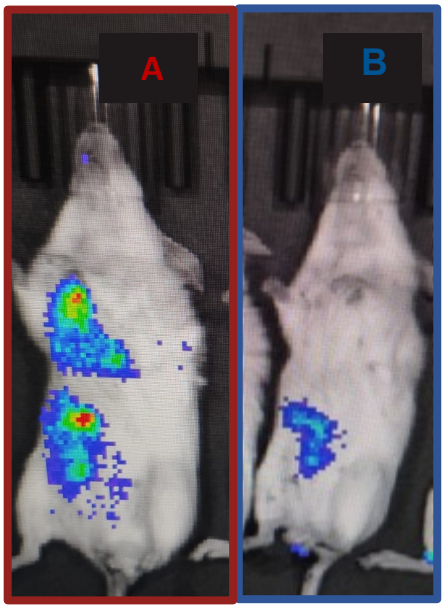

D.

Inoculum concentration	1X10^9 CFU
Inoculum IVIS bioluminescence	3.694 X 10^5 RLU

Bioluminescence 24h After infection		
A	8 W/O maternally unvaccinated offspring	1.551X10^6 RLU
B	8 W/O maternally vaccinated offspring	7.729 X 10^5 RLU

Intraperitoneal Cavity Lavage		
A	8 W/O maternally unvaccinated offspring	Lawn (uncountable)
B	8 W/O maternally vaccinated offspring	1.332 × 10^7 CFU

Figure 4.4 8-week-old maternally vaccinated offspring have significantly reduced T4P2 CFU and bioluminescence activity.
A. T4P2 *pneumococcal* stains were grown in a 96 well plate and bioluminescence (RLU's) was quantified using a LumiGLO plate reader. 8-week-old offspring were either born to unvaccinated or PCV13 vaccinated dams and **B.** infected intraperitoneally for 24h with a bioluminescent strain T4P2 and visualised using the IVIS system. **C.** T4P2 bioluminescence was visualised in mice using the IVIS. **D.** The intraperitoneal cavity was flushed with sterile 1XPBS and RLU's and CFU's were quantified. Data is representative of one experiment with 5 mice per group. Image reflective of representative from each group.

4. 2.3 PCV13 maternal vaccination in offspring elicits reduced bacteria CFU and increased PCV13-specific IgG in a syngeneic setting.

Due to the successful optimisation of the vaccination and infection model, the syngeneic experimental infection model was finalised **(Figure 4.5)**. 7-week-old dams were either left unvaccinated or vaccinated one week before mating. Dams gave birth and offspring were left to age. At 7 weeks of age, offspring were infected intranasally with $1X10^7$ CFU's for 48h and mice were euthanized. The blood, BAL and lungs were collected, processed and further analysed.

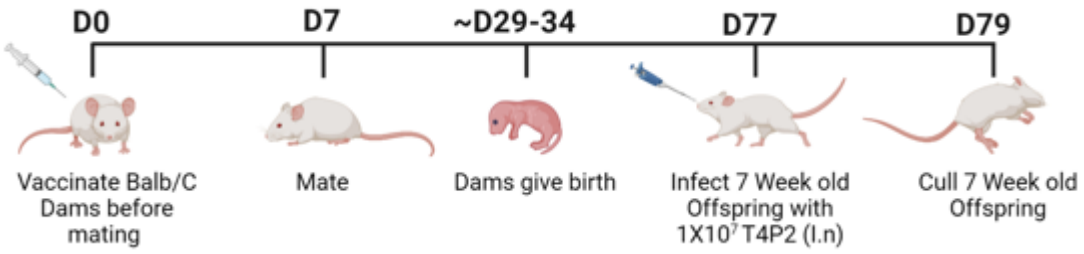

Figure 4.5 Syngeneic experimental infection model
7-week-old female mice (dams) were either unvaccinated or vaccinated one week before mating. Dams gave birth to offspring and were left to age. At 7 weeks of age half of the offspring were infected intranasally with $1X10^7$ CFU and 48h later offspring were euthanized.

Nasal colonisation was achieved after infection, the bacteria travelled from the nasal cavity down the throat into the trachea and into the bronchioles. The bronchioles were flushed with 1X PBS and plated on BAB agar plates and CFU's were recorded. Maternally vaccinated offspring had significantly reduced T4P2 CFU's in the BAL **(Figure 4.6A)**. Cardiac punctures were collected from each mouse and blood was plated on BAB plates. These results suggest that maternally vaccinated offspring had significantly reduced

T4P2 CFU's in the blood **(Figure 4.6B)**. These results indicate that maternally vaccinated offspring have the ability to reduce the spread of bacteria and limit the CFU's in the circulatory system therefore prevent systemic infection.

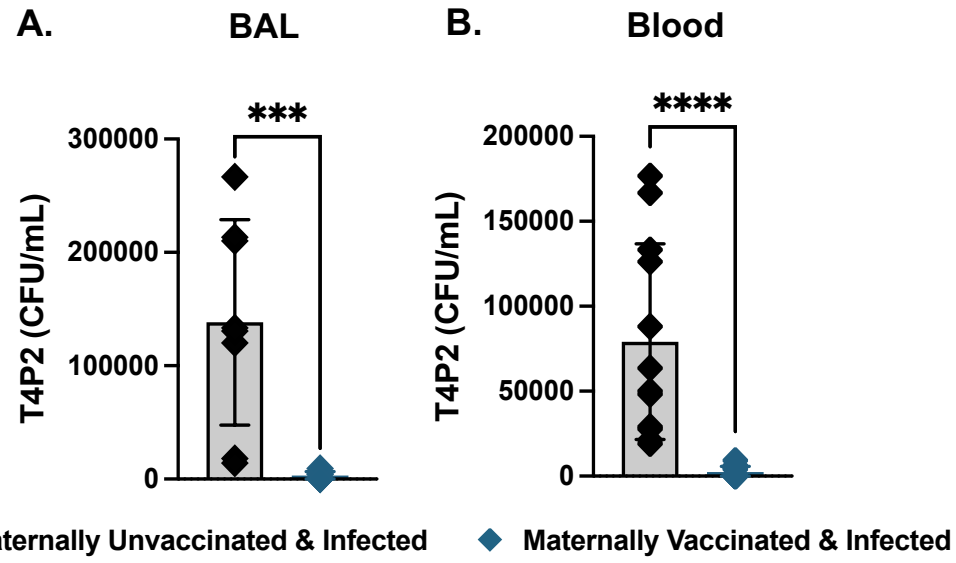

Figure 4.6 7-week-old maternally vaccinated offspring have significantly reduced T4P2 CFU in the BAL and blood.
7-week-old offspring were either born to unvaccinated or PCV13 vaccinated dams and infected intranasally. T4P2 CFU's were recorded in the **A.** BAL and **B.** blood. Data is representative of 2 experiments whereby n = 4-7 mice per group. Statistical analysis was performed using a kruskal-wallis test. P values were regarded as significant if less than 0.05 (* $p<0.05$, ** $p<0.01$, *** $p<0.001$).

PCV13 specific antibodies were investigated in the serum of maternally unvaccinated and vaccinated 7-week-old offspring **(Figure 4.7)**. PCV13 specific IgG was significantly increased in maternally vaccinated offspring and yielded the most significant antibody titres **(Figure 4.7)**. PCV13 specific antibodies were further classified into antibody subgroups IgG1 and IgG2a. PCV13 specific IgG1 and IgG2a antibodies were significantly elevated in maternally vaccinated offspring **(Figure 4.7)**. As expected, the maternally

unvaccinated offspring had no detectable PCV13 specific IgG, IgG1 and IgG2a antibodies **(Figure 4.7)**.

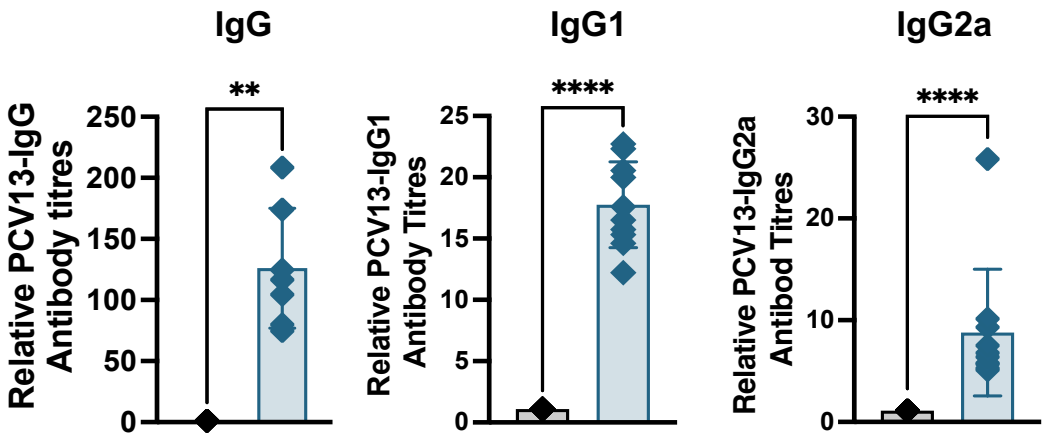

Figure 4.7 PCV13 specific antibodies were significantly elevated in 7-week-old maternally vaccinated offspring.
7-week-old offspring were either born to unvaccinated or PCV13 vaccinated dams and infected with $1X10^7$ T4P2 CFU. PCV13-specific IgG, IgG1 and IgG2a were investigated in serum using ELISA. Data is representative of 2 experiments whereby n = 4-7 mice per group. Statistical analysis was performed using a kruskal-wallis test. P values were regarded as significant if less than 0.05 (* $p<0.05$, ** $p<0.01$, *** $p<0.001$).

4. 2.4 PCV13 maternal vaccination leads to reduced inflammation and increased immune control in the BAL.

The BAL was centrifuged, and cell pellets were processed for flow cytometry. Total $CD45^+$ immune cell populations were significantly reduced in maternally vaccinated offspring **(Figure 4.8A)**. The same trend was observed for total neutrophil ($CD45^+$ $Ly6G^+$ $SiglecF^-$ $CD11b^+$) populations. Maternally vaccinated offspring had reduced neutrophils in the BAL **(Figure 4.8B)**. The presence of a T4P2 infection results in an increase of immune cell and neutrophil recruitment to the BAL in maternally unvaccinated offspring **(Figure 4.8)**.

Total $CD45^+$ immune cells and Neutrophils in the BAL

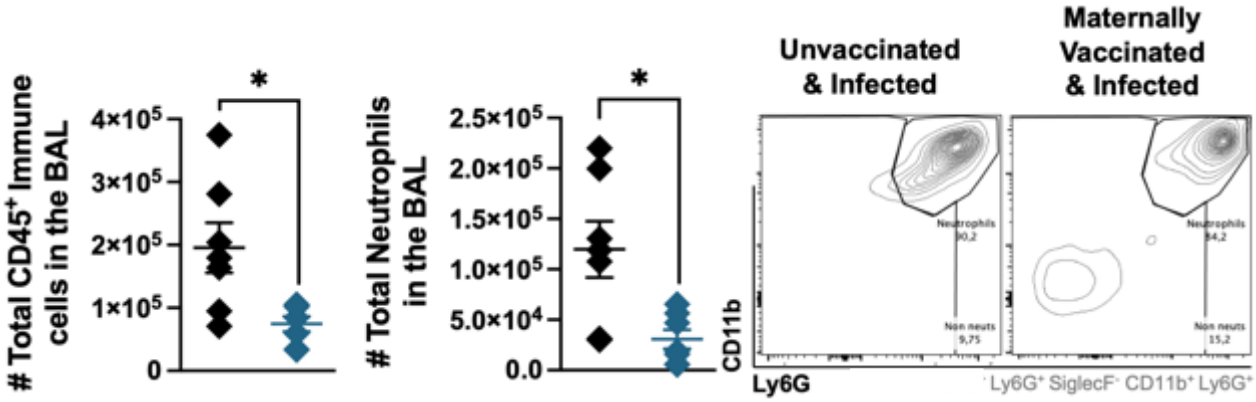

Figure 4.8: Maternally vaccinated and infected 7-week-old offspring have reduced total neutrophil populations in the BAL.
7-week-old offspring were either born to unvaccinated or PCV13 vaccinated dams and infected intranasally with $1X10^7$ T4P2 CFU. **A.** Total immune ($CD45^+$) and **B.** neutrophil ($CD45^+$ $Ly6G^+$ $SiglecF^-$ $CD11b^+$) populations were investigated in the BAL. The results are expressed as individual mice/data points. Representative of 2 experiments whereby n = 5-7 mice per group. Statistical analysis was performed using a Mann-Whitney U test. P values were regarded as significant if less than 0.05 (* $p<0.05$, ** $p<0.01$, *** $p<0.001$).

The lung cell populations were investigated to find important cell populations under the influence of a T4P2 infection. Interestingly, B cells ($CD45^+$ $CD19^+$ $B220^+$) were significantly elevated in maternally vaccinated offspring **(Figure 4.9)**. The above results suggest that maternally vaccinated offspring have reduced CFU in the BAL and in circulation. These offspring not only have increased PCV13 specific antibodies (IgG, IgG1 and IgG2a) but also have reduced cell infiltration to the BAL and increased B cells in the lung.

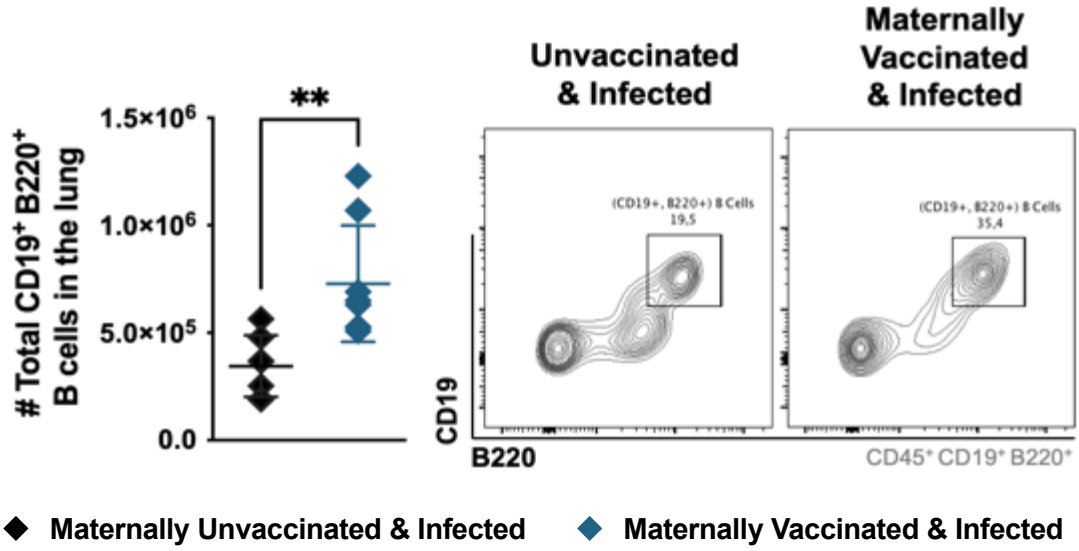

Figure 4.9 7-week-old maternally vaccinated offspring have elevated CD19+ B220+ B cell populations.
7-week-old offspring were either born to unvaccinated or PCV13 vaccinated dams and infected with $1X10^7$ T4P2 CFU. B cell ($CD45^+$ $CD19^+$ $B220^+$) populations were investigated in the lung. Data is representative of 2 experiments whereby n = 4-7 mice per group. Statistical analysis was performed using a Mann-Whitney U test. P values were regarded as significant if less than 0.05 (* $p<0.05$, ** $p<0.01$, *** $p<0.001$).

4.3. Discussion

To investigate the transfer of PCV13 maternal vaccination, a syngeneic mouse model was designed whereby offspring born to unvaccinated and vaccinated dams were left to age but were euthanised at 10 days old and 7 weeks of age. At 10 days of age, the breastmilk pellets and serum were collected to investigated PCV13 and total IgG antibodies using ELISA. In the breastmilk, PCV13 specific IgG could not be detected in breastmilk and no differences in total IgG antibodies were present between maternally unvaccinated and vaccinated offspring. These preliminary results suggests that PCV13 specific antibodies are not transferred via breastfeeding, but this needs to be confirmed performing additional experiments. In the serum, PCV13 specific and total IgG was significantly elevated in maternally vaccinated offspring. In 7-week-old offspring, PCV13 and total IgG were also significantly elevated in older maternally vaccinated offspring. These results suggest that maternal vaccination results in elevated PCV13 specific antibodies that are maternally derived. These preliminary results indicate that transfer of protection is occurring in utero as no PCV13 specific antibodies were detected in the breastmilk. Interestingly, PCV13 specific antibodies were detected in aged 7-week-old offspring which indicates that long lived antibodies are present and that the half-life of these antibodies have potentially increased.

The elevated PCV13 specific antibodies present in maternally vaccinated offspring were incredibly interesting but investigating if the antibodies were functional at reducing bacterial colonisation was important. To investigate if the antibodies were functional,

T4P2 infections were optimised using the IVIS. This method was beneficial as bacteria were bioluminescent so infections could be visualised and measured and in addition less mice were euthanized. $1X10^9$ T4P2 CFU's were injected into the intraperitoneal cavity of maternally unvaccinated and vaccinated mice. The large bacterial dose and route of infection would usually cause sepsis and was used in order to test the functionality of the antibodies and maternal vaccination effects. Interestingly, T4P2 bacteria were restricted to the site of infection in the abdomen of maternally vaccinated mice whereas T4P2 bacteria had migrated in circulation to other sites such as the lungs of maternally unvaccinated mice. These results indicated that maternally vaccinated offspring has antibodies that were efficient at reducing the bacterial burden in infected mice and now the syngeneic experimental infection model could be investigated with a nasal infection using a dose similar to the literature to ensure colonisation(104-106).

PCV13 is a conjugate vaccine that targets specific serotypes included in the vaccine, which stimulates the immune system, including B cells, to produce antibodies against the targeted pneumococcal serotypes. Maternally unvaccinated and vaccinated offspring were infected intranasally with $1X10^7$ CFU's for 48h and the BAL, blood and lungs were collected, processed and further analysed. T4P2 CFU's were significantly reduced in the BAL and blood of 7-week-old maternally vaccinated offspring. In addition, PCV13 specific IgG namely IgG1 and IgG2a were detected in maternally vaccinated offspring. Cell populations were investigated using flow cytometry. Total $CD45^+$ immune cell and neutrophil populations were increased in the BAL of maternally unvaccinated offspring. This result indicates that in the presence of infection, immune cells were recruited to the

BAL resulting in increased inflammation. Total $CD45^+$ immune cell and neutrophil populations in the maternally vaccinated offspring remained low and therefore less inflammation indicating a sense of immune control in the BAL. Total $CD19^+$ $B220^+$ B cells were increased in the lungs of maternally vaccinated offspring while B cells remained relatively low in the lung of maternally unvaccinated offspring. The lung is the site of *pneumococcal* infection and the increase in B cell recruitment to the lung, mimics the effects of PCV13 vaccination(107).

The syngeneic vaccination and infection model used indicates that maternal vaccination induces long lived functional antibodies and reduced T4P2 CFU's in maternally vaccinated offspring. These results indicate that PCV13 maternal vaccination is successful and can be used as a potential vaccination strategy. However, the syngeneic model used is limiting when investigating immune cell responses. Total cell populations can be compared but identifying if maternal cells are playing a role in protection cannot be identified. Therefore, going forward to further investigate the effects of maternal vaccination a more informative model is needed.

Chapter 5: Investigating maternal transfer of protection in an allogenic setting.

5.1. Introduction

Microchimerism is a complex phenomenon which refers to the presence of a low frequency of cells or genetic material that can be exchanged from the mother and their offspring through the placenta or breastfeeding(90, 108-110). These cells can enter the bloodstream and establish in the mother or offspring. This form of microchimerism can be classified into fetomaternal (fMC) and maternofetal microchimerism (mMC) and have important influences on both maternal and offspring health(87, 108, 111).

In pregnancy, syngeneic refers to an immune environment that is genetically and immunologically compatible whereby a mother and offspring have the same major histocompatibility complex (MHC) expression(112). In chapter 4, maternal transfer of protection was investigated in Balb/C mice using a syngeneic setting. This syngeneic setting indicates that Balb/C maternal and offspring cells had the same MHC expression and therefore an offspring would not reject any maternal cells transferred from the mother. Maternal protection was evident in the syngeneic environment as maternally vaccinated offspring had increased long lasting functional PCV13 specific antibodies and reduced T4P2 bacteria in the BAL and blood. Unfortunately, this model would potentially increase the amount of mMC present as no maternal cells would be rejected by the offspring due to the same MHC presence.

To investigate if microchimerism is truly playing a role in this protection, maternal transfer needs to be investigated whereby a mother and offspring are genetically and immunologically incompatible and therefore a MHC mismatch needed to be investigated. This immune environment would be referred to as an allogeneic setting and will be achieved with an intricate mating strategy using Balb/C and C57Bl/6 to allow for mothers to have a MHC mismatch with offspring(109, 112). This model mimics the low frequency of cell transfer present in humans(109, 112). An additional benefit of this allogeneic setting enables tracking of these cells using flow cytometry by measuring the different MHC profiles on the surface of mother and offspring cells.

The aim of this chapter is to investigate if this protection observed in a syngeneic setting remains in an allogeneic setting as well. We aim to investigate proportions of mMC cells and if PCV13 maternal vaccination influences the mMC cell proportion transferred and alters the protection observed in PCV13 maternally vaccinated offspring.

5.2. Results

5. 2.1 The allogeneic maternal vaccination model

At 7 weeks of age, H-$2^{d/d}$ female mice (Balb/C) were mated with H-$2^{b/b}$ males (C57Bl/6) which resulted in H-$2^{b/d}$ offspring. At 3 weeks of age, offspring were weened and separated according to sex. H-$2^{b/d}$ females were selected, and males were culled. At 7 weeks of age H-$2^{b/d}$ females were either vaccinated intraperitoneally with PCV13 one week before mating or left unvaccinated. These females were mated with H-$2^{b/b}$ males resulting in H-$2^{b/d}$ and H-$2^{b/b}$ offspring. At 3 weeks of age, offspring were weaned, tail bleeds were obtained and genotyped. The H-$2^{b/d}$ offspring was culled and H-$2^{b/b}$ offspring were left to age. At 7 weeks of age, H-$2^{b/b}$ offspring were infected with $1X10^7$ T4P2 intranasally and euthanized 48H post infection **(Figure 5.1).**

A. The allogeneic maternal vaccination model:

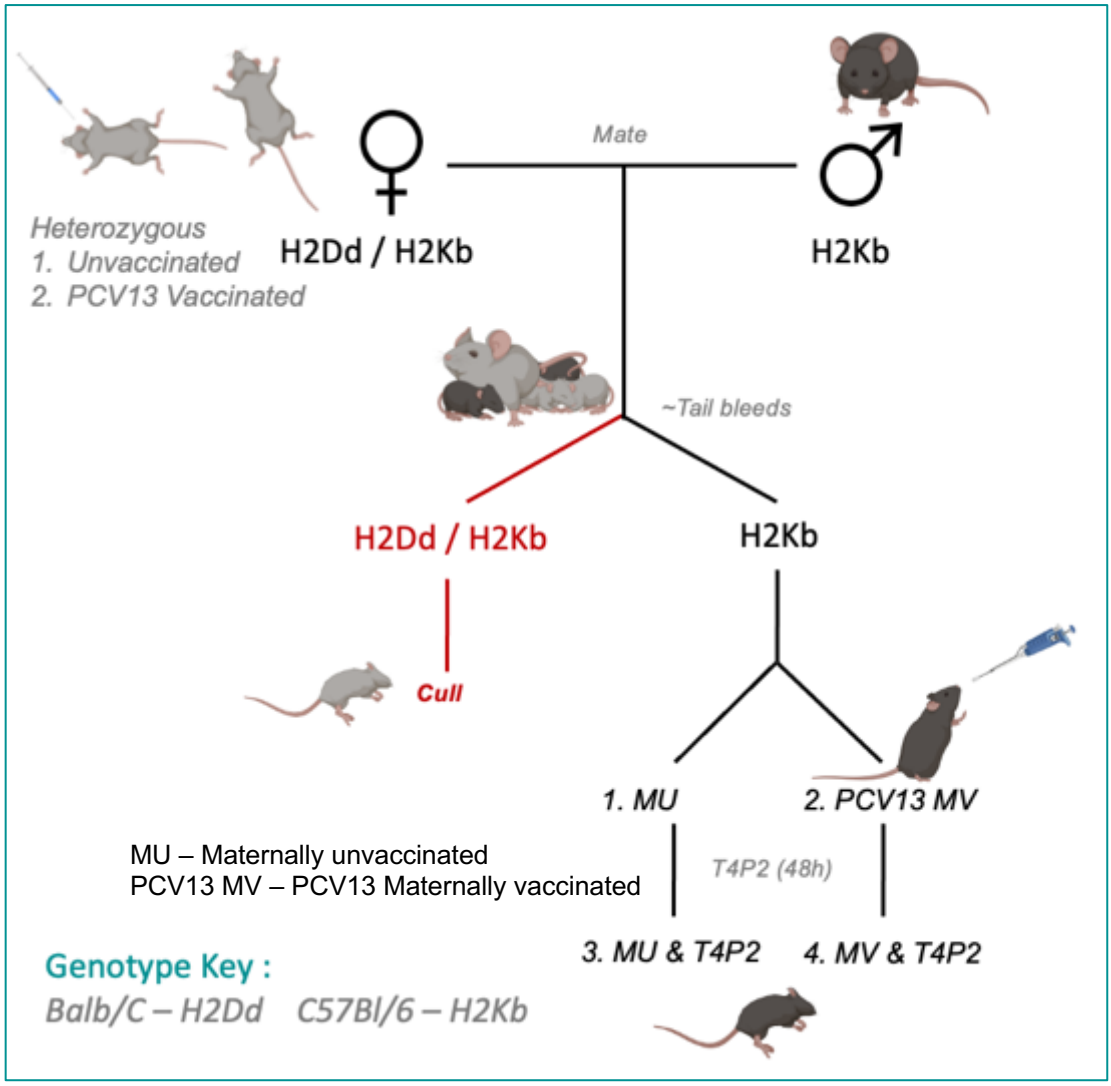

Figure 5.1: The allogeneic maternal vaccination model
At 7 weeks of age, H-$2^{b/d}$ female mice were either vaccinated intraperitoneally with PCV13 before mating or left unvaccinated. These females were then mated with H-$2^{b/b}$ males resulting in H-$2^{b/d}$ and H-$2^{b/b}$ offspring. The H-$2^{b/d}$ offspring was culled and H-$2^{b/b}$ offspring left to age. At 7-weeks-olf half of the offspring were infected with T4P2 intranasally and euthanized 48H post infection.

5. 2.2 PCV13 vaccinated dams have elevated T4P2 and PCV13 specific antibodies.

Three weeks after offspring were born, they were weaned off their dams (mothers) and separated according to sex. Dams were culled and blood, axillary and iliac lymph nodes were collected. Blood was separated into serum for T4P2 and PCV13 specific antibody isotype detection. T4P2 is a serotype 4 strain of pneumococcal bacteria that is covered by PCV13 vaccine. PCV13 vaccinated dams showed increased T4P2 specific total IgG titres in comparison to unvaccinated dams **(Figure 5.2A)**. In addition, PCV13 specific total IgG titres were greatly elevated in PCV13 vaccinated dams **(Figure 5.2B)**. PCV13 vaccinated dams had increased PCV13 specific antibody isotypes with IgG1 having the largest contribution followed by IgG2a and IgG3 **(Figure 5.2B)**. These results suggests that vaccination was successful as PCV13 vaccination not only increases PCV13 specific antibodies but also vaccine specific serotype T4P2 antibodies.

A. PCV13 and T4P2 specific antibody titres in Dams.

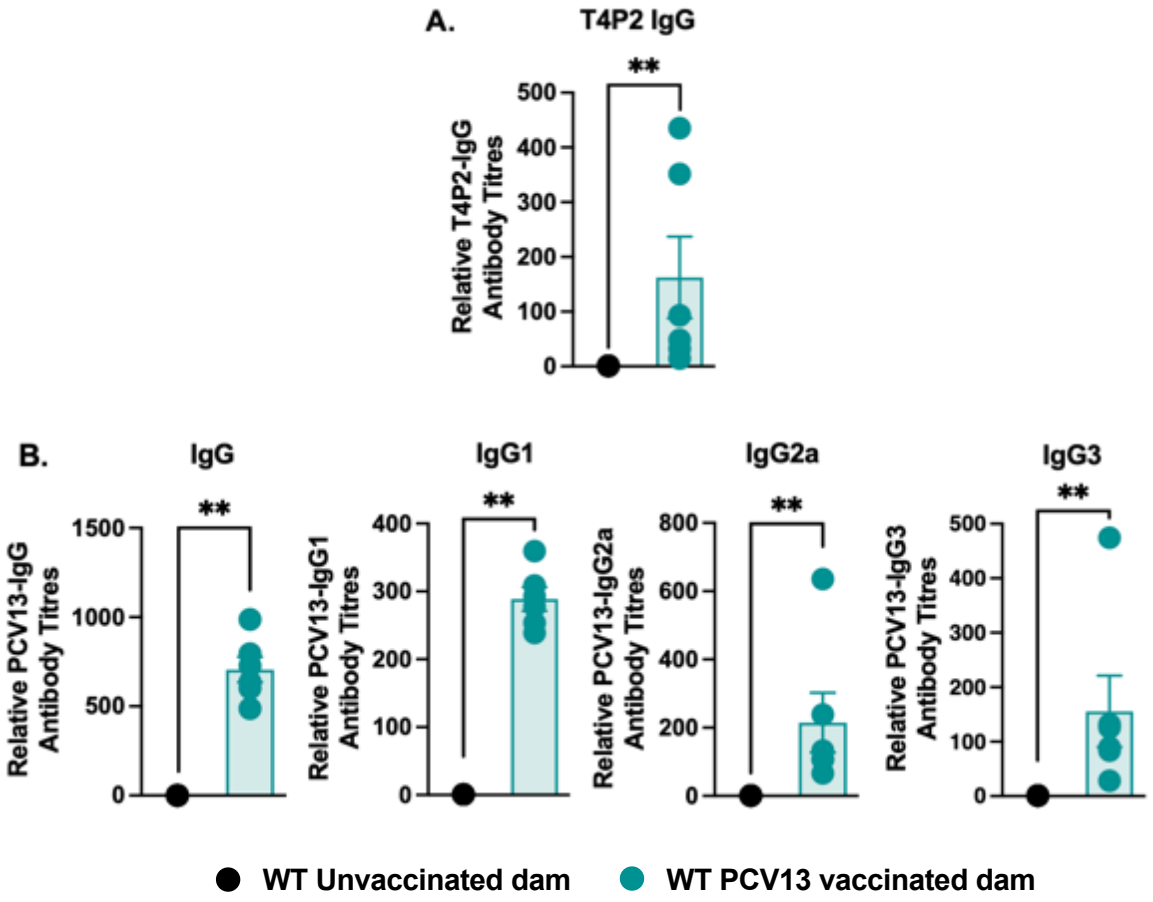

Figure 5.2: PCV13 vaccinated dams acquire antibody mediated anti-T4P2 and anti-PCV13 long lasting immunity.
Dams were either left unvaccinated or vaccinated with PCV13 one week before mating. **A.** T4P2-specific IgG and **B.** PCV13-specific antibodies were screened in the serum using ELISA. The results were expressed as individual mice/data points. Representative of 2 experiments whereby n = 5-7 mice per group. Statistical analysis was performed using a kruskal-wallis test. P values were regarded as significant if less than 0.05 (* $p<0.05$, ** $p<0.01$, *** $p<0.001$).

B cell ($CD45^+$ $CD19^+$ $B220^+$) numbers were increased in both the axillary and illiac lymph nodes **(Figure 5.3A)**. In addition, $IgG1^+$ ($CD45^+$ $B220^+$ $CD138^+$ $IgG1^+$) and $IgG2a^+$ ($CD45^+$ $B220^+$ $CD138^+$ $IgG2a^+$) plasma cells were also investigated in the axillary and illiac lymph nodes **(Figure 5.3B)**. $IgG1^+$ plasma cells in PCV13 vaccinated dams show a slight increase in cell numbers in both the axillary and illiac lymph nodes whereas $IgG2a^+$ cells only show a slight increase in the axillary lymph nodes of PCV13 vaccinated dams **(Figure 5.3B)**.

Dam B Cell profile: Axillary vs Illiac Lymph node.

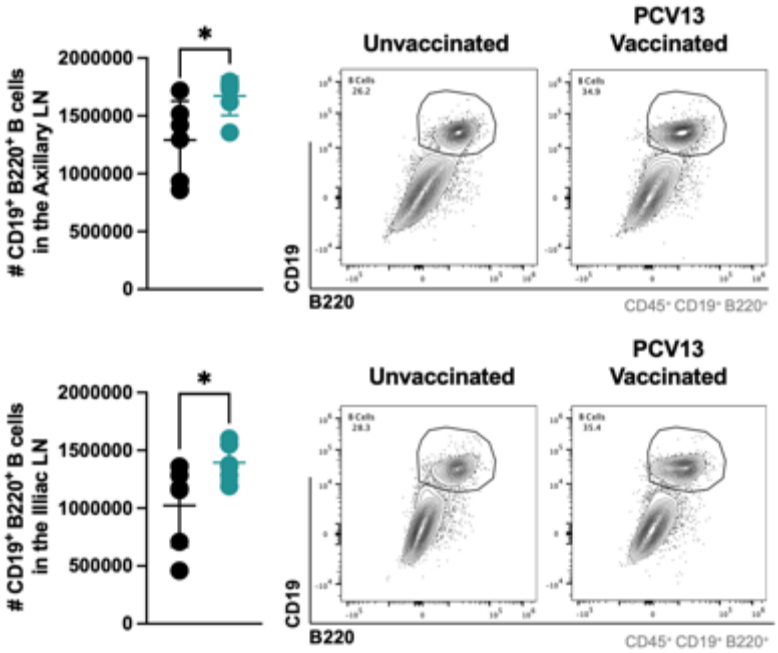

A. Antibodies in dam Lymph nodes

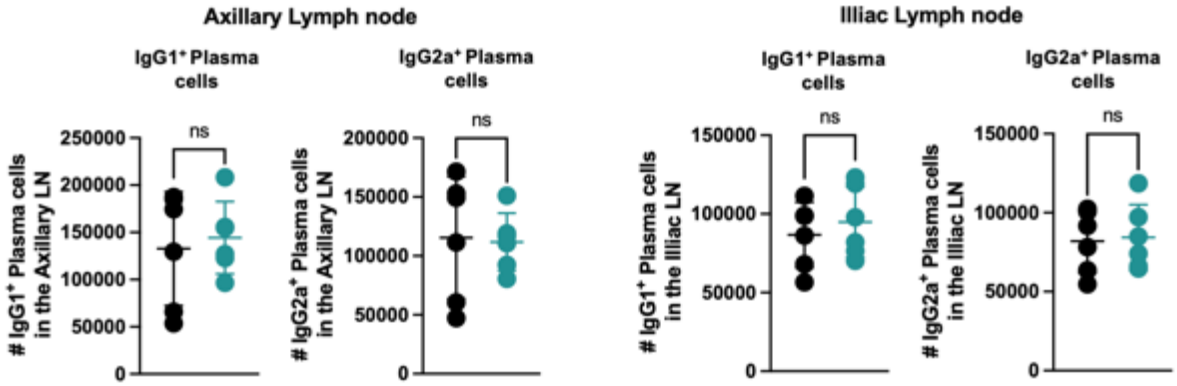

Figure 5.3: PCV13 vaccinated dams acquire elevated CD19$^+$ B220$^+$ B cell populations in the axillary and illiac lymph nodes.
Dams were either left unvaccinated or vaccinated with PCV13 one week before mating. **A.** B cell (CD45$^+$ CD19$^+$ B220$^+$) populations and **B.** IgG1$^+$ (B220$^+$ CD138$^+$ IgG1$^+$) and IgG2a$^+$ (CD45$^+$ B220$^+$ CD138$^+$ IgG2a$^+$) plasma cells were investigated in the axillary and illiac lymph nodes. All cell populations were identified using flow cytometry. The results are expressed as individual mice/data points. Representative of 2 experiments whereby n = 5-7 mice per group. Statistical analysis was performed using a kruskal-wallis test. P values were regarded as significant if less than 0.05 (* p<0.05, ** p<0.01, *** p<0.001).

5. 2.3 PCV13 maternally vaccinated offspring have reduced T4P2 CFU and elevated PCV13 specific antibodies in the serum.

7-week-old maternally unvaccinated and vaccinated and offspring were infected with $1X10^7$ T4P2 bacteria intranasally and euthanized 48h after infection. Blood was collected via cardiac puncture. 30 μL was immediately aliquoted for CFU on BAB agar plates while the rest was processed for serum collection for ELISA quantification.

7-week-old maternally vaccinated and infected offspring had no detectable T4P2 CFU in systemic circulation whereas maternally unvaccinated offspring had increased CFU in circulation **(Figure 5.4A)**. T4P2-specific titres were detected in both maternally unvaccinated and maternally vaccinated and infected offspring **(Figure 5.4B)**. However, maternally vaccinated and infected offspring had significantly higher T4P2 titres **(Figure 5.4B)**. T4P2-specific antibodies were detected in maternally unvaccinated offspring due to the significant CFU titres present in circulation. **(Figure 5.4A,B)**. Maternally vaccinated and infected offspring had significantly elevated PCV13-specific total IgG, IgG1, IgG2a and IgG3 antibody titres were detected in comparison to maternally unvaccinated and infected offspring **(Figure 5.4C)**.

A. T4P2 CFU and antibody-specific antibodies recorded in the serum of 7-week-old offspring.

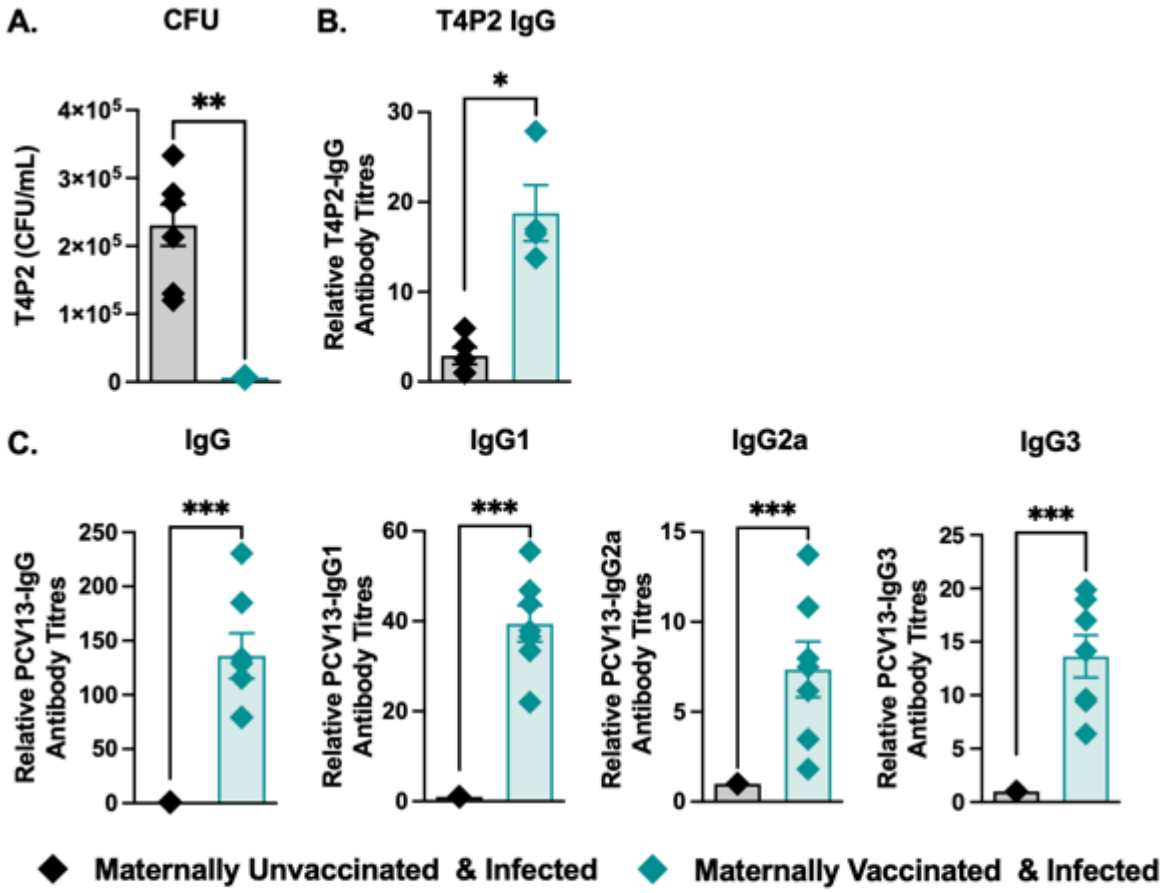

Figure 5.4: Maternally vaccinated 7-week-old offspring have reduced T4P2 CFU's and acquired maternally derived PCV13-specific antibodies in the serum. 7-week-old offspring were either born to unvaccinated or PCV13 vaccinated dams **A.** T4P2 CFU's were recorded in the serum of maternally unvaccinated and vaccinated offspring. **B.** T4P2-specific IgG was identified in serum using ELISA. **C.** PCV13-specific antibody serotypes were investigated in the serum using ELISA. The results are expressed as individual mice/data points. Representative of 2 experiments whereby n = 5-7 mice per group. Statistical analysis was performed using a kruskal-wallis test. P values were regarded as significant if less than 0.05 (* $p<0.05$, ** $p<0.01$, *** $p<0.001$).

Serum collected from unvaccinated and maternally vaccinated offspring was heat inactivated (HI'd) at 56°C for 30 minutes to deactivate complement activity. Once cooled, $1X10^7$ T4P2 was opsonized with serum at 4°C for 1 hour. Opsonized bacteria were infected intranasally into naïve 7-week BALB/c mice and mice were euthanized 48H post infection. Blood was collected and plated on BAB plates for CFU determination. No significant differences were observed between mice infected with $1X10^7$ CFU and mice opsonised with maternally unvaccinated serum or HI maternally unvaccinated serum **(Figure 5.5)**. Mice opsonized with maternally vaccinated serum had significantly reduced T4P2 CFU as no colonies were detected in blood samples **(Figure 5.5)**. Mice opsonized with HI'd maternally vaccinated serum had slightly elevated T4P2 CFU than mice opsonized with maternally vaccinated serum however the CFU were still significantly lower than mice infected with $1X10^7$ CFU and mice opsonized with maternally vaccinated serum **(Figure 5.5)**.

A. Bacteria was opsonized with maternally unvaccinated and vaccinated offspring serum.

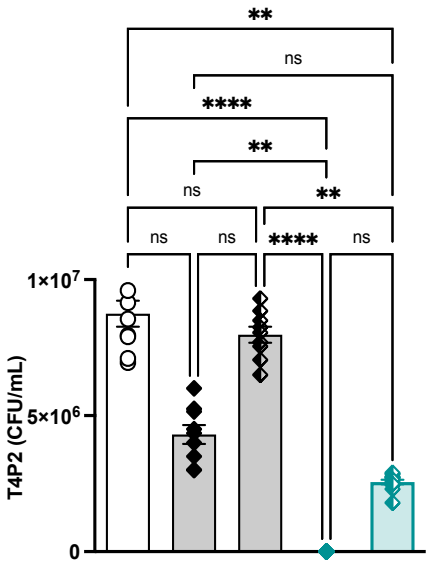

T4P2 Infection
Unvaccinated serum & infected
HI Unvaccinated serum & infected
Maternally Vaccinated serum & Infected
HI Maternally Vaccinated serum & Infected

Figure 5.5: Mice opsonized with PCV13 maternally vaccinated serum had significantly decreased T4P2 CFU's in the blood.
Serum collected from unvaccinated and maternally vaccinated offspring was heat inactivated at 56°C for 30 minutes and cooled. $1X10^7$ T4P2 was opsonized with serum at 4°C for 1 hour. Optimised bugs were infected intranasally into 7-week BALB/c mice and euthanized 48H post infection. The results were expressed as individual mice/data points. Representative of 2 experiments whereby n = 5-7 mice per group. Statistical analysis was performed using a Kruskal-Wallis test. P values were regarded as significant if less than 0.05 (* $p<0.05$, ** $p<0.01$, *** $p<0.001$).

5. 2.4 Maternally vaccinated offspring had reduced CFU tires in the BAL and increased immune control.

7-week-old maternally unvaccinated and vaccinated offspring were infected with $1X10^7$ T4P2 bacteria intranasally and euthanized 48h after infection. The Bronchioles were flushed with 800 μL of sterile 1X PBS and BAL fluid was collected for CFU counts as well as IgA ELISA detection. 7-week-old maternally vaccinated and infected offspring had significantly reduced T4P2 CFU in the BAL **(Figure 5.6A)**. Total IgA was investigated in the BAL, however no differences between maternally unvaccinated and vaccinated offspring was observed **(Figure 5.6B)**. Interestingly, PCV13-specific IgA was detected in high concentrations in the BAL of maternally vaccinated 7-week-old offspring **(Figure 5.6B)**.

A. Bacterial CFU and IgA titers in the BAL

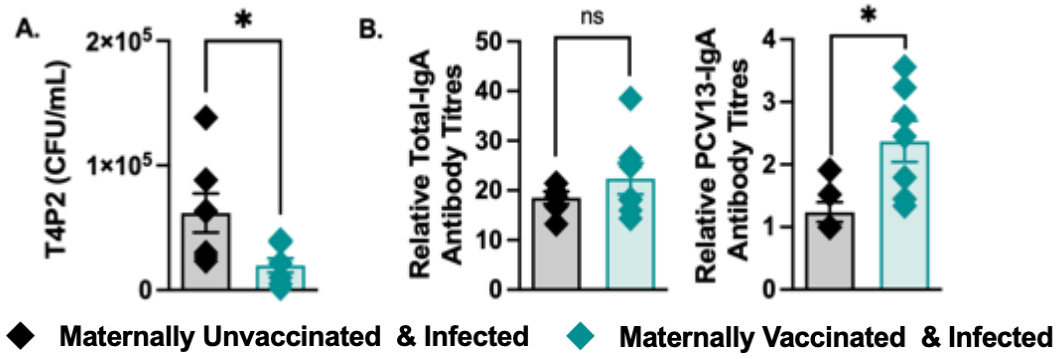

Figure 5.6: Maternally vaccinated 7-week-old offspring have reduced T4P2 CFU's and acquired maternally derived PCV13-IgA antibody in the BAL.
7-week-old offspring were either born to unvaccinated or PCV13 vaccinated dams **A.** T4P2 CFU's were recorded in the BAL of maternally vaccinated and maternally unvaccinated offspring. **B.** Total IgA and PCV13-specific IgA was identified in the BAL using ELISA. The results are expressed as individual mice/data points. Representative of 1 experiment whereby n = 5-7 mice per group. Statistical analysis was performed using a kruskal-wallis test. P values were regarded as significant if less than 0.05 (* $p<0.05$, ** $p<0.01$, *** $p<0.001$).

Total CD45$^+$ immune cells were investigated in the BAL of 7-week-old offspring. Total CD45$^+$ immune cell responses indicate that immune cells were increased in maternally unvaccinated offspring in the presence of an infection **(Figure 5.7)**. No changes in total CD45$^+$ immune cells were observed in maternally vaccinated and maternally vaccinated and infected offspring **(Figure 5.7)**.

A. Total CD45$^+$ immune cells in the BAL: maternal vs offspring cell numbers

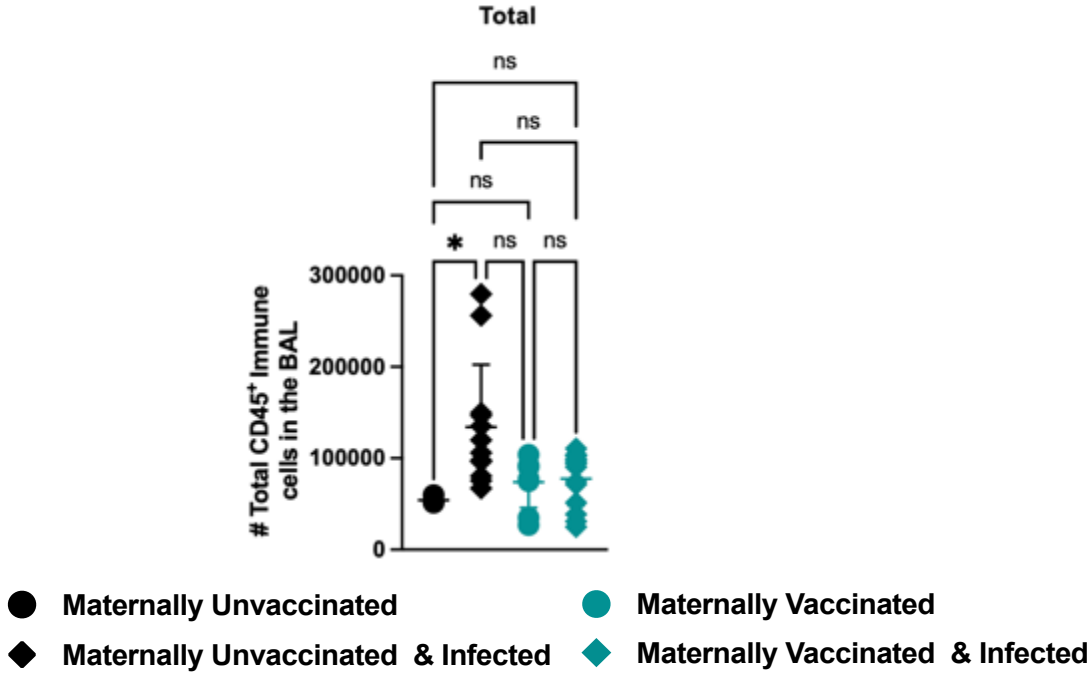

Figure 5.7: Total CD45$^+$ immune cells were significantly increased in the BAL of 7-week-old maternally unvaccinated and infected offspring.
7-week-old offspring were either born to unvaccinated or PCV13 vaccinated dams **A.** Total CD45$^+$ cell populations were investigated in the BAL. The results are expressed as individual mice/data points. Representative of 2 experiments whereby n = 5-7 mice per group. Statistical analysis was performed using a kruskal-wallis test. P values were regarded as significant if less than 0.05 (* $p<0.05$, ** $p<0.01$, *** $p<0.001$).

Total Neutrophil ($CD45^+$ $Ly6G^+$ $SiglecF^-$ $CD11b^+$ $Ly6G^+$) populations were investigated in the BAL. No differences in neutrophil numbers were recorded between maternally unvaccinated, maternally vaccinated and maternally vaccinated and infected offspring **(Figure 5.8A)**. However, neutrophil populations were increased in maternally unvaccinated and infected offspring **(Figure 5.8A)**. Maternal neutrophil ($CD45^+$ $Ly6G^+$ $SiglecF^-$ $CD11b^+$ $Ly6G^+$ $H2Dd^+$) cell populations were investigated in the BAL and no differences were observed between maternally unvaccinated and vaccinated offspring **(Figure 5.8B)**.

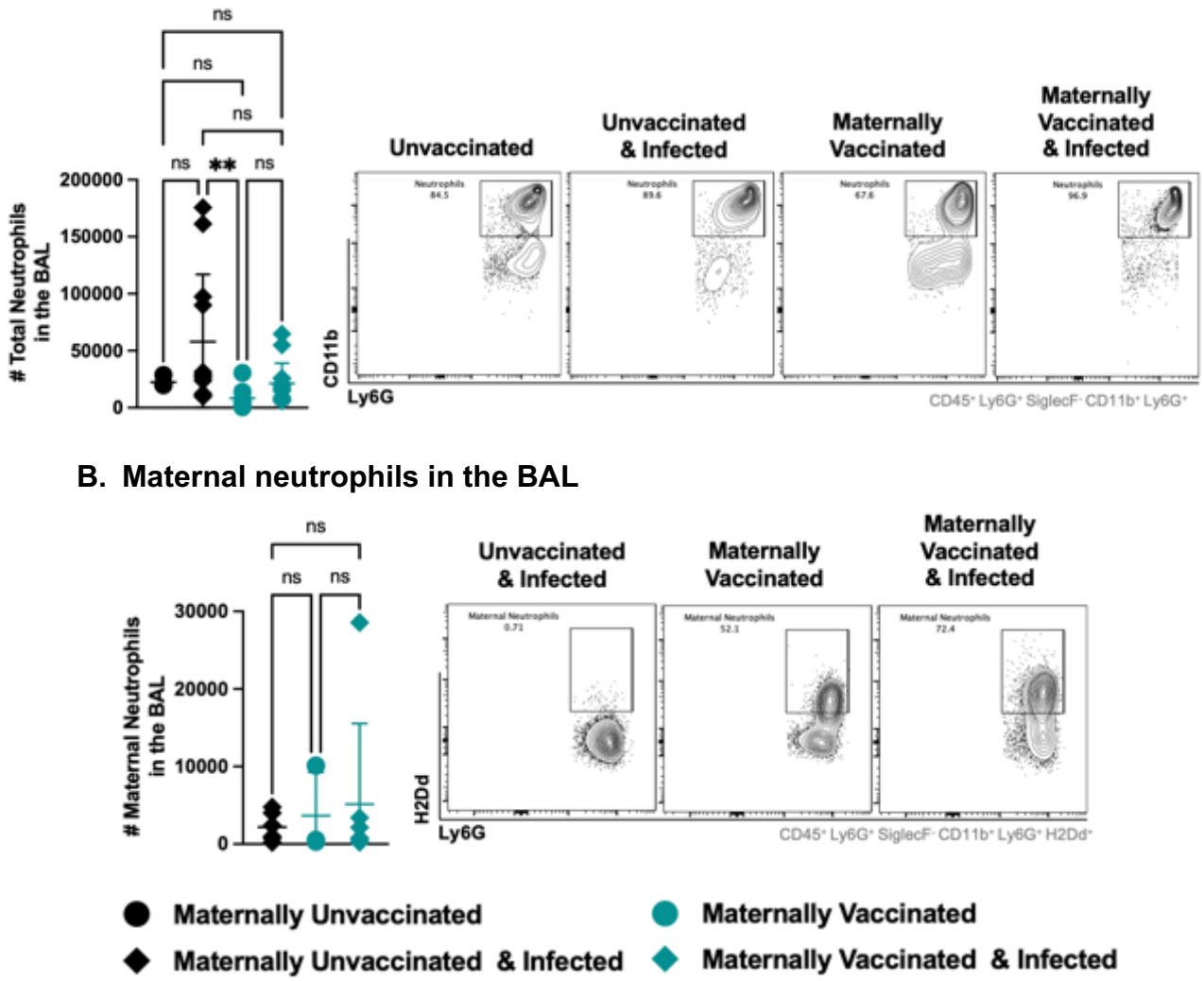

Figure 5.8: Maternally unvaccinated and infected 7-week-old offspring have increased total neutrophil populations in the BAL.
7-week-old offspring were either born to unvaccinated or PCV13 vaccinated dams **A.** Total ($CD45^+$ $Ly6G^+$ $SiglecF^-$ $CD11b^+$) and **B.** maternal ($CD45^+$ $SiglecF^-$ $CD11b^+$ $Ly6G^+$ $H2Dd^+$) neutrophil populations were investigated in the BAL. The results are expressed as individual mice/data points. Representative of 2 experiments whereby n = 5-7 mice per group. Statistical analysis was performed using a kruskal-wallis test. P values were regarded as significant if less than 0.05 (* $p<0.05$, ** $p<0.01$, *** $p<0.001$).

Total Dendritic ($CD45^+$ $Ly6G^-$ $SiglecF^-$ $MHCII^+$ $CD11c^+$) cell (DC) populations were investigated in the BAL. Maternally unvaccinated and infected offspring had significantly higher DC populations in the BAL **(Figure 5.9)**. Maternally unvaccinated, maternally vaccinated and maternally vaccinated and infected offspring had significantly reduced DC numbers when compared to maternally unvaccinated and infected offspring **(Figure 5.9)**. In addition, no differenced were observed between maternally vaccinated and maternally vaccinated and infected offspring **(Figure 5.9)**.

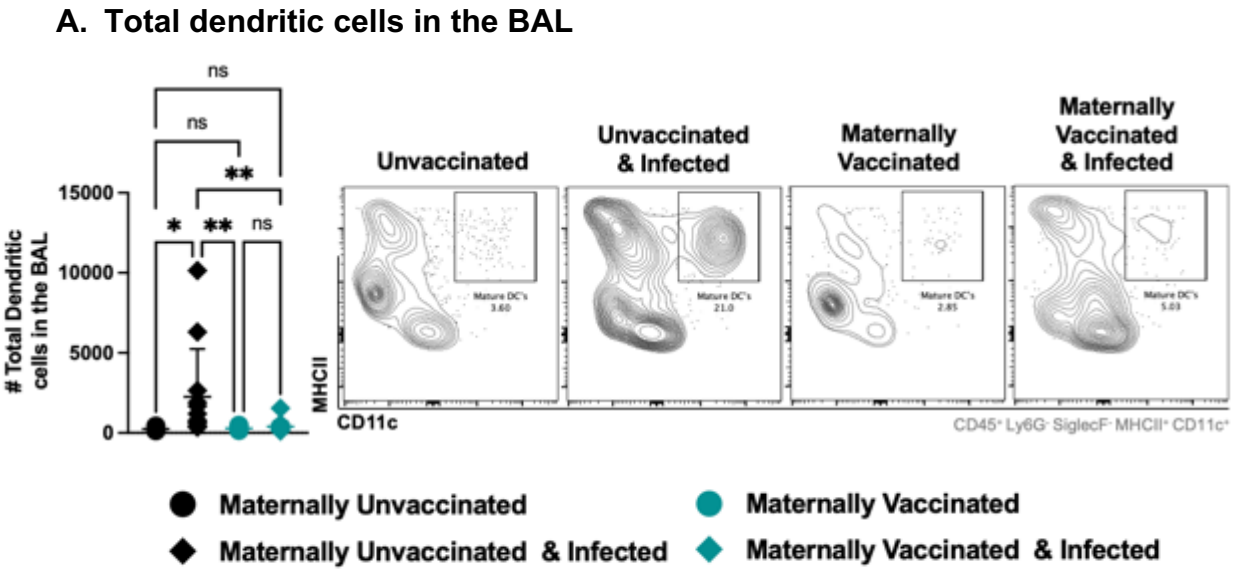

Figure 5.9: Maternally unvaccinated and infected 7-week-old offspring had significantly increased total dendritic cell populations in the BAL.
7-week-old offspring were either born to unvaccinated or PCV13 vaccinated dams **A.** Total dendritic cell ($CD45^+$ $Ly6G^-$ $SiglecF^-$ $MHCII^+$ $CD11c^+$) numbers were investigated in the BAL. The results were expressed as individual mice/data points. Representative of 2 experiments whereby n = 5-7 mice per group. Statistical analysis was performed using a kruskal-wallis test. P value were regarded as significant if less than 0.05 (* $p<0.05$, ** $p<0.01$, *** $p<0.001$).

Total alveolar macrophages ($CD45^+$ $Ly6G^-$ $SiglecF^+$ $CD11b^+$ $CD11c^+$) cell numbers were investigated in the BAL of 7-week-old offspring. No differences in total alveolar macrophages were identified between maternally unvaccinated and maternally vaccinated offspring **(Figure 5.10A)**. Maternal alveolar macrophages ($CD45^+$ $Ly6G^-$ $SiglecF^+$ $CD11b^+$ $CD11c^+$ $H2Dd^+$) were significantly higher in maternally vaccinated and infected offspring **(Figure 5.10B)**. Maternally unvaccinated and infected offspring had significantly less alveolar macrophage cell populations compared to maternally vaccinated offspring **(Figure 5.10B)**.

Total alveolar macrophages in the BAL

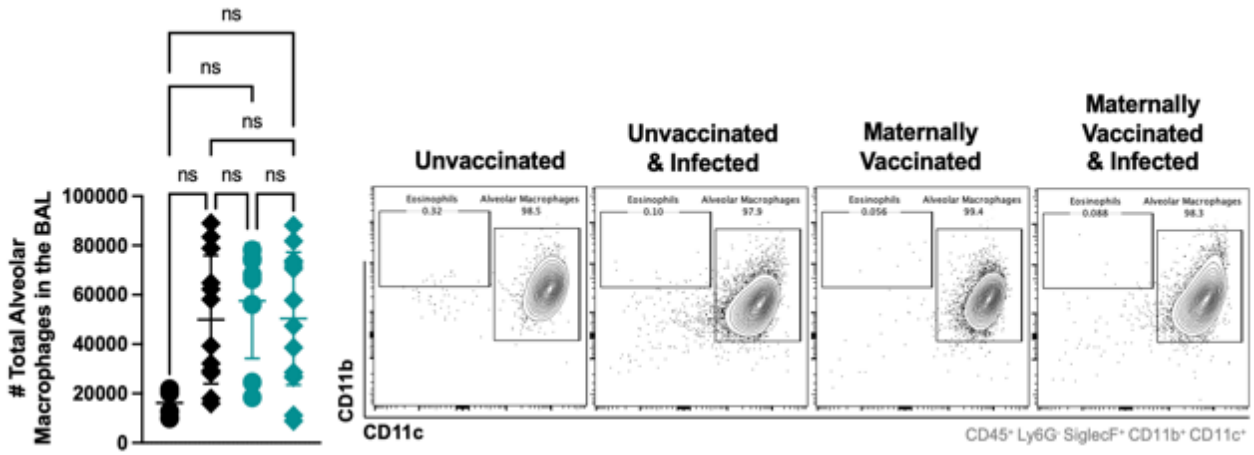

A. Maternal alveolar macrophages in the BAL

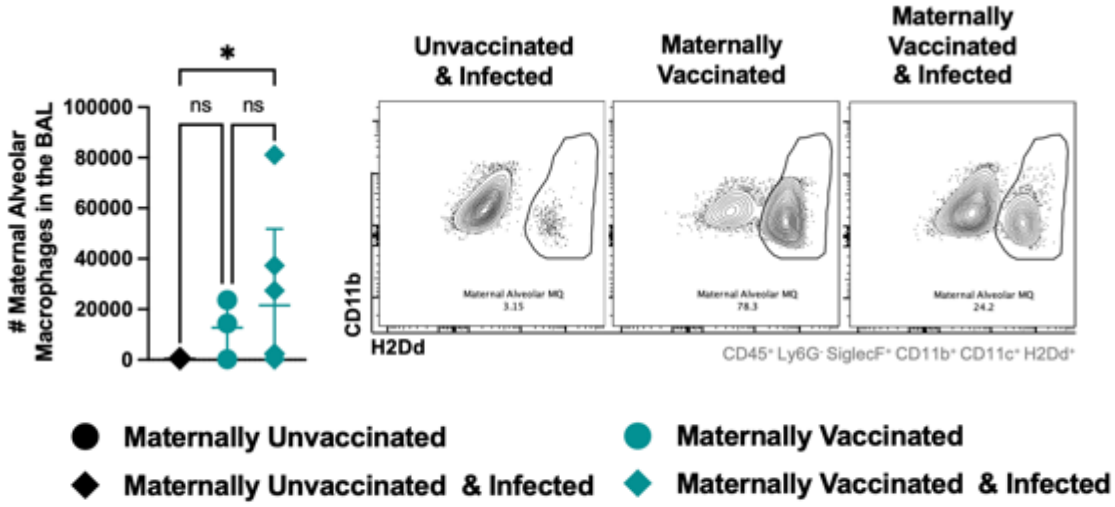

Figure 5.10: Maternally unvaccinated and infected 7-week-old offspring have increased total neutrophil populations in the BAL.
7-week-old offspring were either born to unvaccinated or PCV13 vaccinated dams **A.** Total and **B.** maternal neutrophil populations were investigated in the BAL. The results are expressed as individual mice/data points. Representative of 1 experiments whereby n = 5-7 mice per group. Statistical analysis was performed using a kruskal-wallis test. P values were regarded as significant if less than 0.05 (* p<0.05, ** p<0.01, *** p<0.001).

To investigate cell populations that may be difficult to gate, find niche cell populations and visualise cell populations in a two-dimentional (2D) plot using a unbiased approach, t-SNE (t-Distributed Stochastic Neighbour Embedding) cell population maps were formulated. BAL populations were reduced to 10 000 cells per sample, this was done by an algorithm that allowed for cell ratios to remain the same but allow for the software to function accurately, this was classified as down sampling.

Total cell population t-SNE maps were overlayed with the maternally vaccinated, maternally unvaccinated and infected and maternally vaccinated and infected offspring cell populations in the BAL **(Figure 5.11A)**. The positioning of the group clustering indicated that cells present in the BAL of maternally vaccinated and maternally vaccinated and infected offspring had similar t-SNE immune profiles whereas maternally unvaccinated and infected offspring had a significantly different t-SNE immune profiles **(Figure 5.11A)**.

The maternally unvaccinated and infected t-SNE populations were isolated graphically to visually separate the maternally unvaccinated and maternally vaccinated offspring **(Figure 5.11B)**. Total maternal ($CD45^+$ $H2Dd^+$) cells were isolated and overlayed on the offspring t-SNE map. The visual results indicated that maternal cell populations (indicated in teal) predominantly clustered in the maternally vaccinated and maternally vaccinated and infected offspring groups **(Figure 5.11B)**. However, maternal cells were present in reduced numbers in maternally unvaccinated and infected offspring **(Figure 5.11B)**. Sample ID's of total cells and maternal cells were compared using cell percentages.

Maternally vaccinated offspring accounted for 17.6% of total BAL cells while maternally unvaccinated and infected and maternally vaccinated and infected offspring accounted for 41.2% each **(Figure 5.11B)**. These sample ID's of total cells indicated that the down sampled number of events (10 000) was the same for each sample. The sample ID's of maternal cells were compared between groups and maternal cells were significantly reduced when compared to maternally vaccinated offspring **(Figure 5.11B)**. The unvaccinated and infected offspring contained 24.6% of the maternal cells whereas maternally vaccinated offspring and maternally vaccinated and infected offspring contained 52.9% and 22.5% respectively **(Figure 5.11B)**.

Cell marker intensities were displayed as on t-SNE marker heatmaps in 7-week-old offspring **(Figure 5.11C)**. Neutrophil markers Ly6G, CD11b, H2Dd and alveolar macrophage markers CD11b, CD11c, H2Dd markers were intensified in the maternal cell populations **(Figure 5.11C)**. In addition, DC markers MHCII and CD11c markers were also intensified in marker heatmaps **(Figure 5.11C)**. The results from the t-SNE analysis reiterates the results generated from the manual gating **(Figure 5.11C)**.

A. BAL t-SNE: Group profiles

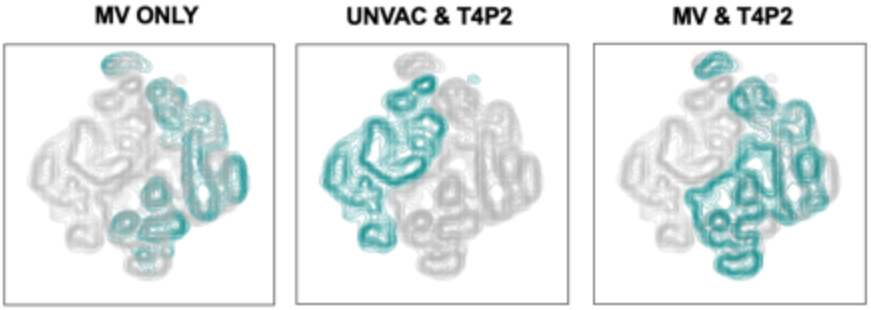

B. Maternal BAL population highlighted in t-SNE plot.

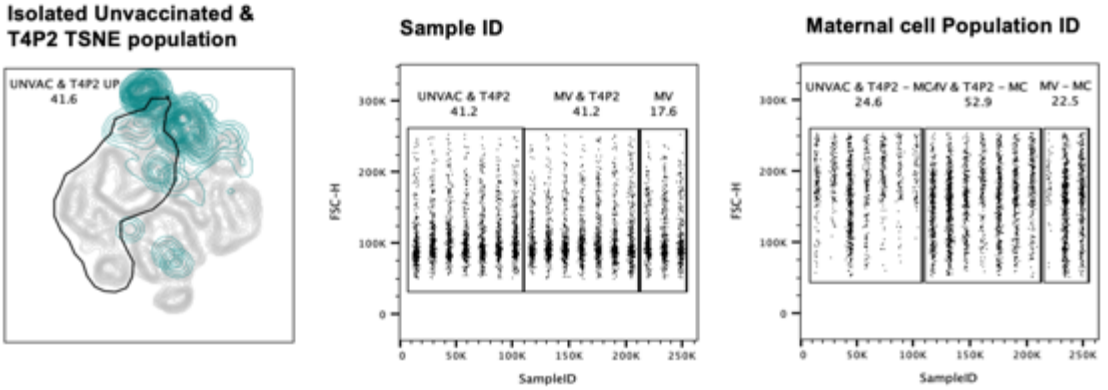

C. Heatmaps of total cell populations

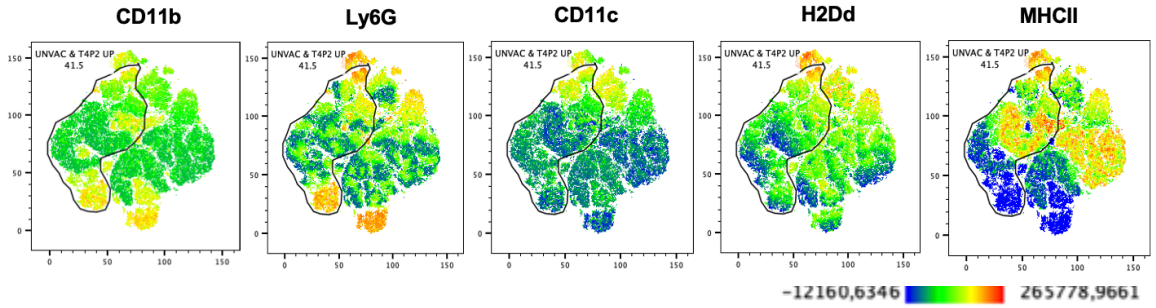

Figure 5.11: t-SNE analysis indicates that offspring have increased maternal neutrophil and alveolar macrophage populations in the BAL of maternally vaccinated 7-week-old offspring.

7-week-old offspring were either born to unvaccinated or PCV13 vaccinated dams **A.** A t-SNE population map was formulated and overlayed each group to display individual group population maps. **B.** The maternally unvaccinated and infected t-SNE population was separated, and maternal cells were isolated. Sample ID's of total cells and maternal cells were compared using cell percentages. **C.** t-SNE heatmaps display marker intensities of maternally unvaccinated and vaccinated offspring. The results are expressed as individual mice/data points. Representative of 1 experiment whereby n = 3-7 mice per group. Statistical analysis was performed using a kruskal-wallis test. P value were regarded as significant if less than 0.05 (* p<0.05, ** p<0.01, *** p<0.001).

5. 2.5 Maternally vaccinated offspring had reduced CFU titres in the lung and a distinct intrinsic IgG2a^{+} expressing B cell population in the lung.

7-week-old maternally unvaccinated and vaccinated and offspring were infected with 1X10^{7} T4P2 bacteria intranasally and euthanized 48h after infection. The lungs were processed into single cell suspensions and plated on BAB agar plates for 16h at 37°C. T4P2 CFU's were significantly elevated in the lungs of maternally unvaccinated and infected offspring whereas no CFU's were recorded in maternally vaccinated and infected offspring **(Figure 5.12)**.

A. T4P2 CFU's present in the lung of 7-week-old offspring.

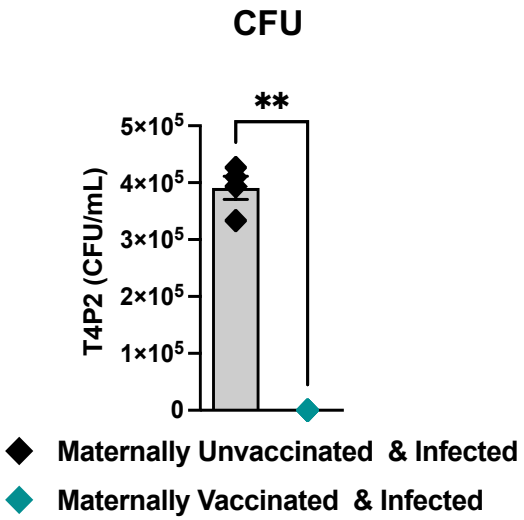

Figure 5.12: Maternally vaccinated 7-week-old offspring have reduced T4P2 CFU's in the lung.
7-week-old offspring were either born to unvaccinated or PCV13 vaccinated dams **A.** T4P2 CFU's were recorded in the lung of maternally unvaccinated and vaccinated offspring. The results are expressed as individual mice/data points. Representative of 2 experiments whereby n = 5-7 mice per group. Statistical analysis was performed using a kruskal-wallis test. P values were regarded as significant if less than 0.05 (* p<0.05, ** p<0.01, *** p<0.001).

The lungs were processed into single cell suspensions and prepared for flow cytometry analysis. Immune cell populations were investigated, and cell markers were used to further classify maternal immune cell populations. Offspring ($CD45^+$ $H2Kb^+$ $H2Dd^-$) and maternal ($CD45^+$ $H2Kb^+$ $H2Dd^+$) cell percentages were displayed graphically **(Figure 5.13)**. Maternally vaccinated offspring had 6% more maternal immune cells compared to maternally unvaccinated offspring **(Figure 5.13)**. Maternally unvaccinated offspring had a 5% increase in maternal cells in the presence of T4P2 infection **(Figure 5.13)**. Maternally vaccinated offspring had an intrinsic maternal immune cell population present in the lungs and therefore maternal cells did not increase significantly in the presence of infection **(Figure 5.13)**.

A. Total $CD45^+$ immune cells in the lung: maternal vs offspring cell percentages

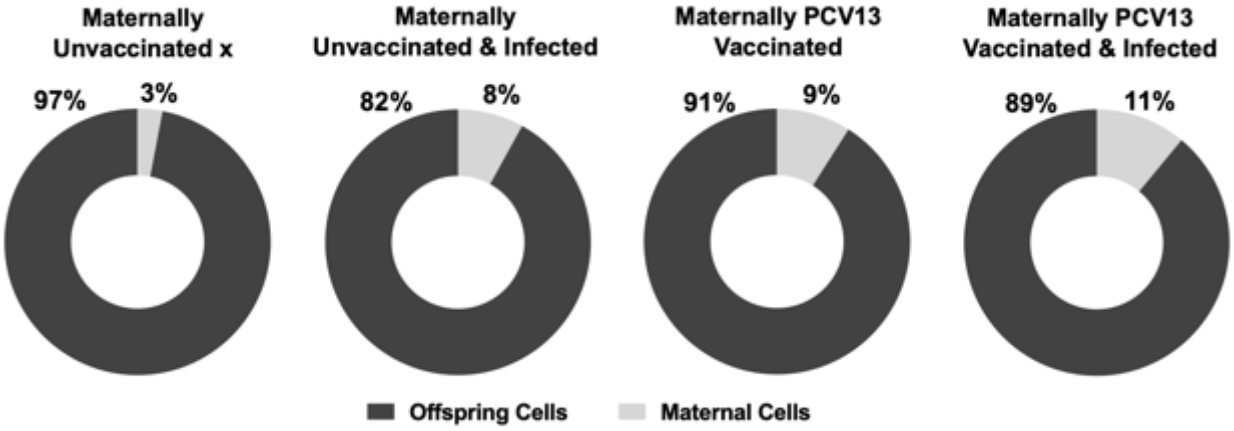

Figure 5.13: Maternally vaccinated offspring have increased maternal cell populations in the lung.
7-week-old offspring were either born to unvaccinated or PCV13 vaccinated dams.
A. Offspring and maternal cell percentages were investigated in the lungs. All cell populations were identified using flow cytometry. The results are expressed as individual mice/data points. Representative of 1 experiment whereby n = 5-9 mice per group. Statistical analysis was performed using a Kruskal-Wallis test. P value were regarded as significant if less than 0.05 (* $p<0.05$, ** $p<0.01$, *** $p<0.001$).

$CD45^+$ immune cell numbers were investigated in the lung. Total $CD45^+$ immune cell populations indicate that maternally unvaccinated offspring had reduced cell numbers however cell numbers increased in the presence of a T4P2 infection **(Figure 5.14A)**. Maternally vaccinated offspring had an increased total $CD45^+$ immune cell numbers which decreased in the presence of infection **(Figure 5.14A)**. Total $CD45^+$ immune cell numbers were significantly decreased in maternally vaccinated and infected offspring when compared to maternally unvaccinated and infected offspring **(Figure 5.14A)**. Offspring ($CD45^+$ $H2Kb^+$ $H2Dd^-$) cells were investigated, and no differences were observed between maternally unvaccinated and vaccinated offspring **(Figure 5.14A)**.

Maternal ($CD45^+$ $H2Kb^+$ $H2Dd^+$) cells were significantly elevated in maternally unvaccinated offspring in the presence of infection **(Figure 5.14A)**. Maternally vaccinated offspring had an increased maternal cell populations however no changes were observed in the presence of infection **(Figure 5.14A)**. The same trend was observed in the FSC plots whereby no differences were observed in offspring cell numbers and only maternally unvaccinated offspring had significantly reduced maternal cells **(Figure 5.14B)**.

$CD19^+$ $B220^+$ B cells were investigated in the lungs of 7-week-old offspring. No differences or trends were observed between total ($CD45^+$ $B220^+$), offspring ($H2Kb^+$ $H2Dd^-$ $B220^+$) and maternal ($H2Kb^+$ $H2Dd^+$ $B220^+$) cells in maternally unvaccinated and vaccinated offspring **(Figure 5.15A-C)**.

A. CD45⁺ immune cells in the lung: maternal vs offspring cell numbers

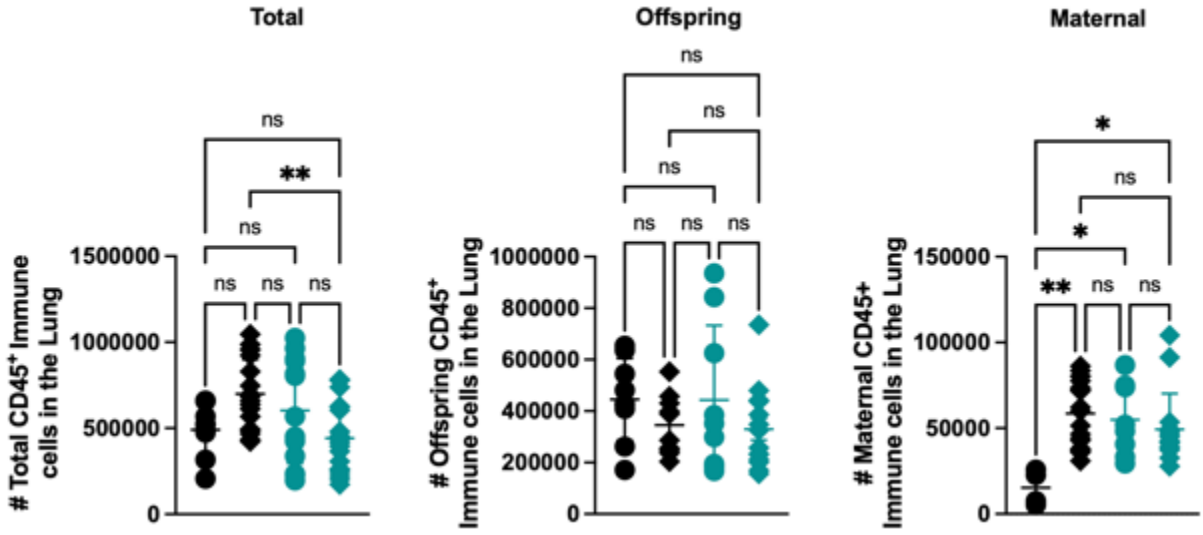

B. Maternal vs offspring CD45⁺ immune cells FSC plots in the lung.

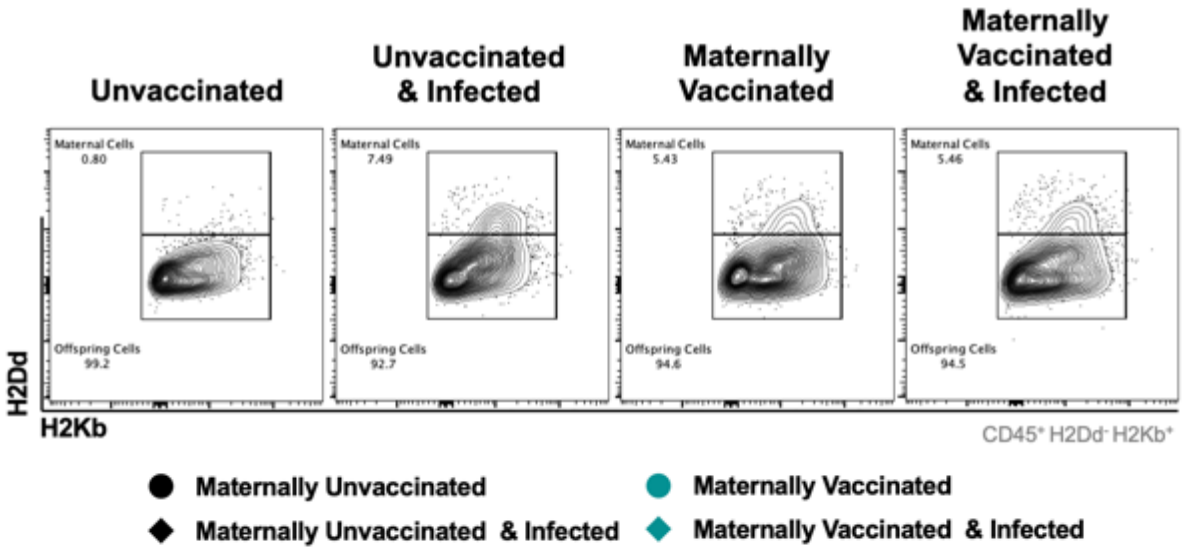

Figure 5.14: Maternally vaccinated offspring have an intrinsic maternal cell population in the lungs.
7-week-old offspring were either born to unvaccinated or PCV13 vaccinated dams **A.** Total (CD45⁺), Offspring (CD45⁺ H2Kb⁺ H2Dd⁻) and maternal (CD45⁺ H2Kb⁺ H2Dd⁺) Immune cell populations were investigated in the lungs. **B.** FCS files of maternal and offspring CD45⁺ cell populations were investigated in the lungs. Representative of 2 experiments whereby n = 5-8 mice per group. Statistical analysis was performed using a Kruskal-Wallis test. P value were regarded as significant if less than 0.05 (* p<0.05, ** p<0.01, *** p<0.001).

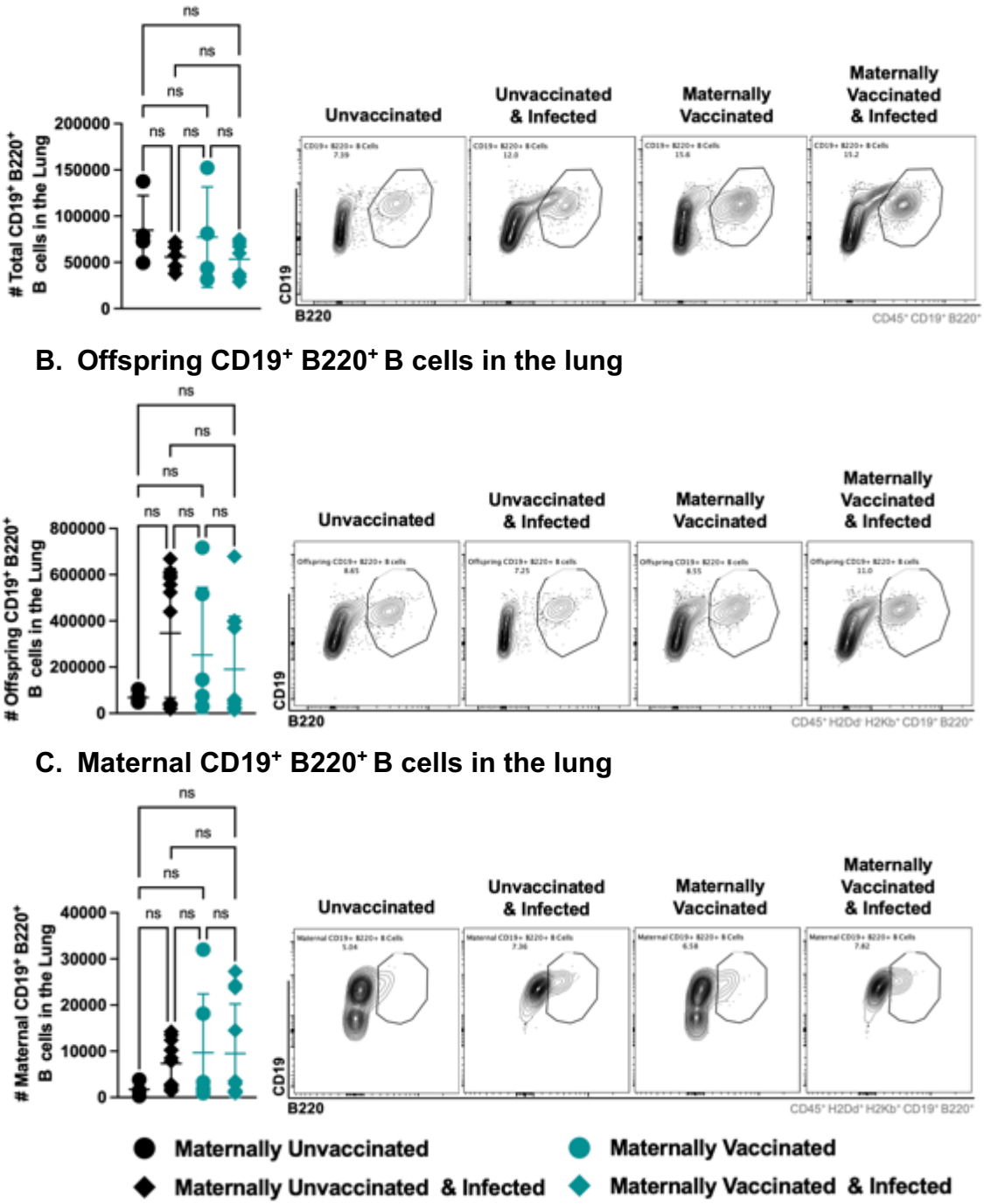

Figure 5.15: No differences in CD19+ B220+ B cells were observed between maternally unvaccinated and vaccinated offspring.
7-week-old offspring were either born to unvaccinated or PCV13 vaccinated dams. **A.** Total ($CD45^+$ $CD19^+$ $B220^+$), **B.** Offspring ($H2Kb^+$ $H2Dd^-$ $CD19^+$ $B220^+$) and **C.** maternal ($H2Kb^+$ $H2Dd^+$ $CD19^+$ $B220^+$) B cell populations were investigated in the lungs. Representative of 2 experiments whereby n = 4-7 mice per group. Statistical analysis was performed using a Kruskal-Wallis test. P value was regarded as significant if less than 0.05 (* $p<0.05$, ** $p<0.01$, *** $p<0.001$).

Total plasma cells ($CD45^+$ $B220^+$ $CD138^+$ $TACI^+$) were investigated in the lungs. Plasma cells were slightly elevated in maternally vaccinated offspring when compared to maternally unvaccinated offspring **(Figure 5.16)**. In addition, T4P2 infection had no significant effect on plasma cell populations in both maternally unvaccinated and vaccinated offspring in the lung **(Figure 5.16)**.

A. Total plasma cells in the lung

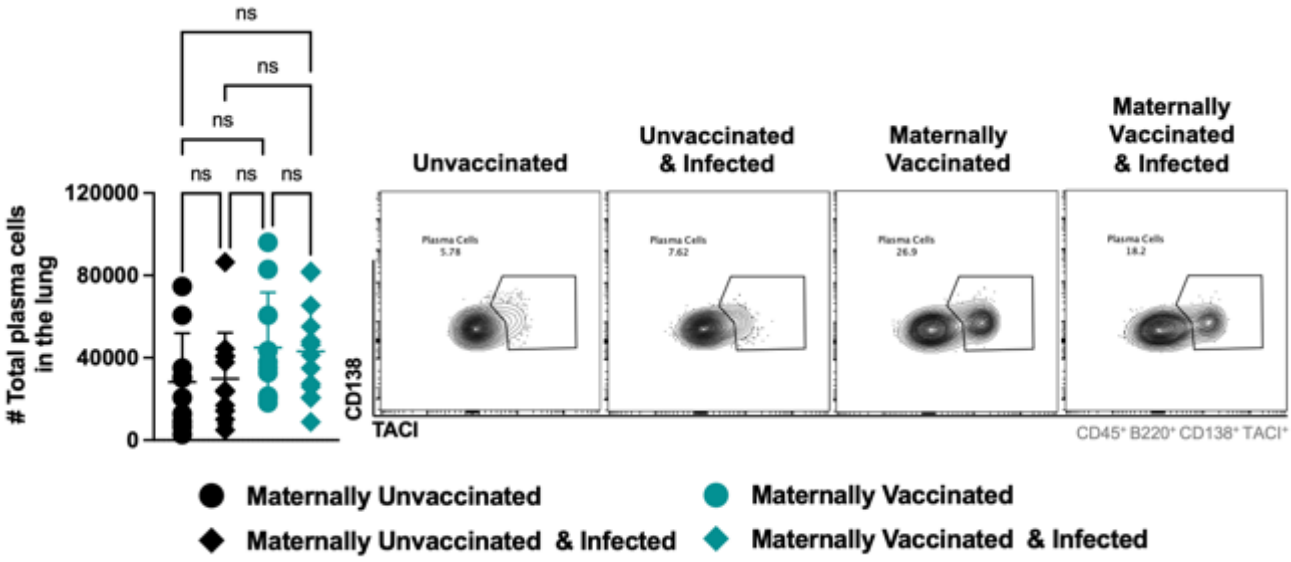

Figure 5.16: Total plasma cell populations were slightly elevated in maternally vaccinated 7-week-old offspring.
7-week-old offspring were either born to unvaccinated or PCV13 vaccinated dams. **A.** Total plasma cells ($CD45^+$ $B220^+$ $CD138^+$ $TACI^+$) populations were investigated in the lung. Representative of 2 experiments whereby n = 5-8 mice per group. Statistical analysis was performed using a Kruskal-Wallis test. P value were regarded as significant if less than 0.05 (* $p<0.05$, ** $p<0.01$, *** $p<0.001$).

Total IgG1$^+$ (CD45$^+$ CD19$^+$ IgG1$^+$) expressing B cells were examined in the lungs and no differences were observed between maternally unvaccinated and vaccinated offspring **(Figure 5.17A)**. No differences in maternal IgG1$^+$ (CD45$^+$ H2Dd$^+$ CD19$^+$ IgG1$^+$) expressing B cells were present between maternally unvaccinated and maternally unvaccinated and infected offspring **(Figure 5.17B)**. Maternal IgG1$^+$ expressing B cells were slightly elevated in the maternally vaccinated offspring but reduced in the presence of infection **(Figure 5.17B)**. Maternal IgG1$^+$ expressing B cell numbers were not altered by infection in both maternally unvaccinated and vaccinated offspring **(Figure 5.17B)**.

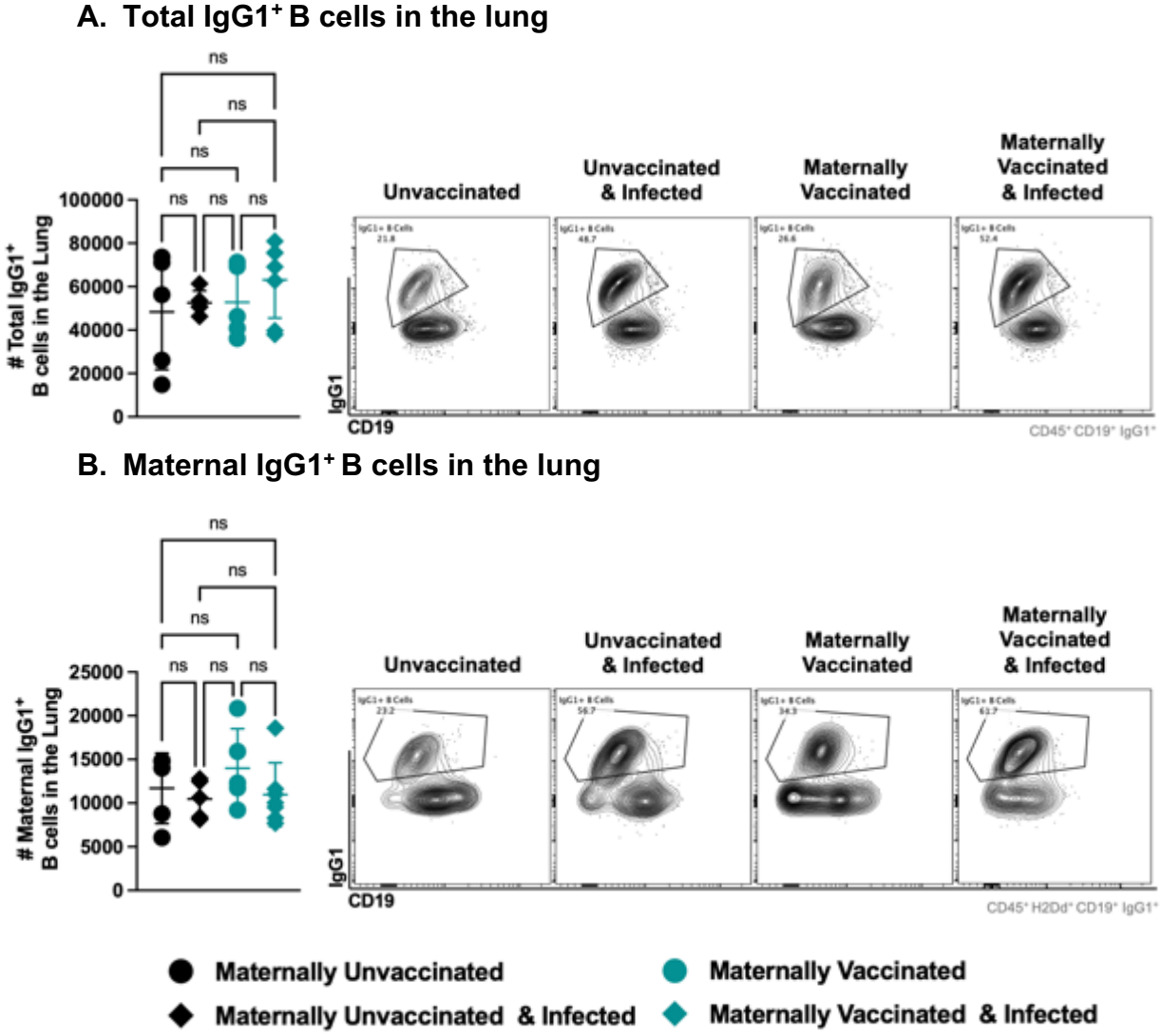

Figure 5.17: Maternal IgG1$^+$ expressing B cell populations were slightly elevated in maternally vaccinated 7-week-old offspring.
7-week-old offspring were either born to unvaccinated or PCV13 vaccinated dams. **A.** Total IgG1$^+$ (CD45$^+$ CD19$^+$ IgG1$^+$) and **B.** maternal IgG1$^+$ (CD45$^+$ H2Dd$^+$ CD19$^+$ IgG1$^+$) expressing B cells populations were investigated in the lungs. Representative of 2 experiments whereby n = 3-6 mice per group. Statistical analysis was performed using a Kruskal-Wallis test. P value were regarded as significant if less than 0.05 (* p<0.05, ** p<0.01, *** p<0.001).

Total IgG2a$^+$ expressing B cells were significantly increased in the maternally vaccinated offspring but no differences were observed in total IgG2a$^+$ expressing B cells in the remaining groups **(Figure 5.18A)**. No significant differences in maternal IgG2a$^+$ expressing B cells were observed in maternally unvaccinated and vaccinated offspring **(Figure 5.18B)**. However, a similar trend was seen as maternally vaccinated offspring had slightly elevated maternal IgG2a$^+$ expressing B cells **(Figure 5.18B)**.

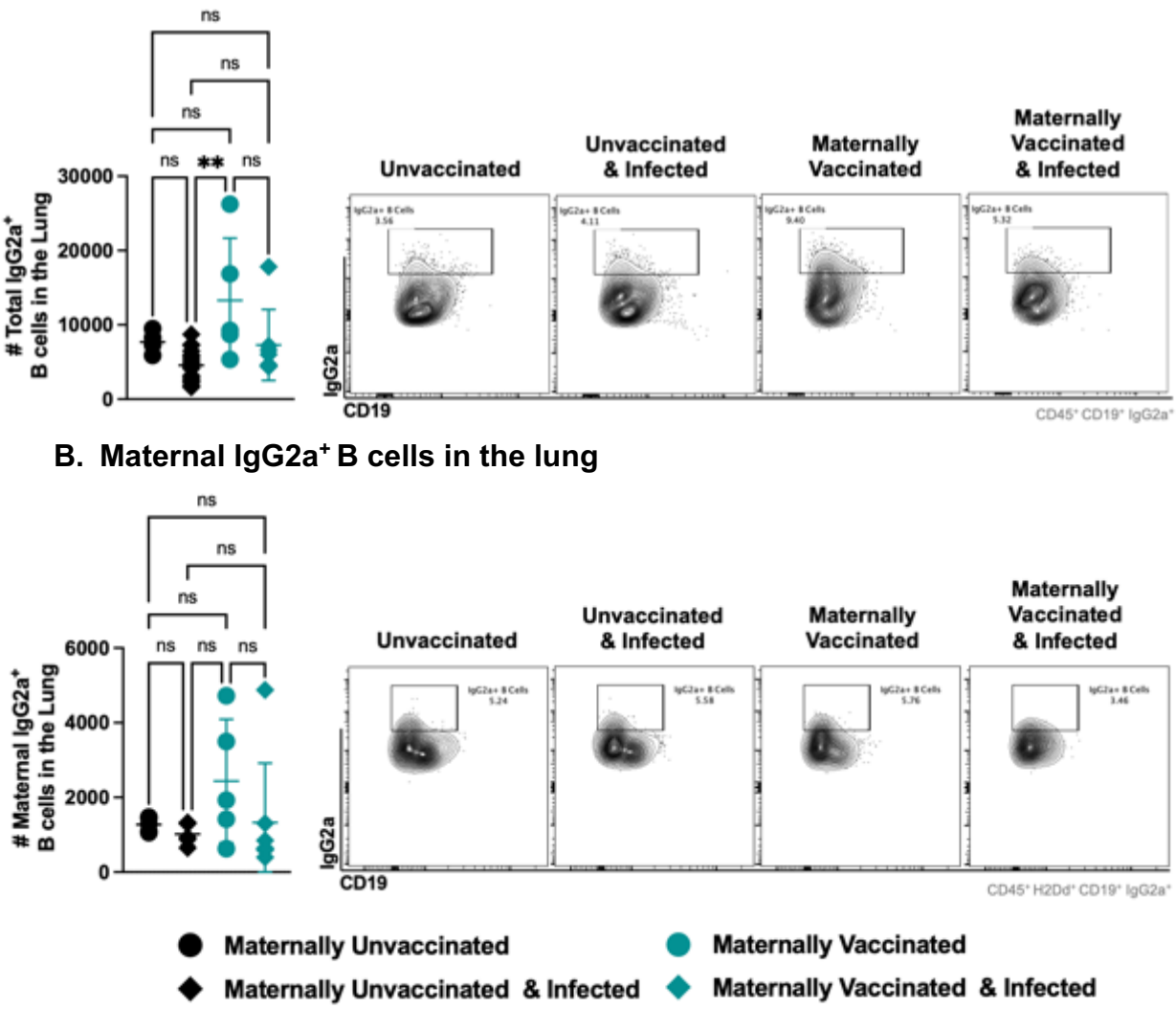

Figure 5.18: No significant differences were observed in Total IgG2a+ expressing B cell populations in the lungs of maternally unvaccined and vaccinated 7-week-old offspring.

7-week-old offspring were either born to unvaccinated or PCV13 vaccinated dams. **A.** Total IgG2a+ (CD45+ CD19+ IgG2a+) and **B.** maternal IgG2a+ (CD45+ CD19+ IgG2a+) expressing B cell populations were investigated in the lungs. Representative of 2 experiments whereby n = 4-7 mice per group. Statistical analysis was performed using a Kruskal-Wallis test. P value was regarded as significant if less than 0.05 (* p<0.05, ** p<0.01, *** p<0.001).

5. 2.6 Maternally vaccinated offspring secrete PCV13 specific antibodies from bone marrow cells.

Femurs were flushed with sterile 1X PBS and bone marrow cells were processed into single cell suspensions. $1X10^7$ bone marrow cells were plated in RPMI media supplemented with 10% FBS and supernatants were collected 24h later. PCV13-specific total IgG, IgG1 and IgG2a antibodies were investigated in supernatants using ELISA. PCV13-specific IgG and IgG1 were detected in maternally vaccinated offspring **(Figure 5.19)**. However, no PCV13-specific IgG2a antibodies were detected in maternally vaccinated offspring. No PCV13-specififc antibodies were detected in the maternally unvaccinated offspring **(Figure 5.19)**.

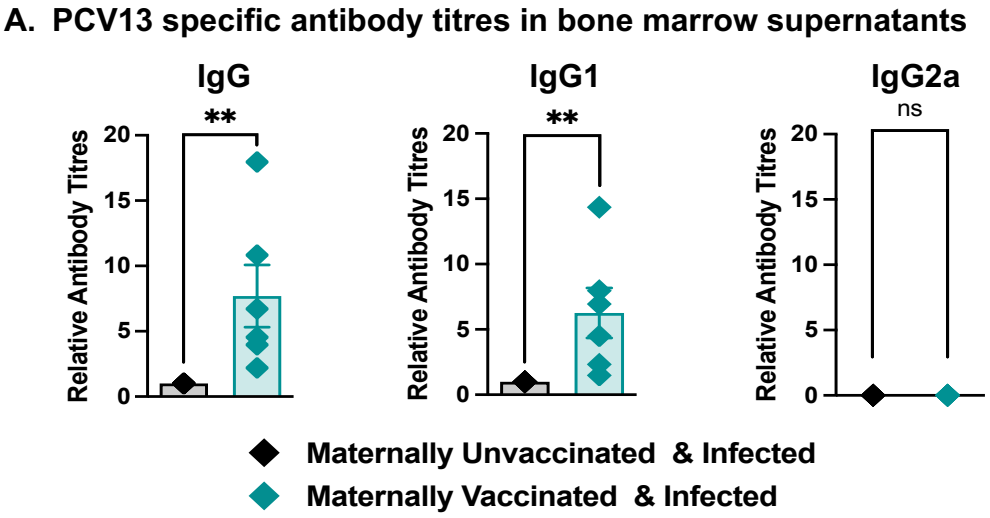

Figure 5.19: 7-week-old maternally vaccinated offspring have bone marrow cells that secrete PCV13 specific IgG and IgG1
Dams were either left unvaccinated or vaccinated with PCV13 one week before mating. **A.** PCV13-specific antibodies were screened in bone marrow supernatants using ELISA. The results are expressed as individual mice/data points. Representative of 1 experiment whereby n = 8 mice per group. Statistical analysis was performed using a Mann-Whitney. P value were regarded as significant if less than 0.05 (* $p<0.05$, ** $p<0.01$, *** $p<0.001$).

CD45$^+$ immune cell percentages were investigated in the bone marrow. No differences were observed between maternally unvaccinated and maternally vaccinated offspring **(Figure 5.20)**. In the presence of infection, maternal immune cells migrate out of the bone marrow and were significantly reduced in both maternally unvaccinated and vaccinated offspring **(Figure 5.20)**.

A. Total CD45$^+$ immune cells in the bone marrow: maternal vs offspring cell percentages

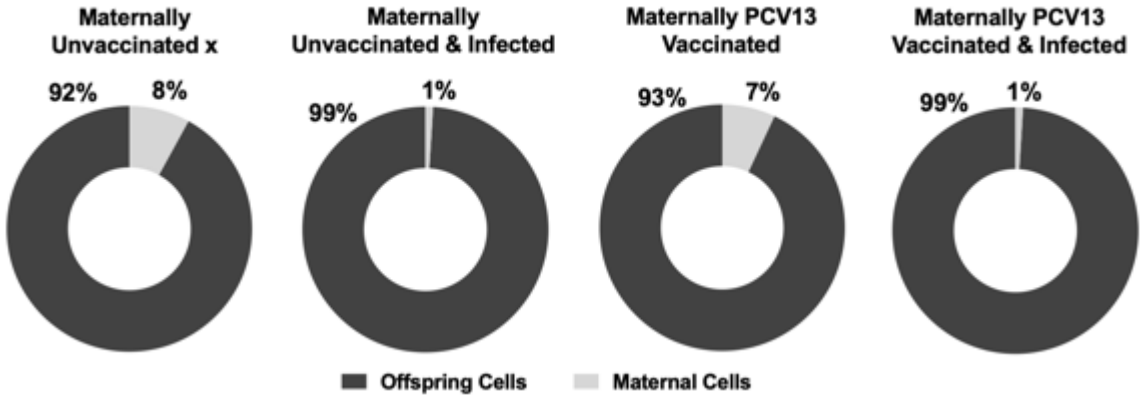

Figure 5.20: Figure 5: Maternal CD45$^+$ cell percentages decrease in the bone marrow upon infection in 7-week-old offspring.
7-week-old offspring were either born to unvaccinated or PCV13 vaccinated dams. **A.** Offspring and maternal cell percentages were investigated in the lung. All cell populations were identified using flow cytometry. The results are expressed as individual mice/data points. Representative of 1 experiment whereby n = 5-9 mice per group. Statistical analysis were performed using a Kruskal-Wallis test. P values were regarded as significant if less than 0.05 (* $p<0.05$, ** $p<0.01$, *** $p<0.001$).

Total $CD45^+$ immune cell numbers in the bone marrow reveal that no difference in cell numbers were observed between maternally unvaccinated and vaccinated offspring. However, in the presence of an infection, both maternally unvaccinated and vaccinated offspring had increased total $CD45^+$ immune cell numbers in the bone marrow **(Figure 5.21A)**. The same trend was observed for offspring ($CD45^+$ $H2Kb^+$ $H2Dd^-$) cells but interestingly the opposite effect was seen for maternal cells **(Figure 5.21A)**. Maternal cells were reduced in maternally unvaccinated and infected offspring and even greater significantly reduced in maternally vaccinated and infected offspring (**Figure 5.21A**). Total $CD45^+$ immune populations were split into maternal and offspring groups and visualised on FCS plots **(Figure 5.21B)**. It was observed that distinct maternal cell populations were present in maternally unvaccinated and vaccinated offspring however populations were significantly reduced in the presence of infection in maternally unvaccinated and vaccinated offspring **(Figure 5.21B)**.

Total ($CD45^+$ $CD19^+$ $B220^+$) and offspring ($H2Kb^+$ $H2Dd^-$ $CD19^+$ $B220^+$) B cells followed the same trend as total and offspring immune cells **(Figure 5.22A, B)**. Total and Offspring B cells increased in the presence of infection in maternally unvaccinated and vaccinated offspring **(Figure 5.22A, B)**. Interestingly no differences or trends were observed in maternal ($H2Kb^+$ $H2Dd^+$ $CD19^+$ $B220^+$) B cells in maternally unvaccinated and vaccinated offspring **(Figure 5.22C)**.

A. CD45⁺ immune cells in the bone marrow: maternal vs offspring cell numbers

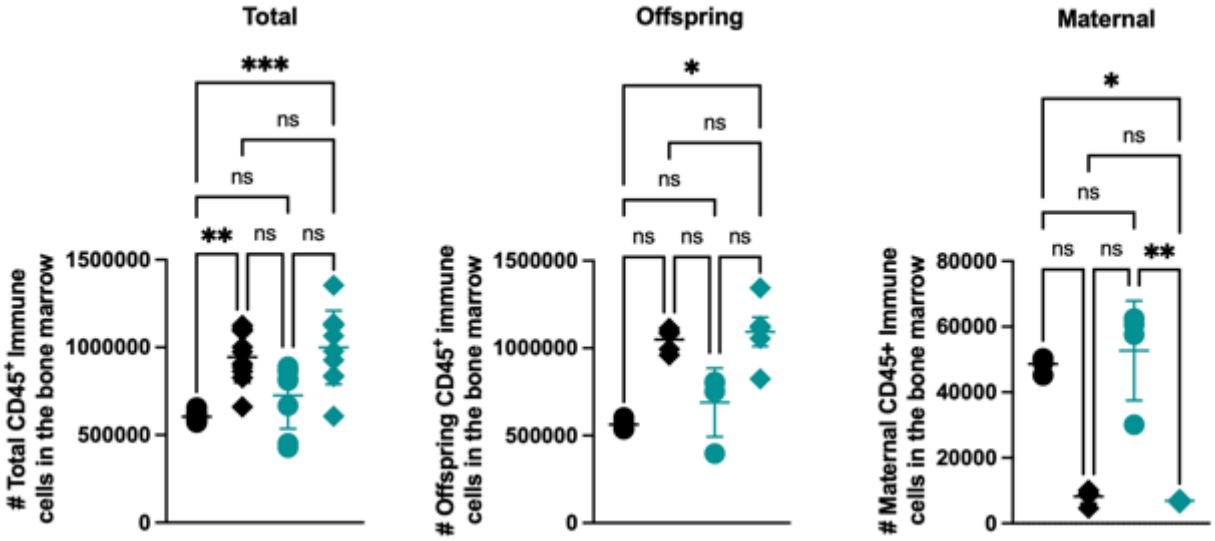

B. Maternal vs offspring CD45⁺ immune cells FSC plots in the bone marrow.

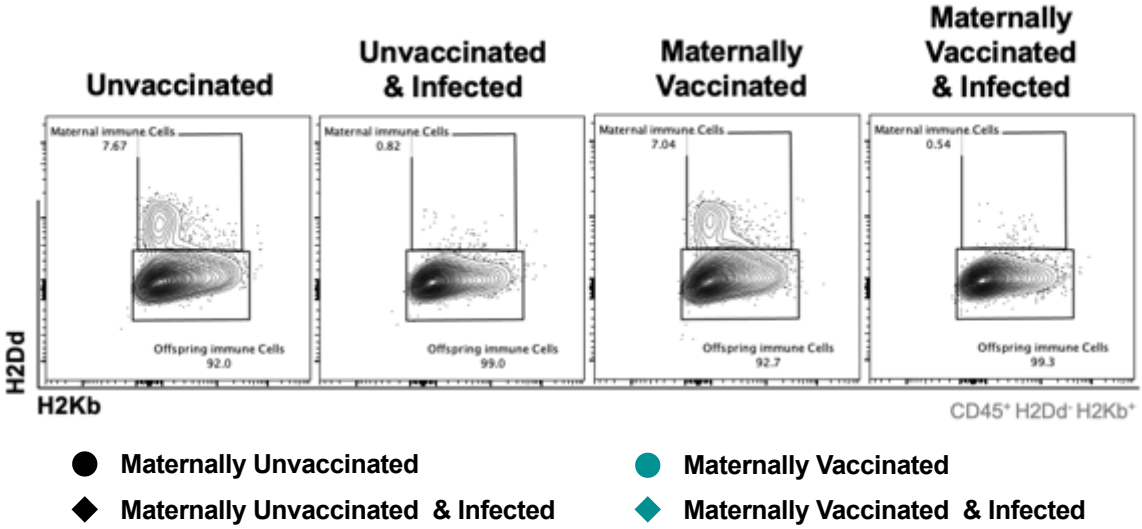

Figure 5.21: Maternal CD45⁺ cells migrate out of the bone marrow upon infection in 7-week-old offspring.

7-week-old offspring were either born to unvaccinated or PCV13 vaccinated dams **A.** Total (CD45⁺), Offspring (CD45⁺ H2Kb⁺ H2Dd⁻) and maternal (CD45⁺ H2Kb⁺ H2Dd⁺) cell populations were investigated in the bone marrow. **B.** FSC plots were investigated and total CD45⁺ cells were divided into offspring and maternal cell populations. The results are expressed as individual mice/data points. Representative of 1 experiment whereby n = 5-8 mice per group. Statistical analysis was performed using a Mann-Whitney. P value were regarded as significant if less than 0.05 (* $p<0.05$, ** $p<0.01$, *** $p<0.001$).

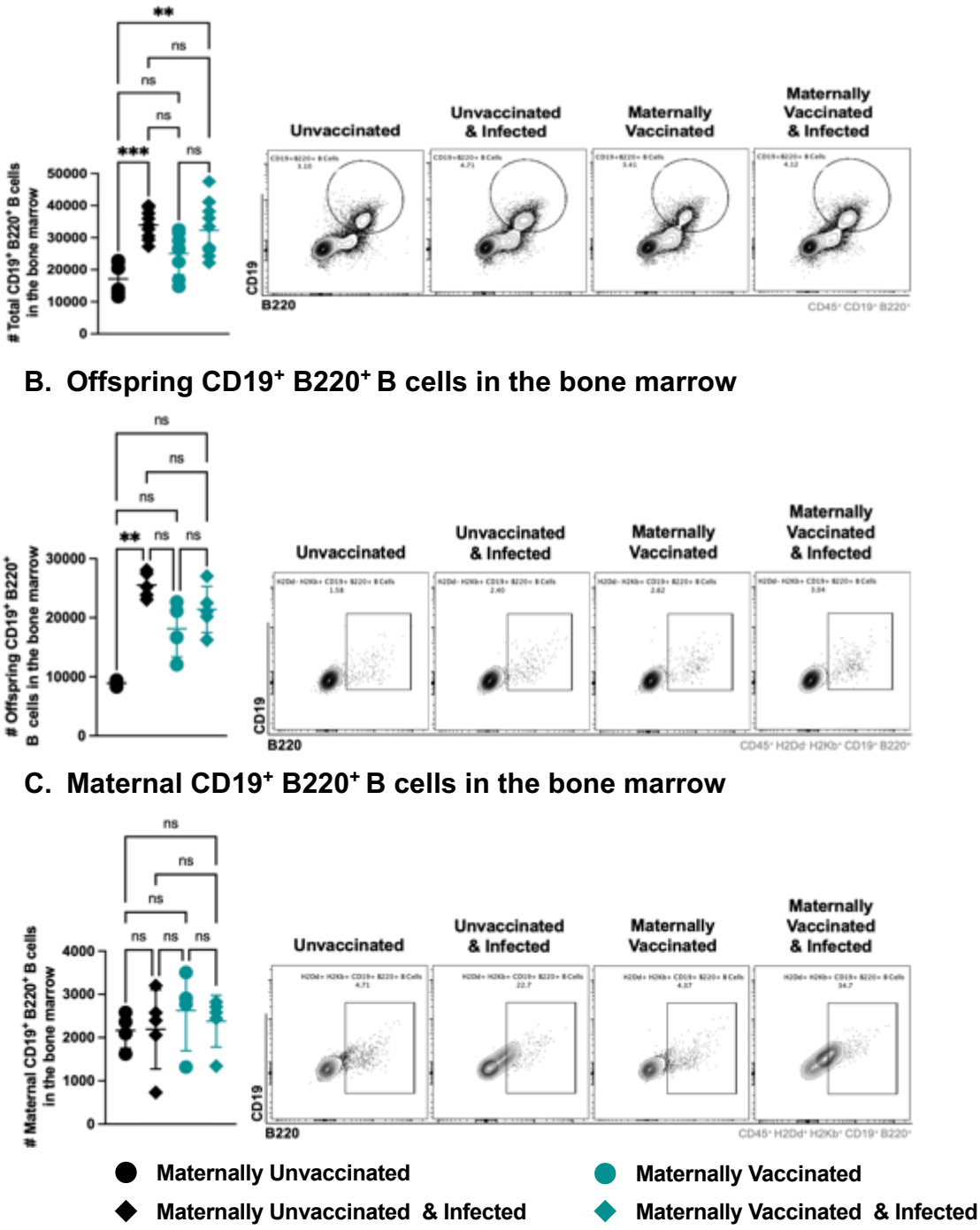

Figure 5.22: Maternal B220+ B cells are reduced in WT maternally vaccinated and infected 7-week-old offspring in the bone marrow.
7-week-old offspring were either born to unvaccinated or PCV13 vaccinated dams. **A.** Total ($CD45^+$ $CD19^+$ $B220^+$), **B.** Offspring ($H2Kb^+$ $H2Dd^-$ $CD19^+$ $B220^+$) and **C.** maternal ($H2Kb^+$ $H2Dd^+$ $CD19^+$ $B220^+$) B cell populations were investigated in the bone marrow. Representative of 1 experiment whereby n = 5-8 mice per group. Statistical analysis was performed using a Kruskal-Wallis test. P values were regarded as significant if less than 0.05 (* $p<0.05$, ** $p<0.01$, *** $p<0.001$).

Total plasma cells ($CD45^+$ $B220^+$ $CD138^+$ $TACI^+$) were slightly elevated in maternally vaccinated offspring but no apparent differences were obsereved in the presence of infection **(Figure 5.23)**.

A. Total plasma cells in the bone marrow

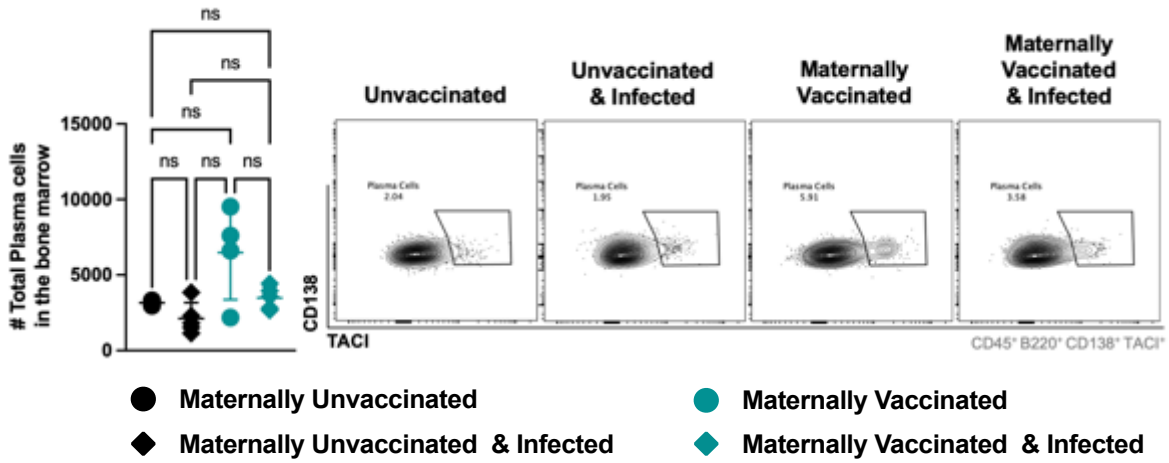

Figure 5.23: No differences in total plasma cell populations were observed between maternally unvaccinated and vaccinated offspring.
7-week-old offspring were either born to unvaccinated or PCV13 vaccinated dams. **A.** Total plasma cells ($CD45^+$ $B220^+$ $CD138^+$ $TACI^+$) populations were investigated in the bone marrow. Representative of 1 experiment whereby n = 5-8 mice per group. Statistical analysis was performed using a Kruskal-Wallis test. P value were regarded as significant if less than 0.05 (* $p<0.05$, ** $p<0.01$, *** $p<0.001$).

Total $IgG1^+$ ($CD45^+$ $CD19^+$ $IgG1^+$) and maternal $IgG1^+$ ($CD45^+$ $H2Dd^+$ $CD19^+$ $IgG1^+$) expressing B cells were increased in maternally unvaccinated and infected offspring **(Figure 5.24)**. However no difference were observed in between maternally vaccinated and maternally vaccinated and infected offspring **(Figure 5.24)**. No differences were observed total $IgG2a^+$ ($CD45^+$ $CD19^+$ $IgG2a^+$) and maternal $IgG2a^+$ ($CD45^+$ $H2Dd^+$ $CD19^+$

IgG2a$^+$) expressing B cells in maternally unvaccinated and vaccinated offspring **(Figure 5.25)**.

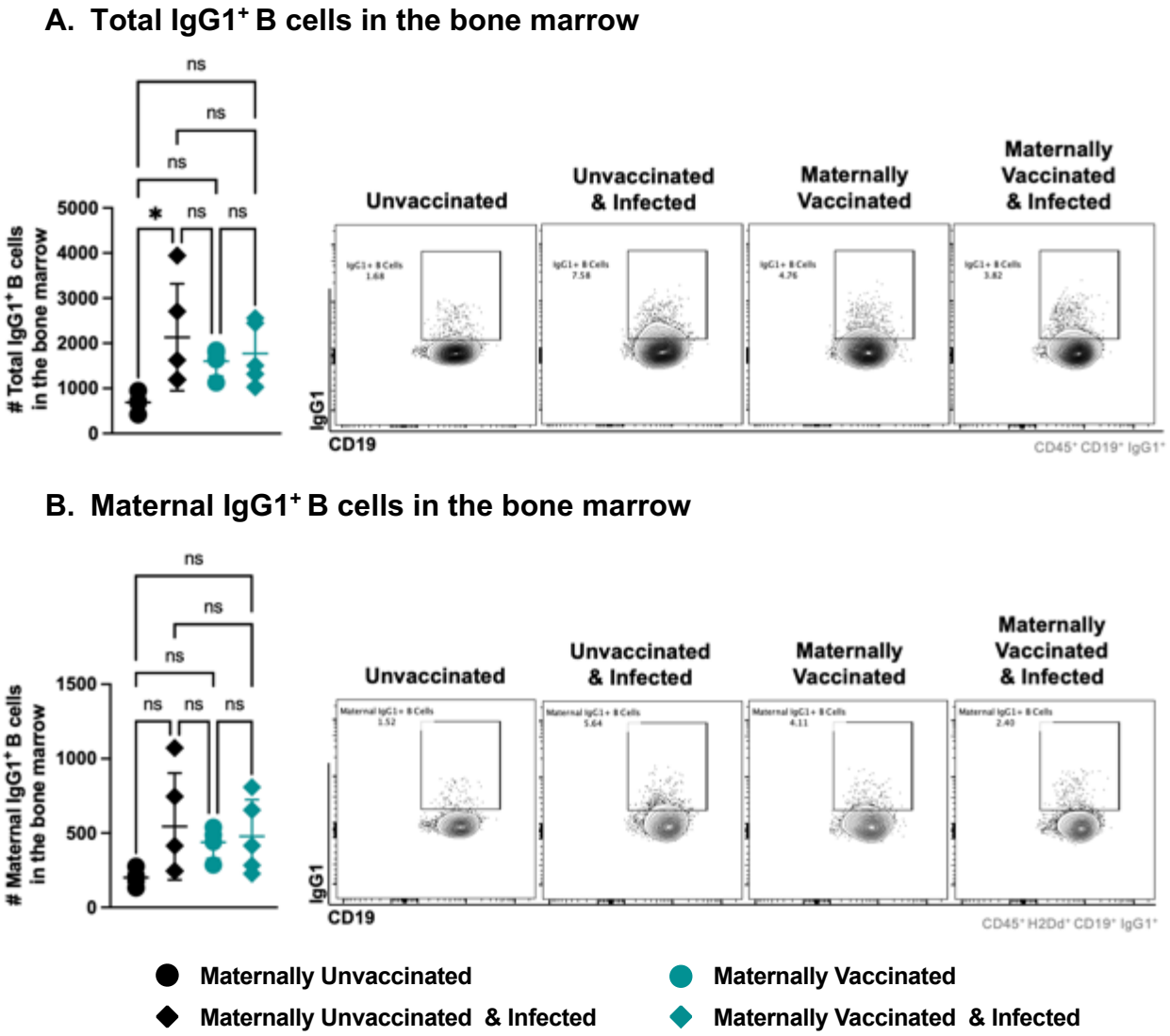

Figure 24: Total IgG1$^+$ expressing B cell populations were increased in the bone marrow of maternally unvaccinated 7-week-old offspring.
7-week-old offspring were either born to unvaccinated or PCV13 vaccinated dams. **A.** Total IgG1$^+$ (CD45$^+$ CD19$^+$ IgG1$^+$) and **B.** maternal IgG1$^+$ (CD45$^+$ H2Dd$^+$ CD19$^+$ IgG1$^+$) B cell populations were investigated in the bone marrow. Representative of 1 experiment whereby n = 5-8 mice per group. Statistical analysis was performed using a Kruskal-Wallis test. P value were regarded as significant if less than 0.05 (* p<0.05, ** p<0.01, *** p<0.001).

A. Total IgG2a⁺ B cells in the bone marrow

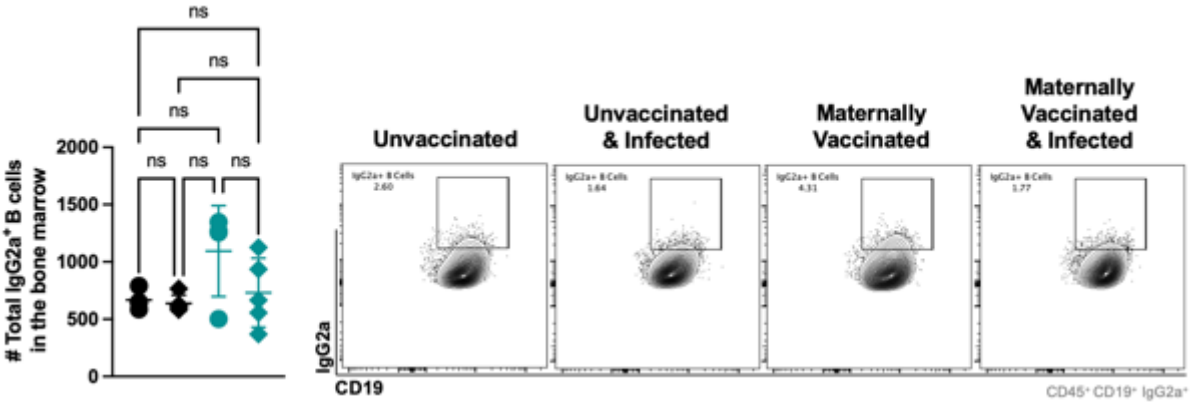

B. Maternal IgG2a⁺ B cells in the bone marrow

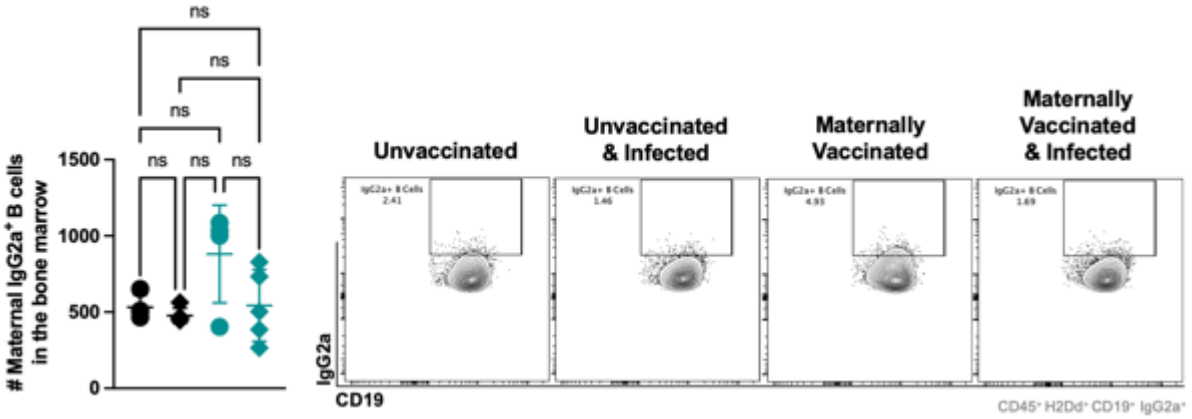

● **Maternally Unvaccinated** ● **Maternally Vaccinated**

◆ **Maternally Unvaccinated & Infected** ◆ **Maternally Vaccinated & Infected**

Figure 25: No significant differences in IgG2a⁺ expressing B cell populations were observed in the bone marrow of 7-week-old offspring.
7-week-old offspring were either born to unvaccinated or PCV13 vaccinated dams. **A.** Total IgG2a⁺ (CD45⁺ CD19⁺ IgG2a⁺) and **B.** maternal IgG2a⁺ (CD45⁺ H2Dd⁺ CD19⁺ IgG2a⁺) B cell populations were investigated in the bone marrow. Representative of 1 experiment whereby n = 5-8 mice per group. Statistical analysis was performed using a Kruskal-Wallis test. P value were regarded as significant if less than 0.05 (* $p<0.05$, ** $p<0.01$, *** $p<0.001$).

5.3. Discussion

Dams were vaccinated 1 week prior to mating and euthanized 55 days later after offspring were weened. Murine average IgG half-life in circulation is approximately 8 days. PCV13 and T4P2 specific antibody results indicate that IgG half-life had significantly increased in PCV13 vaccinated dams as antibody titers were significantly elevated approximately 8 weeks later.

Maternally vaccinated 7-week-old offspring had elevated PCV13 and T4P2 specific antibody titers. The recorded titers were 5 times lower than the titers recorded in dams however these results are incredibly significant as the only possibility for offspring to have acquired long lived antibody would be if antibody producing cells were transferred maternally.

IgA is an important mucosal tissue antibody and is in abundant in the respiratory tract(113, 114). 7-week-old offspring had no difference in total IgA titres however maternally vaccinated and infected offspring had elevated PCV13-specific IgA titres. IgA is regarded as an early neutralising antibody and plays a significant role in inhibiting the colonisation of T4P2 bacteria in the BAL. This can be seen by the reduction in T4P2 bacterial burden in the BAL of maternally vaccinated offspring. Flow cytometry and t-SNE analysis revealed that maternally unvaccinated offspring had increased $CD45^{+}$ immune cell infiltration to the BAL in the presence of infection. These cells were made up of neutrophils, alveolar macrophages and DC's. DCs were significantly recruited to the BAL

of maternally unvaccinated offspring in the presence of infection. This response is not present in maternally vaccinated offspring due to the dramatic reduction in bacterial load present in the BAL. Neutrophils are primarily responsible for initiating phagocytosis while alveolar macrophages are responsible for antigen presentation and phagocytosis, both crucial for initiating an immune response but also eliminating a *pneumococcal* infection(115-117). These cell populations were also recruited to the BAL in the maternally unvaccinated and infected offspring due to the presence of the increased bacterial burden in the BAL. Interestingly, maternally derived DC's, neutrophils and alveolar macrophage populations were increased in the maternally vaccinated and infected offspring whereas maternal innate cells were significantly reduced in maternally unvaccinated and infected offspring. The combination of PCV13 specific IgA and innate maternal cells present indicates that maternally vaccinated offspring have acquired immune control in the BAL.

The same CFU trend observed in the BAL was seen in the lung. Significant T4P2 bacterial colonisation was detected in the lungs of maternally unvaccinated offspring however no CFU's were recorded in maternally vaccinated offspring. Due to the disparate colonisation in the lung, different immune profiles were observed between groups. Total $CD45^+$ immune cells were present in smaller numbers in the maternally unvaccinated offspring, but cell numbers increased 2-fold in the presence of an infection. Maternally vaccinated offspring had an intrinsic total $CD45^+$ immune cell population which was unaffected in the presence of infection. Interestingly, total $CD45^+$ immune cell numbers in maternally vaccinated offspring equated to the same number of total $CD45^+$ immune cell

numbers present in the maternally unvaccinated and infected offspring. In addition, maternally unvaccinated and infected offspring had significantly higher total $CD45^+$ immune cell numbers when compared to maternally vaccinated and infected offspring. The same trend was observed for maternal ($CD45^+$ $H2Kb^+$ $H2Dd^+$) immune cells in the maternally unvaccinated and vaccinated offspring. Maternally unvaccinated offspring numbers were significantly increased in the presence of T4P2 infection, but maternally vaccinated offspring were not influenced by infection and maternal immune cell numbers remained the same. Material $IgG1^+$ and $IgG2a^+$ expressing B cells are slightly elevated in the maternally vaccinated offspring which contributes to the intrinsic $CD45^+$ immune cell population observed. These results indicate that due to more T4P2 CFU's present in the lung a greater immune response and more immune cell infiltration to the lung was present in maternally unvaccinated offspring. Due to the absence of T4P2 CFU's in the lung of maternally vaccinated offspring, less immune cell infiltration was recorded in the presence of infection and cell numbers remained the same at the uninfected maternally vaccinated offspring.

Bone marrow results indicate that maternally unvaccinated and vaccinated offspring had relatively equal immune cell numbers however in the presence of a T4P2 infection, immune cell numbers increase significantly. Interestingly maternal cell numbers decrease in the presence of infection and migrate out of the bone marrow. The migrating immune cells potentially travel in circulation and establish populations in areas crucial for fighting off the infection. For example, in the lung, maternally unvaccinated offspring have reduced maternal cells compared to the larger intrinsic maternally vaccinated offspring.

However, in the presence of infection, maternally unvaccinated offspring have an infiltration of maternal cells in the lung. In addition, bone marrow cells had the ability to secrete PCV13 specific IgG and IgG1 antibodies in the supernatants which not only accounts for the increased antibody half-life seen in 7-week-old offspring but also the ability for bone marrow cells to constantly produce PCV13 specific antibodies.

Chapter 6: Interleukin-4 (IL-4) and its impact on maternal transfer of immunity.

6.1. Introduction

Interleukin-4 (IL-4) is a multifunctional cytokine that plays a crucial role in various aspects of the immune system(118). IL-4 regulates inflammation, B and T cell differentiation and antibody production(118)

Pregnancy is associated with a shift in the immune system towards a T-helper 2 (Th2) cells dominant state(65). IL-4 is a key cytokine that is associated with the Th2 immune environment. The Th2 environment is important for promoting tolerance in reducing inflammation by inhibiting pro-inflammatory cytokines such as interleukin-1 (IL-1) and tumor necrosis factor-alpha (TNF-alpha). This helps maintain an immune balance to prevent the rejection of the developing fetus(119). Excessive inflammation can be detrimental to both the mother and the developing fetus therefore IL-4's role is essential in dampening inflammatory responses to protect the fetus. IL-4 has also been found to play a role in the development and maintenance of the placenta, a crucial organ needed for the exchange of nutrients as well as passive antibody transfer(120).

IL-4 is a critical factor in the differentiation of naïve T cells into Th2 cells. Th2 cells are a distinct subset of T CD4+ T cells that play a regulatory humeral immunity. When T cells are exposed to IL-4 they differentiate into Th2 and produce cytokines such an IL-5 and Il-

13(121). IL-4 acts as a B cell growth factor which it increases the longevity and activation of B cells(122). One of the primary functions of IL-4 is its to induce antibody class switching. B cells are activated by antigen or vaccination and typically produce IgM antibodies. IgM is regarded as the first line of defense against infections. When B cell's encounters an antigen that binds to its receptor, it becomes activated. After activation, B cells interact with helper T cells and receive a signal from cytokines, this will determine which antibody the B cell switches to. If IL-4 is present, this promotes the switch from IgM to either IgE, IgG or IgA depending on the antigen B cells are exposed to.

To the best of our knowledge, it is not known how maternal type 2 immunity influences microchimerism and if maternal cell transfer is altered due to the absence of IL-4. In the absence of IL-4, the TH2 environment will be limited, class switching, and anti-inflammatory properties will be impaired. It is important to note that depending on the specific immune system the lack of IL-4 will vary. IL-4 is one of the many cytokines and signaling molecules present and therefore the absence may be compensated by other cytokines such as IL-13. However, the overall balance of the immune system may be compromised.

In this chapter, we aim to investigate the effect IL-4 has on B cell populations in dams. In addition, we aim to investigate if IL-4 influences the maternal vaccination effects and microchimerism observed previously in WT offspring. We aim to evaluate if any changes are present in CFU's, PCV13 specific antibody production as well as the proportion and location of maternal cells.

6.2. Results

6. 2.1 PCV13 vaccination elicits higher IgG1 B cell populations in WT PCV13 vaccinated dams.

WT and IL-4R$\alpha^{-/-}$ 7-week-old $H2^{Dd}/H2^{Kb}$ dams were either vaccinated with PCV13 one week prior to mating or left unvaccinated. Three weeks after giving birth, offspring were weened, and dams were culled **(Figure 6.1)**. The axillary lymph node, illiac lymph node and spleens were harvested and subjected to flow cytometry analysis.

WT and IL-4Rα$^{-/-}$ Allogeneic Experimental model:

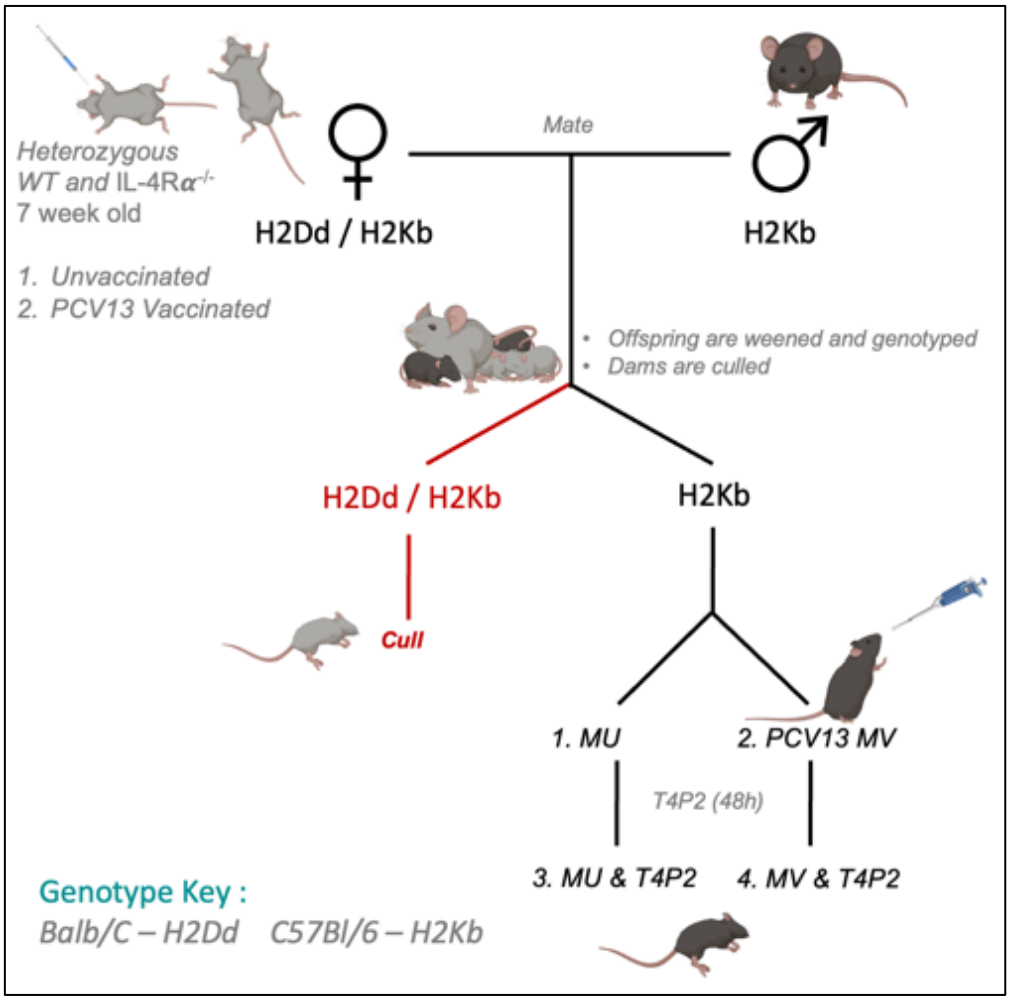

Figure 6.1: The WT and IL-4Rα$^{-/-}$ allogeneic maternal vaccination experimental model.

A. 7-week-old WT and IL-4Rα$^{-/-}$ H-2$^{b/d}$ female mice were either vaccinated intraperitoneally with PCV13 before mating or left unvaccinated. Females were mated with H-2$^{b/b}$ males resulting in H-2$^{b/d}$ and H-2$^{b/b}$ offspring. The H-2$^{b/d}$ offspring was culled and 7-week-old H-2$^{b/b}$ offspring were infected with T4P2 intranasally and culled 48H post infection.

Dam B cells ($CD45^+$ $CD19^+$ $B220^+$) in the axillary lymph nodes were investigated using flow cytometry. There were no differences in B cell numbers between WT and IL-4R$\alpha^{-/-}$ unvaccinated and PCV13 vaccinated dams **(Figure 6.2)**.

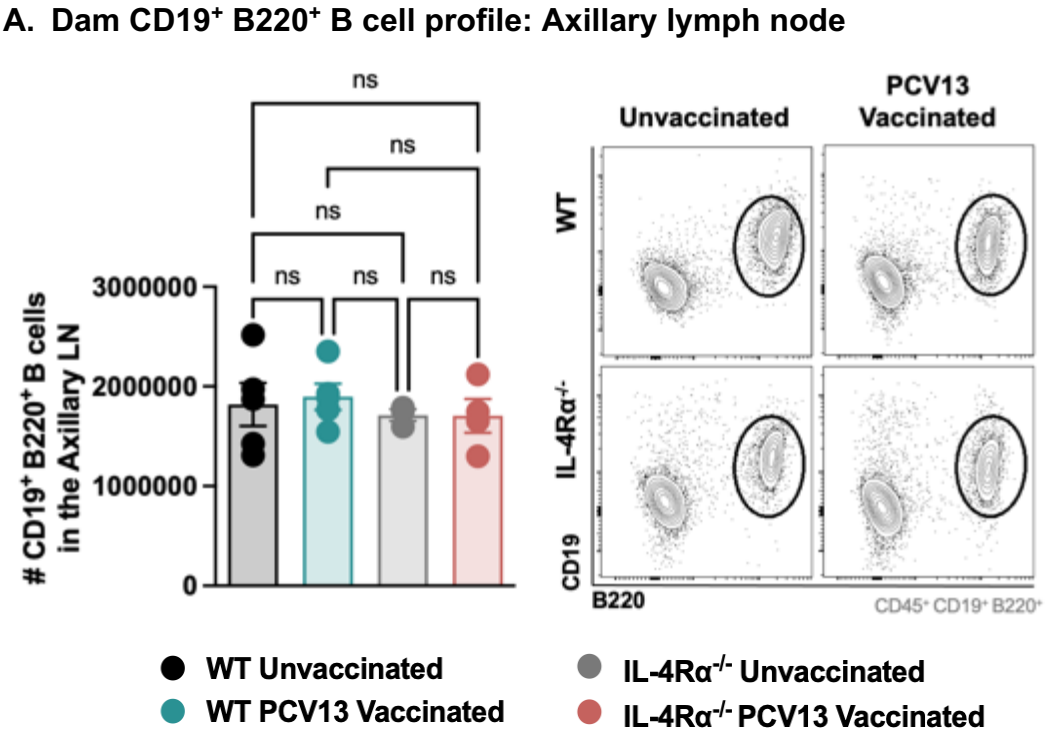

Figure 6.2: No differences in $CD19^+$ $B220^+$ B cell populations were identified in the axillary lymph nodes of unvaccinated and vaccinated dams.
WT and IL-4R$\alpha^{-/-}$ dams were either left unvaccinated or vaccinated with PCV13 one week before mating. **A.** B ($CD19^+$ $B220^+$) cell populations were investigated in the axillary lymph nodes. All cell populations were identified using flow cytometry. The results are expressed as individual mice/data points. Representative of 1 experiment whereby n = 4-6 mice per group. Statistical analysis was performed using a Kruskal-Wallis test. P values was regarded as significant if less than 0.05 (* $p<0.05$, ** $p<0.01$, *** $p<0.001$**).**

IgG1$^+$ (CD45$^+$ CD19$^+$ B220$^+$ IgG1$^+$) and IgG2a$^+$ (CD45$^+$ CD19$^+$ B220$^+$ IgG2a$^+$) B cells were investigated in the axillary lymph nodes. IgG1$^+$ B cell percentages in WT unvaccinated dams are 22% higher than IL-4R$\alpha^{-/-}$ unvaccinated dams **(Figure 6.3)**. In addition, IgG1$^+$ B cell percentages in WT PCV13 vaccinated dams were 28% higher than IL-4R$\alpha^{-/-}$ PCV13 vaccinated dams **(Figure 6.3)**. IgG2a$^+$ B cell percentages were slightly elevated in IL-4R$\alpha^{-/-}$ unvaccinated dams however, no differences were observed in the remaining groups **(Figure 6.3)**.

A. Dam B cell subgroup percentages: Axillary Lymph node

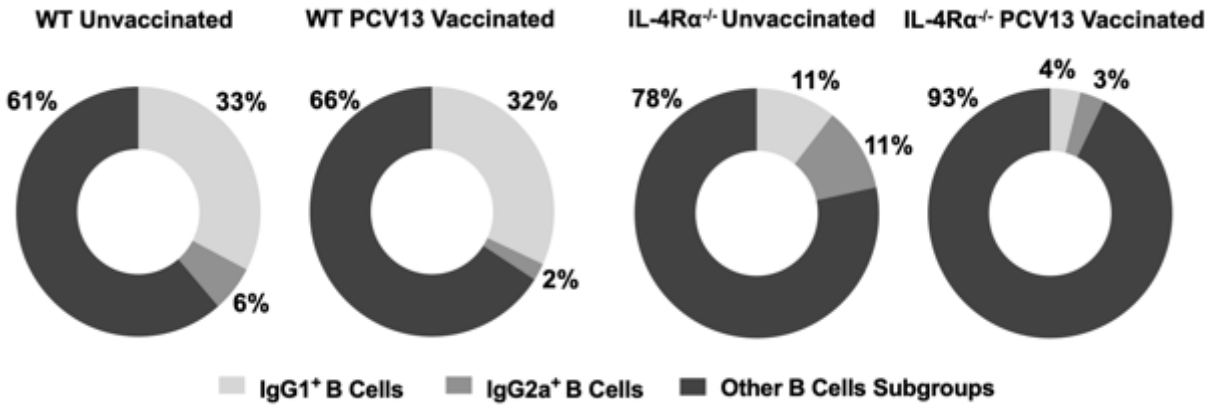

Figure 6.3: IL-4R$\alpha^{-/-}$ dams have decreased IgG1$^+$ B cell populations in the axillary lymph nodes.
WT and IL-4R$\alpha^{-/-}$ dams were either left unvaccinated or vaccinated with PCV13 one week before mating. **A.** IgG1$^+$ (CD19$^+$ B220$^+$ IgG1$^+$) and IgG2a$^+$ (CD19$^+$ B220$^+$ IgG2a$^+$) B cell percentages were investigated in the axillary lymph nodes. All cell percentages were identified using flow cytometry. The results are expressed as individual mice/data points. Representative of 1 experiment whereby n = 4-6 mice per group. Statistical analysis was performed using a Kruskal-Wallis test. P values was regarded as significant if less than 0.05 (* $p<0.05$, ** $p<0.01$, *** $p<0.001$).

A similar trend was observed for $IgG1^+$ and $IgG2a^+$ numbers in the axillary lymph nodes. $IgG1^+$ B cells were significantly reduced in IL-4R$\alpha^{-/-}$ Dams **(Figure 6.4A)**. $IgG2a^+$ B cells were significantly increased in IL-4R$\alpha^{-/-}$ unvaccinated dams while reduced cell populations were present in all remaining groups **(Figure 6.4B)**. PCV13 vaccination had no effect on the proportion of $IgG1^+$ and $IgG2a^+$ cell numbers in the axillary lymph nodes **(Figure 6.3 and 6.4)**.

A. Dam CD19⁺ B220⁺ IgG1⁺ B cell profile: Axillary lymph node

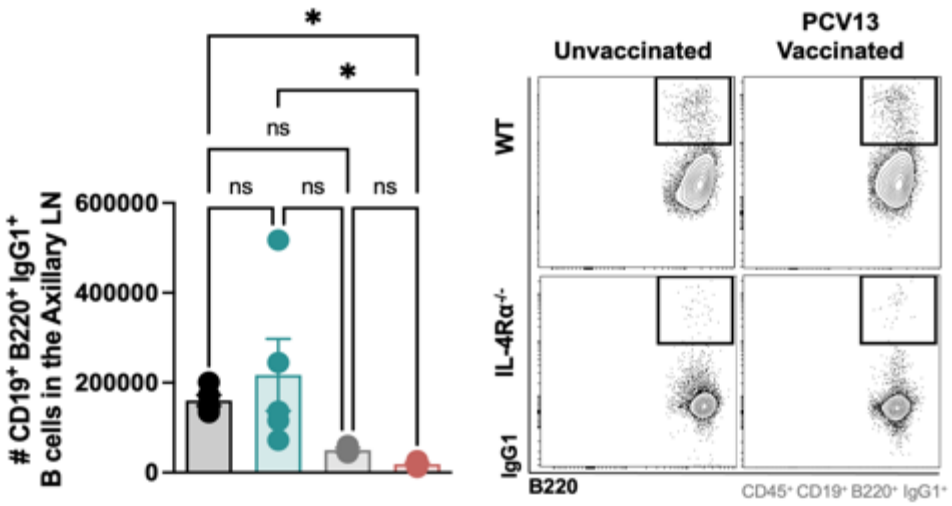

B. Dam CD19⁺ B220⁺ IgG2a⁺ B cell profile: Axillary lymph node

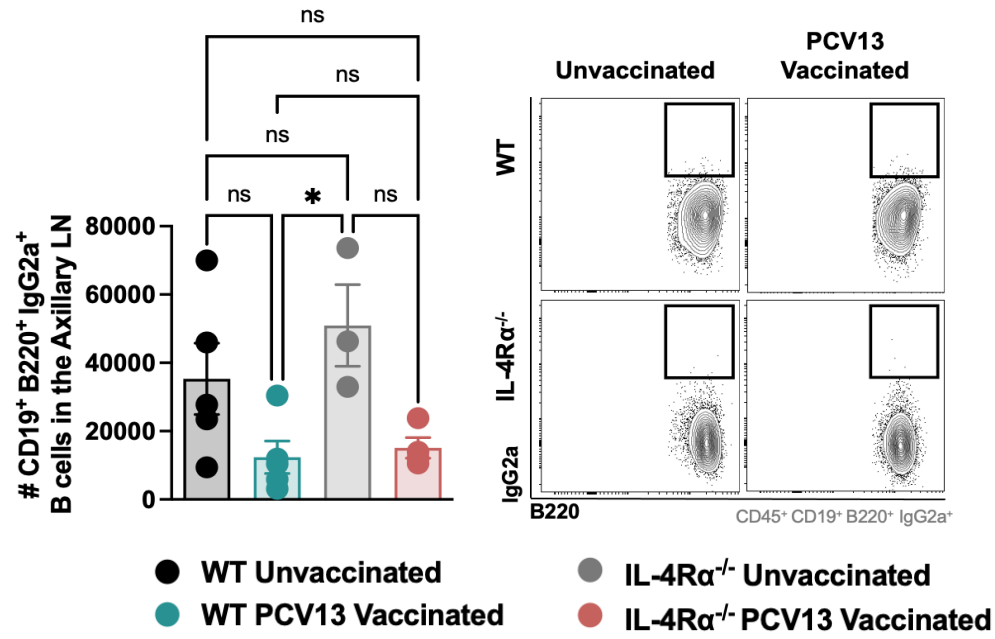

Figure 6.4: IL-4Rα$^{-/-}$ dams have reduced IgG1⁺ B cell populations in the axillary lymph nodes.

Dams were either left unvaccinated or vaccinated with PCV13 one week before mating. **A.** IgG1⁺ B cell (CD19⁺ B220⁺ IgG1⁺) populations and **B.** IgG2a⁺ B cell (CD19⁺ B220⁺ IgG2a⁺) populations were investigated in the axillary lymph nodes. All cell populations were identified using flow cytometry. The results are expressed as individual mice/data points. Representative of 1 experiment whereby n = 4-6 mice per group. Statistical analysis was performed using a Kruskal-Wallis test. P values was regarded as significant if less than 0.05 (* $p<0.05$, ** $p<0.01$, *** $p<0.001$).

CD19^{+} B220^{+} B cells was investigated in the illiac lymph nodes, however no differences in cell numbers were observed in WT and IL-4R$\alpha^{-/-}$ dams **(Figure 6.5)**.

A. Dam CD19^{+} B220^{+} B cell profile: Illiac lymph node

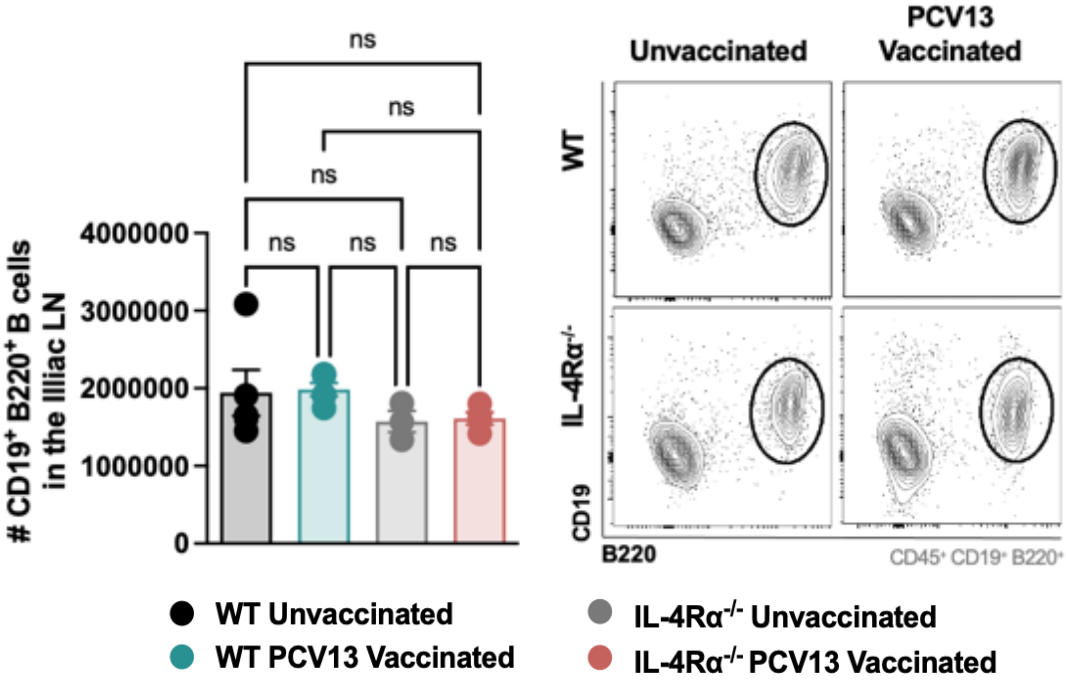

Figure 6.5: No changes in CD19^{+} B220^{+} B cell populations were recorded in the illiac lymph nodes of unvaccinated and vaccinated dams.
WT and IL-4R$\alpha^{-/-}$ dams were either left unvaccinated or vaccinated with PCV13 one week before mating. **A.** CD19^{+} B220^{+} B cell populations were investigated in the illiac lymph nodes. All cell populations were identified using flow cytometry. The results are expressed as individual mice/data points. Representative of 1 experiment whereby n = 4-6 mice per group. Statistical analysis was performed using a Kruskal-Wallis test. P values was regarded as significant if less than 0.05 (* $p<0.05$, ** $p<0.01$, *** $p<0.001$).

Illiac lymph node IgG1$^+$ B cell percentages were significantly reduced in IL-4R$\alpha^{-/-}$ dams **(Figure 6.6)**. This reduction of 13% was evident between WT and IL-4R$\alpha^{-/-}$ PCV13 vaccinated dams. IgG2a$^+$ B cell percentages were increased by 9% in the IL-4R$\alpha^{-/-}$ PCV13 vaccinate dams **(Figure 6.6)**.

A. Dam B cell subgroup percentages: Illiac lymph node

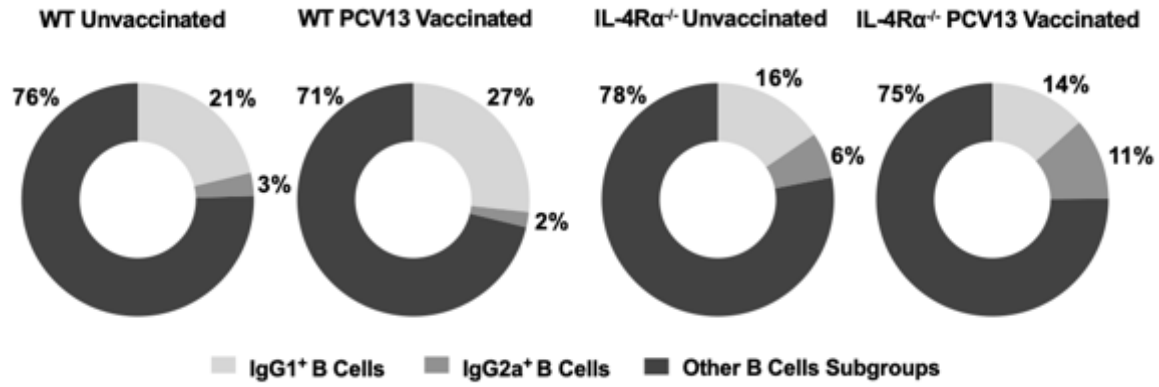

Figure 6.6: IL-4R$\alpha^{-/-}$ dams have decreased IgG1$^+$ and increased IgG2a$^+$ B cell populations in the illiac lymph nodes.
WT and IL-4R$\alpha^{-/-}$ dams were either left unvaccinated or vaccinated with PCV13 one week before mating. **A.** IgG1$^+$ (CD19$^+$ B220$^+$ IgG1$^+$) and IgG2a$^+$ (CD19$^+$ B220$^+$ IgG2a$^+$) B cell percentages were investigated in the axillary lymph nodes. All cell populations were identified using flow cytometry. The results are expressed as individual mice/data points. Representative of 1 experiment whereby n = 4-6 mice per group. Statistical analysis was performed using a Kruskal-Wallis test. P values was regarded as significant if less than 0.05 (* $p<0.05$, ** $p<0.01$, *** $p<0.001$).

The IgG1$^+$ B cell numbers indicate the same trend as the IgG1$^+$ and IgG2a$^+$ cell percentages in the illiac lymph node. IgG1$^+$ B cell numbers were the highest in WT PCV13 vaccinated dams and are significantly reduced in IL-4R$\boldsymbol{\alpha}^{-/-}$ unvaccinated and PCV13 vaccinated dams **(Figure 6.7A)**. IgG2a$^+$ cell numbers are only significantly increased in IL-4R$\boldsymbol{\alpha}^{-/-}$ PCV13 vaccinated dams **(Figure 6.7B)**. These results indicate that in PCV13 vaccination increases IgG1$^+$ B cells in the illiac lymph node in WT dams and decreases IgG1$^+$ B cells in IL-4R$\boldsymbol{\alpha}^{-/-}$ dams **(Figure 6.7B)**. PCV13 vaccination also reduces IgG2a$^+$ B cells in WT dams but increases IgG2a$^+$ B cells in IL-4R$\boldsymbol{\alpha}^{-/-}$ dams **(Figure 6.7B)**.

A. Dam CD19⁺ B220⁺ IgG1⁺ B cell profile: Illiac lymph node.

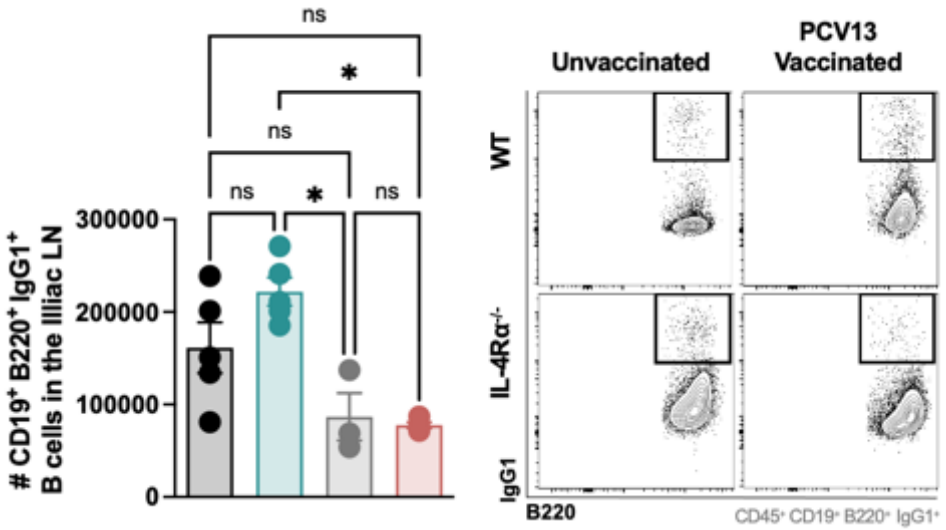

B. Dam CD19⁺ B220⁺ IgG2a⁺ B cell profile: Illiac lymph node

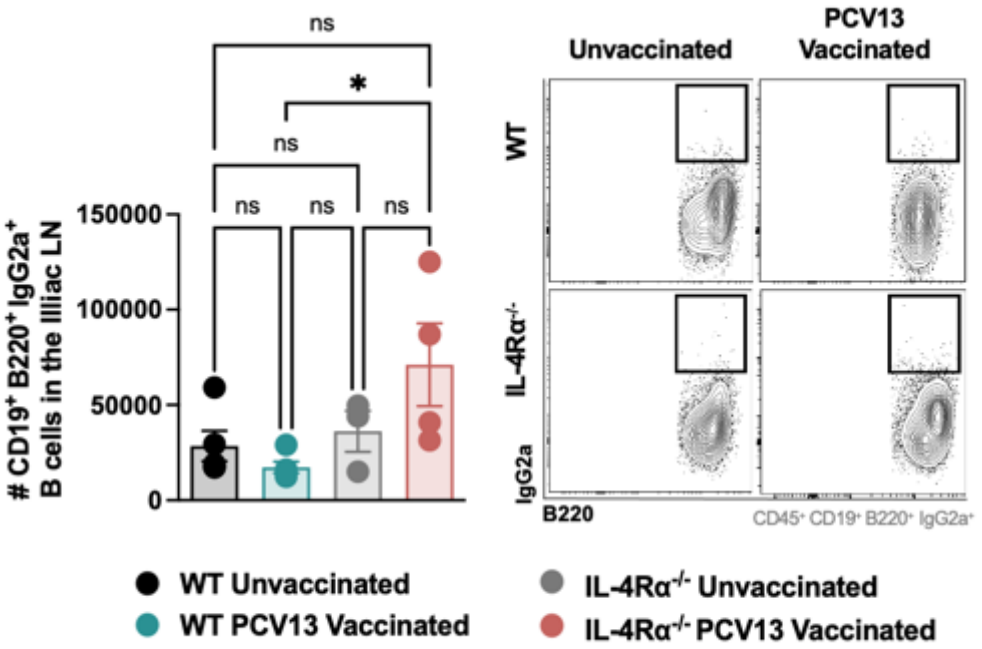

Figure 6.7: WT PCV13 vaccinated dams have increased IgG1⁺ and reduced IgG2a⁺ B cell populations in the illiac lymph nodes.
Dams were either left unvaccinated or vaccinated with PCV13 one week before mating. **A.** IgG1⁺ B cell (CD19⁺ B220⁺ IgG1⁺) populations and **B.** IgG2a⁺ B cell (CD19⁺ B220⁺ IgG1⁺) populations were investigated in the illiac lymph nodes. All cell populations were identified using flow cytometry. The results are expressed as individual mice/data points. Representative of 1 experiment whereby n = 4-6 mice per group. Statistical analysis was performed using a Kruskal-Wallis test. P values was regarded as significant if less than 0.05 (* $p<0.05$, ** $p<0.01$, *** $p<0.001$).

Dam B cells ($CD45^+$ $CD19^+$ $B220^+$) in the spleen were investigated using flow cytometry. There were no differences in B cell numbers between WT and IL-4R$\alpha^{-/-}$ unvaccinated and PCV13 vaccinated dams **(Figure 6.8)**.

A. Dam $CD19^+$ $B220^+$ B cell profile: Spleen

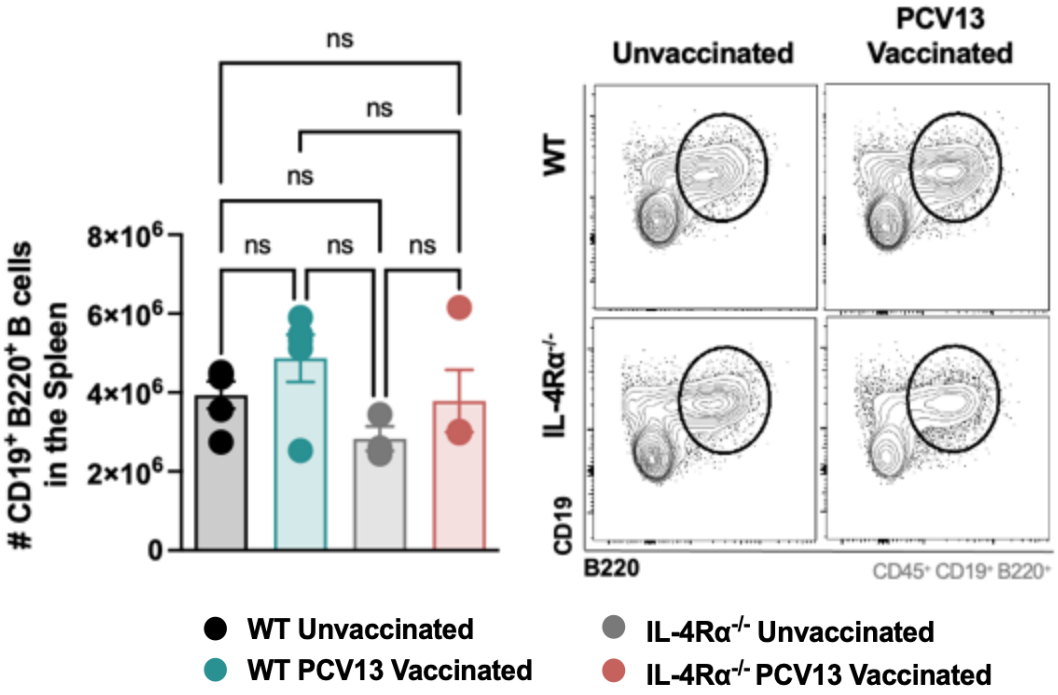

Figure 6.8: $CD19^+$ $B220^+$ B cell populations were elevated in the spleen of WT and IL-4R$\alpha^{-/-}$ vaccinated dams.
WT and IL-4R$\alpha^{-/-}$ dams were either left unvaccinated or vaccinated with PCV13 one week before mating. **A.** $CD19^+$ $B220^+$ B cell populations were investigated in the spleen of unvaccinated and PCV13 vaccinated dams. All cell populations were identified using flow cytometry. The results are expressed as individual mice/data points. Representative of 1 experiments whereby n = 4-6 mice per group. Statistical analysis was performed using a Kruskal-Wallis test. P values was regarded as significant if less than 0.05 (* $p<0.05$, ** $p<0.01$, *** $p<0.001$).

IgG1$^+$ B cell percentages in the spleen were significantly reduced in IL-4R$\alpha^{-/-}$ dams when compared to WT dams **(Figure 6.9)**. WT PCV vaccinated dams had a significant 15% increase in IgG1$^+$ B cell populations. IgG2a$^+$ B cells were slightly reduced in IL-4R$\alpha^{-/-}$ dams however no differences in IgG2a$^+$ B cells were detected between unvaccinated and vaccinated dams in both WT and IL-4R$\alpha^{-/-}$ dams **(Figure 6.9)**.

A. Dam B cell subgroup percentages: Spleen

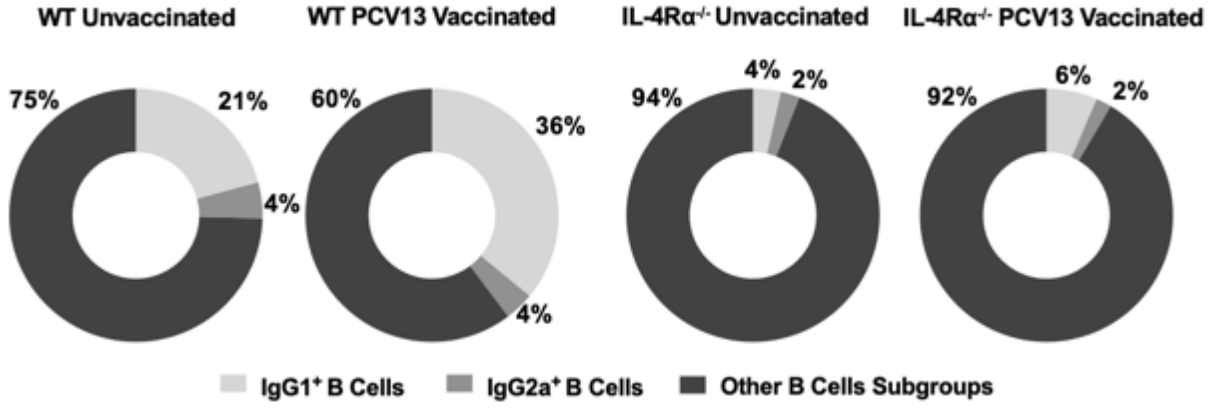

Figure 6.9: IL-4R$\alpha^{-/-}$ dams have decreased IgG1$^+$ B cell populations in the spleen.
WT and IL-4R$\alpha^{-/-}$ Dams were either left unvaccinated or vaccinated with PCV13 one week before mating. **A.** IgG1$^+$(CD19$^+$ B220$^+$ IgG1$^+$) and IgG2a$^+$ (CD19$^+$ B220$^+$ IgG2a$^+$) B cell percentages were investigated in the spleen. All cell populations were identified using flow cytometry. The results are expressed as individual mice/data points. Representative of 1 experiment whereby n = 4-6 mice per group. Statistical analysis was performed using a Kruskal-Wallis test. P value was regarded as significant if less than 0.05 (* $p<0.05$, ** $p<0.01$, *** $p<0.001$).

In the spleen, IgG1$^+$ B cell numbers were significantly reduced in IL-4R$\alpha^{-/-}$ unvaccinated and PCV13 vaccinated dams **(Figure 6.10)**. IgG1$^+$ B cell numbers were the highest in the spleens of WT PCV13 vaccinated dams. No differences in IgG2a$^+$ B cell numbers were observed in the spleen of WT and IL-4R$\alpha^{-/-}$ unvaccinated and PCV13 vaccinated dams **(Figure 6.10)**. These results indicate that PCV13 vaccination increased IgG1$^+$ B cell numbers in WT dams but had no effect on IL-4R$\alpha^{-/-}$ dams **(Figure 6.10)**.

A. Dam CD19⁺ B220⁺ IgG1⁺ B cell profile: Spleen

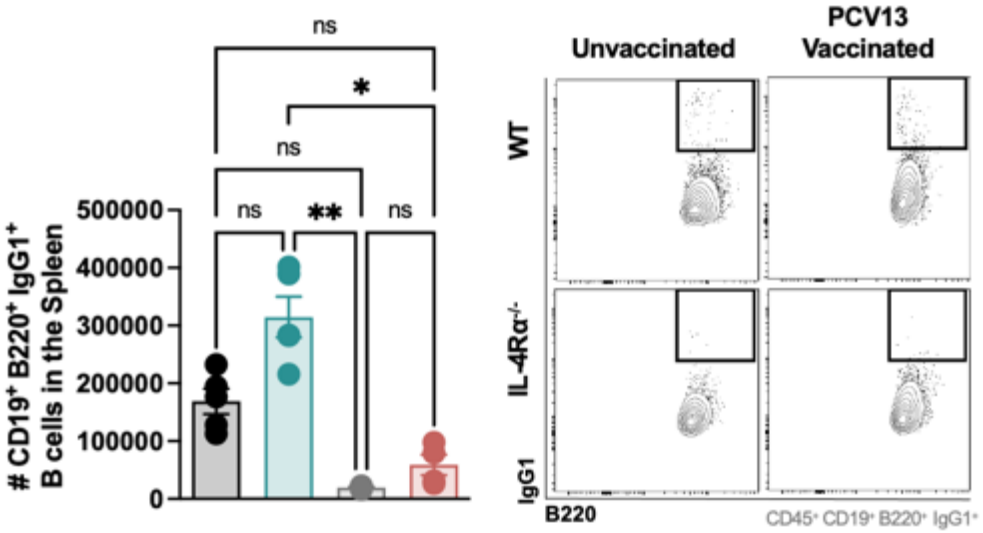

B. Dam CD19⁺ B220⁺ IgG2a⁺ B cell profile: Spleen

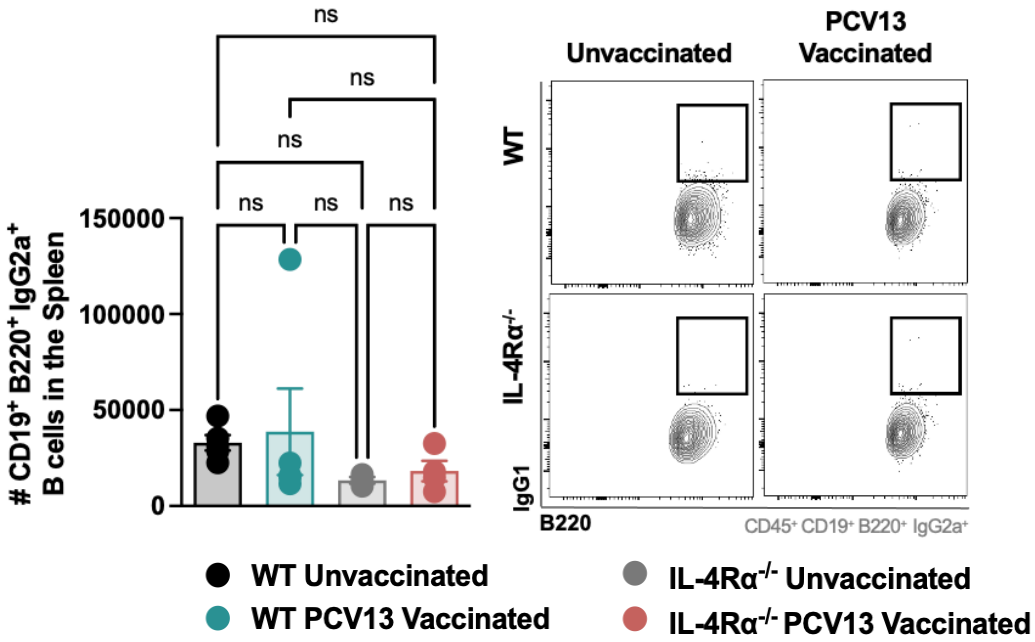

Figure 6.10: IL-4R$\alpha^{-/-}$ dams have significantly reduced IgG1⁺ B cell populations in the spleen.

Dams were either left unvaccinaTable 3: ELISA antibodies concentrations and dilutions. IgTable 4: Flow Cytometry antibodies concentrations, dilutions and panels.tions were investigated in the spleen. All cell populations were identified using flow cytometry. The results are expressed as individual mice/data points. Representative of 1 experiments whereby n = 4-6 mice per group. Statistical analysis was performed using a Kruskal-Wallis test. P values was regarded as significant if less than 0.05 (* $p<0.05$, ** $p<0.01$, *** $p<0.001$).

6. 2.2 Maternal vaccination results in decreased T4P2 CFU and increased PCV13 specific antibodies in the serum of WT 7-week-old offspring.

Blood from infected 7-week-old WT and IL-4R$\alpha^{-/-}$ maternally unvaccinated and vaccinated offspring was collected for CFU quantification. CFU's were significantly decreased in WT maternally vaccinated and infected offspring however CFU's were only slightly reduced in the IL-4R$\alpha^{-/-}$ maternally vaccinated and infected offspring **(Figure 6.11)**. No differences in CFU's were observed between WT and IL-4R$\alpha^{-/-}$ maternally unvaccinated offspring **(Figure 6.11)**.

A. T4P2 CFU in the blood of 7-week-old offspring

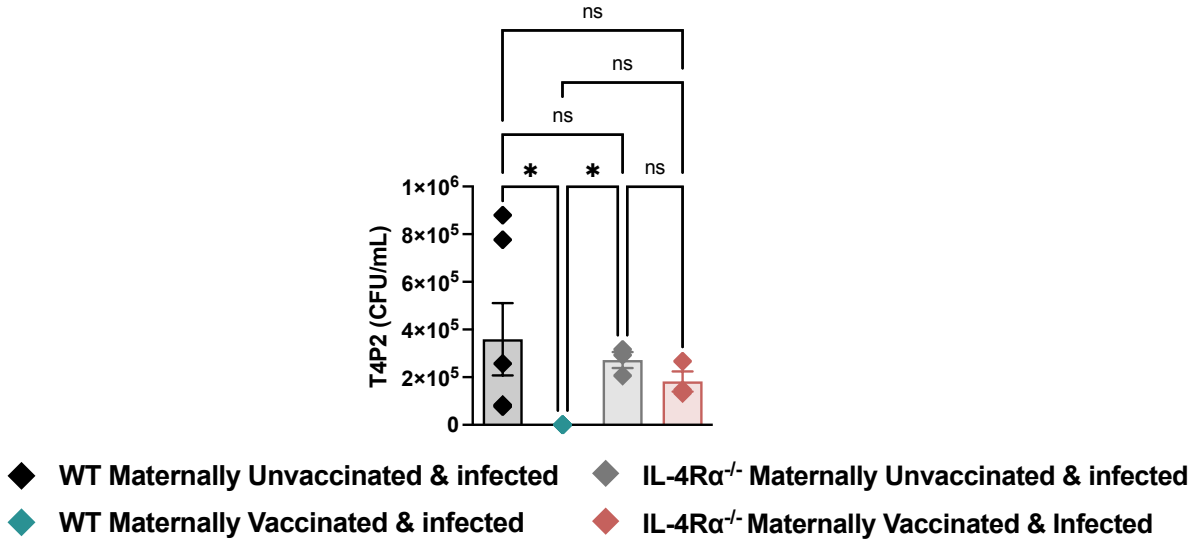

Figure 6.11: WT Maternally vaccinated 7-week-old offspring have reduced T4P2 CFU's in the serum.
7-week-old offspring were either born to unvaccinated or PCV13 vaccinated dams **A.** T4P2 CFU's were recorded in the blood of maternally unvaccinated and vaccinated WT and IL-4R$\alpha^{-/-}$ offspring. The results are expressed as individual mice/data points. Representative of 1 experiment whereby n = 5-8 mice per group. Statistical analysis was performed using a Kruskal-Wallis test. P values was regarded as significant if less than 0.05 (* $p<0.05$, ** $p<0.01$, *** $p<0.001$).

Blood collected was separated into serum and PCV 13 specific total IgG and IgG1 antibodies were investigated in 7-week-old offspring. PCV13 specific total IgG and IgG1 was significantly increased in WT maternally vaccinated and WT maternally vaccinated and infected offspring **(Figure 6.12)**. PCV13 specific total IgG and IgG1 antibodies were not detected in IL-4R$\alpha^{-/-}$ maternally vaccinated and maternally vaccinated and infected offspring. No PCV13 specific total IgG and IgG1 antibodies was detected in WT and IL-4R$\alpha^{-/-}$ maternally unvaccinated and maternally unvaccinated and infected offspring **(Figure 6.12)**.

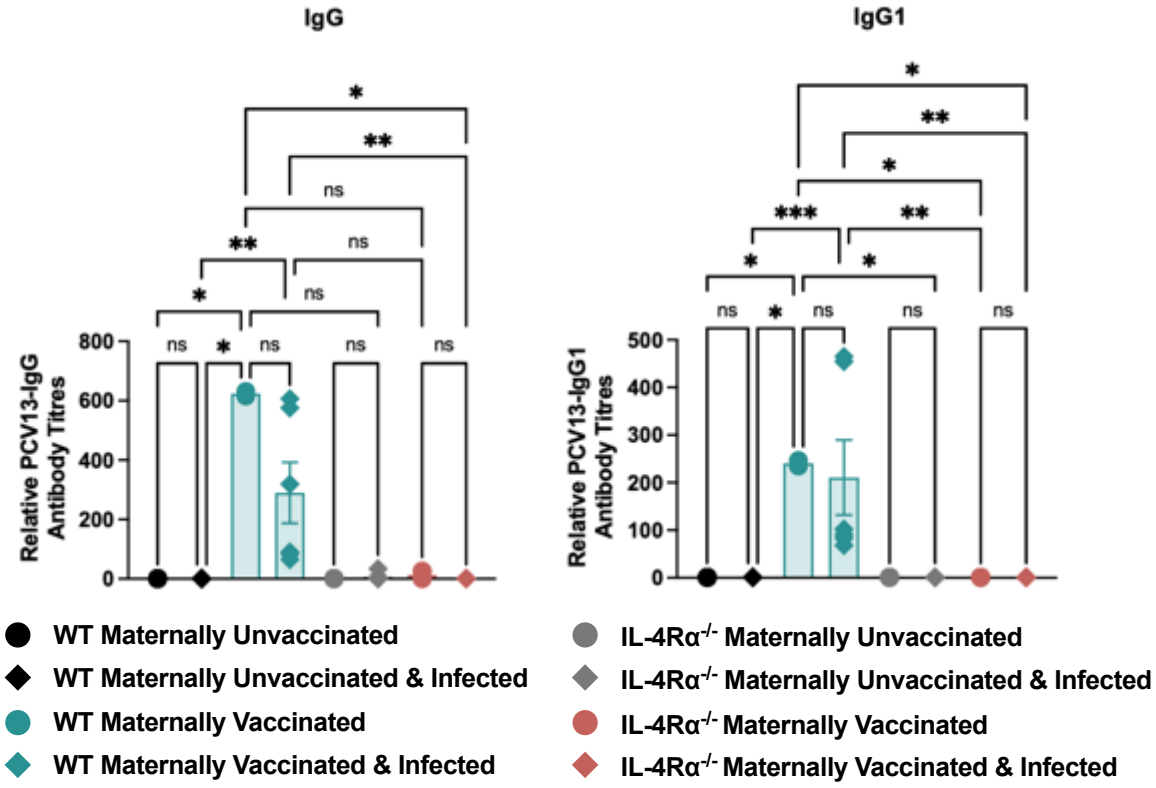

Figure 6.12: WT Maternally vaccinated offspring have acquired maternally derived PCV13-specific antibodies in the serum.
7-week-old offspring were either born to unvaccinated or PCV13 vaccinated dams**.** T4P2-specific IgG and IgG1 antibodies were identified in serum using ELISA. The results are expressed as individual mice/data points. Representative of 1 experiment whereby n = 5-8 mice per group. Statistical analysis was performed using a Kruskal-Wallis test. P values was regarded as significant if less than 0.05 (* p<0.05, ** p<0.01, *** p<0.001).

Serum collected from WT and IL-4R$\alpha^{-/-}$ maternally unvaccinated and maternally vaccinated offspring was heat inactivated at 56°C for 30 minutes and cooled for 15 minutes at 4°C. 1X10^7 T4P2 was opsonized with serum at 4°C for 1 hour. Opsonised bacteria were infected intranasally into 7-week-old BALB/c mice and euthanized 48H post infection. Mice opsonized with WT maternally vaccinated serum had significantly decreased T4P2 CFU's in comparison to the unopsonized T4P2 infection control **(Figure 6.13)**. The mice opsonised with WT and IL-4R$\alpha^{-/-}$ maternally unvaccinated serum as well as IL-4R$\alpha^{-/-}$ maternally vaccinated serum had no significant reduction in T4P2 CFU. These results suggest that only opsonised WT maternally vaccinated serum can reduce CFU in mice.

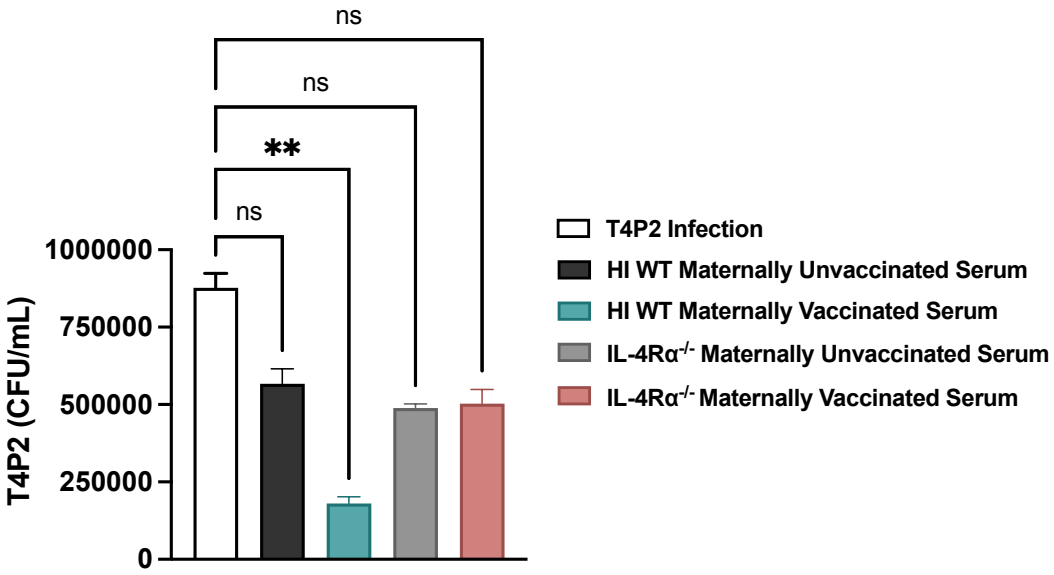

Figure 6.13: Mice opsonized with WT maternally vaccinated serum had significantly decreased T4P2 CFU's in the blood.
Serum collected from unvaccinated and maternally vaccinated offspring was heat inactivated (HI) at 56°C for 30 minutes and cooled. 1X10^7 T4P2 was opsonized with serum at 4°C for 1 hour. Opsonised bacteria were infected intranasally into 7-week BALB/c mice and euthanized 48H post infection. The results are expressed as individual mice/data points. Representative of 1 experiment whereby n = 4-6 mice per group. Statistical analysis was performed using a Kruskal-Wallis test. P values was regarded as significant if less than 0.05 (* $p<0.05$, ** $p<0.01$, *** $p<0.001$).

6. 2.3 Maternal vaccination in 7-week-old WT offspring results in decreased T4P2 CFU and reduced immune cell infiltration to the BAL.

The BAL was collected and plated on BAB agar plates to investigate CFU's. CFU's in WT and IL-4R$\alpha^{-/-}$ maternally unvaccinated and infected offspring were significantly high and no differences were recorded in CFU's of WT and IL-4R$\alpha^{-/-}$ maternally unvaccinated and infected offspring **(Figure 6.14)**. No CFU's were recorded in WT maternally vaccinated and infected offspring whereas CFU's were recorded in IL-4R$\alpha^{-/-}$ maternally vaccinated and infected offspring **(Figure 6.14)**.

A. T4P2 CFU in the BAL of 7-week-old offspring

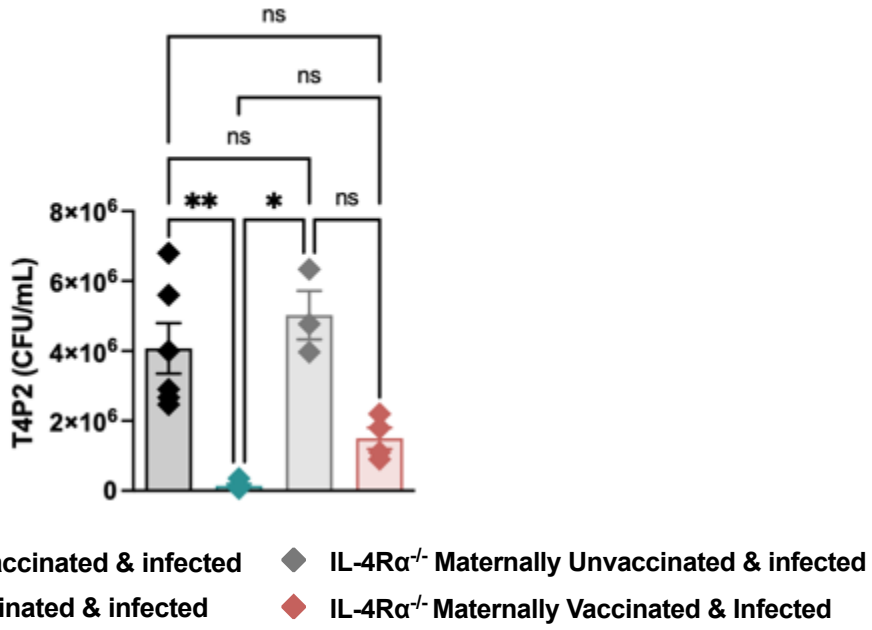

Figure 6.14: WT Maternally vaccinated 7-week-old offspring have reduced T4P2 CFU's in the BAL.
7-week-old offspring were either born to unvaccinated or PCV13 vaccinated dams **A.** T4P2 CFU's were recorded in the BAL of WT and IL-4R$\alpha^{-/-}$ maternally vaccinated and maternally unvaccinated offspring. The results are expressed as individual mice/data points. Representative of 1 experiment whereby n = 5-7 mice per group. Statistical analysis was performed using a Kruskal-Wallis test. P values was regarded as significant if less than 0.05 (* $p<0.05$, ** $p<0.01$, *** $p<0.001$).

BAL supernatants were collected and centrifuged at 4000 rpm for 5 minutes. The pellets were processed and stained for flow cytometry according to section 2.5. Total $CD45^+$ cell numbers were investigated in the BAL. The results suggest that IL-4R$\alpha^{-/-}$ offspring had higher $CD45^+$ numbers compared to WT offspring **(Figure 6.15)**. In addition, IL-4R$\alpha^{-/-}$ maternally unvaccinated and infected as well as IL-4R$\alpha^{-/-}$ maternally vaccinated and infected offspring had significantly increased cell numbers when compared to WT maternally vaccinated and infected offspring **(Figure 6.15)**. WT maternally vaccinated mice had no change in $CD45^+$ Immune cells numbers in the presence on a T4P2 infection **(Figure 6.15**).

A. Total number of CD45⁺ immune cells in the BAL of 7-week-old offspring

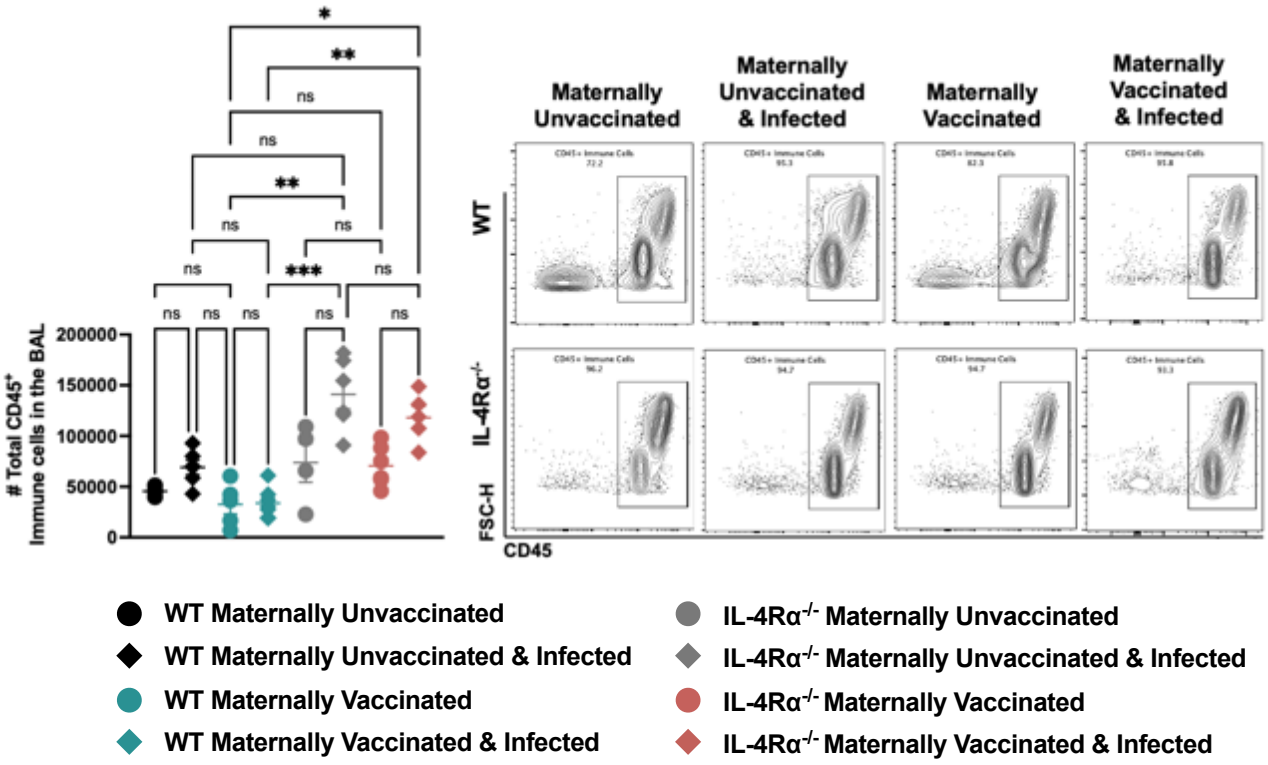

Figure 6.15: 7-week-old IL-4R$\alpha^{-/-}$ offspring acquire increased CD45⁺ immune cell populations upon infection in the BAL.
7-week-old offspring were either born to unvaccinated or PCV13 vaccinated dams. **A.** CD45⁺ immune cell populations were investigated in the BAL. All cell populations were identified using flow cytometry. The results are expressed as individual mice/data points. Representative of 2 experiments whereby n = 5-7 mice per group. Statistical analysis was performed using a Kruskal-Wallis test. P values was regarded as significant if less than 0.05 (* $p<0.05$, ** $p<0.01$, *** $p<0.001$).

Total neutrophil (SiglecF⁻ Ly6G⁺ CD11b⁺) numbers were investigated in the BAL. IL-4R$\alpha^{-/-}$ maternally unvaccinated and vaccinated offspring had a small increase in neutrophil infiltration to the BAL in the presence of an infection when compared to WT offspring **(Figure 6.16)**.

A. Total number of neutrophils in the BAL of 7-week-old offspring

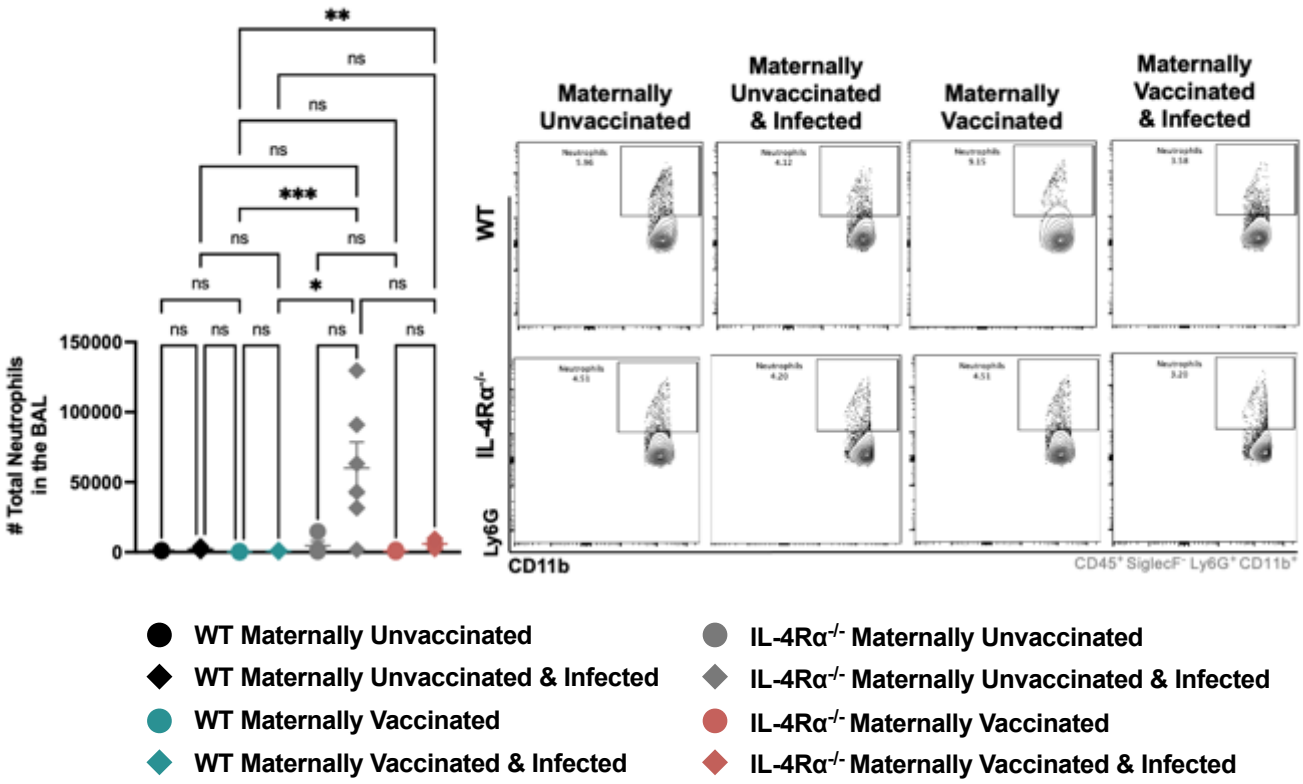

Figure 6.16: 7-week-old IL-4R$\alpha^{-/-}$ maternally unvaccinated and vaccinated offspring acquire increased neutrophil populations in the BAL in the presence of a T4P2 infection.

7-week-old offspring were either born to unvaccinated or PCV13 vaccinated dams. **A.** SiglecF^{+} Ly6G^{+} neutrophil populations were investigated in the BAL. All cell populations were identified using flow cytometry. The results are expressed as individual mice/data points. Representative of 2 experiments whereby n = 5-7 mice per group. Statistical analysis was performed using a Kruskal-Wallis test. P values was regarded as significant if less than 0.05 (* $p<0.05$, ** $p<0.01$, *** $p<0.001$).

Total alveolar macrophages (SiglecF$^+$ Ly6G$^-$ CD11b$^+$ CD11c$^+$) were investigated in the BAL. IL-4R$\alpha^{-/-}$ offspring had increased total cell populations when compared to WT offspring **(Figure 6.17)**. Alveolar macrophages increased in IL-4R$\alpha^{-/-}$ maternally unvaccinated and vaccinated offspring in the presence of infection **(Figure 6.17)**. WT maternally unvaccinated and vaccinated offspring alveolar macrophage numbers remained the same under the influence of infection **(Figure 6.17)**.

A. Total number of alveolar macrophages in the BAL of 7-week-old offspring

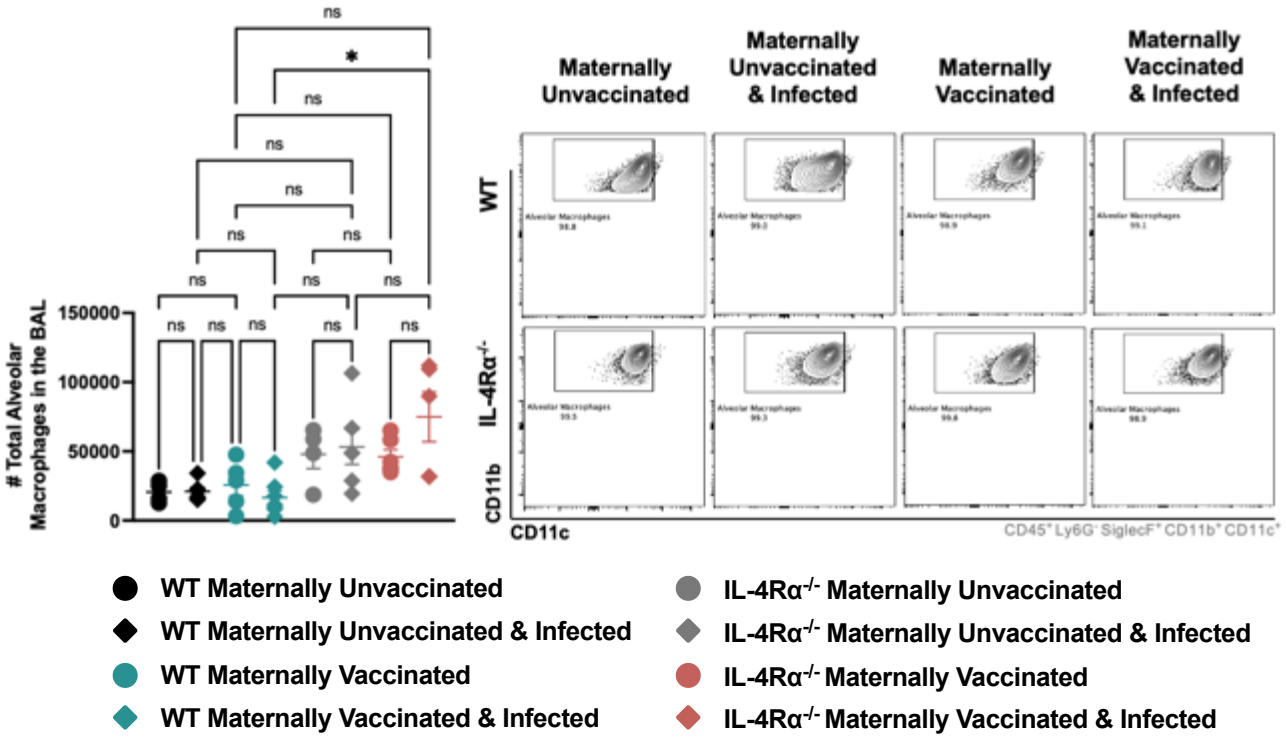

Figure 6.17: 7-week-old IL-4R$\alpha^{-/-}$ maternally vaccinated offspring have slightly increased alveolar macrophages in the BAL in the presence of a T4P2 infection. 7-week-old offspring were either born to unvaccinated or PCV13 vaccinated dams. **A.** Total alveolar macrophage (SiglecF$^+$ Ly6G$^-$ CD11b$^+$ CD11c$^+$) populations were investigated in the BAL. All cell populations were identified using flow cytometry. The results are expressed as individual mice/data points. Representative of 2 experiments whereby n = 5-7 mice per group. Statistical analysis was performed using a Kruskal-Wallis test. P values was regarded as significant if less than 0.05 (* $p<0.05$, ** $p<0.01$, *** $p<0.001$).

Dendritic cell (DC) (SiglecF^{-} Ly6G^{-} MHCII^{+} CD11c^{+}) populations were investigated in the BAL. WT maternally unvaccinated and infected offspring had significantly increased DC populations in 7-week-old offspring **(Figure 6.18)**. The DC infiltration was significantly decreased in WT maternally vaccinated and infected offspring **(Figure 6.18)**. The IL-4R$\alpha^{-/-}$ offspring had no observed differences between the maternally unvaccinated and vaccinated groups **(Figure 6.18)**. However, a significant reduction in DC's was observed between WT maternally unvaccinated and infected and IL-4R$\alpha^{-/-}$ maternally unvaccinated and infected offspring **(Figure 6.18)**.

A. Total number of dendritic cells in the BAL

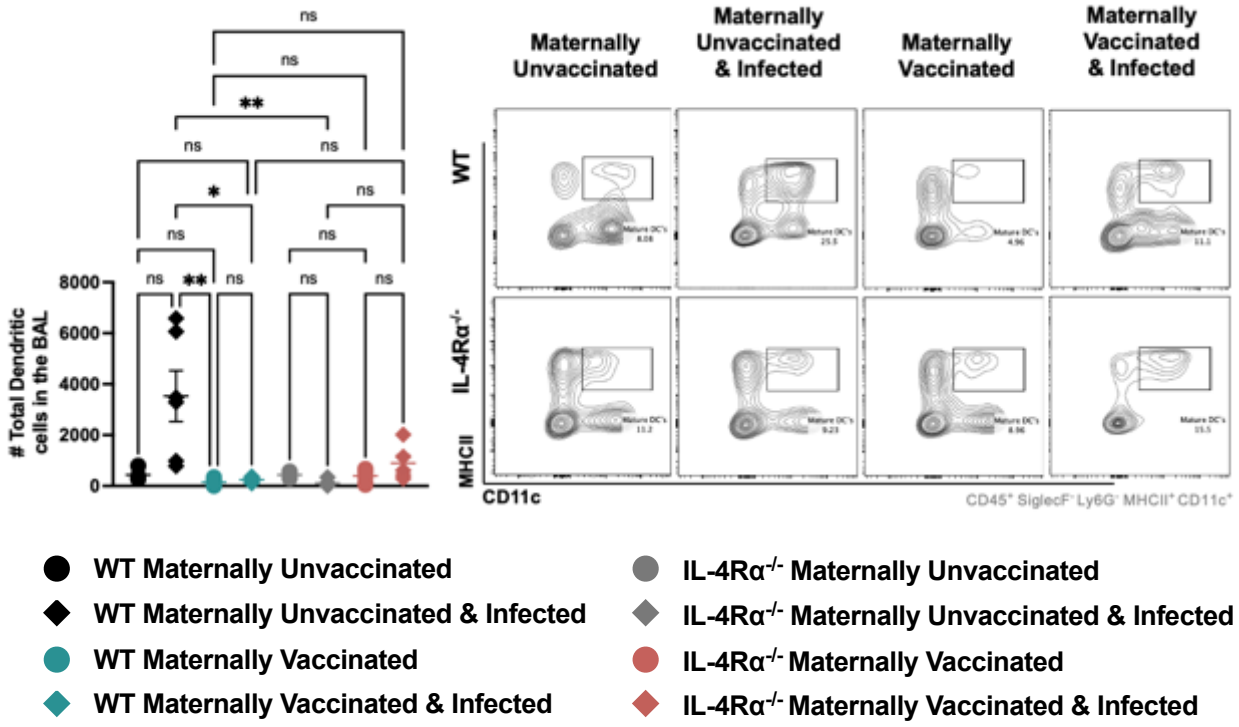

Figure 6.18: 7-week-old WT maternally vaccinated offspring have increased dendritic cells in the BAL in the presence of a T4P2 infection.
7-week-old offspring were either born to unvaccinated or PCV13 vaccinated dams. **A.** Total dendritic cell (SiglecF$^-$ Ly6G$^-$ MHCII$^+$ CD11c$^+$) populations were investigated in the BAL. All cell populations were identified using flow cytometry. The results are expressed as individual mice/data points. Representative of 2 experiment whereby n = 5-7 mice per group. Statistical analysis was performed using a Kruskal-Wallis test. P values was regarded as significant if less than 0.05 (* $p<0.05$, ** $p<0.01$, *** $p<0.001$).

6. 2.4 Maternal vaccination in 7-week-old WT offspring results in decreased T4P2 CFU in the lung.

Lungs were processed into single cell suspensions and plated on BAB agar plates to investigate CFU's. WT and IL-4R$\alpha^{-/-}$ maternally unvaccinated and infected offspring had significantly increased CFU's in the lung **(Figure 6.19)**. Maternal vaccination reduced the overall CFU titre in both WT and IL-4R$\alpha^{-/-}$ groups however the CFU's were significantly reduced only in the WT maternally vaccinated and infected offspring **(Figure 6.19)**.

A. T4P2 CFU in the Lung of 7-week-old offspring

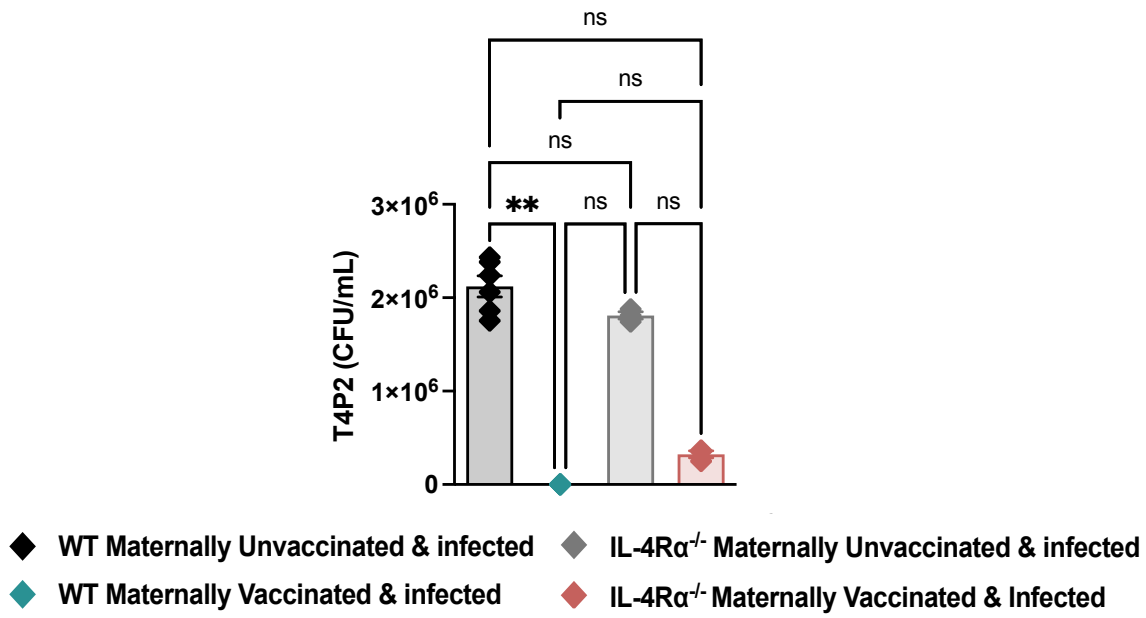

Figure 6.19: WT Maternally vaccinated 7-week-old offspring have reduced T4P2 CFU's in the lung.
7-week-old offspring were either born to unvaccinated or PCV13 vaccinated dams **A.** T4P2 CFU's were recorded in the lung of WT and IL-4R$\alpha^{-/-}$ maternally vaccinated and maternally unvaccinated offspring. The results are expressed as individual mice/data points. Representative of 2 experiments whereby n = 5-8 mice per group. Statistical analysis was performed using a Kruskal-Wallis test. P values was regarded as significant if less than 0.05 (* $p<0.05$, ** $p<0.01$, *** $p<0.001$).

CD45$^+$ immune cell percentages were investigated in the lung. Cell percentages were separated into offspring (CD45$^+$ H2Kb$^+$ H2Dd$^-$) and maternal (CD45$^+$ H2Kb$^+$ H2Dd$^+$) CD45$^+$ immune cell populations. Overall maternal cell populations were higher in IL-4R$\alpha^{-/-}$ offspring when compared to WT offspring **(Figure 6.20)**. Maternal vaccination slightly increased the maternal cell populations in both WT and IL-4R$\alpha^{-/-}$ offspring however cell numbers were further increased in the presence on T4P2 infection **(Figure 6.20)**. These results indicate that maternal cells are recruited to the lung in IL-4R$\alpha^{-/-}$ offspring in the presence of an infection.

A. Total CD45$^+$ Immune cells in the lung: Maternal vs offspring cell percentages

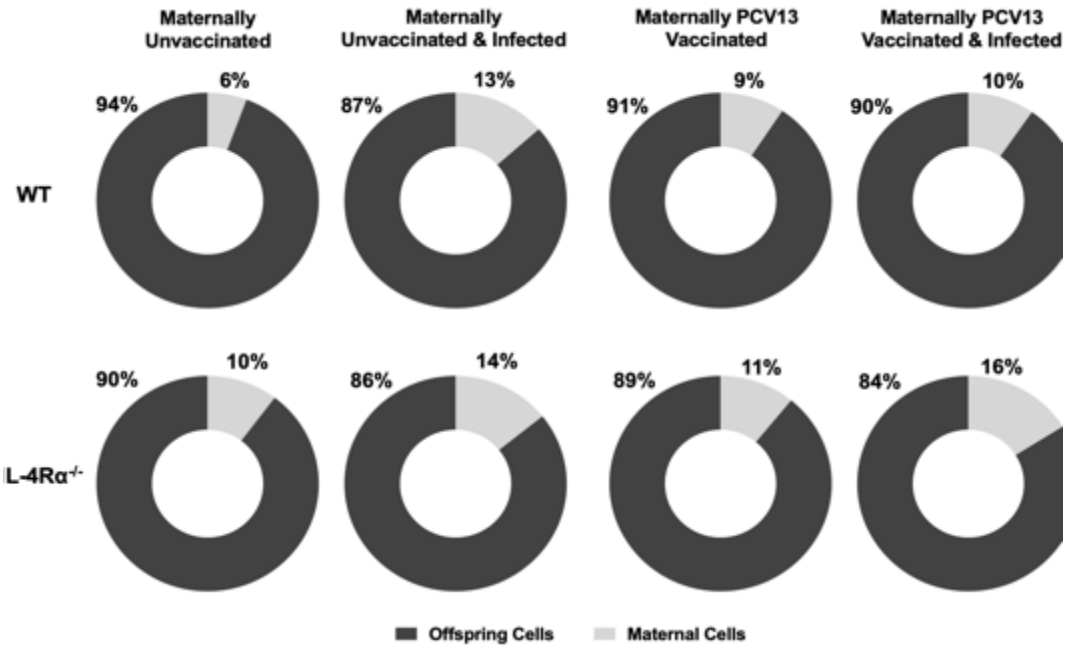

Figure 6.20: IL-4R$\alpha^{-/-}$ offspring have slightly increased maternal CD45$^+$ immune cell populations in the lung.
WT and IL-4R$\alpha^{-/-}$ 7-week-old offspring were either born to unvaccinated or PCV13 vaccinated dams. **A.** Offspring and maternal cell percentages were investigated in the lung. All cell populations were identified using flow cytometry. The results are expressed as individual mice/data points. Representative of 2 experiments whereby n = 5-7 mice per group. Statistical analysis was performed using a Kruskal-Wallis test. P values was regarded as significant if less than 0.05 (* $p<0.05$, ** $p<0.01$, *** $p<0.001$).

$CD45^+$ Immune cell populations were investigated by separating offspring ($CD45^+$ $H2Kb^+$ $H2Dd^-$) and maternal ($CD45^+$ $H2Kb^+$ $H2Dd^+$) cells in the lung **(Figure 6.21)**. WT maternally vaccinated offspring had significantly reduced total $CD45^+$ cell numbers however cell numbers increased in the presence of infection **(Figure 6.21)**. Total $CD45^+$ cell numbers were slightly elevated in the presence on infection in both IL-4R$\alpha^{-/-}$ maternally unvaccinated and maternally vaccinated offspring **(Figure 6.21)**. Maternal cells numbers in the lung were elevated in the presence of infection however more maternal cells were recruited to the lungs of IL-4R$\alpha^{-/-}$ compared to WT offspring **(Figure 6.21)**.

Total $B220^+$ B cell numbers were investigated in the lungs of 7-week-old offspring. Overall total $B220^+$ B cell numbers were increased in the IL-4R$\alpha^{-/-}$ offspring compared to WT offspring **(Figure 6.22)**. WT and IL-4R$\alpha^{-/-}$ maternally vaccinated and infected offspring had elevated recruitment of total $B220^+$ B cells to the lung **(Figure 6.22)**. Offspring $B220^+$ B cells followed a similar trend to overall total $B220^+$ B cell numbers **(Figure 6.23A)**. Maternal $B220^+$ B cells showed a different trend whereby maternal cells were only elevated in the WT maternally vaccinated and infected offspring **(Figure 6.23B)**. The maternal cells had limited recruitment to the lung in IL-4R$\alpha^{-/-}$ offspring **(Figure 6.23B)**.

A. CD45⁺ immune cells in the lung: maternal vs offspring cell numbers

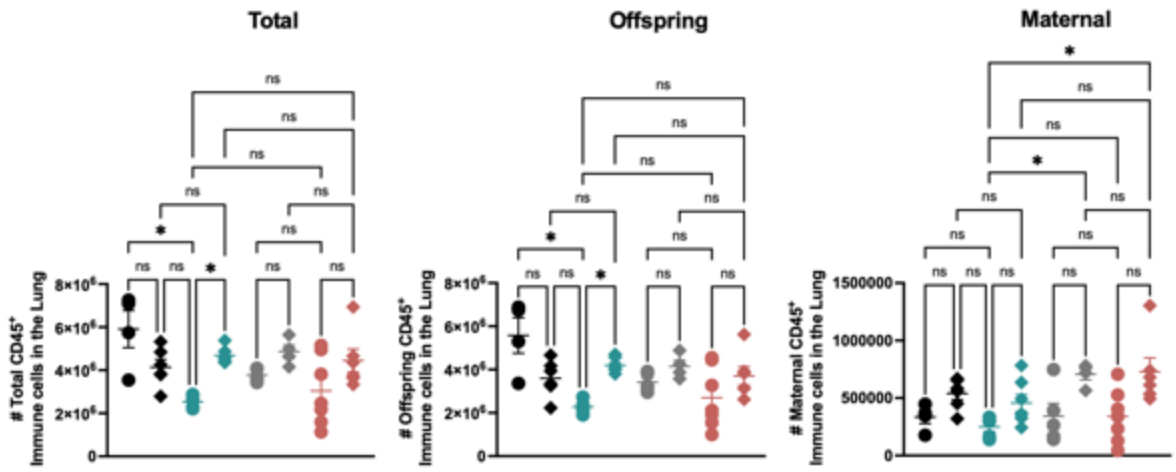

B. Maternal vs offspring CD45⁺ immune cells FSC plots in the lung

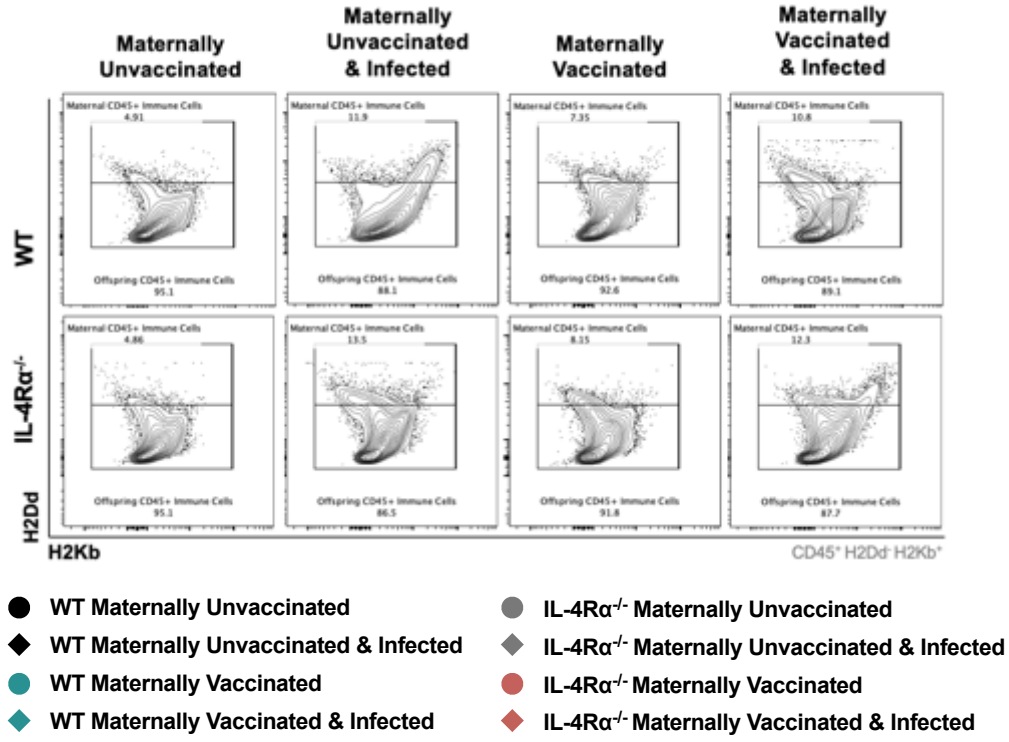

Figure 6.21: IL-4R$\alpha^{-/-}$ infected offspring have increased CD45⁺ immune cell populations in the lung

7-week-old offspring were either born to unvaccinated or PCV13 vaccinated dams **A.** Total (CD45⁺), Offspring (CD45⁺ H2Kb⁺ H2Dd⁻) and maternal (CD45⁺ H2Kb⁺ H2Dd⁺) CD45⁺ Immune cell populations were investigated in the lungs. **B.** FCS files of maternal and offspring CD45⁺ cell populations were investigated in the lungs. Representative of 2 experiments whereby n = 4-7 mice per group. Statistical analysis was performed using a Kruskal-Wallis test. P values was regarded as significant if less than 0.05 (* $p<0.05$, ** $p<0.01$, *** $p<0.001$).

A. Total B220⁺ B cell numbers in the lung

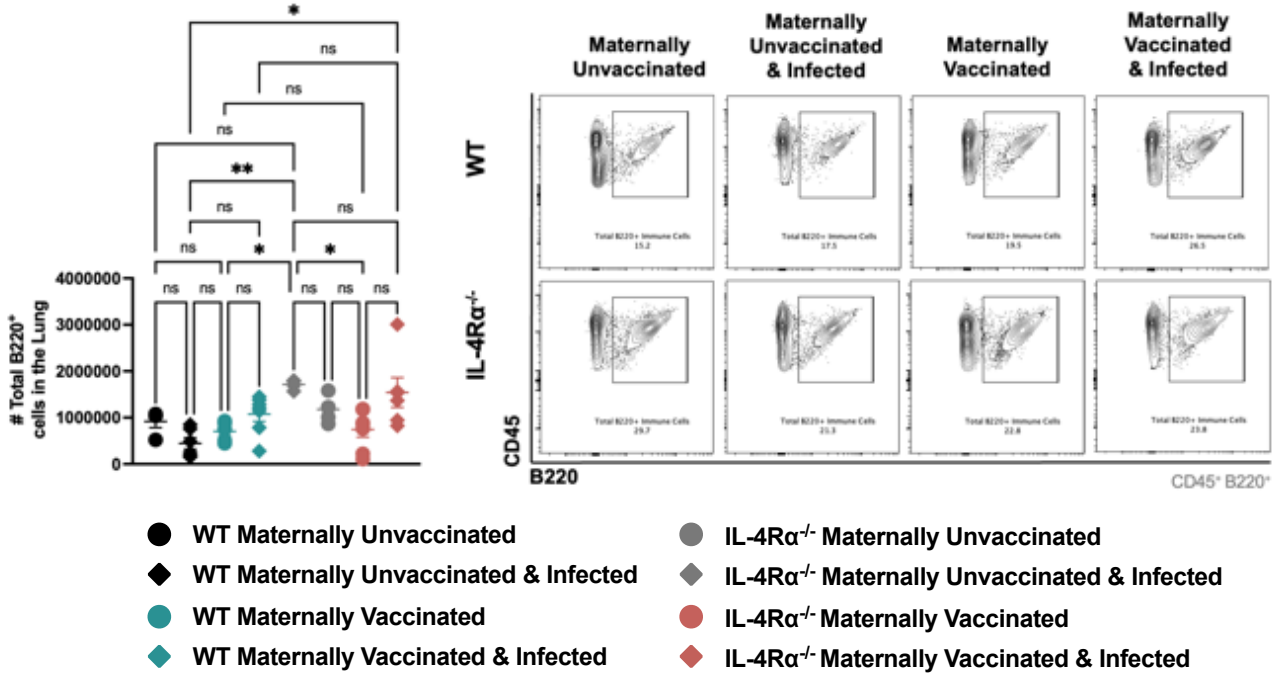

Figure 6.22: IL-4R$\alpha^{-/-}$ offspring have increased maternal B220⁺ cell populations in the lung.
7-week-old offspring were either born to unvaccinated or PCV13 vaccinated dams. **A.** Total B220⁺ B cell (CD45⁺ B220⁺) populations were investigated in the lungs. Representative of 2 experiments whereby n = 4-7 mice per group. Statistical analysis was performed using a Kruskal-Wallis test. P values was regarded as significant if less than 0.05 (* $p<0.05$, ** $p<0.01$, *** $p<0.001$).

A. Offspring B220⁺ B cell numbers in the lung

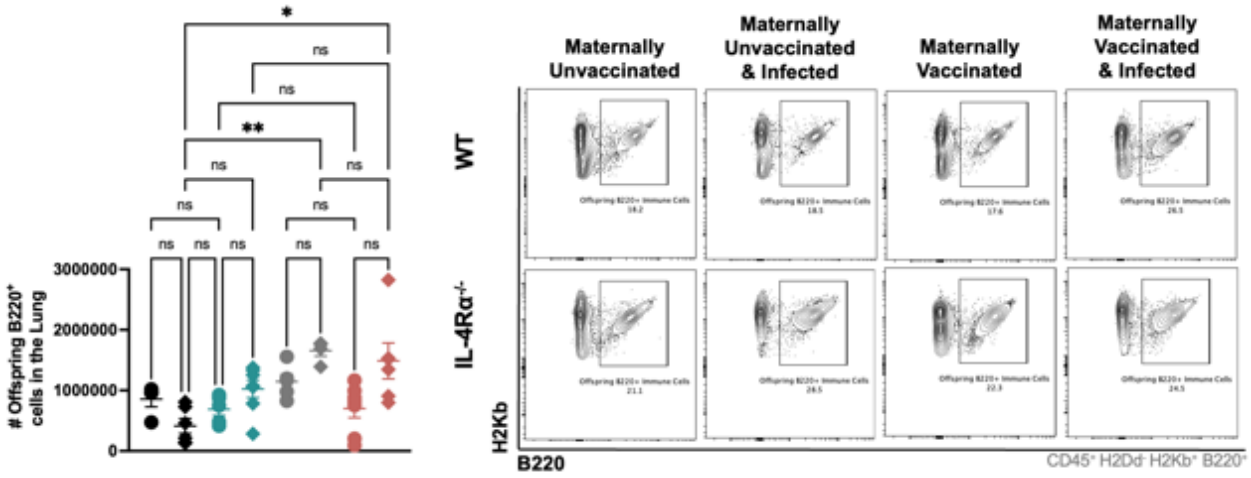

B. Maternal B220⁺ B cell numbers in the lung

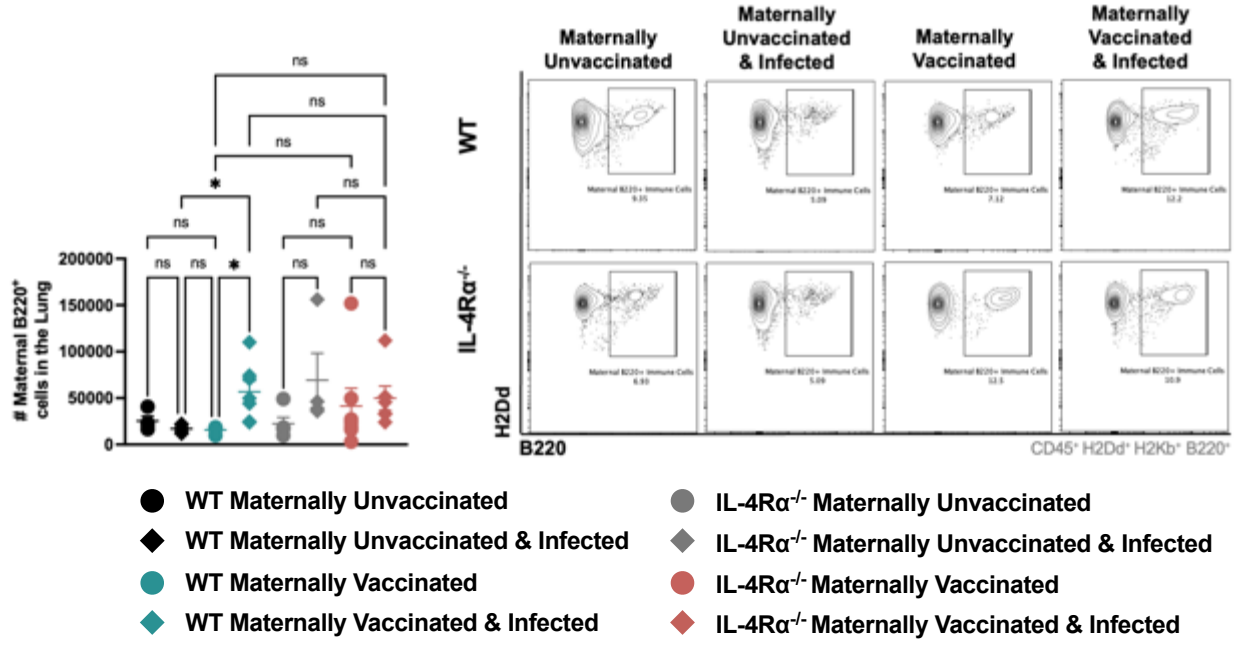

Figure 6.23: Maternally vaccinated and infected offspring have increased maternal B220⁺ cell populations in the lung.
7-week-old offspring were either born to unvaccinated or PCV13 vaccinated dams. **A.** Offspring B220⁺ B cells (H2Kb⁺ H2Dd⁻ B220⁺) and **B.** maternal B220⁺ B cell (H2Kb⁺ H2Dd⁺ B220⁺) populations were investigated in the lungs. Representative of 2 experiments whereby n = 4-7 mice per group. Statistical analysis was performed using a Kruskal-Wallis test. P values was regarded as significant if less than 0.05 (* p<0.05, ** p<0.01, *** p<0.001).

Total plasma cell populations (CD45$^+$ B220$^+$ CD138$^+$TACI$^+$) were investigated in the lungs. Overall total plasma cells were increased in IL-4R$\alpha^{-/-}$ offspring compared to WT offspring **(Figure 6.24)**. Total plasma cells were increased specifically in the presence of an infection in both IL-4R$\alpha^{-/-}$ maternally unvaccinated and vaccinated offspring **(Figure 6.24)**. Offspring plasma cells (CD45$^+$ H2Dd$^-$ H2Kb$^+$ B220$^+$ CD138$^+$ TACI$^+$) and maternal plasma cell (CD45$^+$ H2Dd$^+$ H2Kb$^+$ B220$^+$ CD138$^+$ TACI$^+$) populations all followed a similar trend **(Figure 6.25A, B)**. However no significant differences were observed between populations.

A. Total plasma cell numbers in the lung

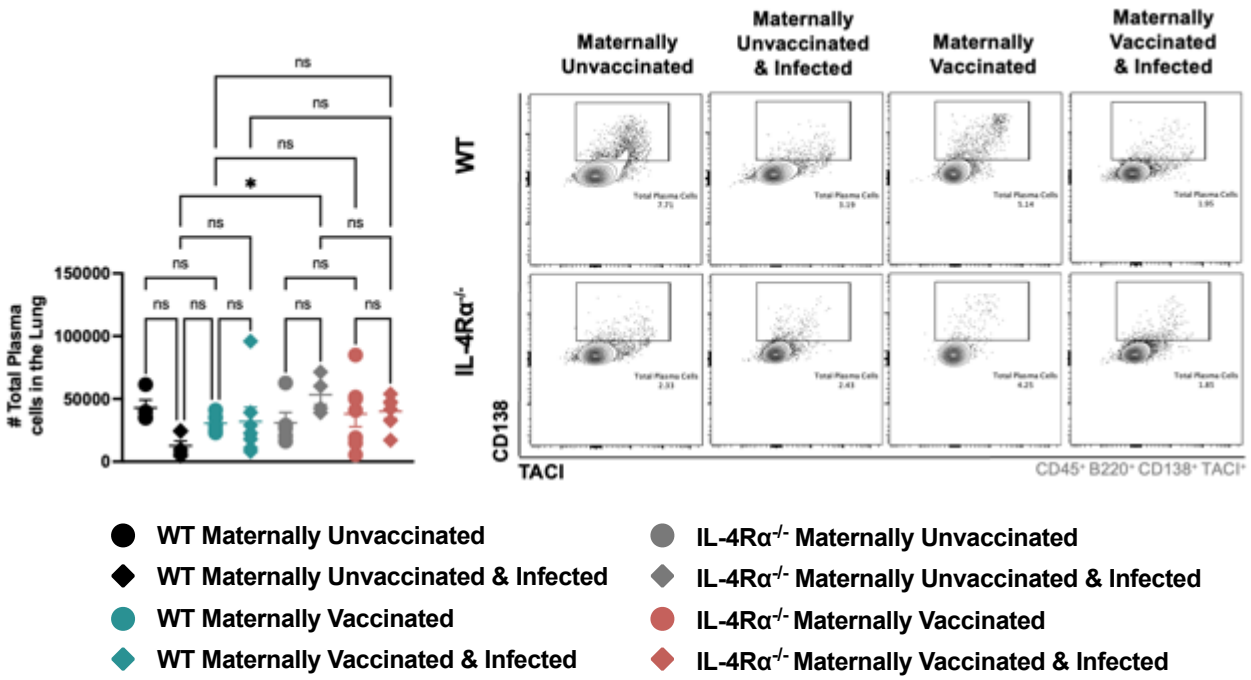

Figure 6.24: IL-4R$\alpha^{-/-}$ offspring have slightly elevated plasma cells in the lung. 7-week-old offspring were either born to unvaccinated or PCV13 vaccinated dams. **A.** Total plasma cell (CD45$^+$ B220$^+$ CD138$^+$ TACI$^+$) populations were investigated in the lungs. Representative of 2 experiments whereby n = 4-7 mice per group. Statistical analysis was performed using a Kruskal-Wallis test. P values was regarded as significant if less than 0.05 (* p<0.05, ** p<0.01, *** p<0.001).

A. Offspring plasma cell numbers in the lung

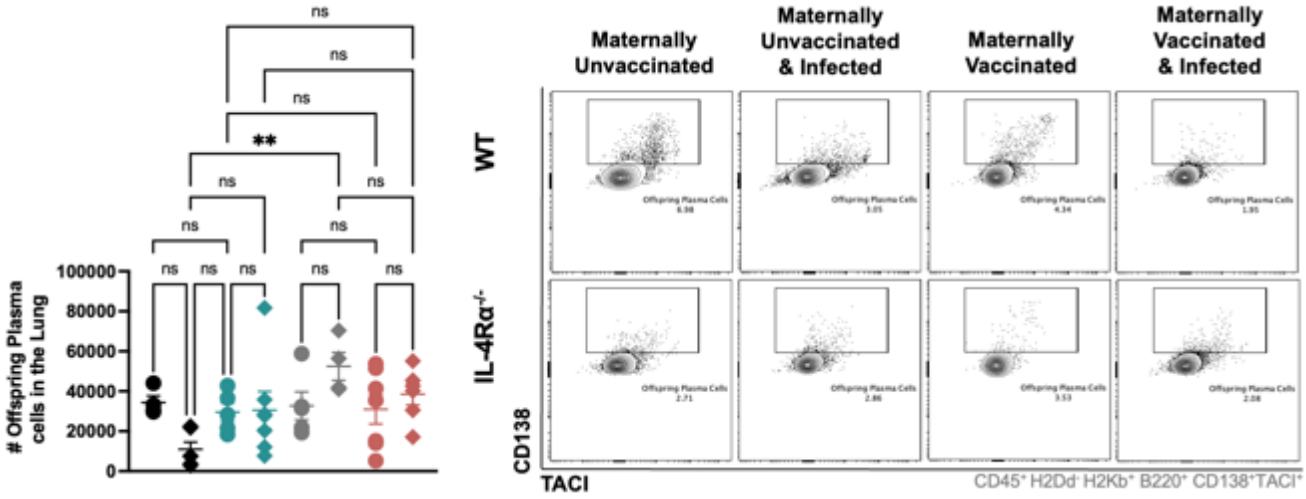

B. Maternal plasma cell numbers in the lung

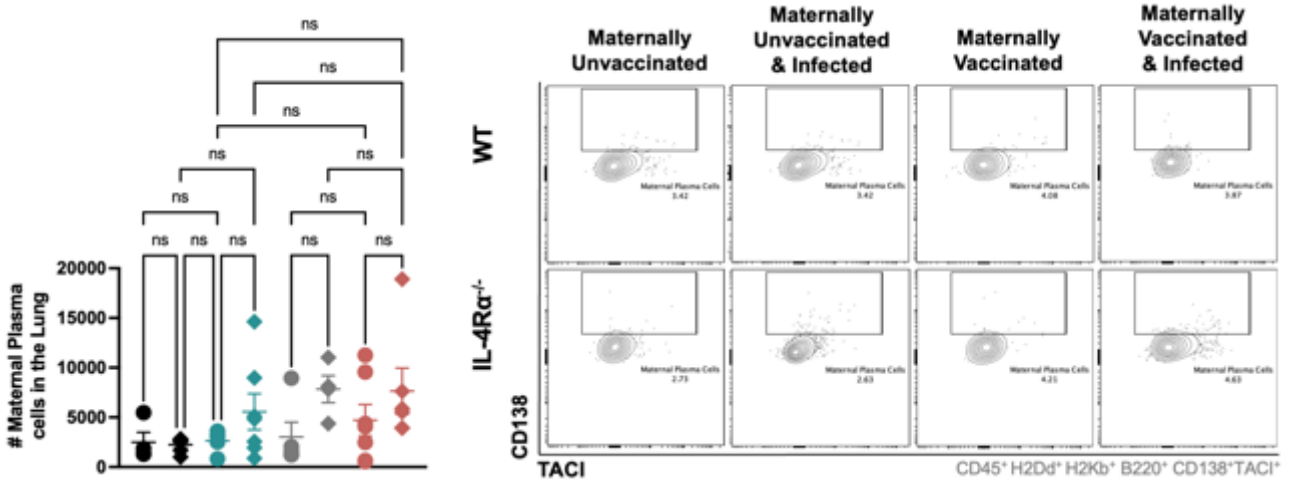

- WT Maternally Unvaccinated
- WT Maternally Unvaccinated & Infected
- WT Maternally Vaccinated
- WT Maternally Vaccinated & Infected
- IL-4Rα$^{-/-}$ Maternally Unvaccinated
- IL-4Rα$^{-/-}$ Maternally Unvaccinated & Infected
- IL-4Rα$^{-/-}$ Maternally Vaccinated
- IL-4Rα$^{-/-}$ Maternally Vaccinated & Infected

Figure 6.25: IL-4R$\alpha^{-/-}$ offspring have slightly elevated plasma cells in the lung. 7-week-old offspring were either born to unvaccinated or PCV13 vaccinated dams. **A.** Offspring plasma cells (CD45$^+$ H2Dd$^-$ H2Kb$^+$ B220$^+$ CD138$^+$TACI$^+$) and **B.** maternal plasma cell (CD45$^+$ H2Dd$^+$ H2Kb$^+$ B220$^+$ CD138$^+$TACI$^+$) populations were investigated in the lungs. Representative of 2 experiments whereby n = 4-7 mice per group. Statistical analysis was performed using a Kruskal-Wallis test. P values was regarded as significant if less than 0.05 (* $p<0.05$, ** $p<0.01$, *** $p<0.001$).

Total IgG1^{+} (CD45^{+} CD19^{+} IgG1$^{+)}$ and IgG2a^{+} B cell (CD45^{+} CD19^{+} IgG2a$^{+)}$ populations were investigated in the lung of 7-week-old offspring. No significant differences or trends were observed between in WT and IL-4R$\boldsymbol{\alpha}^{-/-}$ maternally unvaccinated and vaccinated offspring **(Figure 6.26A, B)**.

A. Total IgG1⁺ plasma cell profile in the lung of 7-week-old offspring

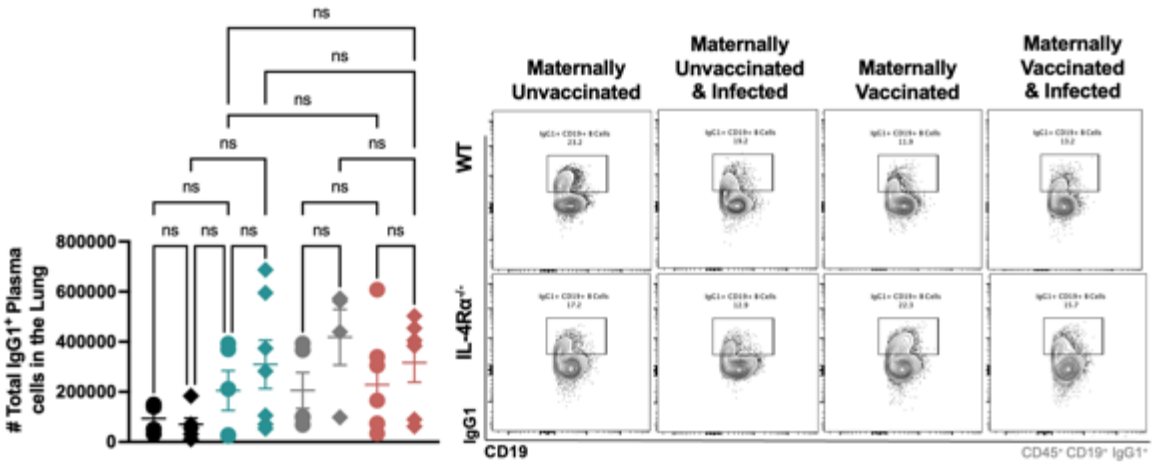

B. Total IgG2a⁺ plasma cell profile in the lung of 7-week-old offspring

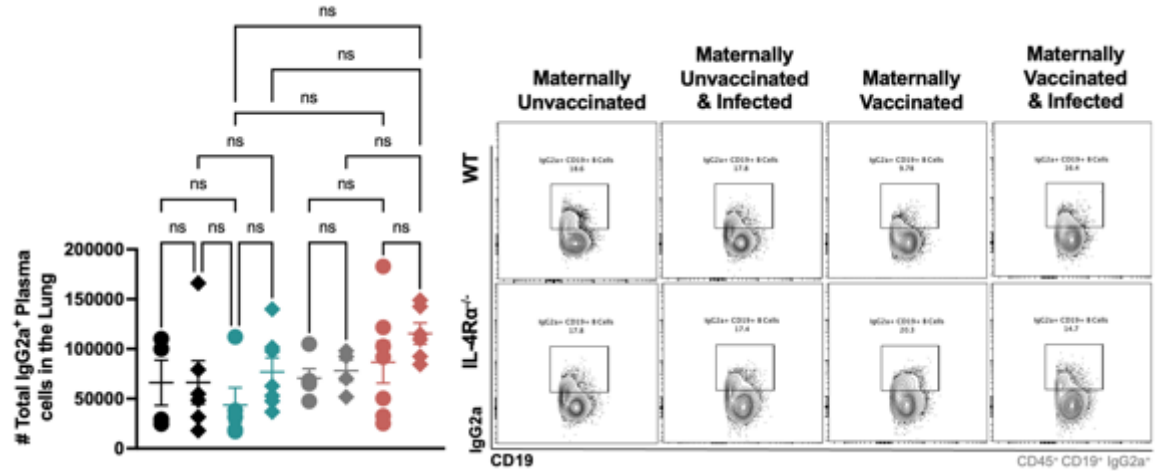

- WT Maternally Unvaccinated
- WT Maternally Unvaccinated & Infected
- WT Maternally Vaccinated
- WT Maternally Vaccinated & Infected
- IL-4Rα$^{-/-}$ Maternally Unvaccinated
- IL-4Rα$^{-/-}$ Maternally Unvaccinated & Infected
- IL-4Rα$^{-/-}$ Maternally Vaccinated
- IL-4Rα$^{-/-}$ Maternally Vaccinated & Infected

Figure 6.26: No differences in total IgG1⁺ and IgG2a+ B Cell populations were present in the lung of 7-week-old offspring.
7-week-old offspring were either born to unvaccinated or PCV13 vaccinated dams. **A.** Total IgG1⁺ B cells (CD45⁺ CD19⁺ IgG1⁺) and **B.** Total IgG2a⁺ B cell (CD45⁺ CD19⁺ IgG2a⁺) populations were investigated in the lungs. Representative of 2 experiments whereby n = 4-7 mice per group. Statistical analysis was performed using a Kruskal-Wallis test. P values was regarded as significant if less than 0.05 (* $p<0.05$, ** $p<0.01$, *** $p<0.001$).

6. 2.5 WT maternally vaccinated offspring bone marrow cells secrete PCV13-specific total IgG and IgG1 antibodies.

Femurs were flushed with sterile 1X PBS and bone marrow cells were processed into single cell suspensions. $1X10^7$ bone marrow cells were plated in RPMI media supplemented with 10% FBS and supernatants were collected 24h later. PCV13-specific total IgG and IgG1 antibodies were investigated in supernatants using ELISA.
PCV13-specific total IgG and IgG1 antibodies were only detected in WT maternally vaccinated and maternally vaccinated and infected offspring **(Figure 6.27)**. No antibody titres were detected in IL-4R$\alpha^{-/-}$ maternally vaccinated and maternally vaccinated and infected offspring **(Figure 6.27)**.

$CD45^+$ immune cell percentages were investigated in the bone marrow. Total cells were separated into offspring ($CD45^+$ $H2Kb^+$ $H2Dd^-$) and maternal ($CD45^+H2Kb^+$ $H2Dd^+$) cell populations. Maternal cell populations were increased in WT maternally unvaccinated and infected, WT maternally vaccinated and infected offspring as well as IL-4R$\alpha^{-/-}$ maternally unvaccinated and infected offspring **(Figure 6.28)**. However maternal cell populations decreased in IL-4R$\alpha^{-/-}$ maternally vaccinated and infected offspring **(Figure 6.28)**.

A. Maternally vaccinated 7-week-old offspring have increased maternally derived PCV13-specific antibodies in the bone marrow.

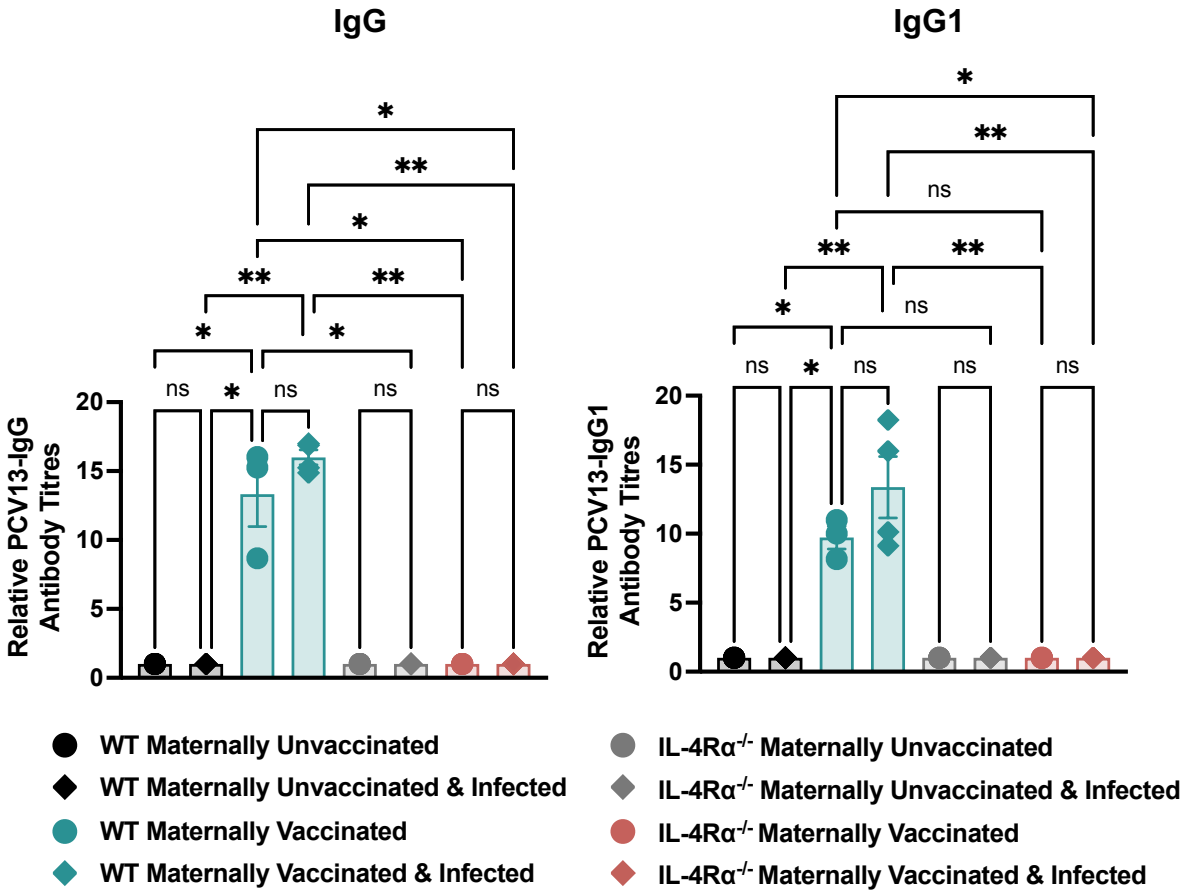

Figure 6.27: Maternally vaccinated 7-week-old offspring have increased maternally derived PCV13-specific antibodies in the bone marrow.
7-week-old offspring were either born to unvaccinated or PCV13 vaccinated dams **A.** 1X10^{7} bone marrow cells were plated in RPMI media and supernatants were collected 24h later. PCV13-specific antibody serotypes were investigated using ELISA. The results are expressed as individual mice/data points. Representative of 2 experiment whereby n = 5 mice per group. Statistical analysis was performed using a Kruskal-Wallis test. P values was regarded as significant if less than 0.05 (* p<0.05, ** p<0.01, *** p<0.001).

A. Total CD45$^+$ Immune cells in the bone marrow: Maternal vs offspring cell percentages

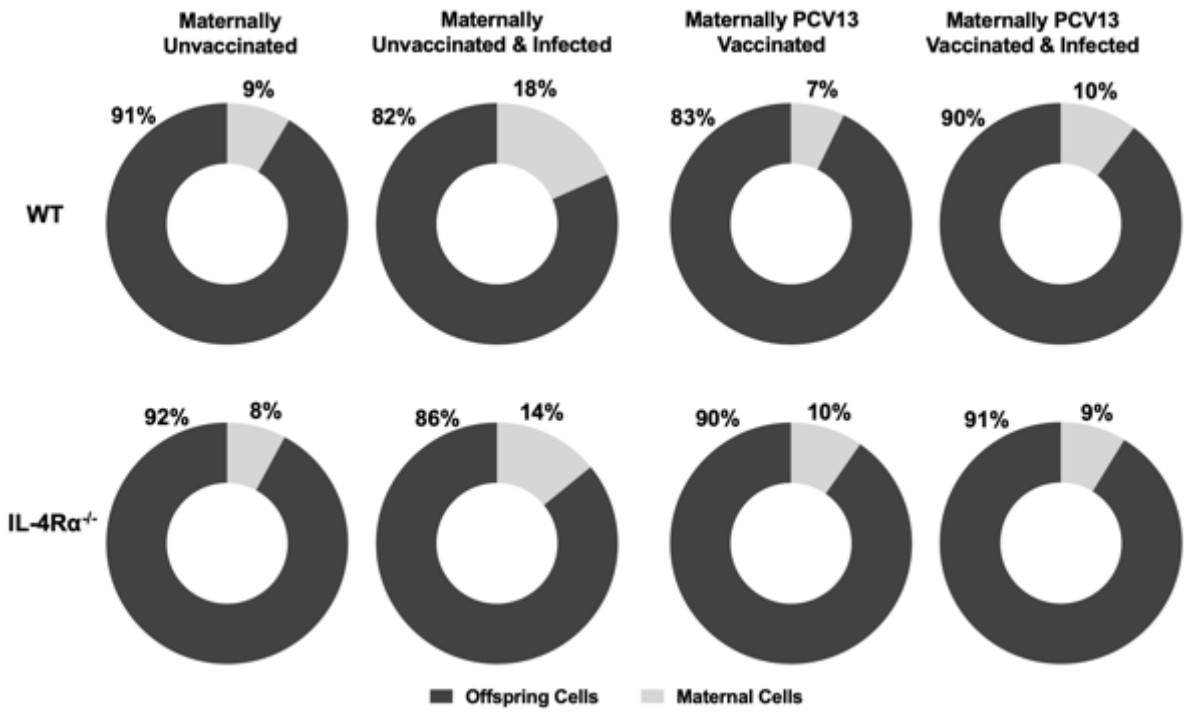

Figure 6.28: WT infected offspring have slightly increased maternal CD45$^+$ immune cell populations in the bone marrow.
WT and IL-4R$\alpha^{-/-}$ 7-week-old offspring were either born to unvaccinated or PCV13 vaccinated dams. **A.** Offspring and maternal cell percentages were investigated in the lung. All cell populations were identified using flow cytometry. The results are expressed as individual mice/data points. Representative of 2 experiments whereby n = 5-9 mice per group. Statistical analysis was performed using a Kruskal-Wallis test. P value was regarded as significant if less than 0.05 (* $p<0.05$, ** $p<0.01$, *** $p<0.001$).

Total (CD45$^+$) and Offspring (CD45$^+$ H2Kb$^+$ H2Dd$^-$) immune cell populations were slightly elevated in IL-4R$\alpha^{-/-}$ maternally unvaccinated and vaccinated offspring **(Figure 6.29)**. Total and offspring immune cell populations increased in IL-4R$\alpha^{-/-}$ maternally vaccinated offspring in the presence of an infection **(Figure 6.29)**. Maternal cells (CD45$^+$ H2Kb$^+$ H2Dd$^+$) were slightly elevated in the presence of infection in both WT

A. CD45⁺ immune cells in the bone marrow: maternal vs offspring cell numbers

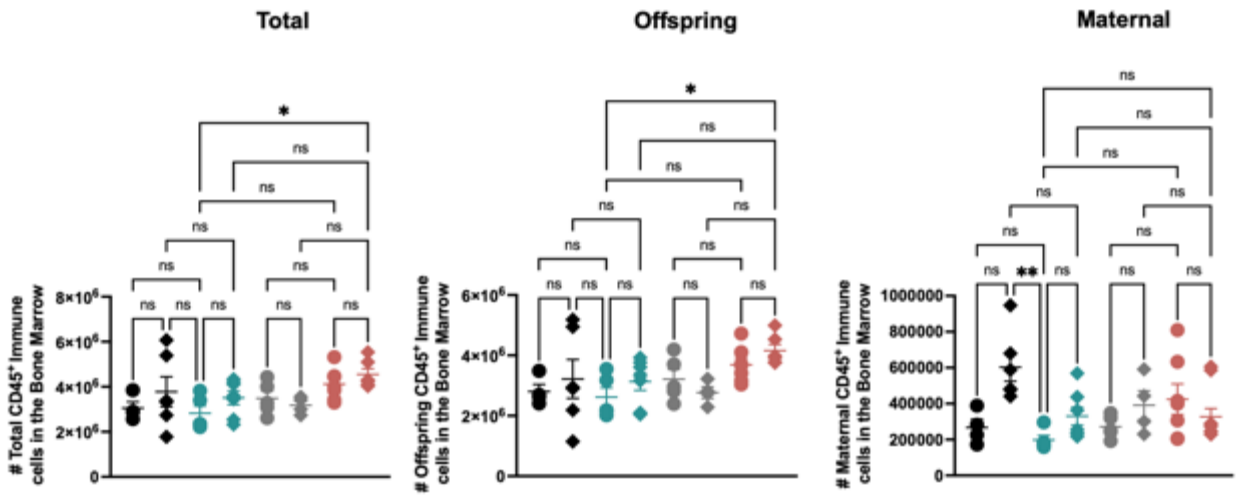

B. Maternal vs offspring CD45⁺ immune cells FSC plots in the bone marrow

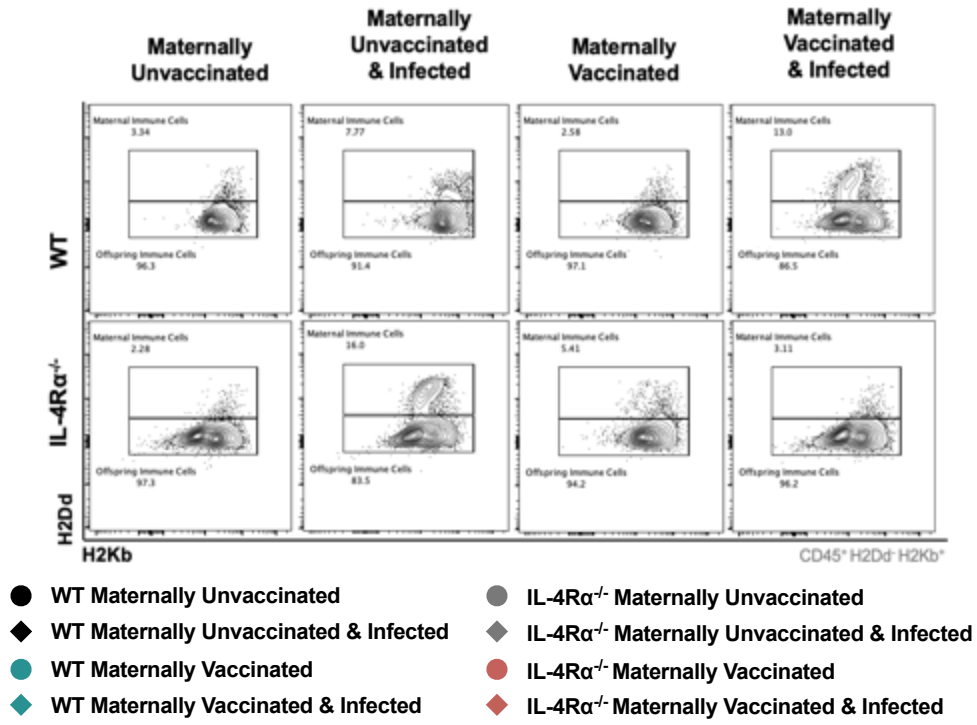

Figure 6.29: WT maternally vaccinated offspring have reduced maternal cells in the bone marrow.

7-week-old offspring were either born to unvaccinated or PCV13 vaccinated dams **A.** Total (CD45⁺), Offspring (H2Kb⁺ H2Dd⁻) and maternal (H2Kb⁺ H2Dd⁺) CD45⁺ Immune cell populations were investigated in the bone marrow. **B.** FCS files of maternal and offspring CD45⁺ cell populations were investigated in the bone marrow. Representative of 2 experiments whereby n = 4-7 mice per group. Statistical analysis was performed using a Kruskal-Wallis test. P values was regarded as significant if less than 0.05 (* $p<0.05$, ** $p<0.01$, *** $p<0.001$).

and IL-4R$\alpha^{-/-}$ maternally unvaccinated and vaccinated offspring **(Figure 6.29)**. Maternal cells in WT maternally unvaccinated and infected offspring were higher than in WT maternally vaccinated and infected offspring. However, no differences in maternal cell numbers were present between IL-4R$\alpha^{-/-}$ maternally unvaccinated and vaccinated offspring under the influence of a T4P2 infection **(Figure 6.29)**.

Total B220^{+} B cells were elevated in WT maternally unvaccinated offspring however no differences were observed between WT maternally vaccinated and IL-4R$\alpha^{-/-}$ maternally unvaccinated and vaccinated offspring **(Figure 6.30)**.

A. Total B220^{+} B cell numbers in the bone marrow

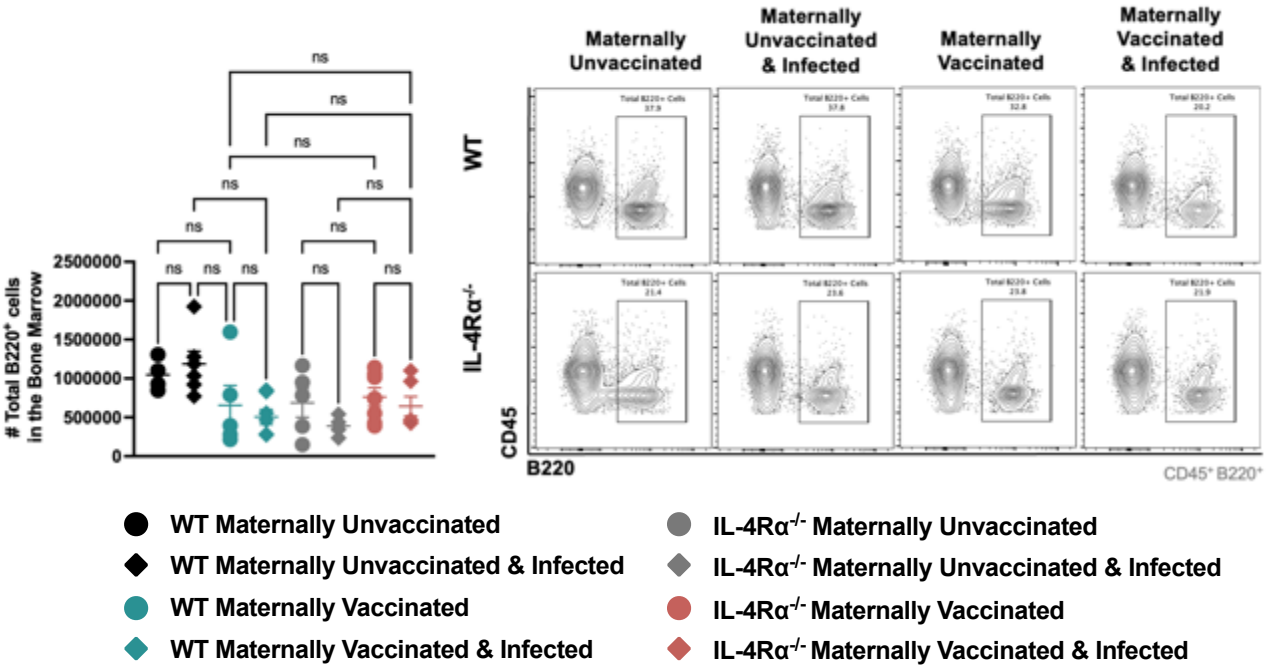

Figure 6.30: Total B220+ B cells were slightly elevated in WT maternally unvaccinated and infected 7-week-old offspring in the bone marrow.
7-week-old offspring were either born to unvaccinated or PCV13 vaccinated dams. **A.** Total B220^{+} B cells (CD45^{+}B220^{+}) populations were investigated in the bone marrow. Representative of 2 experiments whereby n = 4-7 mice per group. Statistical analysis was performed using a Kruskal-Wallis test. P values was regarded as significant if less than 0.05 (* $p<0.05$, ** $p<0.01$, *** $p<0.001$).

A similar trend was observed in offspring $B220^+$ B ($H2Kb^+$ $H2Dd^-$ $B220^+$) cells. WT maternally unvaccinated offspring as well as WT maternally unvaccinated and infected offspring had slightly elevated $B220^+$ B cells in the bone marrow **(Figure 6.31A)**. No differences were observed between WT maternally vaccinated, IL-4R$\alpha^{-/-}$ maternally unvaccinated and vaccinated offspring **(Figure 6.31A)**. Maternal $B220^+$ B cell ($H2Kb^+$ $H2Dd^+$ $B220^+$) numbers were elevated in WT maternally unvaccinated offspring and cells numbers increased in the presence of an infection **(Figure 6.31B)**. Maternal $B220^+$ B cell numbers were significantly reduced in both WT maternally vaccinated and WT maternally vaccinated and infected offspring **(Figure 6.31B)**. No differences were observed in IL-4R$\alpha^{-/-}$ maternally unvaccinated and vaccinated offspring **(Figure 6.31B)**.

Total plasma cells ($CD45^+$ $B220^+$ $CD138^+$ $TACI^+$) were investigated in the bone marrow and no significant changes can be seen between WT and IL-4R$\alpha^{-/-}$ maternally unvaccinated and vaccinated offspring **(Figure 6.32)**. The same trend was observed for offspring plasma cells ($CD45^+$ $H2Dd^-$ $H2Kb^+$ $B220^+$ $CD138^+$ $TACI^+$) whereas maternal plasma ($CD45^+$ $H2Dd^+$ $H2Kb^+$ $B220^+$ $CD138^+$ $TACI^+$) cell numbers were significantly reduced in both WT maternally vaccinated and WT maternally vaccinated and infected offspring **(Figure 6.33A, B)**. No differences were observed in IL-4R$\alpha^{-/-}$ maternally unvaccinated and vaccinated offspring **(Figure 6.33B)**.

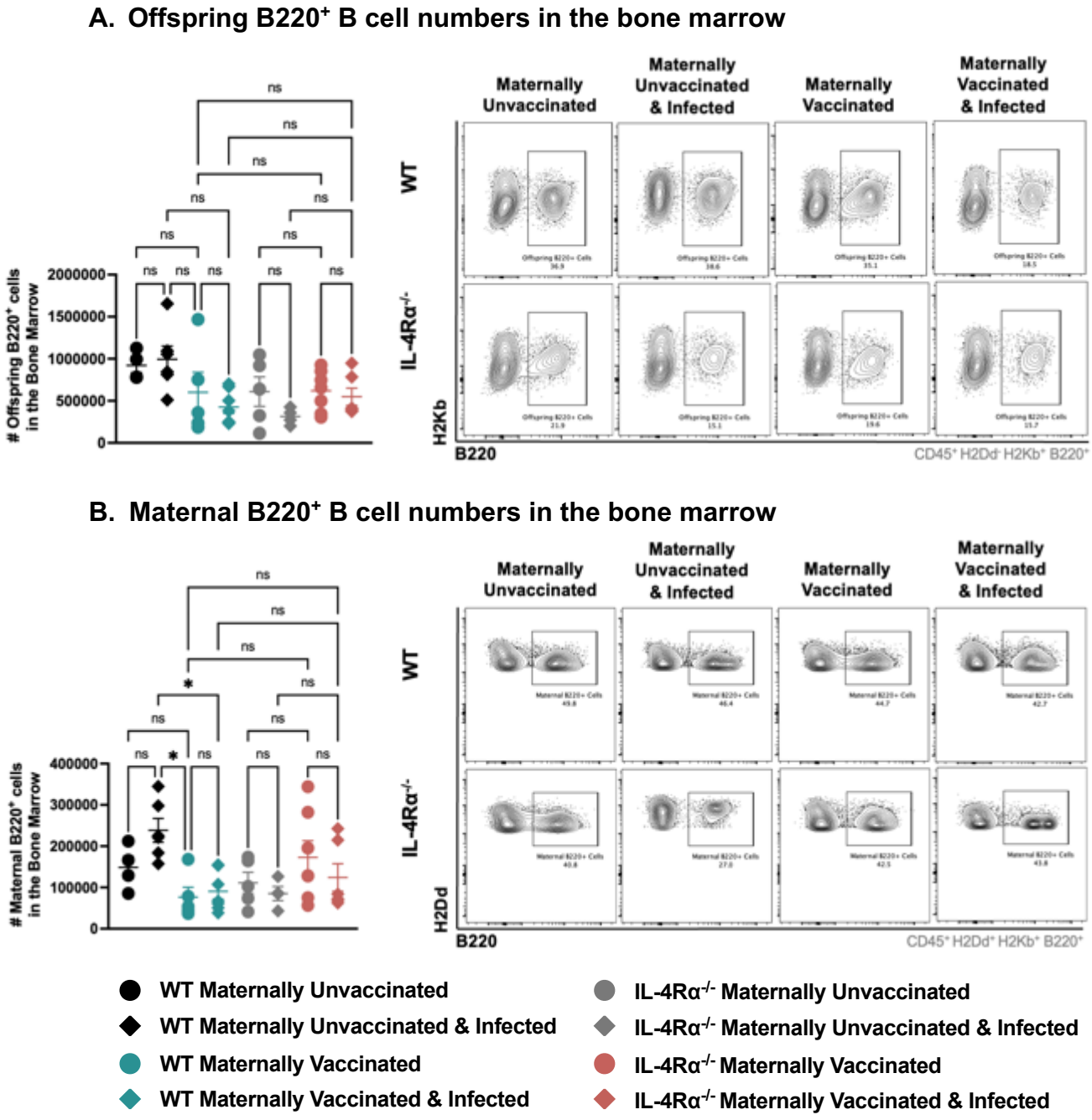

Figure 6.31: Maternal B220+ B cells are reduced in WT maternally vaccinated and infected 7-week-old offspring in the bone marrow.
7-week-old offspring were either born to unvaccinated or PCV13 vaccinated dams. **A.** Offspring B220$^+$ B cells (H2Kb$^+$ H2Dd$^-$ B220$^+$) and **B.** maternal B220$^+$ B cell (H2Kb$^+$ H2Dd$^+$ B220$^+$) populations were investigated in the bone marrow. Representative of 2 experiments whereby n = 4-7 mice per group. Statistical analysis was performed using a Kruskal-Wallis test. P values was regarded as significant if less than 0.05 (* p<0.05, ** p<0.01, *** p<0.001).

A. Total plasma cell numbers in the bone marrow

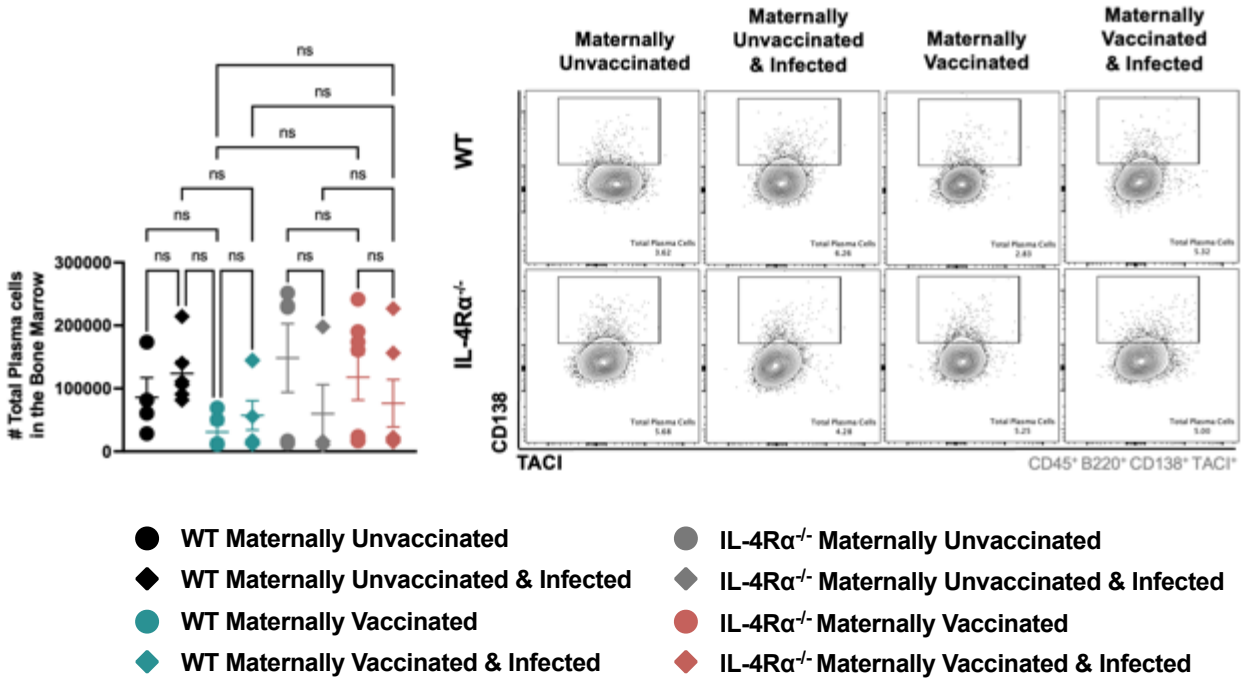

Figure 6.32: No differences were observed in total plasma cell populations were observed in 7-week-old offspring.
7-week-old offspring were either born to unvaccinated or PCV13 vaccinated dams. **A.** Total plasma cells ($CD45^+$ $B220^+$ $CD138^+$ $TACI^+$) populations were investigated in the bone marrow. Representative of 2 experiments whereby n = 4- 7 mice per group. Statistical analysis was performed using a Kruskal-Wallis test. P values was regarded as significant if less than 0.05 (* $p<0.05$, ** $p<0.01$, *** $p<0.001$).

A. Offspring plasma cell numbers in the bone marrow

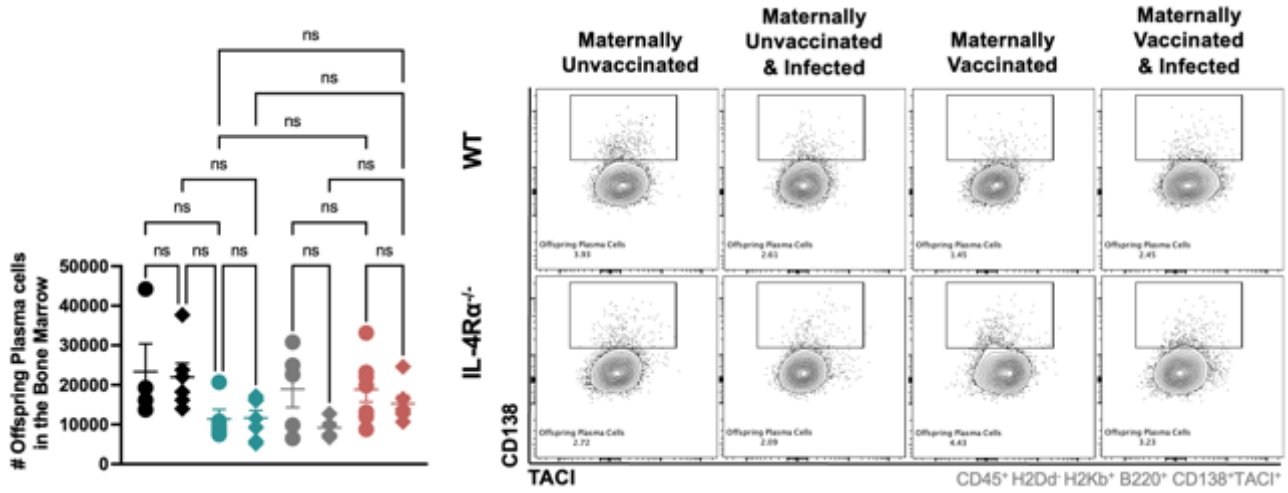

B. Maternal plasma cell numbers in the bone marrow

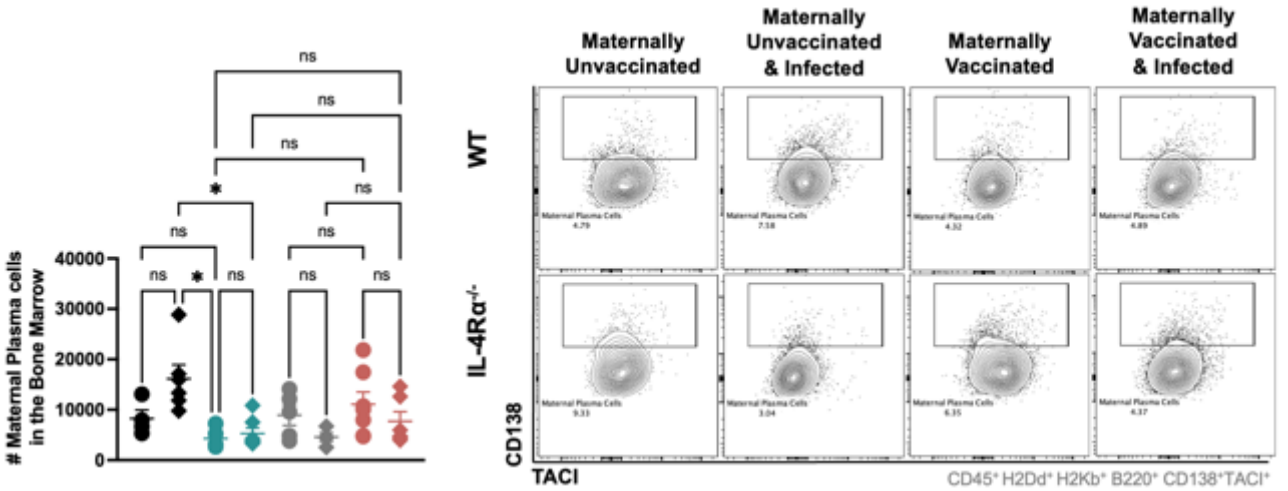

- WT Maternally Unvaccinated
- WT Maternally Unvaccinated & Infected
- WT Maternally Vaccinated
- WT Maternally Vaccinated & Infected
- IL-4Rα$^{-/-}$ Maternally Unvaccinated
- IL-4Rα$^{-/-}$ Maternally Unvaccinated & Infected
- IL-4Rα$^{-/-}$ Maternally Vaccinated
- IL-4Rα$^{-/-}$ Maternally Vaccinated & Infected

Figure 6.33: Maternal plasma cell populations were decreased in the bone marrow of WT maternally vaccinated and infected 7-week-old offspring.
7-week-old offspring were either born to unvaccinated or PCV13 vaccinated dams. **A.** Offspring plasma cells (CD45$^+$ H2Dd$^-$ H2Kb$^+$ B220$^+$ CD138$^+$ TACI$^+$) and **B.** maternal plasma cell (CD45$^+$ H2Dd$^+$ H2Kb$^+$ B220$^+$ CD138$^+$ TACI$^+$) populations were investigated in the bone marrow. Representative of 2 experiments whereby n = 4-7 mice per group. Statistical analysis was performed using a Kruskal-Wallis test. P values was regarded as significant if less than 0.05 (* p<0.05, ** p<0.01, *** p<0.001).

Total IgG1$^+$ (CD45$^+$ CD19$^+$ IgG1$^+$) and IgG2a$^+$ (CD45$^+$ CD19$^+$ IgG2a$^+$) B cells were investigated in the bone marrow of 7-week-old offspring. No differences in IgG1$^+$ B cell populations were observed between WT and IL-4R$\alpha^{-/-}$ maternally unvaccinated and vaccinated offspring **(Figure 6.34A)**. IgG2a$^+$ B cells were significantly reduced in WT maternally vaccinated and infected offspring in comparison to WT maternally unvaccinated and infected offspring **(Figure 6.34B)**. No differences were observed between IL-4R$\alpha^{-/-}$ maternally unvaccinated and vaccinated offspring **(Figure 6.34B)**.

Total plasmoblast (CD45$^+$ B220$^+$ CD138$^+$) cell populations were investigated in the bone marrow. No difference in total plasmoblast cell numbers were present between WT and IL-4R$\alpha^{-/-}$ offspring **(Figure 6.35)**. In addition, no differences was observed in the presence of infection **(Figure 6.35)**. A similar trend was observed for offspring plasmoblast (CD45$^+$ H2Dd$^-$ H2Kb$^+$ B220$^+$ CD138$^+$) cell populations **(Figure 6.36A)**. Maternal plasmoblast (CD45$^+$ H2Dd$^+$ H2Kb$^+$ B220$^+$ CD138$^+$) cell numbers were slightly reduced in WT maternally vaccinated offspring when compared to WT maternally unvaccinated offspring **(Figure 6.36B)**. No differences were observed between IL-4R$\alpha^{-/-}$ maternally unvaccinated and vaccinated offspring. **(Figure 6.36B)**. However, maternal cells were significantly reduced in IL-4R$\alpha^{-/-}$ maternally vaccinated and infected offspring compared to WT maternally vaccinated and infected offspring **(Figure 6.36B)**.

A. Total IgG1⁺ plasma cell profile in the bone marrow of 7-week-old offspring

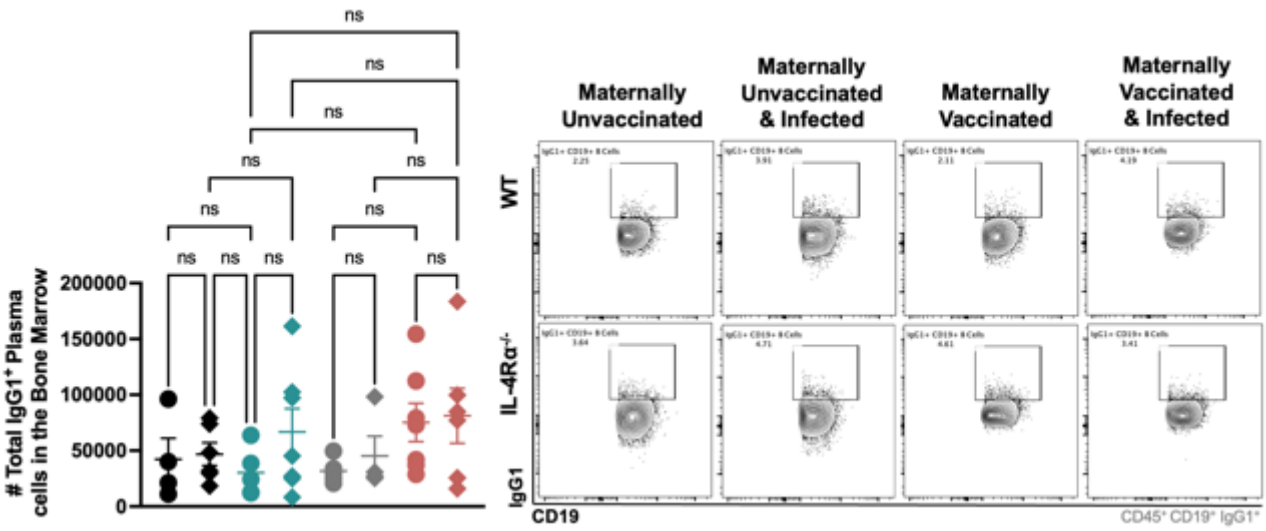

B. Total IgG2a⁺ plasma cell profile in the bone marrow of 7-week-old offspring

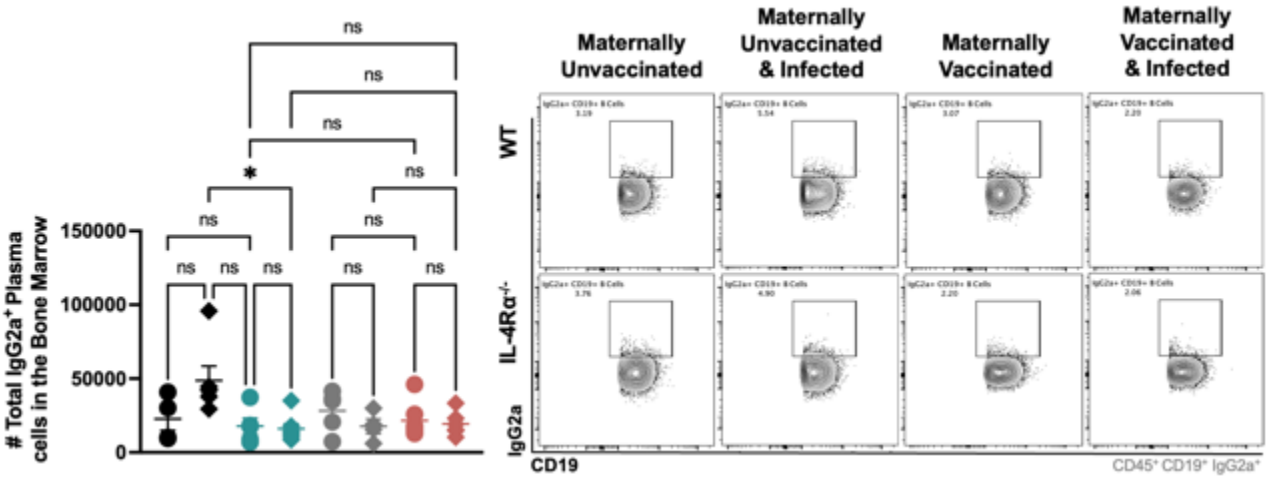

Figure 6.34: IgG2a⁺ B cell populations were decreased in the bone marrow of WT maternally vaccinated and infected offspring.
7-week-old offspring were either born to unvaccinated or PCV13 vaccinated dams. **A.** Total IgG1⁺ B cells (CD45⁺ CD19⁺ IgG1⁺) and **B.** Total IgG2a⁺ B cell (CD45⁺ CD19⁺ IgG2a⁺) populations were investigated in the bone marrow. Representative of 2 experiments whereby n = 4-7 mice per group. Statistical analysis was performed using a Kruskal-Wallis test. P values was regarded as significant if less than 0.05 (* p<0.05, ** p<0.01, *** p<0.001).

A. Total plasmoblast cell numbers in the bone marrow

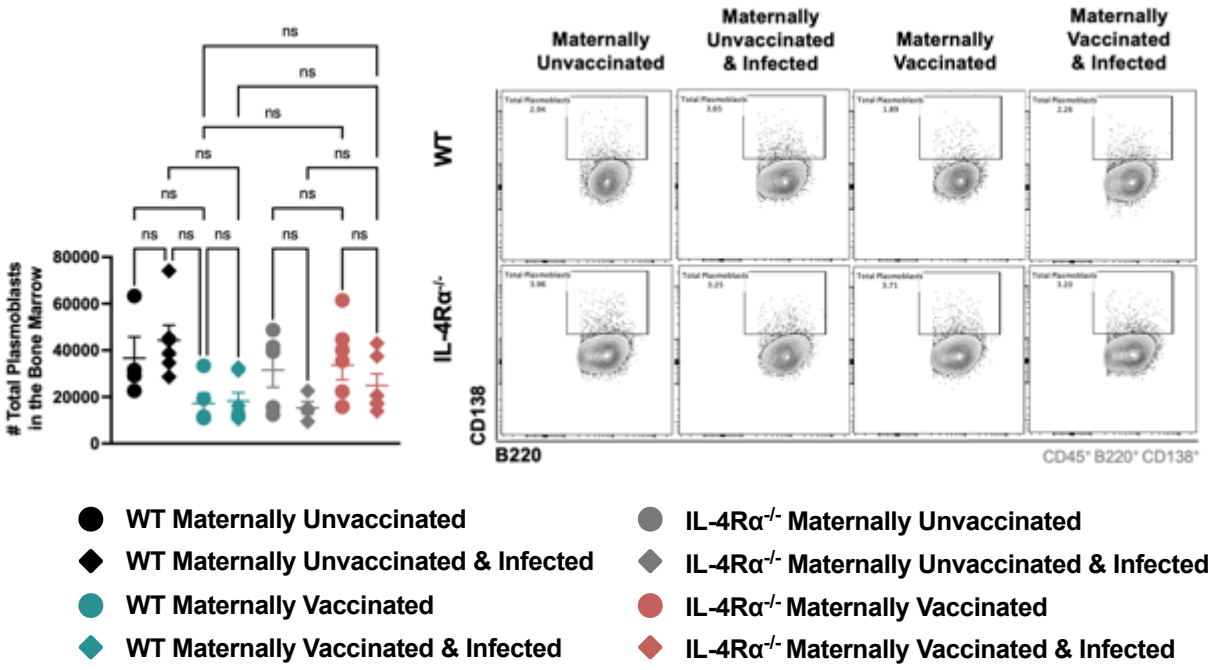

Figure 6.35: No difference in total plasmoblast cell numbers were present in WT and IL-4R$\alpha^{-/-}$ offspring.
7-week-old offspring were either born to unvaccinated or PCV13 vaccinated dams. **A.** Total plasmoblast ($CD45^+$ $B220^+$ $CD138^+$) populations were investigated in the bone marrow. Representative of 2 experiments whereby n = 4-7 mice per group. Statistical analysis was performed using a Kruskal-Wallis test. P value was regarded as significant if less than 0.05 (* $p<0.05$, ** $p<0.01$, *** $p<0.001$).

A. Offspring plasmoblast cell numbers in the bone marrow

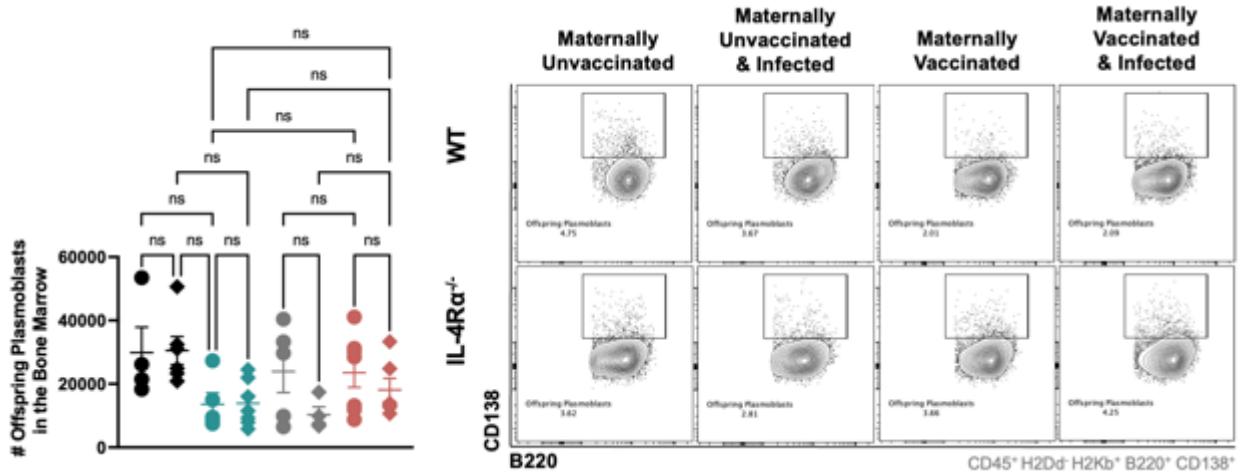

B. Maternal plasmoblast cell numbers in the bone marrow

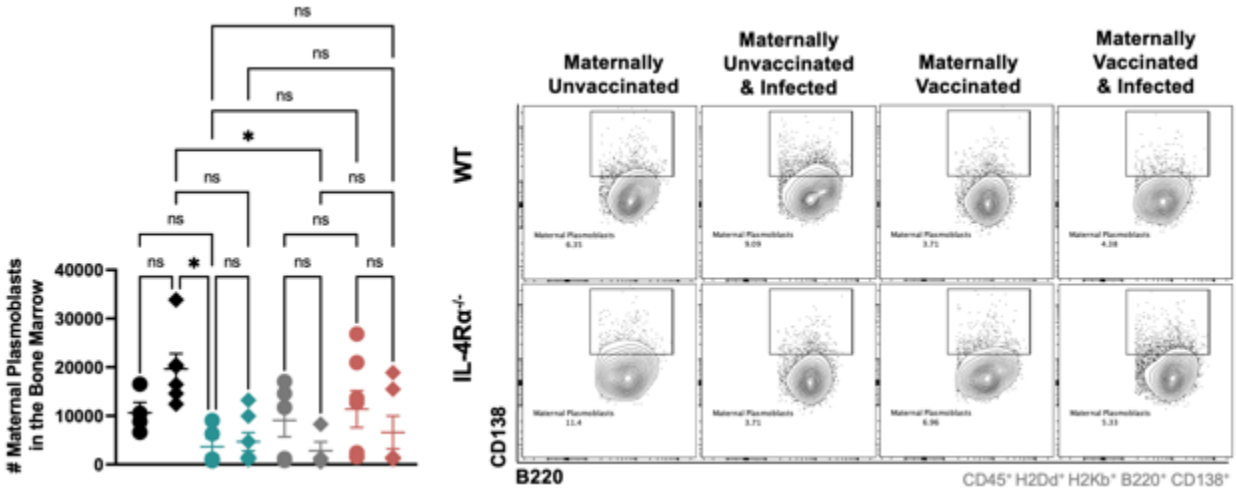

- WT Maternally Unvaccinated
- WT Maternally Unvaccinated & Infected
- WT Maternally Vaccinated
- WT Maternally Vaccinated & Infected
- IL-4Rα$^{-/-}$ Maternally Unvaccinated
- IL-4Rα$^{-/-}$ Maternally Unvaccinated & Infected
- IL-4Rα$^{-/-}$ Maternally Vaccinated
- IL-4Rα$^{-/-}$ Maternally Vaccinated & Infected

Figure 6.36: Maternal cells are significantly reduced in IL-4R$\alpha^{-/-}$ maternally vaccinated and infected offspring compared to WT maternally vaccinated and infected offspring.

7-week-old offspring were either born to unvaccinated or PCV13 vaccinated dams. **A.** Offspring plasmoblast ($CD45^+$ $H2Dd^-$ $H2Kb^+$ $B220^+$ $CD138^+$) and **B.** maternal plasmoblast ($CD45^+$ $H2Dd^+$ $H2Kb^+$ $B220^+$ $CD138^+$) populations were investigated in the bone marrow. Representative of 2 experiments whereby n = 4-7 mice per group. Statistical analysis was performed using a Kruskal-Wallis test. P values was regarded as significant if less than 0.05 (* $p<0.05$, ** $p<0.01$, *** $p<0.001$).

6.3. Discussion

Dam B cell numbers were similar between WT and IL-4R$\alpha^{-/-}$ dams in the spleen, axillary and illiac lymph nodes. However, the differences were observed in the IgG1^{+} B cell and IgG2a^{+} B cell populations. IgG1^{+} expressing B cell numbers were significantly reduced in IL-4R$\alpha^{-/-}$ dams irrespective of PCV13 vaccination. PCV13 vaccination did further elevate IgG1^{+} expressing B cell numbers in the WT dams but this effect was not present in IL-4R$\alpha^{-/-}$ dams. In the axillary and illiac lymph nodes, a shift of IgG1^{+} to IgG2a^{+} expressing B cell dominance was observed in IL-4R$\alpha^{-/-}$ dams. The lack of IgG1^{+} expressing B cells present in IL-4R$\alpha^{-/-}$ dams suggests that less IgG1^{+} is transferred to offspring which may play a crucial role in the quality of immune cells transferred to offspring. The lack of IL-4R$\alpha^{-/-}$ present in dams may also limit the antibody class switching ability of B cells. Therefore, when B cells are activated due to PCV13 vaccination, IgM antibodies are not able to class switch specifically to IgG1^{+} expressing cells B cells but rather to non-specific IgG2a^{+} expressing B cells.

The innate immune system in the BAL seems to be important in WT maternally vaccinated offspring. The T4P2 infection is immediately controlled in BAL's of WT maternally vaccinated offspring which indicates that the BAL would be considered the "first line of defence" against the pneumococcal infection. In WT maternally unvaccinated offspring, IL-4R$\alpha^{-/-}$ unvaccinated and maternally vaccinated offspring had an increased immune cell recruitment to the BAL. These cells are alveolar macrophages and neutrophils which are immediately activated in the presence of infection. WT maternally vaccinated offspring

have a dampened alveolar macrophage, neutrophil response but an increased DC activity. This results in addition with the reduction in CFU indicates that PCV13 maternal vaccination may contribute to immune control which is dependent on IL-4R$\alpha^{-/-}$ in the BAL.

PCV13 specific IgG and IgG1 antibodies were only detected in WT maternally vaccinated offspring. In addition, bacteria opsonised with heat inactivated WT maternally vaccinated offspring serum had the only significant reduction in T4P2 bacteria in the blood of 7-week-old Balb/C mice. Heat inactivation inhibits complement activity in serum further indicating that functional antibodies are present and important for eliminating bacteria in WT maternally vaccinated offspring serum. The lack of IL-4R$\alpha^{-/-}$ in dams not only decreases the complexity of antibodies present but also limits the transfer of functional circulating antibodies in offspring.

T4P2 CFU's were not detectable in the lungs of WT maternally vaccinated and infected offspring however all remaining groups had significantly elevated CFU's present. These results mimic the CFU's present in the BAL with approximately half the bacteria present in the BAL have migrated out and colonised the lungs. Interestingly, in the presence of infection, WT maternally unvaccinated, IL-4R$\alpha^{-/-}$ maternally unvaccinated and vaccinated offspring have significant infiltration of maternal $CD45^+$ immune cell into the lung to help establish immune control of the T4P2 infection. However, maternal $CD45^+$ immune cells remain relatively the same in WT maternally vaccinated and infected offspring therefore the intrinsic maternal $CD45^+$ immune present in the lungs remain unaffected. In addition, WT and IL-4R$\alpha^{-/-}$ offspring have different $B220^+$ B cell profiles in the presence of infection.

Offspring $B220^+$ B cells were significantly increased in IL-4R$\alpha^{-/-}$ maternally unvaccinated and vaccinated offspring while no difference was observed in WT offspring $B220^+$ B cells. Interestingly, maternal $B220^+$ B cells were elevated in WT maternally vaccinated in the presence of infection whereas maternal cells were not increased in WT and IL-4R$\alpha^{-/-}$ maternally unvaccinated as well as IL-4R$\alpha^{-/-}$ maternally vaccinated offspring. The infiltration of maternal $B220^+$ B cells is interesting as bacteria was not detected in the lungs however maternal cells have still been recruited to the lung. Therefore this would indicate that upon an infection, the immune system has been primed to respond with a specialised maternal response which may increase the rate at which the infection can be controlled.

The most significant result was present in the bone marrow as WT maternally vaccinated offspring had the ability to secrete long lasting PCV13-specific IgG and IgG1 antibodies. Bone marrow cells in WT maternally unvaccinated, IL-4R$\alpha^{-/-}$ maternally unvaccinated and vaccinated offspring were unable to secrete PCV13-specific IgG and IgG antibodies. This result was expected in the WT and IL-4R$\alpha^{-/-}$ maternally unvaccinated offspring as they have never been exposed to PCV13. However, the lack of PCV13 antibodies produced in IL-4R$\alpha^{-/-}$ maternally vaccinated offspring is interesting as they have been exposed to maternal vaccination in the same manner as WT maternally vaccinated offspring. This results indicate that IL-4R$\alpha^{-/-}$ is not only important for the transfer of protection but also for the ability for bone marrow cells to constantly produce crucial PCV13-specific IgG and IgG1 antibodies.

Chapter 7: Discussion, conclusions, and future work

7.1 Discussion

A range of maternal cell types have been identified in offspring ranging from maternal neutrophils, alveolar macrophages, $IgG1^+$ to $IgG2a^+$ B cells. The reason for the population of maternal cells found in offspring can be explained by microchimerism, a phenomenon where a small number of cells with a genetic origin different from the host are present in an individual's tissues or bloodstream. This occurs most commonly during pregnancy when cells from the mother and fetus cross the placental barrier(123, 124). Maternal microchimerism involves maternal cells residing in fetal tissue and these exchanged cells can persist and be detected in various organs and can influence immune responses(125).

The preliminary data indicates that bone marrow cells have the ability to secrete PCV13 specific IgG due to the increased PCV13 specific antibody titres found in the bone marrow of PCV13 maternally vaccinated offspring. At this stage in the study, the cells responsible for this significant result is not understood but a reasonable explanation for the array of maternal immune cells present in the offspring could be that the maternal cells being transferred to offspring is maternal stem cells(124, 126).

Evidence of stem cells involved in microchimerism is explained from studies detecting pluripotent and multipotent stem cells in tissues where they are not typically found, originating from a genetically distinct individual(123, 125, 126). Maternal stem cells have

been identified in fetal tissues and organs long after birth as well as fetal stem cells have been found in maternal tissues. Moreover, experiments in mice have shown that transplanted stem cells from one mice can engraft and proliferate in another, mirroring natural microchimerism(123, 126). This body of evidence supports the notion that stem cells play a crucial role in the bidirectional cellular exchange and long-term persistence of microchimerism.

Investigating if any modifications in the antibody structure of PCV13 secreted antibody could further explain the interesting increase in antibody half-life present in PCV13 maternally vaccinated offspring. One of the post-translational antibody modifications of interest is antibody glycosylation(31, 127). Antibody glycosylation refers to the attachment of sugar molecules (glycans) to antibodies. Glycosylation is a post-translational modification that plays a crucial role in the structure and function of antibodies(128, 129). One of the proposed mechanisms is Fc glycosylation which has been associated with extended antibody half-life. Certain glycosylation sites, especially Asparagine (Asn) 297, have been widely studied and alterations in this site have been affiliated with viral and bacterial diseases(129, 130). In various disease conditions, changes occur in antibody glycosylation during infection and changes are shown to act as potential biomarkers of disease state but may also functionally contribute to control of the disease(127, 131).

Cells in the bone marrow are able to secrete antibodies that can circulate throughout the body. Once antibodies are secreted into the bloodstream they can travel to different parts

of the body through the circulatory system and settle in different tissues and organs where they might be needed. In some cases antibodies produce may be specific to target specific pathogens that are localised into different parts in certain organs or tissues. In this body of work, we see that bone marrow cells are able to secrete PCV13 specific antibodies that may settle in the lungs. This is evident as an intrinsic population of maternal cells are found in the lungs of maternally vaccinated offspring.

The benefits of B cells producing antibody in the bone marrow are especially involved in long-term immunity(132). The constant secretion of antibodies in the bone marrow contributes to the establishment and maintenance of long-term immune responses and ensures a rapid and robust immune response upon re-exposure to the a reoccurring pathogen or to vaccination(132). In addition, constant antibody secretion provides immediate protection against pathogens. If the circulating antibody levels decrease over time, the presence of antibody secreting cells in the bone marrow can ensure the production of cells capable of rapidly producing antibodies upon exposure to pathogens(76). The constant antibody production ensures that the immune system is primed and ready to mount an effective immune response(133). This can be seen in the maternally vaccinated offspring as T4P2 bacterial titre is significantly reduced in the BAL, Lung and serum. The degree of inflammation is also reduced due to the decreased bacterial titres present when compared to maternally unvaccined offspring as well as IL-4R$\boldsymbol{\alpha}^{-/-}$ maternally unvaccinated and vaccinated offspring.

7.2 Conclusions

PCV13 maternal vaccination in WT dams induces maternal transfer and this protection can be seen in WT maternally vaccinated offspring. Maternally vaccinated offspring have reduced T4P2 titre in the BAL, lung and blood. In addition, maternally vaccinated offspring had increased PCV13 specific IgA in the BAL and PCV13 specific IgG (IgG1 and IgG2a) in the serum. Maternally vaccinated offspring have increased immune control in the BAL compared to maternally unvaccinated offspring. Maternal cells ($H2Dd^+$ $H2Kb^+$) were tracked using flow cytometry and results indicate that maternal immune cells leave the bone marrow in the presence of infection. Preliminary results indicate that maternal cells migrate to other areas such as the lung as an intrinsic maternal immune cell population was present in WT maternally vaccinated offspring lungs. WT Maternally vaccinated offspring have increased PCV13 specific antibody in bone marrow supernants and preliminary results indicate that bone marrow cells are actively secreting PCV13 specific IgG (IgG1 and IgG2a) antibodies. Finally, IL-4 is essential for the transfer of protection. In the absence of IL-4, dams have reduced PCV13 specific antibody responses in the serum and reduced $IgG1^+$ B cell populations. This result is then transferred to offspring as PCV13 specific antibodies are reduced in the serum and bone marrow supernatants of IL-4R$\alpha^{-/-}$ maternally vaccinated offspring.

7.3 Future work

This body of work indicates that WT maternally vaccinated 7 week old offspring have maternal $CD45^+$ immune cell populations present in the bone marrow that migrate out of the bone marrow in the presence of infection. In addition, preliminary data suggests that these maternal cells in PCV13 maternally vaccinated offspring have the ability to secrete PCV13 specific antibody's. These PCV13 specific antibodies are also present in the serum and BAL of PCV13 maternally vaccinated offspring. This significant result indicates that PCV13 specific antibodies are being secreted, circulating and have a potential increase in antibody half-life. To validate if bone marrow cells are able to secrete enzyme-linked immunospot (ELISPOT) specific to PCV13 will need to be performed on bone marrow cells. This ability for bone marrow cells to secrete PCV13 specific antibodies is a novel finding and therefore needs to be confirmed.

Breastmilk isolated from pups was added to PCV13 specific ELISA coated plates however no PCV13 specific antibodies could not be detected in breastmilk pellets using the ELISA protocol described. Breastmilk pellets are filled with an abundant amount of proteins and the lack of antibodies detected could be masked by non-specific binding of larger proteins. In order to confirm that is no antibodies are being transferred via the breastmilk, litter swop experiment needed to be performed. The same allogeneic mating model will be applied but once offspring are born maternally vaccinated offspring will be breastfed off an unvaccinated dams and maternally unvaccinated offspring will be breastfed on maternally vaccinated offspring. Half of the offspring will be infected with $1x10^7$ CFU for

48h while the remaining offspring remain uninfected. All offspring will be euthanized after 48h and cardiac blood, BAL and bone marrow will be collected. Antibody titres will be checked in the BAL, serum and bone marrow supernatants. PCV13-specific antibody (IgG, IgG1, IgG2 and T4P2) titres will be checked in the serum and bone marrow while IgA titres will be detected in the BAL. If the maternally unvaccinated offspring acquired PCV13 specific antibodies to the same extent as previous experiments we can be assured that maternal transfer is occurring through the breastmilk. If antibody transfer is occurring at a reduced level we can say that maternal transfer is occurring though utero as well as through the breastmilk. If no maternal transfer is occurring, then maternal transfer is only happening via utero. In addition to collecting and analysing antibody supernatants for PCV13 specific antibodies, bone marrow cells will be collected to measure PCV13 specific antibody titres as well as perform ELISPOT's. This will validate that bone marrow cells are secreting antibody specific to PCV13 and results will be compared to the results explained in chapter 5 and 6.

The next list of experiments will be honing into further classifying the differences between maternal ($H2Dd^+$ $H2Kb^-$) and offspring cells ($H2Dd^-$ $H2Kb^+$). We have previously used flow cytometry to separate total immune cell populations from an allogeneic mating experiment into maternal and offspring cells. Next, we aimed to sort the bone marrow immune cells into maternal and offspring cells. Once cells were sorted into these two populations we will plate maternal and offspring cells separately and collect supernatant to investigate if PCV13 specific antibody was secreted only in the maternal cell populations. In addition, bone marrow cells will be plated and ELISPOT experiments will be performed against

PCV13 to investigate if cells isolated maternal and offspring cells are able to secrete PCV13 specific antibodies. If maternal cells in the bone marrow cells secrete PCV13 specific antibody but no PCV13 specific antibody is secreted from offspring cells we can validate that maternal cells are responsible for the protection observed and offspring cells don't play a role in secreting PCV13 specific antibodies.

To validate the model used to investigate maternal vs offspring cells an additional model can be used using Fluorescently labelled mice. This experiments will be planned in collaboration with the Toellner lab at the University of Birmingham. At 7 weeks of age tomato labelled female mice will be mated with GFP labelled males which will result in offspring with 50% tomato and 50% GFP labelled cells ($WT^{tomato/GFP}$). At 3 weeks of age, $WT^{tomato/GFP}$ offspring will be weaned and separated according to sex. females will be selected, and males will be culled. At 7 weeks of age $WT^{tomato/GFP}$ females will either be vaccinated intraperitoneally with PCV13 one week before mating or left unvaccinated. These females will be mated with GFP labelled males resulting in $WT^{tomato/GFP}$ and $WT^{GFP/GFP}$ offspring. At 3 weeks of age, offspring will be weaned once again and tail bleeds will be collected. Mice will be selected for only GFP positive cells ($WT^{GFP/GFP}$). The $WT^{tomato/GFP}$ offspring will be culled and $WT^{GFP/GFP}$ offspring will be left to age. At 7 weeks of age, $WT^{GFP/GFP}$ offspring will be infected with $1X10^7$ T4P2 intranasally and euthanized 48H post infection. The BAL, bone marrow and serum will be collected. Maternal cells will be tomato labelled while offspring will be GFP labelled. Using flow cytometry, cells can be gated accordingly with GFP and Tomato antibodies. In addition, sorting will be done,

and the same protocols as above will be used to investigate if maternal cells are actively playing a role in maternal protection observed.

To investigate if the maternal cells that are being transferred to offspring are stem cells, flow cytometry experiments need to be performed with a focus on stem cell markers. To increase the probability and of detecting the stem cells, maternally unvaccinated and vaccinated offspring will be euthanized at 10 days of age, 3 weeks of age and 7 weeks of age. Bone marrow cells will be processed and stained with stem cell markers: CD49f (Integrin alpha-6), Sca-1 (Stem cell antigen-1), CD34, CD38, CD90, CD117, lineage marker and $H2Dd^+$ and $H2Kb^+$.

Finally, the last experiment planned will be investigating if any antibody post translational modifications are occurring in the bone marrow supernatants and serum of both dams and offspring. Antibody glycosylation is difficult process to investigate and therefore we would do this in collaboration with other groups such as the Crouch-Meyers group at the University of Birmingham or with the Ragon institute at Harvard University.

Chapter 8: Appendix

8.1. Appendix A:

8.1.1 Antibodies

8.1.1.1 ELISA Antibody

Table 3: ELISA antibodies concentrations and dilutions.

Coating Antibody	Coating Antibody Concentration	Clone	Detection Antibody	Detection Antibody Concentration	Clone
T4P2	10 µg/mL (80 µL in 10 mL)	Purified in lab	Total IgG	1:1000 (10 µL in 10 mL)	Poly4053
TiGR4	10 µg/mL (105 µL in 10 mL)	Purified in lab	Total IgG	1:1000 (10 µL in 10 mL)	Poly4053
PCV13	1:1000 (10 µL in 10 mL	Purified in lab	IgA	1:1000 (10 µL in 10 mL)	RMA-1
Total IgG	1:1000 (10 µL in 10 mL)	Poly4053	Total IgG	1:1000 (10 µL in 10 mL)	Poly4053
PCV13	10 µg/mL (10 µL in 10 mL)	Purified in lab	Total IgG	1:1000 (10 µL in 10 mL)	Poly4053
PCV13	10 µg/mL (10 µL in 10 mL)	Purified in lab	IgG1	1:1000 (10 µL in 10 mL)	RMG1-1
PCV13	10 µg/mL (10 µL in 10 mL)	Purified in lab	IgG2a	1:1000 (10 µL in 10 mL)	RMG2a-62
PCV13	10 µg/mL (10 µL in 10 mL)	Purified in lab	IgG3	1:1000 (10 µL in 10 mL)	RMG3-1

8.1.1.2 Flow Cytometry antbodies

Table 4: Flow Cytometry antibodies concentrations, dilutions and panels.

Marker	Antibody fluorophore	Clone	Antibody Dilution	Source
B Cell Panel Options				
Viability Dye	eFlour 520	-	1:500	BD Biosciences
CD19	A488	1D3	1:200	BD Biosciences
B220	BV421	RA3-6B2	1:200	eBioscience™
CD45	BV510	30-F11	1:200	eBioscience™
CD138	APC Cy7	DL-101	1:200	eBioscience™
IgG1	PE	M1-14D12	1:200	eBioscience™
IgG2a	APC	m2a-15F8	1:200	eBioscience™
CD21	APC	7G6	1:200	eBioscience™
CD23	PE	B3B4	1:200	eBioscience™
T Cell Panel Options				
Viability Dye	eFlour 520	-	1:500	BD Biosciences
CD45	BV510	30-F11	1:200	eBioscience™
CD3	A700	145-2C11	1:600	eBioscience™
CD4	PercpCy5/BV421	RM4-5	1:600	eBioscience™
CD44	FITC/APC	IM7	1:200	eBioscience™
CD62L	BV605	MEL-14	1:200	eBioscience™
Myeloid Panel Options				
Viability Dye	eFlour 520	-	1:500	BD Biosciences
CD45	BV510	30-F11	1:200	eBioscience™
CD11b	APC/Cy7	M1/70	1:200	eBioscience™
CD11c	Alexa Fluor® 700	N418	1:200	eBioscience™
Ly6G	BV605™	HK1.4	1:200	eBioscience™
Siglec-F	Alexa Flour® 647	E50-2440	1:400	eBioscience™
MHCII	FITC	M5/114.15.2	1:200	eBioscience™
CD206	PE-Cy7-A	MR6F3	1:200	eBioscience™

Maternal Cell Panel				
Viability Dye	eFlour 520	-	1:500	BD Biosciences
CD45	BV510	30-F11	1:200	eBioscience™
H2Dd	PE	34-5-8S	1:200	eBioscience™
H2Kb	PE-Cy7-A	25-D1.16	1:200	eBioscience™
Ki67	FITC	SolA15	1:200	eBioscience™
CD19	A488	1D3	1:200	BD Biosciences
B220	BV421	RA3-6B2	1:200	eBioscience™
CD21	APC	7G6	1:200	eBioscience™
CD23	PerCP-Cy5-5	B3B4	1:200	eBioscience™
IgD	BV605	11-26c.2a	1:300	eBioscience™
Plasma cell Panel				
CD45	Alexa Flour 700	30-F11	1:200	eBioscience™
CD138	APC Cy7	DL-101	1:200	eBioscience™
IgD	BV605	11-26c.2a	1:300	eBioscience™
TACi	PE	ebio8F10-3	1:200	eBioscience™
CD38	PE-CY-594	HIT2	1:200	eBioscience™
CD19	PE-Cy7-A	1D3	1:200	eBioscience™
GL7	PerCP-Cy5-5	GL-7 (GL7)	1:200	eBioscience™
Additional Markers				
Fc block	-	-	1:200	BD Biosciences
Rat serum	-	-	1:50	BD Biosciences

8.1.2 Gating Strategies

8.1.2.1 Dam B cell gating strategies in the spleen, axillary and illiac lymph nodes

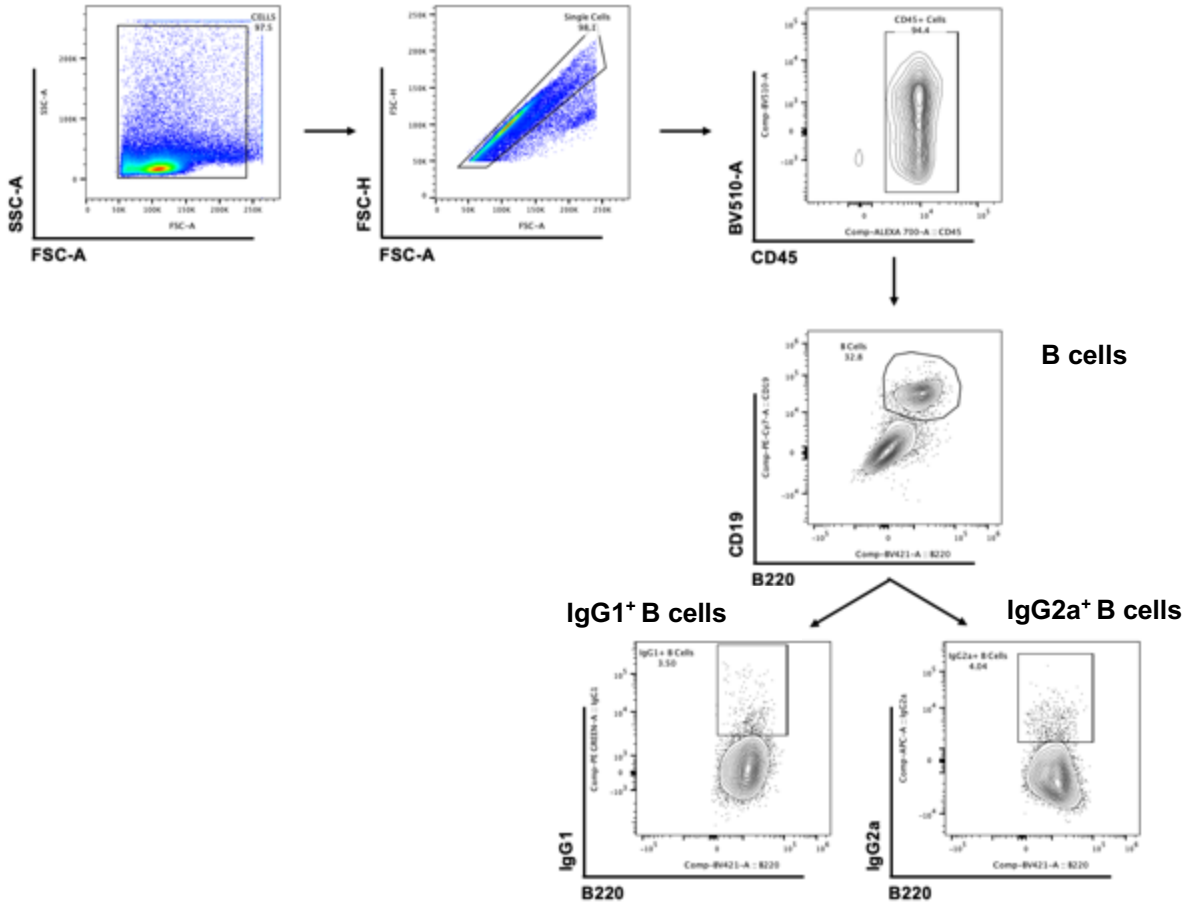

8.1.2.2 Dam T cell gating strategies in the spleen, axillary and illiac lymph nodes

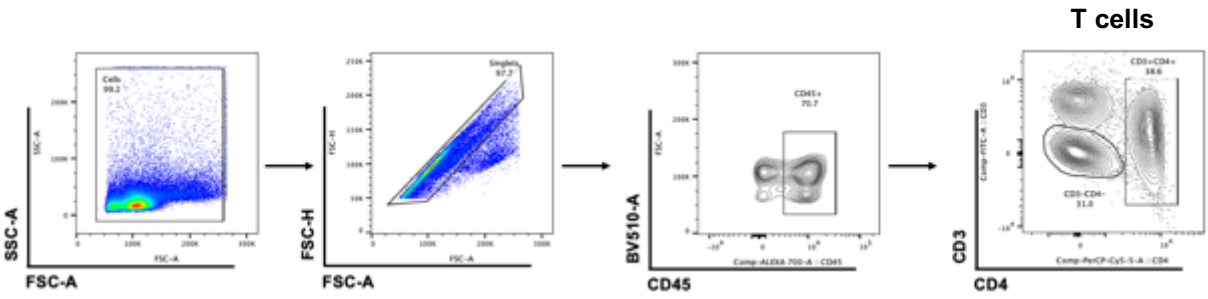

8.1.2.3 Offspring myeloid gating strategies in the BAL

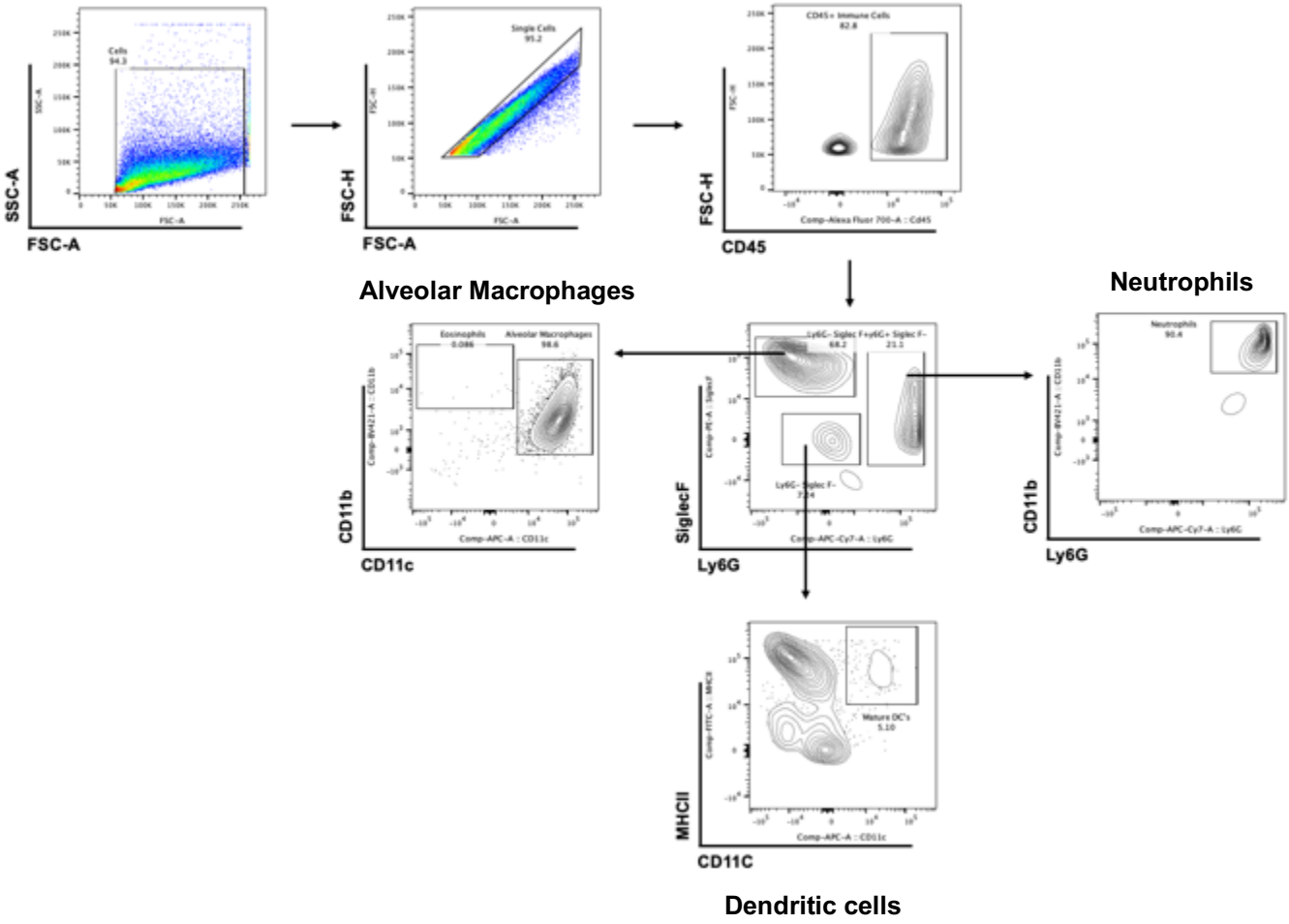

8.1.2.4 Offspring B and T cell gating strategies in the lung and bone marrow

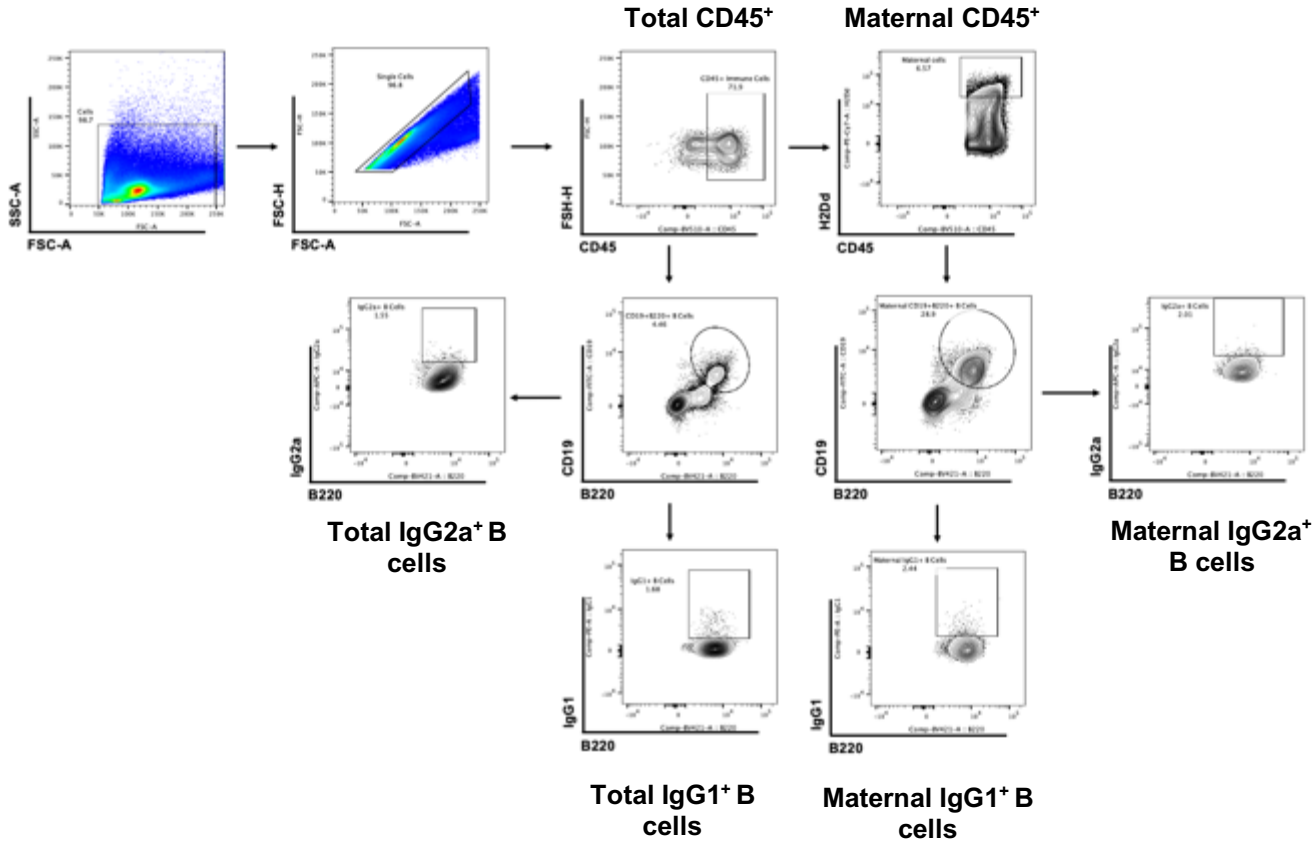

8.1.2.5 Offspring Plasma cell gating strategies in the lung and bone marrow

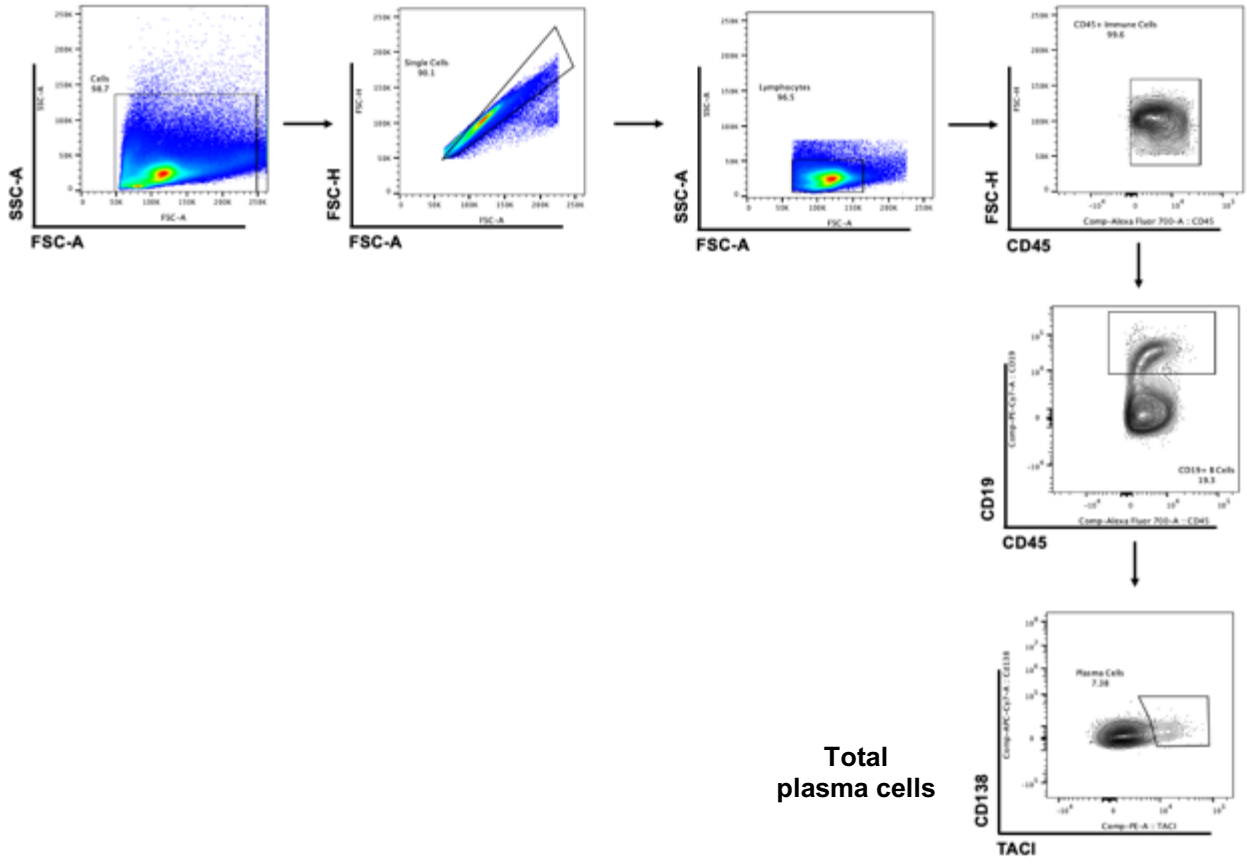

8.1.2.6 Offspring Maternal vs offspring cell gating strategies in the lung

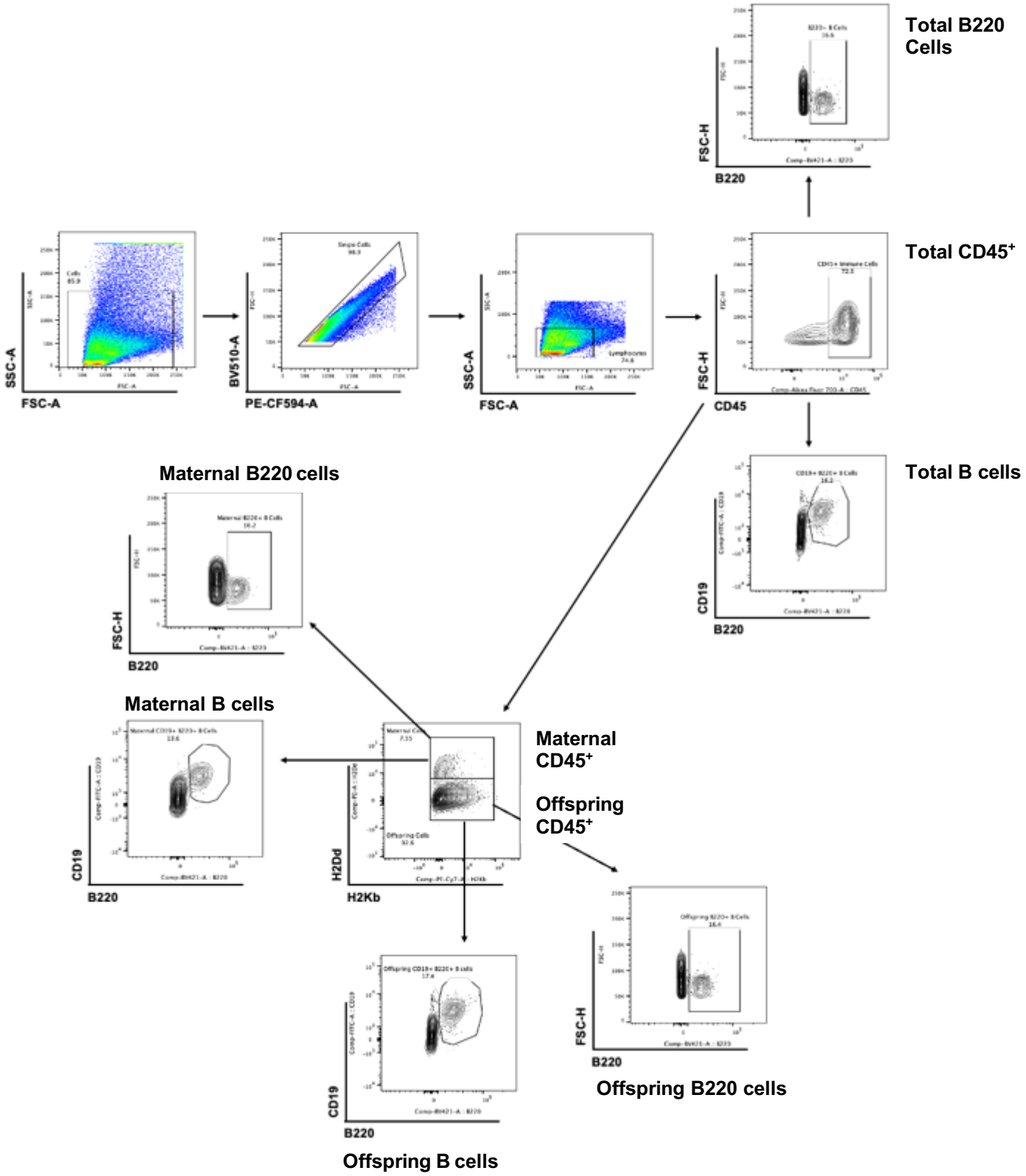

8.1.2.7 Offspring Maternal vs offspring cell gating strategies in the bone

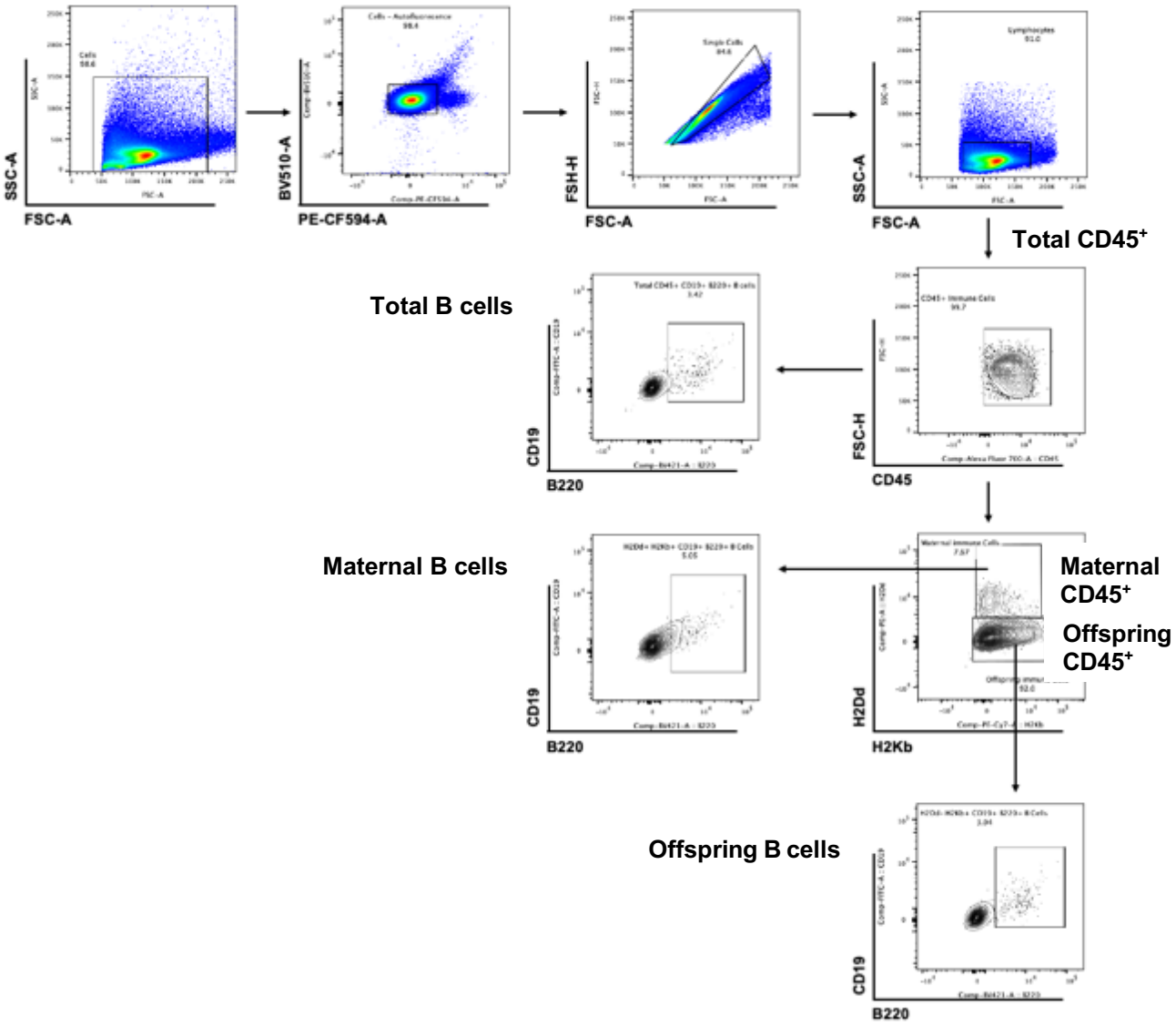

8.2. Appendix B: Media and buffer recipes

Complete Media

Roswell Park Memorial Institute (RPMI) 1640, 50 mL heat-inactivated Fetal Calf Serum (Gibco™), 5 mL Penicillin/streptomycin (100X)

FACS Buffer

0.1% bicinchoninic acid (BSA), 0.05% NaN3 (Merck), Made up in 1X PBS

ELISA Wash buffer

1X PBS (Gibco), 0. 05% Tween 20 (National diagnostics)

p-Nitrophenol phosphate (pNPP) Substrate (per 20 mL)

Open one pNPP tablet package (silver foil) and Trizma buffer tablet package (gold foil) and place in 20 mL of sterile H_2O. Cover the tube with foil and place the tubes on a vertical rotator until all contents have been dissolved.

Blocking buffer

1X PBS, 2g Bovine Serum Albumin (BSA) (Sigma)

Dilution Buffer

1X PBS, 1g BSA

8.3. Appendix C: References

1. Organisation WH. Revised WHO classification and treatment of childhood pneumonia at health facilities 2014.
2. (UNICEF) WHOTUNCsF. Ending Preventable Child Deaths from Pneumonia and Diarrhoea by 2025. 2013.
3. The World Health Organisation UNCf. Pneumonia the forgotten killer of children 2006.
4. Oliwa JN, Marais BJ. Vaccines to prevent pneumonia in children – a developing country perspective. Paediatric Respiratory Reviews. 2017;22:23-30.
5. Drijkoningen JJ, Rohde GG. Pneumococcal infection in adults: burden of disease. Clin Microbiol Infect. 2014;20 Suppl 5:45-51.
6. Grant A Mackenzie AJL, Jonathan R Carapetis, Janelle Fisher, Peter S Morris. Epidemiology of nasopharyngeal carriage of
respiratory bacterial pathogens in children and
adults: cross-sectional surveys in a population
with high rates of pneumococcal disease. BMC Infectious Disease. 2010;304:1471-82.
7. Amari S, Warda K, Bouraddane M, Katfy M, Elkamouni Y, Arsalane L, et al. Antibiotic Resistance of Streptococcus pneumoniae in the Nasopharynx of Healthy Children Less than Five Years Old after the Generalization of Pneumococcal Vaccination in Marrakesh, Morocco. Antibiotics (Basel). 2023;12(3).
8. Karcic E, Aljicevic M, Bektas S, Karcic B. Antimicrobial Susceptibility/Resistance of Streptococcus Pneumoniae. Mater Sociomed. 2015;27(3):180-4.
9. Rybak A, Levy C, Ouldali N, Bonacorsi S, Bechet S, Delobbe JF, et al. Dynamics of Antibiotic Resistance of Streptococcus pneumoniae in France: A Pediatric Prospective Nasopharyngeal Carriage Study from 2001 to 2022. Antibiotics (Basel). 2023;12(6).
10. Simell B, Auranen K, Kayhty H, Goldblatt D, Dagan R, O'Brien KL, et al. The fundamental link between pneumococcal carriage and disease. Expert Rev Vaccines. 2012;11(7):841-55.
11. Ramos-Sevillano E, Ercoli G, Brown JS. Mechanisms of Naturally Acquired Immunity to Streptococcus pneumoniae. Front Immunol. 2019;10:358.
12. Almeida ST, Paulo AC, Froes F, de Lencastre H, Sa-Leao R. Dynamics of Pneumococcal Carriage in Adults: A New Look at an Old Paradigm. J Infect Dis. 2021;223(9):1590-600.
13. Lee LH, Gu XX, Nahm MH. Towards New Broader Spectrum Pneumococcal Vaccines: The Future of Pneumococcal Disease Prevention. Vaccines (Basel). 2014;2(1):112-28.
14. Daniels CCR, P.D.; Shelton, C.M. . A review of pneumococcal vaccines: Current polysaccharide vaccine recommendations
and future protein antigens. . 2016;J. Pediatr. Pharmacol. Ther.(21):27–35.
15. Javaid N, Olwagen C, Nzenze S, Hawkins P, Gladstone R, McGee L, et al. Population genomics of pneumococcal carriage in South Africa following the introduction of the 13-valent pneumococcal conjugate vaccine (PCV13) immunization. Microb Genom. 2022;8(6).

16. Rowe HM, Karlsson E, Echlin H, Chang TC, Wang L, van Opijnen T, et al. Bacterial Factors Required for Transmission of Streptococcus pneumoniae in Mammalian Hosts. Cell Host Microbe. 2019;25(6):884-91 e6.
17. Ogunniyi ADF, R.L.; Briles, D.E.; Hollingshead, S.K.; Paton, J.C. . mmunization of mice with combinations of pneumococcal
virulence proteins elicits enhanced protection against challenge with Streptococcus pneumoniae. . Infect Immun
. 2000(68):3028–33.
18. Masomian M, Ahmad Z, Gew LT, Poh CL. Development of Next Generation Streptococcus pneumoniae Vaccines Conferring Broad Protection. Vaccines (Basel). 2020;8(1).
19. Reglinski M, Ercoli G, Plumptre C, Kay E, Petersen FC, Paton JC, et al. A recombinant conjugated pneumococcal vaccine that protects against murine infections with a similar efficacy to Prevnar-13. NPJ Vaccines. 2018;3:53.
20. Mazumder L, Shahab M, Islam S, Begum M, Oliveira JIN, Begum S, et al. An immunoinformatics approach to epitope-based vaccine design against PspA in Streptococcus pneumoniae. J Genet Eng Biotechnol. 2023;21(1):57.
21. Zhang Y, Edmonds KA, Raines DJ, Murphy BA, Wu H, Guo C, et al. The Pneumococcal Iron Uptake Protein A (PiuA) Specifically Recognizes Tetradentate Fe(III)bis- and Mono-Catechol Complexes. J Mol Biol. 2020;432(19):5390-410.
22. Chan WY, Entwisle C, Ercoli G, Ramos-Sevillano E, McIlgorm A, Cecchini P, et al. A Novel, Multiple-Antigen Pneumococcal Vaccine Protects against Lethal Streptococcus pneumoniae Challenge. Infect Immun. 2022;90(1):e0084618a.
23. Bahadori Z, Shafaghi M, Madanchi H, Ranjbar MM, Shabani AA, Mousavi SF. In silico designing of a novel epitope-based candidate vaccine against Streptococcus pneumoniae with introduction of a new domain of PepO as adjuvant. J Transl Med. 2022;20(1):389.
24. Feng S, Xiong C, Wang G, Wang S, Jin G, Gu G. Exploration of Recombinant Fusion Proteins YAPO and YAPL as Carrier Proteins for Glycoconjugate Vaccine Design against Streptococcus pneumoniae Infection. ACS Infect Dis. 2020;6(8):2181-91.
25. Shafaghi M, Bahadori Z, Madanchi H, Ranjbar MM, Shabani AA, Mousavi SF. Immunoinformatics-aided design of a new multi-epitope vaccine adjuvanted with domain 4 of pneumolysin against Streptococcus pneumoniae strains. BMC Bioinformatics. 2023;24(1):67.
26. Faucette AN, Unger BL, Gonik B, Chen K. Maternal vaccination: moving the science forward. Hum Reprod Update. 2015;21(1):119-35.
27. Atyeo C, Shook LL, Nziza N, Deriso EA, Muir C, Baez AM, et al. COVID-19 booster dose induces robust antibody response in pregnant, lactating, and nonpregnant women. Am J Obstet Gynecol. 2023;228(1):68 e1- e12.
28. Boudreau CM, Burke JSt, Shuey KD, Wolf C, Katz J, Tielsch J, et al. Dissecting Fc signatures of protection in neonates following maternal influenza vaccination in a placebo-controlled trial. Cell Rep. 2022;38(6):110337.
29. Le Doare K, Faal A, Jaiteh M, Sarfo F, Taylor S, Warburton F, et al. Association between functional antibody against Group B Streptococcus and maternal and infant colonization in a Gambian cohort. Vaccine. 2017;35(22):2970-8.

30. Nyangahu DD, Lennard KS, Brown BP, Darby MG, Wendoh JM, Havyarimana E, et al. Disruption of maternal gut microbiota during gestation alters offspring microbiota and immunity. Microbiome. 2018;6(1):124.
31. Turfkruyer M, Verhasselt V. Breast milk and its impact on maturation of the neonatal immune system. Curr Opin Infect Dis. 2015;28(3):199-206.
32. Saso A, Kampmann B. Vaccination against respiratory syncytial virus in pregnancy: a suitable tool to combat global infant morbidity and mortality? The Lancet Infectious Diseases. 2016;16(8):e153-e63.
33. Paul T Heath* FJC, Christine E Jones, Beate Kampmann, Kirsty Le Doare, Marta C Nunes, Manish Sadarangani, Zain Chaudhry,, Carol J Baker PJMO. Group B streptococcus and respiratory syncytial virus immunisation during pregnancy: a landscape analysis. The Lancet Infectious Diseases. 2017;17.
34. Hall J, Adams NH, Bartlett L, Seale AC, Lamagni T, Bianchi-Jassir F, et al. Maternal Disease With Group B Streptococcus and Serotype Distribution Worldwide: Systematic Review and Meta-analyses. Clin Infect Dis. 2017;65(suppl_2):S112-S24.
35. Procter SR, Goncalves BP, Paul P, Chandna J, Seedat F, Koukounari A, et al. Maternal immunisation against Group B Streptococcus: A global analysis of health impact and cost-effectiveness. PLoS Med. 2023;20(3):e1004068.
36. Swamy GK, Metz TD, Edwards KM, Soper DE, Beigi RH, Campbell JD, et al. Safety and immunogenicity of an investigational maternal trivalent group B streptococcus vaccine in pregnant women and their infants: Results from a randomized placebo-controlled phase II trial. Vaccine. 2020;38(44):6930-40.
37. Dabrera G, Amirthalingam G, Andrews N, Campbell H, Ribeiro S, Kara E, et al. A case-control study to estimate the effectiveness of maternal pertussis vaccination in protecting newborn infants in England and Wales, 2012-2013. Clin Infect Dis. 2015;60(3):333-7.
38. Gall SA, Myers J, Pichichero M. Maternal immunization with tetanus-diphtheria-pertussis vaccine: effect on maternal and neonatal serum antibody levels. Am J Obstet Gynecol. 2011;204(4):334 e1-5.
39. Annette K. Regan HCM, Michael J. Binks, Lisa McHugh, Christopher C. Blyth, Gavin Pereira, Karin Lust, MBBS,i Mohinder Sarna, Ross Andrews,, Damien Foo PVE, Stephen Lambert Van Buynder. Maternal Pertussis Vaccination, Infant Immunization, and Risk of Pertussis. PEDIATRICS. 2023;152.
40. Kandeil W, van den Ende C, Bunge EM, Jenkins VA, Ceregido MA, Guignard A. A systematic review of the burden of pertussis disease in infants and the effectiveness of maternal immunization against pertussis. Expert Rev Vaccines. 2020;19(7):621-38.
41. Golub R, Cumano A. Embryonic hematopoiesis. Blood Cells Mol Dis. 2013;51(4):226-31.
42. Rieger MA, Schroeder T. Hematopoiesis. Cold Spring Harb Perspect Biol. 2012;4(12).
43. Orkin SH. Hematopoiesis: how does it happen? Current biology. 1995;7:870-7.
44. Zon LI. Developmental Biology of Hematopoiesis. Blood. 1995;86:2876-91.
45. Doulatov S, Notta F, Laurenti E, Dick JE. Hematopoiesis: a human perspective. Cell Stem Cell. 2012;10(2):120-36.
46. Jagannathan-Bogdan M, Zon LI. Hematopoiesis. Development. 2013;140(12):2463-7.

47. Kelly B, O'Neill LA. Metabolic reprogramming in macrophages and dendritic cells in innate immunity. Cell Res. 2015;25(7):771-84.
48. Navegantes KC, de Souza Gomes R, Pereira PAT, Czaikoski PG, Azevedo CHM, Monteiro MC. Immune modulation of some autoimmune diseases: the critical role of macrophages and neutrophils in the innate and adaptive immunity. J Transl Med. 2017;15(1):36.
49. Hunt JS, Petroff MG, Burnett TG. Uterine leukocytes: key players in pregnancy. Semin Cell Dev Biol. 2000;11(2):127-37.
50. Hirayama D, Iida T, Nakase H. The Phagocytic Function of Macrophage-Enforcing Innate Immunity and Tissue Homeostasis. Int J Mol Sci. 2017;19(1).
51. Xuan W, Qu Q, Zheng B, Xiong S, Fan GH. The chemotaxis of M1 and M2 macrophages is regulated by different chemokines. J Leukoc Biol. 2015;97(1):61-9.
52. Italiani P, Boraschi D. From Monocytes to M1/M2 Macrophages: Phenotypical vs. Functional Differentiation. Front Immunol. 2014;5:514.
53. Deng H, Li Z, Tan Y, Guo Z, Liu Y, Wang Y, et al. A novel strain of Bacteroides fragilis enhances phagocytosis and polarises M1 macrophages. Sci Rep. 2016;6:29401.
54. Zhang M, Hutter G, Kahn SA, Azad TD, Gholamin S, Xu CY, et al. Anti-CD47 Treatment Stimulates Phagocytosis of Glioblastoma by M1 and M2 Polarized Macrophages and Promotes M1 Polarized Macrophages In Vivo. PLoS One. 2016;11(4):e0153550.
55. Bonilla FA, Oettgen HC. Adaptive immunity. J Allergy Clin Immunol. 2010;125(2 Suppl 2):S33-40.
56. Cooper MD, Alder MN. The evolution of adaptive immune systems. Cell. 2006;124(4):815-22.
57. Iwasaki A, Medzhitov R. Control of adaptive immunity by the innate immune system. Nat Immunol. 2015;16(4):343-53.
58. Naito T, Tanaka H, Naoe Y, Taniuchi I. Transcriptional control of T-cell development. Int Immunol. 2011;23(11):661-8.
59. Kumar BV, Connors TJ, Farber DL. Human T Cell Development, Localization, and Function throughout Life. Immunity. 2018;48(2):202-13.
60. Germain RN. T-cell development and the CD4-CD8 lineage decision. Nat Rev Immunol. 2002;2(5):309-22.
61. Luckheeram RV, Zhou R, Verma AD, Xia B. CD4(+)T cells: differentiation and functions. Clin Dev Immunol. 2012;2012:925135.
62. T Cell Development, Activation and Effector Functions. Primer to the Immune Response2014. p. 197-226.
63. Kaech SM, Cui W. Transcriptional control of effector and memory CD8+ T cell differentiation. Nat Rev Immunol. 2012;12(11):749-61.
64. Allison CACaJP. Costimulatory regulation of T cell function. Current Opinion in Cell Biology 1999;11:203–10.
65. Akdis CA, Arkwright PD, Bruggen MC, Busse W, Gadina M, Guttman-Yassky E, et al. Type 2 immunity in the skin and lungs. Allergy. 2020;75(7):1582-605.
66. Agrawal S, Smith SA, Tangye SG, Sewell WA. Transitional B cell subsets in human bone marrow. Clin Exp Immunol. 2013;174(1):53-9.

67. Shahaf G, Zisman-Rozen S, Benhamou D, Melamed D, Mehr R. B Cell Development in the Bone Marrow Is Regulated by Homeostatic Feedback Exerted by Mature B Cells. Front Immunol. 2016;7:77.
68. Pieper K, Grimbacher B, Eibel H. B-cell biology and development. J Allergy Clin Immunol. 2013;131(4):959-71.
69. Schatz DG, Ji Y. Recombination centres and the orchestration of V(D)J recombination. Nat Rev Immunol. 2011;11(4):251-63.
70. Michael S Neuberger CsM. Somatic hypermutation. Current Opionion in immunology. 1995;7.
71. Christopher J. Jolly SDW, Cristina Rada, Norman Klix,, Neuberger CeaMS. The targeting of somatic hypermutation. Immunology 1996;8:159-68.
72. Schatz DG, Swanson PC. V(D)J recombination: mechanisms of initiation. Annu Rev Genet. 2011;45:167-202.
73. Frederick W. Alt EMO, Faith Young, James Gorman, Guillermo Taccioli and Jianzhu Chen. VDJ recombination. Immunology today. 1992;13(8).
74. Peled JU, Kuang FL, Iglesias-Ussel MD, Roa S, Kalis SL, Goodman MF, et al. The biochemistry of somatic hypermutation. Annu Rev Immunol. 2008;26:481-511.
75. Di Noia JM, Neuberger MS. Molecular mechanisms of antibody somatic hypermutation. Annu Rev Biochem. 2007;76:1-22.
76. Sallusto F, Lanzavecchia A, Araki K, Ahmed R. From vaccines to memory and back. Immunity. 2010;33(4):451-63.
77. Teng G, Papavasiliou FN. Immunoglobulin somatic hypermutation. Annu Rev Genet. 2007;41:107-20.
78. Reed JH, Jackson J, Christ D, Goodnow CC. Clonal redemption of autoantibodies by somatic hypermutation away from self-reactivity during human immunization. J Exp Med. 2016;213(7):1255-65.
79. Schramm CA, Douek DC. Beyond Hot Spots: Biases in Antibody Somatic Hypermutation and Implications for Vaccine Design. Front Immunol. 2018;9:1876.
80. Domon H, Terao Y. The Role of Neutrophils and Neutrophil Elastase in Pneumococcal Pneumonia. Front Cell Infect Microbiol. 2021;11:615959.
81. Bordon J, Aliberti S, Fernandez-Botran R, Uriarte SM, Rane MJ, Duvvuri P, et al. Understanding the roles of cytokines and neutrophil activity and neutrophil apoptosis in the protective versus deleterious inflammatory response in pneumonia. Int J Infect Dis. 2013;17(2):e76-83.
82. Craig A, Mai J, Cai S, Jeyaseelan S. Neutrophil recruitment to the lungs during bacterial pneumonia. Infect Immun. 2009;77(2):568-75.
83. Rigby KM, DeLeo FR. Neutrophils in innate host defense against Staphylococcus aureus infections. Semin Immunopathol. 2012;34(2):237-59.
84. Noske N, Kammerer U, Rohde M, Hammerschmidt S. Pneumococcal interaction with human dendritic cells: phagocytosis, survival, and induced adaptive immune response are manipulated by PavA. J Immunol. 2009;183(3):1952-63.
85. Dommaschk A, Ding N, Tort Tarres M, Bittersohl LF, Maus R, Stolper J, et al. Nasopharyngeal colonization with Streptococcus pneumoniae triggers dendritic cell dependent antibody responses against invasive disease in mice. Eur J Immunol. 2017;47(3):540-51.

86. Bouras M, Asehnoune K, Roquilly A. Contribution of Dendritic Cell Responses to Sepsis-Induced Immunosuppression and to Susceptibility to Secondary Pneumonia. Front Immunol. 2018;9:2590.
87. Jennewein MF, Abu-Raya B, Jiang Y, Alter G, Marchant A. Transfer of maternal immunity and programming of the newborn immune system. Semin Immunopathol. 2017;39(6):605-13.
88. Marchant A, Sadarangani M, Garand M, Dauby N, Verhasselt V, Pereira L, et al. Maternal immunisation: collaborating with mother nature. The Lancet Infectious Diseases. 2017;17(7):e197-e208.
89. Siegrist C-A. Neonatal and early life vaccinology. Elsevier Science. 2001.
90. Matthew G. Darby AC, Dunja Mrjden1, Marion Rolot, Katherine Smith, Claire Mackowiak DS, Donald Nyangahu, Heather Jaspan, Kai-Michael Toellner,, Ari Waisman VQ, Bernhard Ryffel, Adam F. Cunningham, Benjamin G. Dewals, Frank Brombacher, William G. C. Horsnell. Pre-conception maternal helminth infection transfers via nursing long-lasting cellular immunity against helminths to offspring. Science Advances 2019.
91. Svensson-Arvelund J, Ernerudh J. The Role of Macrophages in Promoting and Maintaining Homeostasis at the Fetal-Maternal Interface. Am J Reprod Immunol. 2015;74(2):100-9.
92. Erlebacher A. Immunology of the maternal-fetal interface. Annu Rev Immunol. 2013;31:387-411.
93. Ziegler KB, Muzzio DO, Matzner F, Bommer I, Ventimiglia MS, Malinowsky K, et al. Human pregnancy is accompanied by modifications in B cell development and immunoglobulin profile. J Reprod Immunol. 2018;129:40-7.
94. Ernerudh J, Berg G, Mjosberg J. Regulatory T helper cells in pregnancy and their roles in systemic versus local immune tolerance. Am J Reprod Immunol. 2011;66 Suppl 1:31-43.
95. Thomas G. Wegmann HL, Larry, Mosmann GaTR. Bidirectional cytokine interactions in the maternal-fetal relationship: is successful pregnancy a Th2 phenomenon? Immunology today. 1993;14(7).
96. Svensson-Arvelund J, Ernerudh J, Buse E, Cline JM, Haeger JD, Dixon D, et al. The placenta in toxicology. Part II: Systemic and local immune adaptations in pregnancy. Toxicol Pathol. 2014;42(2):327-38.
97. Sarit Aschkenazi SS, Karlijn M.A. Verwer, Harald Foellmer, Thomas Rutherford, and Gil Mor. Differential Regulation and Function of the Fas/Fas Ligand System in Human Trophoblast Cells1. Biology of reproduction. 2002;66:1853-61.
98. Atyeo CG, Shook LL, Brigida S, De Guzman RM, Demidkin S, Muir C, et al. Maternal immune response and placental antibody transfer after COVID-19 vaccination across trimester and platforms. Nat Commun. 2022;13(1):3571.
99. Pullen KM, Atyeo C, Collier AY, Gray KJ, Belfort MB, Lauffenburger DA, et al. Selective functional antibody transfer into the breastmilk after SARS-CoV-2 infection. Cell Rep. 2021;37(6):109959.
100. Blanco JCG, Pletneva LM, Oue RO, Patel MC, Boukhvalova MS. Maternal transfer of RSV immunity in cotton rats vaccinated during pregnancy. Vaccine. 2015;33(41):5371-9.

101. Madhi SA, Anderson AS, Absalon J, Radley D, Simon R, Jongihlati B, et al. Potential for Maternally Administered Vaccine for Infant Group B Streptococcus. N Engl J Med. 2023;389(3):215-27.
102. Apiwattanakul N, Thomas PG, Iverson AR, McCullers JA. Chronic helminth infections impair pneumococcal vaccine responses. Vaccine. 2014;32(42):5405-10.
103. Clark CE, Fay MP, Chico ME, Sandoval CA, Vaca MG, Boyd A, et al. Maternal Helminth Infection Is Associated With Higher Infant Immunoglobulin A Titers to Antigen in Orally Administered Vaccines. Journal of Infectious Diseases. 2016;213(12):1996-2004.
104. Douce G, Ross K, Cowan G, Ma J, Mitchell TJ. Novel mucosal vaccines generated by genetic conjugation of heterologous proteins to pneumolysin (PLY) from Streptococcus pneumoniae. Vaccine. 2010;28(18):3231-7.
105. Badgujar DC, Anil A, Green AE, Surve MV, Madhavan S, Beckett A, et al. Structural insights into loss of function of a pore forming toxin and its role in pneumococcal adaptation to an intracellular lifestyle. PLoS Pathog. 2020;16(11):e1009016.
106. Herbert JA, Mitchell AM, Ritchie R, Ma J, Ross-Hutchinson K, Mitchell TJ. Expression of the lux genes in Streptococcus pneumoniae modulates pilus expression and virulence. PLoS One. 2018;13(1):e0189426.
107. Duke JA, Avci FY. Emerging vaccine strategies against the incessant pneumococcal disease. NPJ Vaccines. 2023;8(1):122.
108. Moles JP, Tuaillon E, Kankasa C, Bedin AS, Nagot N, Marchant A, et al. Breastmilk cell trafficking induces microchimerism-mediated immune system maturation in the infant. Pediatr Allergy Immunol. 2018;29(2):133-43.
109. Dutta P, Molitor-Dart M, Bobadilla JL, Roenneburg DA, Yan Z, Torrealba JR, et al. Microchimerism is strongly correlated with tolerance to noninherited maternal antigens in mice. Blood. 2009;114(17):3578-87.
110. Nigar Shahid MS, S Hoque, Tahmina Begum, Claudette Thompson, George Siber. Serum, breast milk, and infant antibody after maternal
immunisation with pneumococcal vaccine. The Lancet 1995;346:1252-7.
111. Kinder JM, Stelzer IA, Arck PC, Way SS. Immunological implications of pregnancy-induced microchimerism. Nat Rev Immunol. 2017;17(8):483-94.
112. Stelzer IA, Urbschat C, Schepanski S, Thiele K, Triviai I, Wieczorek A, et al. Vertically transferred maternal immune cells promote neonatal immunity against early life infections. Nat Commun. 2021;12(1):4706.
113. Mathias A, Pais B, Favre L, Benyacoub J, Corthesy B. Role of secretory IgA in the mucosal sensing of commensal bacteria. Gut Microbes. 2014;5(6):688-95.
114. Melo-Gonzalez F, Kammoun H, Evren E, Dutton EE, Papadopoulou M, Bradford BM, et al. Antigen-presenting ILC3 regulate T cell-dependent IgA responses to colonic mucosal bacteria. J Exp Med. 2019;216(4):728-42.
115. Preston JA, Bewley MA, Marriott HM, McGarry Houghton A, Mohasin M, Jubrail J, et al. Alveolar Macrophage Apoptosis-associated Bacterial Killing Helps Prevent Murine Pneumonia. Am J Respir Crit Care Med. 2019;200(1):84-97.
116. Tchalla EYI, Wohlfert EA, Bou Ghanem EN. Neutrophils are required during immunization with the pneumococcal conjugate vaccine for protective antibody responses and host defense against infection. bioRxiv. 2020.

117. Watson K, Russell CD, Baillie JK, Dhaliwal K, Fitzgerald JR, Mitchell TJ, et al. Developing Novel Host-Based Therapies Targeting Microbicidal Responses in Macrophages and Neutrophils to Combat Bacterial Antimicrobial Resistance. Front Immunol. 2020;11:786.
118. Heeb LEM, Egholm C, Boyman O. Evolution and function of interleukin-4 receptor signaling in adaptive immunity and neutrophils. Genes Immun. 2020;21(3):143-9.
119. Wagner B, Perkins G, Babasyan S, Freer H, Keggan A, Goodman LB, et al. Neonatal Immunization with a Single IL-4/Antigen Dose Induces Increased Antibody Responses after Challenge Infection with Equine Herpesvirus Type 1 (EHV-1) at Weanling Age. PLoS One. 2017;12(1):e0169072.
120. Taylor M, Pillaye J, Horsnell WGC. Inherent maternal type 2 immunity: Consequences for maternal and offspring health. Semin Immunol. 2021;53:101527.
121. Gonzalez DG, Cote CM, Patel JR, Smith CB, Zhang Y, Nickerson KM, et al. Nonredundant Roles of IL-21 and IL-4 in the Phased Initiation of Germinal Center B Cells and Subsequent Self-Renewal Transitions. J Immunol. 2018;201(12):3569-79.
122. Chakma CR, Good-Jacobson KL. Requirements of IL-4 during the Generation of B Cell Memory. J Immunol. 2023;210(12):1853-60.
123. Gammill HS, Nelson JL. Naturally acquired microchimerism. Int J Dev Biol. 2010;54(2-3):531-43.
124. Iwai S, Okada A, Sasano K, Endo M, Yamazaki S, Wang X, et al. Controlled induction of immune tolerance by mesenchymal stem cells transferred by maternal microchimerism. Biochem Biophys Res Commun. 2021;539:83-8.
125. Ichinohe T, Teshima T, Matsuoka K, Maruya E, Saji H. Fetal-maternal microchimerism: impact on hematopoietic stem cell transplantation. Curr Opin Immunol. 2005;17(5):546-52.
126. Sunku CC, Gadi VK, de Laval de Lacoste B, Guthrie KA, Nelson JL. Maternal and fetal microchimerism in granulocytes. Chimerism. 2010;1(1):11-4.
127. Irvine EB, Alter G. Understanding the role of antibody glycosylation through the lens of severe viral and bacterial diseases. Glycobiology. 2020;30(4):241-53.
128. Hayes JM, Cosgrave EF, Struwe WB, Wormald M, Davey GP, Jefferis R, et al. Glycosylation and Fc receptors. Curr Top Microbiol Immunol. 2014;382:165-99.
129. Roy Jefferís JL. Glycosylation of Antibody Molecules:
Structural and Functional Significance. Antibody Engineering. 1997;65:111-28.
130. Jefferies R. Glycosylation of Natural and Recombinant Antibody Molecules. Glycobiology and Medicine. 2005:143-8.
131. Liu L. Antibody glycosylation and its impact on the pharmacokinetics and pharmacodynamics of monoclonal antibodies and Fc-fusion proteins. J Pharm Sci. 2015;104(6):1866-84.
132. Ian J. Amanna NEC, Mark K. Slifka. Duration of Humoral Immunity
to Common Viral and Vaccine Antigens. The New England Journal of Medicine. 2007.
133. Mark K Slifka MM, Rafi Ahmed. Bone Marrow Is a Major Site of Long-Term Antibody
Production after Acute Viral Infection. Journal of Virology. 1995:1895-902.